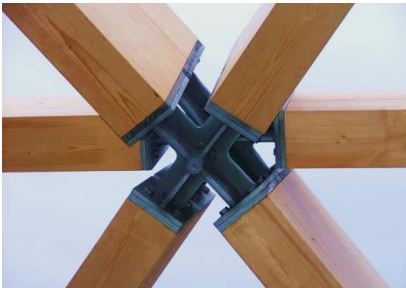


Proceedings of the Conference of COST Action FP1402
Graz University of Technology, Institute of Timber Engineering and Wood Technology
Graz, Austria, 13.09.2017

International Conference on Connections in Timber Engineering – From Research to Standards



Editors:
Reinhard Brandner, Andreas Ringhofer & Philipp Dietsch

**Proceedings of the Conference of COST Action FP1402
Graz University of Technology, Institute of Timber Engineering and Wood Technology
Graz, Austria, 13.09.2017**

International Conference on Connections in Timber Engineering – From Research to Standards

Editors: Reinhard Brandner, Andreas Ringhofer & Philipp Dietsch

Editors Reinhard Brandner, Andreas Ringhofer & Philipp Dietsch

Cover Photos Above: Graz from the Clock Hill (source: Reinhard Brandner)
 Below Left & Right: Joints in Timber Structures (source: WIEHAG GmbH)

Printed by Medienfabrik Graz GmbH

© 2017 Verlag der Technischen Universität Graz

www.ub.tugraz.at/Verlag

ISBN (print) 978-3-85125-553-9

ISBN (e-book) 978-3-85125-554-6

DOI 10.3217/978-3-85125-553-9



This work is licensed under a Creative Commons Attribution 4.0 International License.

<https://creativecommons.org/licenses/by/4.0/deed.en>

Table of Contents

Motivation <i>P. Dietsch</i>	p. 2
The practical design of dowel-type connections in timber engineering structures according to EC5 <i>A. Brunauer</i>	p. 6
Assessment of existing safety formats for timber connections – How probabilistic approaches can influence connection design in timber engineering <i>R. Jockwer, G. Fink & J. Köhler</i>	p. 16
Considerations of connection ductility within the design of timber structures <i>F. Brühl & U. Kuhlmann</i>	p. 32
Impact of standards and EADs on the determination of single fastener properties <i>J. Munch-Andersen</i>	p. 46
Nailed joints: Investigation on parameters for Johansen Model <i>C. Sandhaas & R. Görlacher</i>	p. 64
Design approaches for dowel-type connections in CLT structures and their verification <i>A. Ringhofer, R. Brandner & H. J. Blaß</i>	p. 80
Performance of dowel-type fasteners for hybrid timber structures <i>A. Dias</i>	p. 112
Push-out vs. beam: Can the results of experimental stiffness of TCC-connectors be transferred? <i>J. Schänzlin & S. Mönch</i>	p. 122
Numerical modeling of the load distribution in multiple fastener joints <i>T. K. Bader, J.-F. Bocquet, M. Schweigler & R. Lemaitre</i>	p. 136
Brittle failure of connections loaded parallel to grain <i>P. Quenneville</i>	p. 154
Brittle failure of connections loaded perpendicular to grain <i>R. Jockwer & P. Dietsch</i>	p. 166
Reinforcement of timber structures – a new section for EC 5 <i>P. Dietsch & A. Brunauer</i>	p. 184
Summary and recommendations regarding the seismic design of timber connections <i>R. Tomasi & D. P. Pasca</i>	p. 212
List of authors, reviewers and participants	p. 224

Motivation

It is well known that timber structures succeed or fail in their connections and significant technical advances and developments in the field of timber connections have fostered the recent renaissance of timber as a structural material. Self-tapping screws are prominent amongst these innovations. They increase timber's potential by enabling strong, stiff and economic connections, widening the range for structural applications. An increased range of connection types and corresponding applications gives designers both opportunity and challenge. The result is a noticeable trend towards systemized solutions enabling quick and reliable assembly on site.

The behaviour of structures must be both reliable and safe and, for this reason, construction is highly controlled. This poses the challenge that innovation has to take place inside a framework of regulation. A lack of standardized design and construction principles for new developments could result in a variety of applied approaches that might lead to a lower reliability of structures at higher cost. A core objective for COST Action FP1402 is to provide the knowledge and methods necessary to bring these new developments into regulated building practice.

The objective of this Conference is to record the current state-of-the-art for connections in timber engineering, and to illustrate how new developments will be adopted in the next generation of Timber Design Standards (e.g. Eurocode 5:2022). It is an opportunity to hear presentations from some of the world's leading experts and to join discussions on the design, application and performance of Connections in Timber Engineering. There will be presentations on current performance indicators, (e.g. strength, stiffness and ductile vs. brittle failure modes), as well as applications of connections in cross-laminated timber and timber-concrete composite structures. The Conference will also include presentations on current developments of design rules (e.g. for brittle failure modes, reinforcement and seismic design) and give an outlook on the potential of numerical modelling and probabilistic methods for future design of efficient and reliable connections.

It is intended that this COST Action FP1402 Conference will contribute to a high-quality and open scientific and technical dialogue within the timber engineering community. It thereby adheres to the main principle of the COST Programme, which is to strengthen Europe in scientific and technological research, for peaceful purposes, through the support of cooperation and interaction between researchers and practitioners.

For many years, the team of the Institute of Timber Engineering and Wood Technology at TU Graz has been working at the forefront of timber engineering research and innovation. In 2013, in collaboration with COST Action FP1004, they hosted a very successful "Conference on Cross Laminated Timber". For this current Conference on "Connections in Timber Engineering", TU Graz, with COST Action FP1402, is once again bringing together researchers and practitioners from around the world to increase understanding of current and future timber connection research and to discuss applications.

Philipp Dietsch, Chair COST FP1402

Conference of COST Action FP1402
Graz University of Technology, Institute of Timber Engineering and Wood Technology
Graz, Austria, 13.09.2017

International Conference on Connections in Timber Engineering – From Research to Standards

Scientific Papers

The Practical Design of Dowel-Type Connections in Timber Engineering Structures according to EC 5

Alfons Brunauer
Technical Director Timber Engineering
WIEHAG GmbH
Altheim, Austria

1. Introduction

In fact, connections determine the costs of a structure. Their related influence increases disproportionately with the number of joints in the single structural member. In Fig. 1 the roof structure of a hall, realized with solid web fish belly beams, is illustrated, while Fig. 2 shows a similar situation, wherefore a trussed system was applied. Although the amount of glued laminated timber (GLT, glulam) used for the prior mentioned construction was twice as much as that of the latter one, related costs were only about two third – amongst others because comparatively few joints had to be created. So, the phrase “the simplest structure is the cheapest structure” fully applies. Consequently, the current chapter 8 of EN 1995-1-1 [1] (Eurocode 5 or EC 5) including design provisions for timber engineered connections is one of the most important contents of this European design standard for timber being competitive to other materials.



Fig. 1 Assembly of a roof structure with fish belly beam

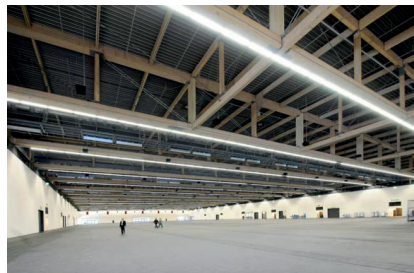


Fig. 2 Roof structure of an exhibition hall realized as trussed system

In the frame of this paper the view of a practicing engineer on current regulations of Eurocode 5, chapter 8 “connections” is summarized and discussed. This especially concerns such topics, which are missing or which are too conservative and where a strong demand improving them by the currently ongoing revision process of this document is given.

2. Some Comments to Missing or on the Safe-Side Rules of EC 5, Chapter 8

As mentioned in the previous section 1, aim of this paper is to point out specific chapter 8 content, which should be improved in the ongoing revision process. Currently missing rules or on the safe-side ones are listed as follows:

- Minimum spacings and edge and end distances for staples. Spacing distance a_2 (perpendicular to grain) and $a_{4,c}$ (unloaded edge) must be affected by the angle between the crown and the direction of the grain of the timber. At the moment, it is necessary to use a greater width for beams in timber-framed elements where boards are jointed.
- Minimum spacing requirements for connections composed by nails or staples with wood based panels should be improved.
- Bolted connections: a rule for the design of bolted connections with threaded rods in EC 5 is missing. Threaded rods are often used, e.g. for the supporting of timber beams on concrete columns.
- The design provisions should contain the phrase that a moisture content change in timber structures during life time must be taken into account.
- Bolted and dowelled connections: splitting of the timber has to be always prevented by sufficient reinforcement perpendicular to the grain and $n_{ef} = n$.
- The height of a fitch plate dowel connection perpendicular to the grain should be limited to a certain value.
- The block shear failure mechanism should be considered for the design of all connections with metal fasteners ruled in chapter 8.
- The group effect of axially loaded screws: the existing provision given in eq. (8.41) of Eurocode 5 is far too conservative – so far the right equipment for assembly is used.

3. Proposals for Improving the Topics Listed in Section 2

3.1 Minimum Spacing and Edge and End Distances for Staples

There is a certain need of improving the minimum spacings for staples situated in solid timber and also in wood based panels. Both the Austrian and the German National Annex, the ÖNORM B 1995-1-1 [2] and the DIN EN 1995-1-1/NA [3] contain additional regulations related, which allow reducing the timber post's width about 40 %, see:

- a_2 (perpendicular to grain):

$$\begin{aligned} \theta \geq 30^\circ & \quad a_2 = (5 + 10 \cdot \sin \alpha) d \\ \theta < 30^\circ & \quad a_2 = 10 \cdot d \end{aligned} \quad (1)$$

- $a_{4,c}$ (unloaded edge):

$$a_{4,c} = (5 + 5 \cdot \sin \theta) d \quad (2)$$

Thereby, d is the staple's shaft diameter and α and θ the angles between the force direction and between the staple crown and grain direction. Furthermore, for staples and nails inserted in wood based panels (WP) there are additional regulations, c. f. Eq. (3) and (4) as well as Fig. 2.

$$\text{unloaded edge: } a_{4,c} = 3 \cdot d \quad (3)$$

$$\text{loaded edge: } a_{4,t} = 7 \cdot d \quad (4)$$

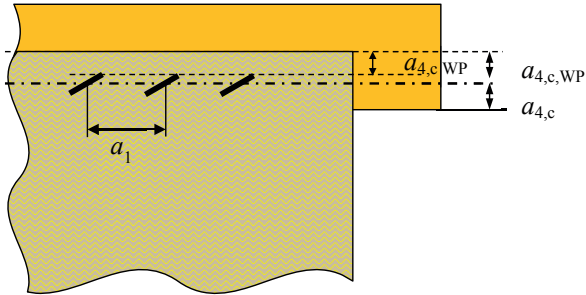


Fig. 2 Spacing and end distances of staples situated in wood based panels

The following example given in Table 1 shall express the given difference between European standardisation and national Non-Contradictory Information (NCI) regarding minimum spacing and edge distances of staples ($d = 1.83$ mm) connecting an OSB board with a timber post. Comparing both required timber widths w_i , a 61 % higher amount of timber results when the provisions given in EN 1995-1-1 [1] are applied.

Table 1 Consequences of different minimum spacing and edge distances of staples exemplarily connecting an OSB board with a timber post: EN 1995-1-1 [1] vs. ÖNORM B 1995-1-1 [2]

standard	EN 1995-1-1 [1]	ÖNORM B 1995-1-1 [2]
spacing a_2 timber	$a_2 = 15 \cdot d = 15 \cdot 1.83 = 27.5$ mm	$a_2 = 10 \cdot d = 10 \cdot 1.83 = 18.3$ mm
spacing $a_{4,c}$ timber	$a_{4,c} = 2 \cdot 10 \cdot d =$ $2 \cdot 10 \cdot 1.83 = 36.6$ mm	$a_{4,c} = 2 \cdot 7.5 \cdot d =$ $2 \cdot 7.5 \cdot 1.83 = 27.5$ mm
spacing $a_{4,c}$ OSB	$a_{4,c} = 2 \cdot 10 \cdot d =$ $2 \cdot 10 \cdot 1.83 = 36.6$ mm	$a_{4,c} = 2 \cdot (3 + 3 \cdot \sin \theta) \cdot d =$ $2 \cdot (3 + 3 \cdot \sin 30) \cdot 1.83 = 16.5$ mm
required timber width	$w = 2 \cdot a_{4,c} = 2 \cdot 36.6 \approx 74$ mm	$w = 27.5 + 18.3 \approx 46$ mm

3.2 Joint Design with Laterally Loaded Threaded Rods

As mentioned in section 2, threaded rods as illustrated in Fig. 3 are often applied in timber engineered structures, e.g. for the supporting of timber beams on concrete columns. If compared to conventional bolts, their advantage is the availability of all necessary customized lengths due to the threaded section along their total length. This in fact saves money since it reduces the delivery time of bolts with specific dimensions (custom-made products).



Fig. 3 Threaded rod with washer and nuts

For the design of laterally loaded threaded rods, the company WIEHAG therefore currently applies NCI NA.8.5.3 given in DIN EN 1995-1-1/NA [3], which consists of the phrase:

“(NA.2) Instead of bolts also threaded rods according to DIN 976-1 [4] may be used.”

Furthermore, the yield moment $M_{y,Rk}$ of the rods shall be determined according to Eurocode 5, eq. (8.30), see

$$M_{y,Rk} = 0.3 \cdot f_{u,k} \cdot d^{2.6}, \quad (5)$$

where d is the average of the rod’s outer and inner thread diameter. The following example shall illustrate the applicability of these provisions given in DIN EN 1995-1-1/NA [3]. Comparing tight-fitting bolts with $d = 20$ mm and steel grade 8.8 with M20 8.8 steel rods ($d = 18.47$ mm), both applied in a steel-to-timber lap joint, the load-carrying capacities R_k according to the European Yield Model (EYM) result in form of:

$$\left. \begin{array}{l} d = 20 \text{ mm } 8.8 \quad R_k = 27.1 \cdot 10 = 271 \text{ kN} \\ d = 18.47 \text{ mm } 8.8 \quad R_k = 24.44 \cdot 10 = 244.4 \text{ kN} \end{array} \right\} \Delta = 11 \%$$

In order to validate this theoretical assumption, the company WIEHAG conducted shear tests with both different joint configurations. Related results are subsequently illustrated in Fig. 4. Even though the experimentally determined load-carrying capacities of both connections are somewhat higher than the characteristic ones, their deviation in form of $\Delta = 9 \%$ is quite similar. So, the regulation according to DIN EN 1995-1-1/NA [3] seems to adequately cover the application of threaded rods applied instead of tight-fitting bolts.

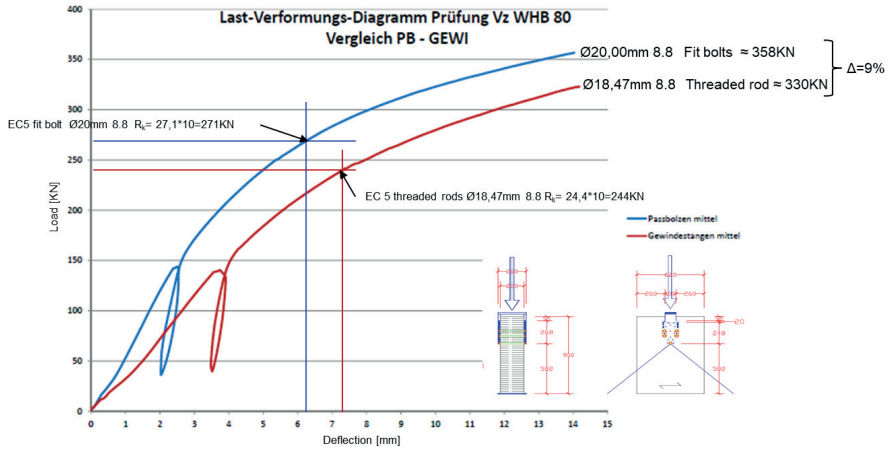


Fig. 4 Comparison of the force-displacement curves for tight-fitting bolts ($d = 20.00 \text{ mm}$) and threaded rods ($d = 18.47 \text{ mm}$) applied in a steel-to-timber shear connection with outer steel plates

3.3 The Consideration of Moisture Content Variation During Building Life Time

As consequence of a missing regulation related, a WIEHAG internal design provision says:

“If no other requirements are given, all connections must be designed to accommodate a change of moisture content by $u = \pm 5 \%$.”

That means that the engineer has to think about possible moisture changes, which will occur during the structure’s life time. In some cases, the changes of timber moisture might be quite low. But also in air-conditioned buildings, moisture changes will appear; at least in form of $\pm 2\div 3 \%$.

As it is well known, a change in moisture content leads to shrinkage or swelling of the timber member. This especially affects comparatively high glulam beams connected with flitch plates and laterally loaded dowel-type fasteners: as illustrated in Fig. 5, missing elongated holes may lead to the occurrence of cracks in the joint area as consequence of shrinking due to dry indoor conditions ($u = 5\div 6 \%$) and a built-in moisture of $u = 12\div 15 \%$. This combined with a beam height of at least 700 mm and a dowel diameter of $d = 20 \text{ mm}$ leads to a further WIEHAG design provision, which limits the maximum height of the dowelled connection (without elongated holes) to $h = 360 \text{ mm}$. This value may be increased by $10\div 15 \%$, when a sufficient reinforcement perpendicular to grain is applied.



Fig. 5 Appearance of shrinkage cracks in the area of a flitch plate dowel - rigid connection in very dry conditions

3.4 The Reinforcement of Bolted and Dowelled Connections

Concentrating on the failure mechanisms of bolted or dowelled connections, splitting of the timber should be always prevented by a sufficient reinforcement perpendicular to the grain. This advantageously consequences that the effective number of fasteners parallel to grain direction, n_{ef} can be set equal to the total number of fasteners n .

The company WIEHAG carried out some tests together with Graz University of Technology on large dowel-type connections, see Fig. 6. The results clearly show that the approach $n_{ef} = n$ is correct (even on a large scale) – so far splitting is prevented by a sufficient reinforcement perpendicular to the grain, here in form of self-tapping screws.

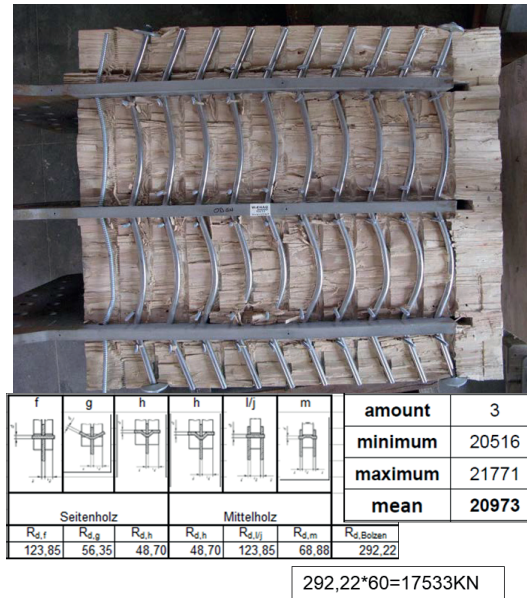


Fig. 6 Comparison Johansen equations – test result of large dowel-type connections

In some cases, an external reinforcement in form of plywood or other wooden based panels or lamellas may be a better alternative. One related example is a framework with a rigid dowel-type corner joint, c. f. Fig. 7.



Fig. 7 Reinforced two-hinged frame with dowel circle (UCD Dublin Library, 2005). Plywood board (beech) 4 x20 mm fully glued on both sides (columns and crossbar) to avoid cracks

3.5 Group Effect of Axially Loaded Screws

In the currently valid version of Eurocode 5, the group effect of connections with predominately axially loaded self-tapping screws is considered quite conservatively, c. f. Eq. (6):

$$n_{ef} = n^{0.9}, \quad (6)$$

with n_{ef} as the effective number of inserted screws and n as their total number. In some European Technical Assessments dedicated to self-tapping screws – c. f. ETA 11/0190 [5] for instance – this harsh restriction has been modified as follows:

$$n_{ef} = 0.9 \cdot n. \quad (7)$$

Eq. (7) corresponds to the experience of the company WIEHAG, which is based on internal testing. For example, a truss joint as steel-to-timber connection with $n = 214$ fully threaded, inclined positioned screws was tested at the University of Stuttgart, c. f. Brunauer [6] and Fig. 8.



Fig. 8 Test arrangement at the University of Stuttgart

Thereby, the steel failure of the screws (see Fig. 8, right) appeared at a test load of 13,000 kN. This clearly points out a global safety factor of > 300 % and that a group effect could not be observed. Another test, done at the WIEHAG workshop, showed the same results. So, the current design provision of Eurocode 5 in form of

$$n_{ef} = n^{0.9} = 214^{0.9} = 125, \quad (8)$$

is far too conservative, while when following Eq. (7)

$$n_{ef} = 0.9 \cdot n = 0.9 \cdot 214 = 193, \quad (9)$$

a secure system is given.

But note in all cases, and this is content of the European Technical Assessments as well, we applied a torque controlled equipment to make sure all screws are equally attracted, see Fig. 9.



Fig. 9 Torque controlled screw driver

4. Conclusions

The current missing or on safe side rules in Eurocode 5 for dowel-type connections should be adapted to the state-of-the art. This contribution gives an overview about the design in practise and possible approaches to make timber structures more competitive.

5. References

- [1] EN 1995-1-1: 2004 + AC:2006 + A1:2008 + A2:2014, “Eurocode 5: Design of timber structures – Part 1-1: General – Common rules and rules for buildings”, CEN, 2014.
- [2] ÖNORM B 1995-1-1, “Eurocode 5: Design of timber structures – Part 1-1: General – Common rules and rules for buildings – National specifications for the implementation of ÖNORM EN 1995-1-1, national comments and national supplements”, ASI, 2015 (in German).
- [3] DIN EN 1995-1-1/NA, “National Annex – Nationally determined parameters – Eurocode 5: Design of timber structures – Part 1-1: General – Common rules and rules for buildings”, DIN, 2013 (in German).
- [4] DIN 976-1, “Fasteners – Stud bolts – Part 1: Metric thread”, DIN, 2016.
- [5] Deutsches Institut für Bautechnik (DIBt), “European Technical Assessment ETA-11/0190 Würth screws“, Berlin, 2013.
- [6] Brunauer A., “Frankfurt Trade Fair Hall“, In: *15. Internationales Holzbau-Forum IHF*, Garmisch-Partenkirchen, Germany, 2009 (in German).

Assessment of Existing Safety Formats for Timber Connections – How Probabilistic Approaches can Influence Connection Design in Timber Engineering

**Robert Jockwer
Senior Scientist
ETH Zurich
Zurich, Switzerland**

**Gerhard Fink
Assistant Professor
Aalto University
Helsinki, Finland**

**Jochen Kohler
Professor
NTNU
Trondheim, Norway**

Summary

Connections are important details in timber construction, connecting single members and elements to larger structures. The design of connections is regulated by structural standards that in general make use of the so called semi-probabilistic safety concept. This concept contains reliability elements, i.e. a conventional deterministic representation of strength and stiffness related properties and action effects as specified fractile values of the underlying probability distributions, partial factors and load combination factors. Standardisation bodies ascertain the reliability elements in order to provide sufficient reliability for the design solutions that result from the application of the code.

This is also done for the semi-probabilistic design basis for timber connections. However, despite of the fundamental differences in mechanical and material behaviour, in general the same reliability elements as for the design of timber structural components are used.

The present article takes a critical appraisal of the existing safety format for timber connections as implemented in the Eurocode.

1.1 Introduction

Due to the natural origin of the wood the dimensions of timber elements are limited. In order to be able to build larger structures, individual timber elements are connected by means of different types of connections. The types of connections

most commonly used in modern timber engineering are amongst others: glued-connections, dowelled, bolted, nailed or stapled connections, connections with screws or glued-in rods. The performance of the above-mentioned connections depends on their applications; e.g. used as shear or tensile connector, type of connecting materials like timber or engineered wood products.

The structural performance of a timber structure is considerably influenced by the performance of the connections between the individual structural members. These connections are often the cause of failure of timber structures [1,2]. Despite their importance timber connection design frameworks are not based on a consistent basis compared to the design regulations of timber structural components.

1.2 Design of Timber Members

For the determination of the load-carrying capacity and for the design of individual timber members their behaviour is characterized by the principal mechanical properties, e.g. the tensile and compression strength of the timber loaded parallel and perpendicular to the grain, respectively, the shear strength and rolling shear strength. The design can be performed by comparison of the acting stresses and the corresponding strength of the members.

1.3 Design of Connections in Timber Structures

The structural performance of single connections depends on different elements with individual material strength and stiffness and individual geometrical properties. Due to this complexity a straight forward comparison of acting stresses and corresponding strength as compared to timber members is hardly possible for the design of connections.

Mechanical models have been developed in order to explain the structural behaviour of connections and in order to handle the variety of possible arrangement of connections in timber structures. Certain material related parameters and system properties are used in the mechanical models that represent a specific performance of the material. These material related parameters or system properties can be determined in material tests or in simplified tests on representative connections or parts of it, respectively. An example of a material related parameter is the tensile strength of steel determined according to EN ISO 6892-1 [3]. An example of a system property is the embedment strength of the timber determined according to EN 383 [4].

One of the challenges for the implementation of mechanical models and provisions for the design of connections in codes is to account for the different characteristic properties of the elements and the different failure modes of a connection. For a reliable design of connections the entire system of the individual members of the connection has to be assessed.

1.4 Ductility Aspects for Design of Timber Structures

The performance of a structure depends not only on its resistance but also on its deformation capacity. Besides elastic deformations of the structure especially the non-linear behaviour of connections is of interest. Especially ductile behaviour of connections offers the potential for redistribution of loads in the structure as shown by [5]. Different design codes like DIN 1052 [6] or SIA 265 [7] set the ductile failure mode of connections as the basis for the design. A detailed discussion of the importance of ductile failure modes in connections can be found in [8,9].

Due to e.g. geometrical constraints it can be necessary to reduce the dimensions of the connections necessary to achieve ductile failures. This seems adequate especially if the desired load-carrying capacity can be obtained, however, the consequences of brittle failures should be minimized by implementing additional measures for guaranteeing sufficient robustness.

2. Safety Concept of Eurocode

2.1 Load and Resistance Factor Design Format

Both, the loads and the resistances are subject to uncertainties. In order to ensure an adequate level of reliability almost all design codes, including the Eurocodes, introduced design values for resistances and actions in the design equations; the so-called load and resistance factor design (LRFD) format.

The optimal partial factors for achieving the desired failure probability can be determined in dependency of the loading situation and the relevant material parameters as discussed in [10]. The calibration of these partial factors for timber structures is based mainly on loading situations of members in pure bending [11].

2.2 Load-Carrying Capacity and Resistance in the Eurocodes

Different formats for representing the design value of the load-carrying capacity can be set up. The design resistance is defined as:

$$R_d = \frac{R\{X_d\}}{\gamma_{Rd}} \quad (1)$$

where:

X_d design value of the relevant material property;

γ_{Rd} partial factor accounting for uncertainty in the resistance model; and

$R\{ \}$ outcome of the resistance model.

The design values of the material property (X_d) that is used in Eq. (1) to verify ultimate limit states should be calculated from:

$$X_d = \frac{\eta\{X_k\}}{\gamma_m} \quad (2)$$

where:

X_k characteristic value of the relevant material property;

η conversion factor that takes account of volume and scale effects, effects of moisture and temperature, and any other relevant parameters; and

γ_m partial factor accounting for uncertainty in the material property.

Besides the separate consideration of the partial factors either on the resistance level or on the material property level a joint consideration of the partial factors related to the material property and to the resistance model could be set up. In this regard the following two equations are considered.

The following formulation is known as the ‘material factor approach’ (MFA) as given in Equation 6.6a in EC 0.

$$R_d = R \left\{ \frac{\eta X_k}{\gamma_M} \right\} \quad (3)$$

where:

$$\gamma_M = \gamma_m \cdot \gamma_{Rd}$$

Alternatively to Eq. (3), the design resistance may be obtained directly from the characteristic value of a resistance, without explicit determination of design values for the individual material property. This formulation is known as the ‘resistance factor approach’ (RFA):

$$R_d = \frac{R \{ \eta X_k \}}{\gamma_R} \quad (4)$$

where:

$$\gamma_R = \gamma_M = \gamma_m \cdot \gamma_{Rd}$$

2.3 Application in EN 1995-1-1 [12]

EN 1995-1-1 (Eurocode 5, EC 5) [12] specifies design rules for the use of timber and timber based products in structural design. Timber and most of the derived building products are complex inhomogeneous materials and it cannot be referred to material properties without reference to the corresponding test conditions in terms of loading mode, size, time, surrounding climate, etc. However, in EC5 [12] the term “material property” is used for simplicity (as in the entire timber engineering profession) as a proxy for the more correct term “properties of standardized test specimen examined under standardized test conditions”.

2.3.1 General Definition of the Design Material Property

The design material property as defined in Eq. (2) is applied in EC 5 [12] as follows.

$$X_d = k_{\text{mod}} \frac{X_k}{\gamma_M} \quad (5)$$

where:

X_k characteristic value of strength property;

γ_M partial factor for a material property;

k_{mod} modification factor taking into account the effect of the duration of load and moisture content.

The factor k_{mod} is a conversion factor from standardized test load duration and moisture conditions to the anticipated conditions in the structure.

2.3.2 General Definition of the Design Resistance

The design resistance or load-carrying capacity is defined as:

$$R_d = k_{\text{mod}} \frac{R_k}{\gamma_M} \quad (6)$$

where:

R_k characteristic value of load-carrying capacity.

The conversion factor is here directly multiplied to the resistance. The partial factor for the partial material property is also used directly on the resistance. The universal use of the partial material factor is illustrated in Tab. 1, where different partial factors are suggested for both, material properties and resistances.

Tab. 1 Recommended partial factors γ_M for material properties and resistances [12].

Fundamental combinations	
Solid Timber	1.30
Glued laminated timber	1.25
LVL, plywood, OSB	1.20
Connections	1.30
Punched metal plate fasteners	1.25
Accidental combinations	
	1.30

2.4 Design of Connections in Eurocode 5 [12]

As an example the design value of the load-carrying capacity can be derived as follows:

$$F_{v,Rd} = k_{\text{mod}} \frac{F_{v,Rk} \{f_{h,i,k}; M_{y,Rk}; F_{ax,Rk}\}}{\gamma_M} \quad (7)$$

where:

$f_{h,i,k}$ characteristic value of embedment strength in the timber member i ;

$M_{y,Rk}$ characteristic value of the yield moment of the fastener;

$F_{ax,Rk}$ characteristic value of the axial withdrawal capacity of the fastener.

An additional factor k_γ is used for certain failure modes in order to account for the different partial factors for the material of timber and steel. The factor can be derived e.g. as follows for the failure modes with plastic hinges in the fastener:

$$k_\gamma = \sqrt{\frac{\gamma_M}{\gamma_{M,steel} \cdot k_{mod}}} = \sqrt{\frac{1.3}{1.1 \cdot 0.9}} = 1.15 \quad (8)$$

2.5 Discussion of the Implementation of the EC 0 Safety Format to the Design of Connections in EC 5 [12]

The design value of the resistance of a connection is calculated in Eurocode 5 [12] by applying the general values of the partial factor γ_M and the modification factor k_{mod} to the characteristic value of the resistance of a connection. This procedure is correct only if (a) the coefficient of variation and (b) the distribution function of the resistance of the connection are the same as assumed for the determination of the general values γ_M . Existing differences in the variation of the resistance are considered currently by the factor k_γ . However, the differences of the distribution functions are not accounted for in the current design format for connections in EC 5 [12].

3. Structural Behaviour of Connections with Metal Dowel-Type Fasteners

The structural behaviour of connections is discussed e.g. in [13,14]. The estimation of the resistance of connections is based on extensive mechanical models that include several material properties. The load-carrying capacity of dowel type fasteners is governed by four main characteristics:

- The embedment strength of the timber f_h . The embedment strength is the system property that is associated to the resistance of solid timber against the lateral penetration of a stiff fastener. Additional properties like dowel geometry or surface roughness have an important impact on the embedment strength.
- The bending moment capacity of the dowel M_y . The bending moment capacity is mainly influenced by the dowel diameter and the yield strength of the dowel material. A plastic deformation capacity is necessary to provide bending moment capacity even after considerable deformation of the dowel.
- The pulling out resistance of the dowel F_{ax} . Under special circumstances the so called pulling out resistance of dowel type fasteners can be activated even in lateral loading. In that case a large bending deformation of the fastener is required. This effect is also referred to as the rope effect. For smooth dowels the rope effect is commonly neglected.
- The resistance against splitting, block or plug shear failure. This resistance is mainly governed by a fracture mechanical phenomena and depends on the spacing, edge and end-distances as well as the member thickness and penetration depth of the fasteners.

In addition to those four main characteristics, also effects such as the effective number of fasteners or the impact of friction between the members due to the rope effect influence the load-carrying capacity. However, they are not considered in the present study.

3.1 Mechanical Models

3.1.1 Fastener Failure: European Yield Model

The resistance of laterally loaded dowel type timber connections is commonly determined as the minimum of the capacities according to the so called European Yield model (EYM) that is based on the studies by Johansen [15]. These failure modes describe the embedment failure of the timber and/or the plastic failure of the dowel in dependency of the thickness t_i of the timber members i (failure modes $R_{I,i}$ to $R_{III,i}$ in Fig. 1). The load-carrying capacities of the different failure modes according to the EYM for a single shear plane in a wood-steel-wood connection are given in Eqs. (9)-(11).

Failure mode I: Embedment failure

$$R_{I,i} = f_{h,i} t_i d \tag{9}$$

Failure mode II: Mixed failure with plastic deformation of the dowel in the steel plate

$$R_{II,i} = t_i f_{h,i} d \left[\sqrt{2 + \frac{4M_y}{f_{h,i} d t_i^2}} - 1 \right] \tag{10}$$

Failure mode III: Failure with plastic deformation of the dowel in the timber member

$$R_{III,i} = \sqrt{4M_y f_{h,i} d} \tag{11}$$

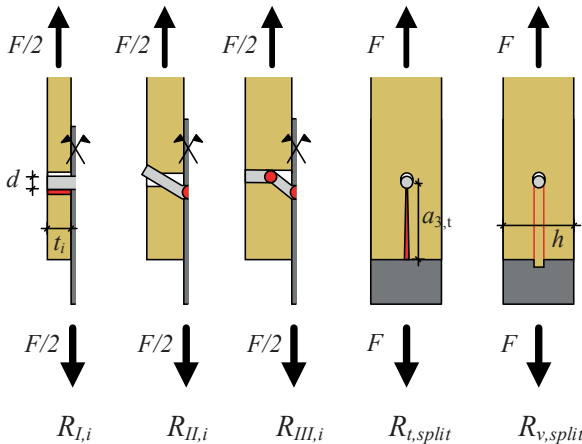


Fig. 1 Simplification of failure modes of the EYM for the symmetric half of a dowelled timber-steel-timber connection and splitting and block shear failure modes.

3.1.2 Timber Failure: Splitting and Block Shear Failure

Failure modes in the timber members are often characterized by brittle failure mechanisms in shear and tension perpendicular to the grain. So far only a design equation for the situation of block shear failure of laterally loaded groups of fasteners is given in the Appendix A of EC 5 [12]. Additional failure modes with tension perpendicular to the grain splitting and shear fracture of the connection as shown for the cases $R_{t,\text{split},i}$ and $R_{v,\text{split},i}$ in Fig. 1 are not accounted for in EC 5 [12]. Brittle failure modes are relevant especially for thin side members of double shear connections and small spacing or end-grain distances.

A very simple model for considering impact of the end-grain distance $a_{3,t}$ can be based on a verification of tension perpendicular to grain strength $f_{t,90}$ (Eq. (12)). The relation between force F_{90} acting perpendicular to the grain induced by a dowel loaded parallel to the grain by force F_0 is $F_{90} \approx 0.3 F_0$ according to [16].

$$R_{t,\text{split},i} = \frac{1}{0.3} t_i a_{3,t} f_{t,90} \quad (12)$$

The model in Eq. (12) can be used in analogy for describing the impact of spacing a_1 on the fracture in tension perpendicular to the grain.

[17] presented a fracture mechanics based design approach for brittle failure of a connection (Eq. (13)). Due to the complex stress state the fracture process is described by mixed mode fracture with $G_{f,\text{mixed}}$. An angle of friction $\varphi = 30^\circ$ between dowel and timber is used by Jorissen.

$$R_{v,\text{split},i} = 2t_i \sqrt{\frac{G_{f,\text{mixed},i} E_{0,i} d \sin \varphi (h - d \sin \varphi)}{h}} \quad (13)$$

A conservative estimate can be made by assuming the mixed mode fracture energy to be equal to the mode I fracture energy with crack opening: $G_{f,\text{mixed}} = G_I$. Other more sophisticated fracture mechanics based approaches can be found e.g. in [18].

3.2 Material Properties

The determination of different material property values and their impact on the load-carrying capacity of connections with dowel type fasteners was discussed by [19].

The distribution characteristics of the relevant material property values and a probabilistic assessment of the load-carrying capacity of shear connections with dowels was presented by [13]. In the following the most important characteristics of the material property values are summarized.

3.2.1 Embedment Strength f_h

The distribution characteristics of embedment strength were determined by [20] as summarized in Eq. (14) and Tab. 2.

$$f_h = A \rho^\beta d^C \varepsilon \quad (14)$$

Tab. 2 Regression parameters for Eq. (14) from [20].

Parameter	Distribution function	Mean value	stDev
A	Lognormal	0.097	0.23
B	Normal	1.07	0.04
C	Normal	-0.25	0.012
ϵ	Lognormal	1	0.11

3.2.2 Yield Moment M_y

The relevant resistance of a fastener in bending is between the elastic and full plastic bending capacity (e.g. [21]). The empirically derived Eq. (15) is given in EC 5 and is based on studies by [22].

$$M_y = 0.3 f_u d^{2.6} \quad (15)$$

The variation of material properties of the steel within one batch is rather small. [23] proposes $CoV \approx 4\%$. In Tab. 3 the yield and tensile strength of common steel grades are summarized. Recent studies by [24] show that there can be a considerable difference between steel qualities of different batches and overstrength is a common issue.

Tab. 3 Yield strength f_y and tensile strength f_u in dependency of steel grades for a $CoV = 4\%$ and lognormal distribution properties.

Grade	$f_{y,k}$ [N/mm ²]	$f_{u,k}$ [N/mm ²]	$f_{u,mean}$ [N/mm ²]
S235	$\approx 190 - 360$	$\approx 360 - 510$	$\approx 385 - 545$
5.6	300	500	534
8.8	640	800	854
ETG 100	> 865	$\approx 960 - 1100$	$\approx 1025 - 1175$

3.2.3 Additional Material Properties and Correlations

The distribution characteristics of density ρ , modulus of elasticity parallel to the grain E_0 and tension perpendicular to grain strength $f_{t,90}$ can be found in [25]. The mode 1 fracture energy G_I is based on studies by [26]. All distribution characteristics used in this study are summarized in Tab. 4.

Tab. 4 Distribution characteristics of material parameters.

	Distribution function	Mean value	CoV
ρ	Lognormal	420	10%
E_0	Lognormal	11500	23%
$f_{t,90}$	Weibull	2.0	30%
G_I	Lognormal	0.3	20%

The correlations between the material property values is based on JCSS [25] (Tab. 5) and [20] (Tab. 6). No correlation is assumed between G_1 and the other material properties as discussed in [27] which leads to a larger impact of $R_{v,split}$.

Tab. 5 Correlation between material properties values [25].

	E_0	$f_{t,90}$
ρ	0.6	0.4
E_0	–	0.4

Tab. 6 Correlation between embedment strength parameters [20].

	B	C	ε
A	-0.99	-0.24	0
B	–	0.11	0
C	–	–	0

4. Load-Carrying Capacity of Connections

4.1 Impact of Varying Material Properties on the Load-Carrying Capacity of Connections

The geometrical parameters of relevance for the load-carrying capacity according to EYM are the thickness of the timber member(s) t_i and the dowel diameter d . These geometrical parameters can be expressed by the slenderness $\lambda = t/d$. The steel quality has an impact only on the load-carrying capacity in failure mode II and III. At the transition between the failure modes II to III the critical slenderness $\lambda_{II/III} = t/d$ for achieving ductile failure can be defined. The end-grain distance $a_{3,t}$ of a connection with a single fastener has an impact on the failure mode. For small end-grain distance the splitting failure modes cause a reduction of load-carrying capacity. In the example shown in Fig. 2 in addition to the values specified in Tab. 4 the following material and geometric properties have been chosen: steel quality 5.6, $d = 12$ mm, $h = 10 d$, $a_{3,t} = 7.5 d$.

In Fig. 2 the impact of varying material properties on the variability of the relevant load-carrying capacity is shown in dependency of the relative thickness of the side members $\lambda = t_i/d$. For each thickness $n = 10^5$ simulations were performed. It is obvious that with increasing λ the load-carrying capacity is increasing. However, a closer look also indicates that the variability decreases and the shape of the distribution function changes, in particular the lower and most important tale of the distribution function. This is a result of the different types of failure (see also Fig. 1) with the different corresponding strength parameters: For small relative thickness of the side members (approx. $\lambda < 2.5$) about 3/4 of the simulated connections failed in R_I and 1/4 in $R_{t,split}$. For larger relative thickness λ failure mode R_{II} (approx. $2.5 < \lambda < 5.5$) and failure mode R_{III} (approx. $\lambda > 5.5$) become dominant.

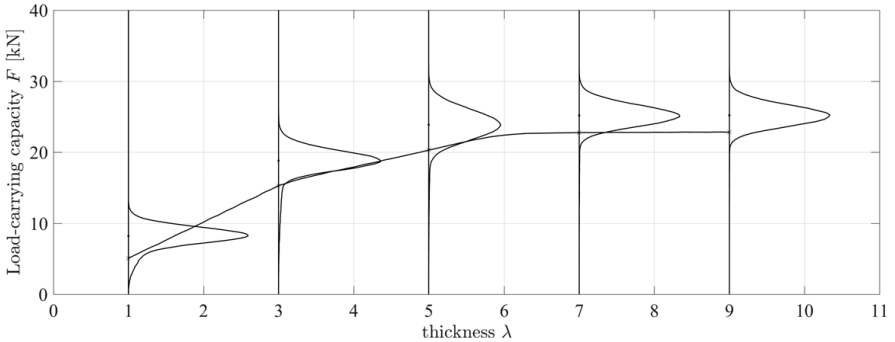


Fig. 2 Load-carrying capacity according to EYM and timber failure modes in dependency of the relative side member thickness $\lambda = t/d$.

In Fig. 3 the load-carrying capacity normalized with the mean value is illustrated. Comparing the black lines (5 % and 1 % fractile) and the grey lines (95 % and 99 % fractile) the skewness of the distribution becomes obvious. Furthermore, the change of the leading failure modes, for different relative thicknesses, is visible. This change in skewness has to be accounted for when defining and specifying a partial factor for the failure mode. A solution would be the consideration of individual partial factors for the different strength properties.

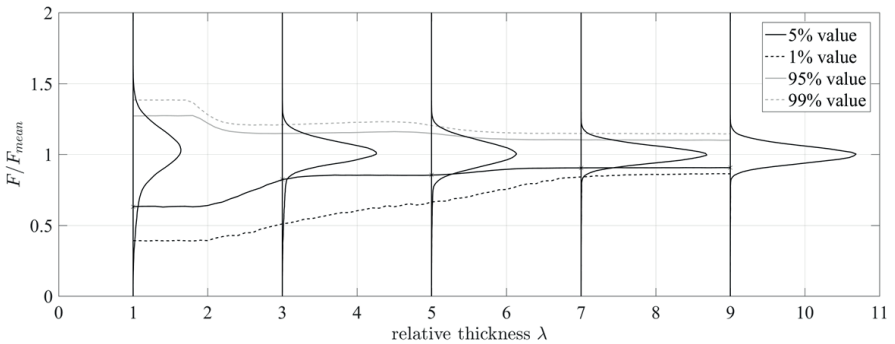


Fig. 3 Normalized load-carrying capacity in dependency of the relative side member thickness $\lambda = t/d$.

4.2 Variation of Load-Carrying Capacity of Connections in Tests by [17]

[17] reports a large number of tests with various configurations. The tests were carried out as bolted shear connection in timber-to-timber double lap joints. Teflon sheets in the contact areas were used to reduce the impact of friction induced by the

rope effect. [23] confirmed the validity of the fracture mechanics design approach derived by [17] (Eq. (13)) for the load-carrying capacity of a single dowel of small slenderness $\lambda = d/t$.

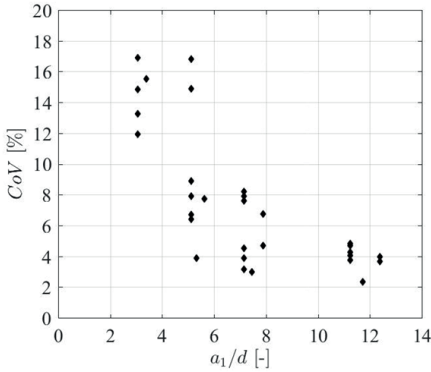


Fig. 4 *CoV of the load-carrying capacity at density $\rho_{mean} = 420 \text{ kg/m}^3$ for different test series from [19].*

In this paper the impact of spacing a_1 on the variation of load-carrying capacity shall be studied. In Fig. 4 the coefficient of variation of the load-carrying capacity at a reference density is shown in dependency of the spacing a_1 of the dowels. A considerable increase of variation with decreasing spacing can be observed. The reason for the increase of variation with decreasing spacing between the dowels can be explained by the change of the failure mode: for small spacing the material properties of the timber ($f_{t,90}$, G_I) featuring high variation govern the failure whereas for large spacing the steel properties (M_y) are decisive.

5. Discussion

5.1 Reliability of Connections with Dowel Type Fasteners

The dimensions and properties of shear connections with dowel type fasteners should be designed in a way to achieve the target reliability level. Most beneficial are failure modes that cause a low variability of the load-carrying capacity as e.g. plastic failure of the metal fasteners. As already stated by [17] for the different failure modes of connections with different level of ductility different partial factors might be necessary. For the ductile failure mode EYM III the variability is in the range of $CoV \approx 5\%$. For other, brittle failure modes not only the reduction in resistance but also the increased variability should be accounted for.

5.2 Other Types of Connections

In the framework of this paper only dowel type connections were discussed in detail. However, similar considerations can be made for all kind of connections. In the following an overview about other selected connections, in respect to the reliability analysis are presented:

5.2.1 Glued-in Rods

For glued-in rods so far no homogenous design standard exists; however, the different failure modes are well-known (see e.g. [28,29]): bondline failure along the

rod, tensile failure of the net cross section, block shear, splitting, and yielding of the rod. As for dowel type connections, the occurring failure type depends on different parameters such as the number of rods, the spacing and end and edge distances as well as the relative slenderness of the rods. Based on the different failure modes with the associated strength properties of the timber, steel and adhesive, the resistance of the glued-in rod connection will have different variability in dependency of the geometric properties of the system. The ductile failure mode of the rod loaded in axial tension shows commonly the highest predictability and lowest variability and, hence, should be targeted.

5.2.2 Axially Loaded Screws

The design of axially loaded screws is standardized in EC 5 [12]; accordingly the following failure types should be considered: withdrawal of the threaded part of the screw, pull-through and tear-off failure of the screw head, tensile failure of the core cross-section of the screw as well as group effects, such as pull-out of a block. The occurring type of failure depends on similar material strength parameters as described above. Screws made of high grade steel wire and hardened screws show commonly a reduced ability for ductile deformation. This may lead to limited redistribution of forces in connections with multiple screws and may result in premature brittle failure due to unequal loading of single screws.

5.2.3 Finger Joint Connections

Typical failure types of finger joint connections are a failure of the timber net cross-section, shear failure along the fingers in the timber or in the bondline. Due to inhomogeneity of timber also a timber failure outside the finger joint connections can occur. In particular, for lower strength grades the failure often occurs outside the finger joint connections. However, the quality of the finger joint connections have to be guaranteed by the producer and the resulting uncertainties are already considered in the safety factors of the corresponding engineered wood product. The same applies for other glued connections that are used for the fabrication of engineered wood products and as well as for universal finger joint connections.

6. Conclusions

From the study presented in this paper, the following conclusions can be drawn:

- the current implementation of the safety format in the design rules for timber structures is based mainly on individual member design
- connections are complex compounds of different parts and materials exhibiting a wide range of possible failure modes
- the different failure modes are governed by different geometrical parameters and material properties
- depending on the failure mode these different material properties cause different variability of the resistance of a connection

- the reliability and the resulting optimal partial factor depend on the failure mode of the connection and the variability of its resistance
- failure modes with a plastic failure of the steel allow for a low partial factor and, hence, an economic design
- brittle failure modes require a larger safety margin

The following recommendations for an optimal design can be given:

- In order to allow for an economic and reliable design the geometry and configuration of a connection should be chosen in a way to obtain high load-carrying capacity with only a small variability. This can be achieved by sufficiently large spacing, end and edge distances and timber member thickness (large dowel slenderness λ) in order to reach a failure mode with ductile deformation of the fasteners. This allows benefiting from the small variability of these ductile failure modes and the consequent small partial factors.
- The unfavourable brittle failure modes due to splitting or plug-shear should be accounted for in the design but charged with sufficient safety margin in order to account for the higher variability and reduced reliability compared to ductile failure modes.
- Reinforcement by means of e.g. self-tapping screws can be a good solution to reduce the risk of brittle failure of dowelled connections due to splitting failure [30]. It can be used to reduce the variability of load-carrying capacity also for small spacing and end and edge distances and sustain an adequate level of reliability for this type of connection geometries. Nevertheless, possible restraint in case of moisture variation might lead to negative consequences.

7. Acknowledgement

The work presented in this paper was written in the framework of the COST Action FP 1402 (www.costfp1402.tum.de).

8. References

- [1] Foliente G.C., "Design of timber structures subjected to extreme loads", *Progress in Structural Engineering and Materials*, Vol. 1, 1998, pp. 236–244.
- [2] Frühwald E., Serrano E., Toratti T., Emilsson A., and Thelandersson S., *Design of safe timber structures - how can we learn from structural failures in concrete, steel and timber?*, 2007, Division of Structural Engineering, Lund University, Sweden.
- [3] EN ISO 6892-1, *Metallic materials - Tensile testing - Part 1: Method of test at room temperature*, European Committee for Standardization (CEN), 2016, Brussels Belgium.

- [4] EN 383, *Timber structures - Test methods - Determination of embedment strength and foundation values for dowel type fasteners*, European Committee for Standardization (CEN), 2007, Brussels, Belgium.
- [5] Dietsch P., "Robustness of large-span timber roof structures - Structural aspects", *Engineering Structures*. Vol. 33, 2011, pp. 3106–3112.
- [6] DIN 1052, *Entwurf, Berechnung und Bemessung von Holzbauwerken - Allgemeine Bemessungsregeln und Bemessungsregeln für den Hochbau*, DIN Deutsches Institut für Normung e.V., 2008, Berlin, Germany (in German).
- [7] SIA 265:2012, *Holzbau*, SIA - Schweizerischer Ingenieur- und Architektenverein, 2012, Zurich, Switzerland (in German).
- [8] Mischler A., "Influence of ductility on the load-carrying capacity of joints with dowel-type fasteners", *Proceedings of the 30th CIB-W18 Meeting*, 1997, p. CIB-W18/30-7-6, Vancouver, BC, Canada.
- [9] Mischler A., "Design of joints with laterally loaded dowels", *Proceedings of the 31st CIB-W18 Meeting*, 1998, p. CIB-W18/31-7-2, Savonlinna, Finland.
- [10] Kohler J., Steiger R., Fink G., and Jockwer R., "Assessment of selected Eurocode based design equations in regard to structural reliability", *Proceedings of the 45th CIB-W18 Meeting*, 2012, p. CIB-W18/45-102-1, Växjö, Sweden.
- [11] Sørensen J.D., "Calibration of partial safety factors in Danish structural codes", *Proceedings of the JCSS Workshop on Reliability Based Code Calibration*, 2002, Zurich, Switzerland.
- [12] EN 1995-1-1, *Eurocode 5: Design of timber structures - Part 1-1: General - Common rules and rules for buildings*, European Committee for Standardization (CEN), 2004, Brussels, Belgium.
- [13] Köhler J., *Reliability of Timber Structures*, 2007, Institute of Structural Engineering, ETH, vdf, Zurich, Switzerland.
- [14] Jockwer R., "Impact of varying material properties and geometrical parameters on the reliability of shear connections with dowel type fasteners", *Proceedings of the 49th INTER Meeting*, 2016, p. INTER/49-7-1, Graz, Austria.
- [15] Johansen K.W., "Theory of Timber Connections", *IABSE Publications*, Vol. 9, 1949, pp. 249–262.
- [16] Schmid M., *Anwendung der Bruchmechanik auf Verbindungen mit Holz*, 2002, Universität Karlsruhe, Germany (in German).
- [17] Jorissen A., *Double shear timber connections with dowel type fasteners*, 1998, University Press Delft, The Netherlands.
- [18] Schmid M., Blaß H.-J., and Frasson R.P.M., "Effect of distances, spacing, and number of dowels in a row on the load carrying capacity of connections with

- dowels failing by splitting", *Proceedings of the 35th CIB-W18 Meeting*, 2002, pp. CIB-W18/35-7-5, Kyoto, Japan.
- [19] Werner H., "Tragfähigkeit von Holz-Verbindungen mit stiftförmigen Verbindungsmitteln unter Berücksichtigung streuender Einflussgrößen", PhD Thesis, 1993, Technical University Karlsruhe, Germany (in German).
- [20] Leijten A.J.M., Köhler J., and Jorissen A., "Review of probability data for timber connections with dowel-type fasteners", *Proceedings of the 37th CIB-W18 Meeting*, 2004, p. CIB-W18/37-7-12, Edinburgh, UK.
- [21] Jorissen A., and Leijten A.J.M., "The yield capacity of dowel type fasteners", *Proceedings of the 38th CIB-W18 Meeting*, 2005, p. CIB-W18/38-7-5, Kyoto, Japan.
- [22] Blaß H.-J., Bienhaus A., and Kramer V., "Effective bending capacity of dowel-type fasteners", *Proceedings of the 33th CIB-W18 Meeting*, 2000, p. CIB-W18/33-7-5, Delft, The Netherlands.
- [23] Kohler J., "A probabilistic framework for the reliability assessment of connections with dowel type fasteners", *Proceedings of the 38th CIB-W18 Meeting*, 2005, p. CIB-W18/38-7-2, Karlsruhe, Germany.
- [24] Blaß H.-J., and Colling F., "Load-carrying capacity of dowelled connections", *Proceedings of the 48th INTER Meeting*, 2015, p. INTER/48-7-3, Šibenik, Croatia.
- [25] JCSS, *Probabilistic Model Code*, Joint Committee of Structural Safety, 2001.
- [26] Jockwer R., *Structural behaviour of glued laminated timber beams with unreinforced and reinforced notches*, PhD Thesis Nr. 21825, 2014, IBK ETH Zurich, Switzerland.
- [27] Jockwer R., Steiger R., Frangi A., and Kohler J., "Impact of material properties on the fracture mechanics design approach for notched beams in Eurocode 5", *Proceedings of the 44th CIB-W18 Meeting*, 2011, p. CIB-W18/44-6-1, Alghero, Italy.
- [28] Stepinac M., Hunger F., Tomasi R., Serrano E., Rajcic V., and Van de Kuilen J.W.G., "Comparison of design rules for glued-in rods and design rule proposal for implementation in European standards", *Proceedings of the 46th CIB-W18 Meeting*, 2013, p. CIB-W18/46-7-10, Vancouver, BC, Canada.
- [29] Tlustochowicz G., Serrano E., and Steiger R., "State-of-the-art review on timber connections with glued-in steel rods", *Materials and Structures*. Vol. 44, 2011, pp. 997–1020.
- [30] Bejtka I., *Verstärkung von Bauteilen aus Holz mit Vollgewindeschrauben*, PhD Thesis, 2005, Technical University Karlsruhe, Germany.

Consideration of Connection Ductility within the Design of Timber Structures

Frank Brühl
Head of WiEHAG Engineering
WiEHAG GmbH
4950 Altheim, Austria

Ulrike Kuhlmann
Full Professor
Institut of Structural Design
Universität Stuttgart
70569 Stuttgart, Germany

Summary

This paper presents a first approach to a closer comprehension on the ductility in timber structures realized connection ductility. In order to introduce the ductility as part of the design of timber structures, it is necessary to set a comprehensive understanding of possibilities and requirements. The aim of this paper is to show a possible classification of different fasteners, and to give a first approach to define the non-linear behavior of dowel type fasteners in a reliable manner. Reliable not only in the view of the ultimate load, but also in the deformability. The inherent material properties of timber allow only a formation of plastic hinges within the joint. Hence a Monte-Carlo simulation was conducted to give a first approach of an over-strength factor for various reliability indexes β , which ensures that the joint is in the state of yielding, before a brittle failure occurs.

1. Introduction

The ability to form plastic hinges within a structure has become more and more of interest within the recent years. The demand on ductile connections is widespread. The plastic behavior of a connection is important in the consideration of robustness (see EN 1991-1-7 [21]), in the seismic design (see EN 1998-1 [26]) and in the application to redistribute internal forces (see 5.1(3) in EN 1995-1-1 [24]).

For structures able to redistribute the internal forces via connections of adequate ductility, elastic-plastic methods may be used for the calculation of the internal forces in the members.

However, no information about the non-linear behavior of fasteners is given in the currently valid standard [24]. Furthermore, no basic principles are given how to carry out a structural design based on the elastic-plastic design method. Hence it is necessary to bridge that gap to enable also a guaranteed application of ductile structural elements within the design of timber structures.

2. Fundamentals to Describe the Ductile Behavior

2.1 General

The currently valid design standards (e.g. [24] and [27]) consider only the linear elastic behavior of fasteners. In order to introduce also the non-linear behavior it is necessary to initiate regulations to classify different types of fasteners in respect to their deformation behavior.

Fig. 1 shows certain parameters to set a uniform declaration. The failure is defined as a rupture of the specimen or as a decrease of the ultimate load to 80 % [29].

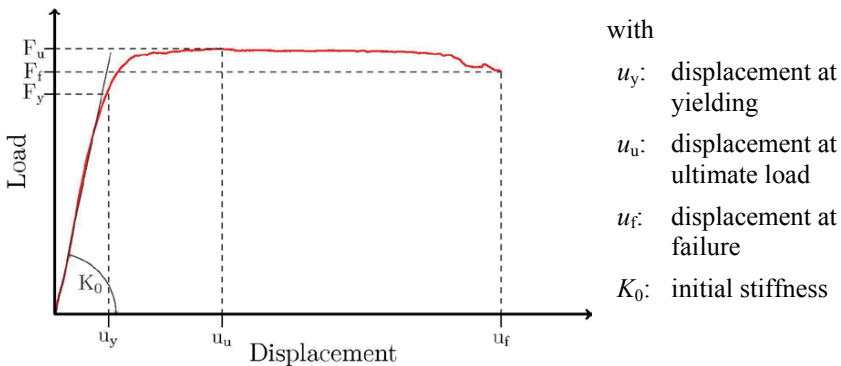


Fig. 1 Definition of certain parameters of a non-linear load-displacement behavior

2.2 Determination of the Yield Point

One of the most important parameters within the consideration of the non-linear behavior is the yield point. It separates the elastic behavior and the plastic behavior clearly. There are several different definitions on the appraisal of the yield point which are summarized by Muñoz et al. [1] and discussed in [13].

It has been shown, that some of the considerations are inappropriate. For example, Karacabeyli and Ceccotti [3] define the yield point at 50 % of the maximum load. Thus, no attention is given to the plasticity and a point of yielding is found for every load displacement behavior. The method given by AF & PA [4] describes the yield point as a setup of the initial stiffness by 5 % of the diameter of the fastener. Therefore also no consideration of the plasticity is given. Yasumura and Kawai [19] introduce an interesting method to describe the yield point. According to them, the yield point is defined by a horizontal copy of an intersection point of the initial stiffness, given as a secant at 10 % and 40 % of the ultimate load, and a secant found between 40 % and 90 % of the ultimate load to the load-displacement behavior. Hence, a further defined stiffness is required in order to find the yield

point. It has been shown, that a yield point is found for a rather brittle behavior as well as for a ductile behavior.

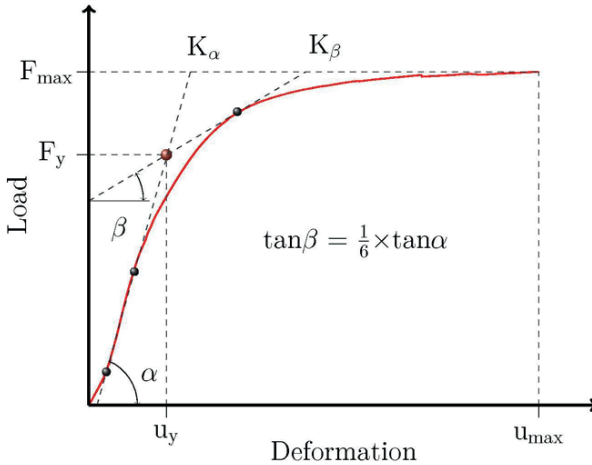


Fig. 2 Definition of the yield point based on EN 12512 [29]

On the other hand, the definition given in [29] and [27] demands at least a second stiffness, which is one sixth of the initial stiffness, given as a secant between 10 % and 40 % of the ultimate load (comp. Fig. 2). This method gives reliable results since the deformation behavior needs to turn to a defined lower stiffness in order to find a yield point.

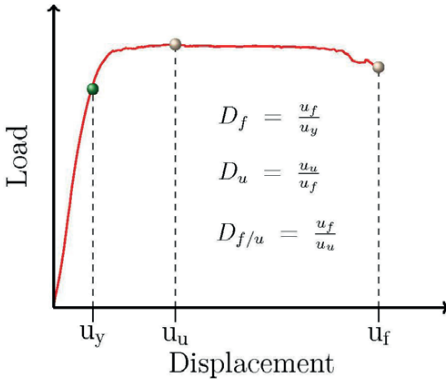
2.3 Evaluation of Certain Connectors

Smith et al [5] give a classification of fasteners with respect to the ductility ratio D_f (comp Fig. 3).

Based on the regulations given in EN 12512 [29] and SIA 265:2012 [27] the ductility ratio is given as the proportion of the displacement at failure (u_f) and the displacement at yielding (u_y) (comp. Eq. (1)).

$$D_f = \frac{u_f}{u_y} \tag{1}$$

Certain connectors have been evaluated based on the described method and characterized by their mean values calculated from a number of experiments within one test setup. The results are either realized directly by the authors, or taken from literature and described in the following.



Classification	Ductility ratio
Brittle	$D_f \leq 2$
Low ductility	$2 < D_f \leq 4$
Moderate ductility	$4 < D_f \leq 6$
High ductility	$D_f > 6$

Fig. 3 Classification of fasteners with respect to the ductility ratio D_f [5]

Split Ring and Shear Plate Connectors

Investigations on connections with split rings (type A1) and shear plate connectors (type C10) were conducted at the Karlsruhe Institute of Technology (KIT) [7]. The aim was to evaluate the load-bearing resistance and the displacement behavior of a row of connectors parallel to the grain. The evaluated connections are related to one unit, consisting of a bolt and two connectors [24, Figure 8.12].

Besides the experiments performed at the KIT, additional experiments were conducted at the Ruhr-Universität Bochum on shear plate connectors (type C2 & C11) [8]. The purpose was to evaluate the possibility of activating the strength of the required bolt on the load-bearing resistance of the connection unit.

Considering the classification of Smith et al. [5] and EN 12512 [29] it is possible to evaluate such kind of connections as low to moderate ductile (see Fig. 3). Since the experiments were stopped at a displacement of 15 mm [30], the conducted results show a lower boundary of the ductile behavior.

Unreinforced Dowel Connections

Doweled connections are most commonly used in timber engineering structures. Within the investigations different types of doweled connections are evaluated. All of the required spacing, end and edge distances comply with EN 1995-1-1 [24]. Experiments on self-drilling steel dowels from SFS intec AG were conducted on the ETH Zurich [6] with the aim to study the load-bearing resistance. All of the evaluated connections were performed with flitch plates and multi-shear fasteners. Special attention was given to the steel grade of the dowel itself, the thickness of the timber element and the end distance.

Among other aspects, Jorissen [9] studied the load-bearing resistance of double shear timber-to-timber connections with the focus on the behavior of a row of

connectors parallel to the grain. The spacing of the dowels parallel to the grain (a_1), the end distance ($a_{3,c}$) and the thickness of the timber elements were varied. Further investigations are conducted at the TU Delft [10]. Besides the variation of the dowel diameter, the steel grade of the dowels, the number of fasteners in a row and the wood species were varied.

The investigations have shown that unreinforced dowel connections feature in general a low or moderate ductility. The arrangement of fasteners in a row parallel to the grain has not only an influence on the load-bearing resistance, but also a significant influence on the realizable ductility. The risk of splitting, and therefore a brittle failure of the timber within the connection, increases with the number of fasteners in a row. Furthermore, the risk of splitting decreases with an increasing slenderness (λ). The slenderness of a connection is defined as the ratio of the timber thickness (t) to the diameter of the doweled type fastener (d) (comp. Eq. (2)).

$$\lambda = \frac{t}{d} \quad (2)$$

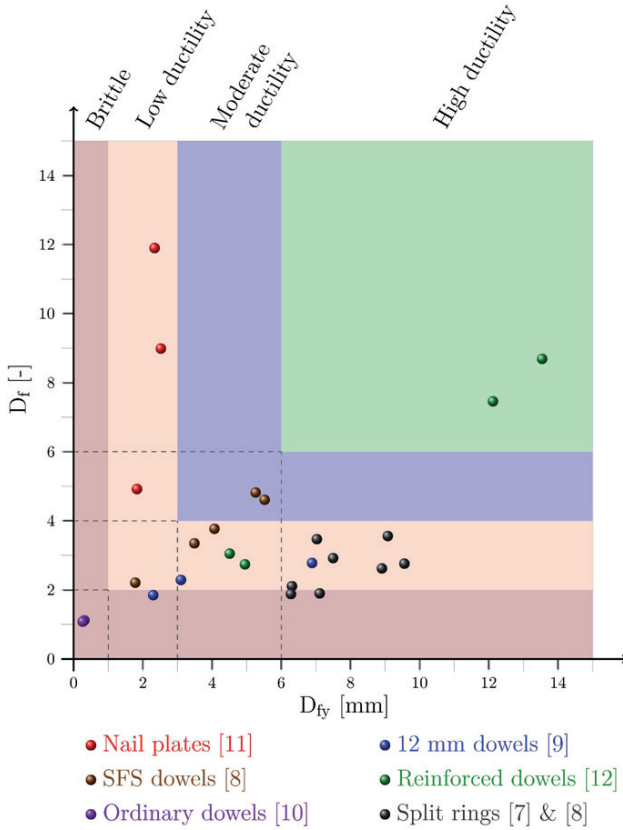
Punched Metal Plate Fasteners

Kevarinmäki [11] conducted experiments on punched metal plate connections. The aim was to study the plastic behavior of such connections with respect to the consequence on a structure. Considering the approach of Smith et al. [5] and EN 12512 [29], this kind of connection behaves in a highly ductile manner (see Fig. 3).

Although such kind of connections exhibit a displacement at failure (u_f) of approximately 3 mm, the high ductility is achieved due to a displacement at yielding (u_y) at an early stage. EN 1994-1-1 [23] requires a deformability of at least 6 mm to ensure, that a sufficient deformability of the connector is given. Besides the relative classification of [5] it is advisable to consider a second absolute constraint (D_{fy}) ($u_f - u_y$) to evaluate the ductile behavior (comp. Fig. 4). Therefore the classification based on Smith et al. [5] is extended by a further requirement, to classify connections in timber structures (comp. Tab. 1).

Tab. 1 Extension of the classification based on Smith et al. [5]

Classification	Relative consideration	Absolute consideration
Brittle	$D_f \leq 2$	$D_{fy} \leq 1 \text{ mm}$
Low ductility	$2 < D_f \leq 4$	$1 \text{ mm} < D_{fy} \leq 3 \text{ mm}$
Moderate ductility	$4 < D_f \leq 6$	$3 \text{ mm} < D_{fy} \leq 6 \text{ mm}$
High ductility	$D_f > 6$	$D_{fy} > 6 \text{ mm}$



$$F_1 = \frac{2}{3} \cdot F_{v,Rk} \quad (3)$$

$$u_1 = \frac{F_1}{K_1} = \frac{\frac{2}{3} \cdot F_{v,Rk}}{\frac{\rho_k^{1.5}}{23} \cdot d} \quad (4)$$

The stiffness of the second part is given by a stiffness of one third of the initial stiffness. Hence the second point is achieved by:

$$u_2 = u_1 + \frac{\Delta F}{\frac{1}{3} \cdot K_1} = u_1 + \frac{F_{v,Rk}}{K_1}$$

$$F_2 = F_{v,Rk} \quad (5)$$

$$= \frac{2}{3} \cdot F_{v,Rk} + \frac{F_{v,Rk}}{K_1} = \frac{5}{3} \cdot F_{v,Rk} \quad (6)$$

The third part is characterized by an infinitesimal stiffness.

Figure 5 shows the comparison of the gained load-displacement behavior based on the simplified model and the mean value of conducted experiments with a diameter of 12 mm [13]. Two different approaches are displayed: on the one hand the simplified behavior based on the initial material properties, and on the other hand with the material properties according to the standard. For calculating the load-bearing resistance, within the standardized determination a steel grade of S355 ($f_{u,k} = 510 \text{ N/mm}^2$) was chosen and for the density a mean value of $\rho_{g,mean} = 420 \text{ kg/m}^3$ [28].

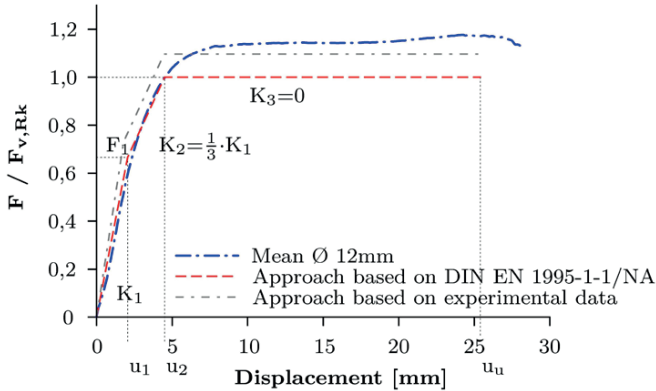


Fig. 5 Comparison of the load-displacement curve of the trilinear approach with the mean value of conducted experiments in tension ($\text{\O} 12 \text{ mm}$) [13]

The load-bearing resistance of the conducted experiments shows a good conformity with the trilinear approach based on the initial properties. Since the input values of the standardized determination are lower than the actual properties, the load-bearing resistance underestimates the experimental value. On the other hand, the initial stiffness given by the mean density $\rho_{g,mean}$ based on [28] confirms the experimental studies.

The ultimate displacement (u_u) is determined as the 2 % quantile based on all conducted experiments with a diameter of 12 mm. Assuming a log-normal distribution, a 2 % quantile value of 25.4 mm is determined, together with a mean of 32.1 mm and a coefficient of variation of 11 %.

4. Introduction of an Over-Strength Factor

4.1 General

The previous chapter has shown that the variation of the material properties has a significant influence on the load-bearing resistance of the dowel type fastener (see Fig. 5).

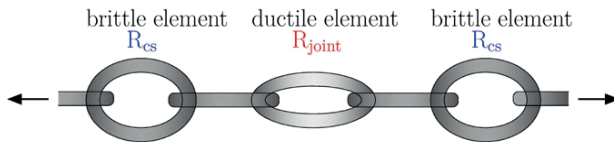


Fig. 6 Series of different structural elements [21]

Regardless of the application of the ductility in timber structures, it is important to ensure that the plasticizing of the ductile element takes place before a brittle element fails.

The capacity design method was developed by Paulay and Priestley [14] with the view on the earthquake safety in reinforced concrete structures. The general idea is displayed in Figure 6. An over-strength factor k_{cs} is introduced (comp. Eq. (7)), which ensures that no brittle failure occurs with a certain probability.

$$\frac{M_{joint}}{M_{CS}} \leq k_{CS} \quad \text{with } k_{CS} < 1.0 \quad (7)$$

The current version of the Swiss timber code [27, 4.6.3.1] already implies an over-strength factor. Hence the brittle element must consist a 20 % higher load-bearing resistance as the ductile element.

4.2 Determination of an Over-Strength Factor

The over-strength factor is determined based on a Monte-Carlo Simulation. The investigations are conducted following the geometrical and material properties of experiments loaded in bending [13]. All of the properties are displayed in Table 2. The reliability index β is determined with a C++ program based on 10^{10} calculations following the equation given in EN 1990 [20]:

$$\beta = \frac{\mu_g}{\sigma_g} \quad (8)$$

where μ_g in Eq. (8) represents the mean value of the limit state function and σ_g the corresponding standard deviation. The limit state function is given by [20]

$$g = R - E \quad (9)$$

where R represents the resistance and E the effect on the system.

Within this consideration, the load-bearing resistance of the dowel type fasteners is set as an effect on the brittle element. The limit state function is therefore turning to:

$$g = W_{\text{net}} \cdot f_m - X_M \cdot \kappa_{\text{cs}} \cdot n \cdot e \cdot F_{\text{E,con}} = M_{\text{CS}} - X_M \cdot \kappa_{\text{cs}} \cdot M_{\text{joint}} \quad (10)$$

with:

W_{net} : net-section modulus	f_m : bending stress
X_M : model uncertainty	κ_{cs} : variable to determine k_{cs}
n : number of dowels	e : inner lever arm

The ultimate characteristic load for flitch plate connections is given by [24, 25]:

$$F_{\text{E,con}} = \min \begin{cases} f_{\text{h},1,\text{k}} \cdot t_1 \cdot d & \text{(f)} \\ f_{\text{h},1,\text{k}} \cdot t_1 \cdot d \left(\sqrt{2 + \frac{4 \cdot M_{\text{y,Rk}}}{f_{\text{h},1,\text{k}} \cdot d \cdot t^2}} - 1 \right) & \text{(g)} \\ \sqrt{2} \cdot \sqrt{M_{\text{y,Rk}} \cdot f_{\text{h},1,\text{k}} \cdot d} & \text{(h)} \end{cases} \quad (11)$$

Table 2 shows the main input variables of the Monte-Carlo simulations. The material properties of the lamellae were recorded during the manufacturing process. Therefore it was possible to gain knowledge about the density and the tension strength of the fabricated lamellae within the different specimens. The bending strength of the beams was determined based on the tension strength of the boards, following the equation given in [28].

The designation ($n \times m$) of the experiments given in Table 2 indicates the number of fasteners in grain direction (n) and perpendicular to the grain (m).

The material properties of timber correlate with a certain dependency on each other [16]. According to [16] a correlation coefficient of 0.6 was introduced to pay

attention to the dependency of the bending strength to the density within the beam element.

Tab. 2 Input variables

experiment	tensile strength f_u [MPa]	diameter	timber density ρ [kg/m ³]	bending strength f_m [MPa]	width [mm]	height [mm]	model uncertainty [-]
dist.	log-normal [15]	normal	normal [16]	log-normal [16]	normal [16]	normal [16]	log-normal [15]
2x4 mean	↑	↑	441.7	33.8	↑	↑	↑
3x3 mean	581	12	449.6	33.9	180	320	1
5x2 mean	↓	↓	440.3	33.4	↓	↓	↓
COV	0.04 [15]	0.001	0.1 [16]	0.15 [16]	0.0025	0.0015	0.1 [15]

4.3 Results of the Monte-Carlo Simulation

Figure 7 (a) shows the reliability index β conducted with the Monte-Carlo simulation for different input values of κ_{cs} . The effect of the load-bearing capacity of the fasteners has a direct influence on the reliability index. The decrease of the reliability index for a dowel arrangement of 5x2 with a larger inner lever arm and a larger number of fasteners is greater compared to a dowel arrangement of 2x4 dowels with a shorter lever arm.

It is hardly possible to design a joint with the same load-bearing capacity compared to the load-carrying capacity of the timber itself. Therefore, a hidden over-strength factor is inevitably integrated within the design of joints. An over-strength factor between 0.5 and 0.75 was considered in the design of the experimental joint. Therefore the normalized over-strength factor k_{cs} can be found by:

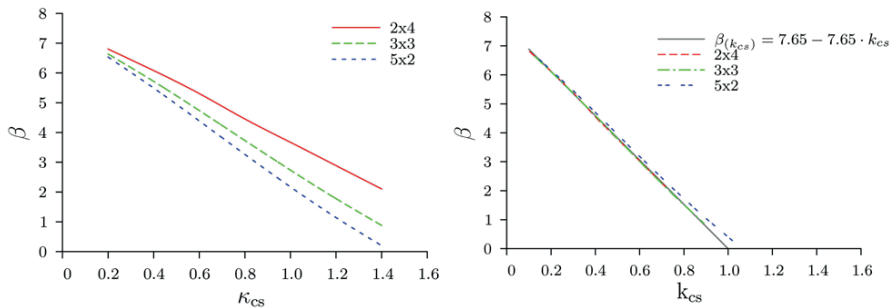
$$k_{cs} = \kappa_{cs} \cdot \frac{M_{joint}}{M_{cs}} \quad (12)$$

The design values M_{joint} and M_{cs} are determined based on the mean input values of the Monte-Carlo simulation (comp. Table 2). Figure 7 (b) shows the normalized over-strength factors k_{cs} of the different reliability indexes β for the considered joints [13]. The obtained reliability line can be expressed by:

$$\beta_{k_{cs}} = 7.65 - 7.65 \cdot \kappa_{cs} \quad (13)$$

The verification of the conducted reliability line shows a reliability index β of zero for a k_{cs} value of one. A reliability index of zero gives a failure probability (P_f) of

0.5. This means that the system is in an indifferent condition. This is a reasonable number since both, the effect and the resistance, are of the same magnitude.



(a) Factor k_{cs} for different reliability indexes β (b) Normalized factor k_{cs} different reliability indexes β

Fig. 7 Over-strength factor depending on the reliability index β [13]

5. Conclusions and Outlook

Based on the classification of various fasteners it has been shown, that it is important to categorize fasteners not only on the relative ductility ratio (D_t), but also on the absolute ductility value D_{fy} . Hence it is ensured that fasteners have a certain ductile displacement and a minimum ductile deformability compared to the elastic deformation.

A simplified model is given to describe the non-linear behavior of connections based on known parameters. Therefore it is possible to describe the non-linear behavior of fasteners within the structural analysis.

Regardless of the application of the ductility it is important to ensure that the ductility is activated before a brittle member fails. A reliability line is determined based on a Monte-Carlo simulation, which gives certain over-strength factors. Depending on the application of the ductility an over-strength factor can be chosen.

Further investigations on the reliability line need to be conducted to consolidate.

Acknowledgement

This research work (16184N) within the International Association for Technical Issues related to Wood (iVTH e.V.), is supported in the program of “Industriellen Gemeinschaftsforschung (IGF)” and financed by the German Federation of Industrial Research Association (AiF) [17]. Furthermore we would like to thank the “Deutsches Institut für Bautechnik (DIBt)” for their support [18].

6. References

- [1] Muñoz W., Mohammad M., Salenikovich A., and Quenneville P., “Need for a harmonized approach for calculations of ductility of timber assemblies”, *Proceedings of the 41th Working Commission CIB-W18 Meeting - Timber Structures*, August 2008, St. Andrews, Canada.
- [2] Brühl F., Kuhlmann U., and Jorissen A., „Consideration of plasticity within the design of timber structures due to connection ductility”, *Structural Engineer*, Vol. 33, 2011, pp. 3007–3017.
- [3] Karacabeyli E., and Ceccotti A., “Nailed wood-frame shear walls for seismic loads: test results and design considerations”. *Structural Engineering World Wide. Proceedings of the Structural Engineering Congress*, July 1998, San Francisco, USA, ISBN 0-08-042845-2, Paper Ref. T207-6.
- [4] AF & PA. Design Specification (NDS) for Wood Construction - Commentary. American Forest & Paper Association, 2005, Washington, DC, USA.
- [5] Smith I., Asiz A., Snow M., and Chui I.H., Possible Canadian/ISO approach to deriving design values from test data. *Proceedings of the 39th Working Commission CIB-W18 Meeting - Timber Structures*, August 2006, Florence, Italy.
- [6] Mischler A.. Untersuchungen zum Tragverhalten des SFS WS-Verbindungssystem, Januar 2001, Eidgenössische Technische Hochschule Zürich, Switzerland (in German).
- [7] Blaß H.-J., Ehlbeck J., Krämer V., and Werner H., Sicherheitsrelevante Untersuchungen zum Trag- und Verformungsverhalten von mehreren in Krafrichtung hintereinanderliegenden Dübeln besonderer Bauart, 1997, Universität Karlsruhe, Versuchsanstalt für Stahl, Holz und Steine, Abteilung Ingenieurholzbau (in German).
- [8] Reyer E., Bretländer Th., and Linzner P., Untersuchungen über die mögliche Übertragung von Scher- und Lochleibungskräften durch die Gewindebereiche von Passbolzen bzw. Gewindestangen, 1993, Lehrstuhl für Baukonstruktionen, Ingenieurholzbau und Bauphysik, Ruhr-Universität Bochum, Germany (in German).
- [9] Jorissen A., Double shear timber connections with dowel type fasteners, Dissertation, 1998, Delft University of Technology.
- [10] Sandhaas C., Mechanical behaviour of timber joints with slotted-in steel plates. Dissertation, 2012, Delft University of Technology.
- [11] Kevarinmaki A., Semi-rigid behaviour of nail plate joints. Dissertation, March 2000, Helsinki University of Technology.

- [12] Bejtka I., Verstärkungen von Bauteilen aus Holz mit Vollgewindeschrauben, 2005, Universität Karlsruhe, Lehrstuhl für Ingenieurholzbau und Baukonstruktionen, Dissertation (in German).
- [13] Brühl F., Ductility in timber structures - possibilities and requirements with regard to dowel type fasteners. Dissertation, Institut für Konstruktion und Entwurf, Universität Stuttgart, (in preparation).
- [14] Paulay T., and Priestley M.J.N., *Seismic design of reinforced concrete and masonry buildings*. John Wiley & Sons, Inc., 1992.
- [15] Köhler J., Reliability of timber structures. Dissertation, April 2006, Swiss Federal Institute of Technology, Zürich, Switzerland.
- [16] Joint Committee on Structural Safety (JCSS). Probabilistic model code, August 2006.
- [17] Kuhlmann U., and Brühl F., Vorteilhafte Bemessung von Holztragwerken durch duktile, plastische Anschlüsse, Mai 2012, Research work (16184N) within the international association for technical issues related to wood (iVTH e.v.), was supported in the program of “Industrielle Gemeinschaftsforschung (IGF)“ and financed by the German Federation of Industrial Research Association (AiF), Institute of Structural Design (in German).
- [18] Kuhlmann U., and Brühl F., Robuste Holztragwerke durch duktile Anschlüsse mit stiftförmigen Verbindungsmitteln, 2011, Research work supported and financed by Deutschen Instituts für Bautechnik DIBt, Institute of Structural Design (in German).
- [19] Yasumura M., and Kawai N., “Estimating seismic performance of wood-framed structures” *Proceedings of I.W.E.C. Switzerland, Vol. 2*, 1998, pp. 564–571.

Standards

- [20] EN 1990: Eurocode 0: Basis of structural design, European Committee for Standardization (CEN), 2002, Brussels, Belgium.
- [21] EN 1991-1-7: Eurocode 7: Actions on structures; Part 1-7: General actions - Accidental actions, European Committee for Standardization (CEN), 2010, Brussels, Belgium.
- [22] EN 1993-1-8: Eurocode 3: Design of steel structures- Part 1-8: Design of joints, European Committee for Standardization (CEN), 2005, Brussels, Belgium.
- [23] EN 1994-1-1: Eurocode 4: Design of composite steel and concrete structures - Part1-1: General rules and rules for buildings, European Committee for Standardization (CEN), 2010, Brussels, Belgium.

- [24] EN 1995-1-1: Eurocode 5: Design of timber structures - Part 1-1: General - Common rules and rules for buildings, European Committee for Standardization (CEN), 2004, Brussels, Belgium.
- [25] DIN EN 1995-1-1/NA: National Annex - Design of timber structures - Part 1-1: General rules and rules for buildings, DIN-Deutsches Institut für Normung e.V., 2010.
- [26] EN 1998-1: Eurocode 8: Design of structures for earthquake resistance – Part 1: General rules, seismic actions and rules for buildings, European Committee for Standardization (CEN), 2010, Brussels, Belgium.
- [27] SIA 265: Holzbau. Schweizerischer Ingenieur- und Architektenverein, März 2003, Zürich, Schweiz (in German).
- [28] DIN EN 14080: Holzbauwerke - Brettschichtholz und Balkenschichtholz - Anforderungen; Deutsche Fassung. DIN Deutsches Institut für Normung e.V., September 2013 (in Deutsch).
- [29] EN 12512: Timber structures - Test methods - Cyclic testing of joints made with mechanical fasteners, European Committee for Standardization (CEN), Brussels, Belgium.
- [30] EN 26891. Timber structures - Joints made with mechanical fasteners- General principles for the determination of strength and deformation characteristics. European Committee for Standardization (CEN), Brussels, Belgium.

Impact of Standards and EADs on the Determination of Single Fastener Properties

**Jørgen Munch-Andersen
Senior Advisor
Danish Timber Information
Lyngby, Denmark**

Summary

Strength parameters of fasteners are one of the essential information needed for designing connections in timber structures. It is important both that they are correct and that they are easy to find and use for the structural designer. Introduction of strength classes is one mean.

The methods to determine the parameters are not sufficiently accurate to ensure that the results can be repeated. Part of the problem is that the selected timber specimen has a larger influence on the results than the differences between two brands of fasteners. It is discussed how the use of reference fasteners can improve the accuracy of tests.

The use of reference fasteners can also be used to obtain strength parameters for other wood materials than softwood structural timber. Presently it is quite difficult to find consolidated information that enables design of connections in other materials than structural timber.

Rules for declaration of dimensions and tolerances are also discussed as they are unclear.

1. Introduction

It is essential for the competitiveness of timber constructions compared to other materials that the structural designers feel confident when they are designing the connections. This subject is suffering from Eurocode 5 [1] not really covering 'modern' fasteners like self-tapping screws. Also, the requirements to edge distances and spacings appear outdated. Therefore, various supplements in national annexes, ETA's and unofficial design guides have emerged, but it is not easy neither to find the information nor fulfil the formal requirements in building regulations. Improvements are necessary for the next Eurocode 5, where ensuring 'Ease of use' is a major task.

It is therefore extremely important to improve the situation, which, among other things, requires that manufacturers of wood based materials and fasteners work together, considering their main competitors to be steel and concrete, not the colleague manufacturing a similar product.

Another step is to clarify the design procedure. The principle for designing a connection in the future Eurocode 5 is assumed to involve the following steps:

1. Determine the load distribution among the fasteners
2. Check if the single fastener has sufficient load-carrying capacity
3. Check if the timber in the connection has sufficient load-carrying capacity
4. Adjust for group effects not comprised by 1 and 3
5. Check that the fasteners can be installed without risk of splitting

In the present Eurocode 5 [1] most of step 3 and 4 is done by using rules based on the fastener diameter, even it is obvious that the load per fastener must have an influence. Presently, only the block shear failure modes in Annex A for steel to timber connections takes the load into account.

This paper deals with fastener properties that are used to determine the withdrawal and lateral load carrying capacity of a single fastener applied for step 2, i.e. assuming the capacities are not influenced by edge and end distances, spacing or other circumstances that might reduce the load carrying capacity. The other steps are dealt with in [2, 3, 4, 5] in these proceedings.

Three main problems are addressed:

1. The specified test methods do not ensure that similar fasteners obtain similar strength parameters. A second test using fasteners from the very same batch as the previous test might give a quite different result. This is to a large extent due to the influence of the timber used, but probably also the procedures at the test institute or of the operator.
2. The properties given in the CE-marking of the fastener only provides properties for structural timber. They can also be used for glulam, but for all other wood materials, it is quite diverse which parameters that are available to the structural designer.
3. How dimensions are declared and tolerances handled is also important to ensure that correct load carrying capacities are estimated using Eurocode 5 [1]. For e.g. the outer thread diameter of a screw there is a nominal value, a target value and a minimum value. It is not clearly defined which diameter the declared strength parameter should refer to.

2. Declaration of Strength Parameters

The harmonized standard for fasteners EN 14592 [6] specifies, among other things, how the major design parameters, yield moment, the withdrawal strength and head pull-through strength, for softwood shall be determined and declared in the CE-marking. Embedment strength is, as an exception, given in Eurocode 5 [1] and is not among the properties that can be declared. Together, the necessary strength parameters for softwood are available to the designer.

For smooth nails and lag screws, Eurocode 5 [1] gives equations to calculate all parameters. These equations can be used by the manufacturer as an alternative to

testing. The result must be given in the CE-marking, so the equations are formally of no use for the designer.

For other wood based materials, it is quite sparse which parameters are available. Some embedment strengths are given in Eurocode 5 [1]. For e.g. wood based panels covered by the harmonized standard EN 13986 [7], an embedment strength can be declared in the CE-marking, but if not determined from Eurocode 5 [1] by calculation the value applies only to the fastener type and diameter used for the testing. The value is therefore not adequate for use in general design.

Further, some national annexes to Eurocode 5 [1] and other national guidelines comprise some values for head pull-through and withdrawal strength for some types of fasteners in some wood products. They are probably on the safe side, but not well documented.

EN 320 [8] gives a method to determine the withdrawal strength of screws in particleboards and fibreboards using a screw with a specified geometry. The standard is probably not widely used because it not referred to in EN 13986 [7] (or in 14592 [6]), so the result cannot be declared in the CE-marking. The standard applies only to screws, probably because the strength might depend on more than the geometry for other types of fasteners.

A similar standard for other wood products and structural timber does not exist, but the results presented in section 4.2 of this paper indicate that withdrawal strength of screws depends only on geometry.

2.1 ETA and EAD

For products not or not fully covered by a harmonized standard, it is possible to do the CE-marking based on an ETA (European Technical Assessment) for a specific product, which in turn is based on an EAD (European Assessment Document), which replaces the harmonized standard. An EAD can be proposed by any manufacturer. It is approved within EOTA, without any public hearing. It only becomes public when published by the European Commission in the Official Journal of the European Union (OJEU).

There are a number of EAD's for fasteners [9, 10, 11]. To some extent they add information compared to what can be declared based on the harmonized standard, mending that the needed properties are not fully covered.

There is no problem in adding information compared to the harmonized standard, but in several cases the EAD change the requirements in the harmonized standard or in Eurocode 5, even these requirements were operative for the products not fully covered.

An example is the EAD on screws for use in timber constructions [9], which allows about twice as large tolerances on the dimensions of the screws as the harmonized standard does. This causes the coefficient of variation of the load carrying capacity to increase, which would require a (slightly) larger partial factor to obtain the same safety level. Tolerances are further discussed in section 6. This EAD also reduces

the minimum penetration depth of the thread (including the point length) from $6d$ in Eurocode 5 [1] to $4d$, and specifies a test method, that might allow for smaller spacing of the fasteners than Eurocode 5. It also gives some strength parameters for wood based panels which can be given in the ETA without testing.

The changes and possibilities might be sensible, but they should be introduced in the harmonized standard or Eurocode 5 [1] rather than in an EAD as they hardly are related to the specific products. Further, it is quite complicated for the user to take advantage of these possibilities as they must be found in the ETA-document for the specific products.

2.2 Strength Classes

A major simplification for the users (structural designers and contractors), will be if fasteners are classified into strength classes, which define all relevant strength parameters. This will be similar to timber strength classes (like C24 or GL28c). Then the designer can specify dimensions and a strength class, and it is simple for the contractor to pick a correct fastener product. Special products could still be declared individually.

There can be a number of classes for each fastener type. For screws, they can e.g. take different ratios between core diameter and thread diameter into account. For nails, different profiles like twisted or ringed can give rise to different classes.

The manufactures can optimize a product to meet the requirements of a class, e.g. by changing the target diameter, see section 6.1. The scheme can easily be extended to classes for e.g. LVL or plywood, provided of course that the strength parameters are available.

3. Variability of Declared Value

The accuracy of the load-carrying capacities obtained from Eurocode 5 [1] depends on the accuracy of the declared strength parameters. Despite of specifications in test standards on how to determine the strength parameters, very significant differences between the declared values for very similar products might occur.

In general, a declared value is based on 20 tests. Timber specimens used shall fulfil the requirements to density in EN ISO 8970 [12], which states: 'The sampling method is based on the principle that all selected pieces have a density comparable with that of the wood to which the connection test results shall be applied'. The standard gives a maximum range of the densities of the used specimens, but there is no minimum range, so it could be interpreted such that all specimens can be taken from the same board [13, 14]. The coefficient of variation (CoV) of the density for a class of structural timber like C24 is assigned to be 10 %, which is in fact quite difficult to create in a sample (CoV = 10 % can be deduced from the ratio between the characteristic density and the mean density given in EN 338 [15]).

20 tests to establish a characteristic strength parameter is very little. Roughly, the characteristic value is the mean minus twice the standard deviation. Assuming the

true mean is 10 MPa and the true CoV of the strength is 20 %, the true characteristic value is $10 - 2 \cdot 40 \% \cdot 10 = 6$ MPa.

The influence of the number of tests is studied by numerical simulations. When simulating 20 tests many times, 95 % of the cases will give mean values within 10 % of the true mean value, but the characteristic values will only be within 25 % of the true value because the variability of the estimated CoV is much larger than of the mean value. Using 60 tests will reduce these uncertainties to 5 % and 13 % - and for 300 tests to 2 % and 6 %. These numbers show that it is possible to establish a fair estimate for the mean, but the CoV continues to be quite badly estimated, so there is a huge gain in accuracy if the CoV can be assumed known. On top of these statistical uncertainties adds the real differences caused by using a new sample of timber for each test or fasteners from a new batch. This is discussed in section 4.

3.1 Example – Withdrawal Strength of Ring Shank Nail

Ring shank nails from the same production batch have been used in several test series using structural timber. In some series were included both other fasteners and LVL. The observed results for structural timber, corrected to density 420 kg/m³ assuming a linear relation between density and strength, are summarized in Table 1.

Tab. 1 Withdrawal strengths in structural timber for similar nails obtained from different test series. Strengths are adjusted to density 420 kg/m³ assuming a linear relation to the density. The point length is ignored.

	No of tests	Density		Withdrawal strength			
		Mean, kg/m ³	CoV	Same batch		Other batch	
				Mean, MPa	CoV	Mean, MPa	CoV
Series 1	20	397	7.2 %			15.5*	14.7 %
Series 2	20	408	7.5 %	13.8	9.3 %	13.8*	15.6 %
Series 4	30	419	7.0 %	14.1	16.9 %	13.7 [#]	13.6 %
Series 5	20	422	7.3 %	15.7	16.0 %	15.9	17.5 %
Series 6	10	404	5.5 %	–	–	13.7 [#]	16.5 %

* Same batch used in Series 1 and 2. [#] Same batch used in Series 4 and 6

Results from tests with nails of same type from other production batches and in Series 1 also with slightly different types of nails, are also shown in Table 1. The results from Series 2 are further discussed in [16] and from Series 6 in section 4.2.

It is seen that:

1. The mean densities and their CoV's are quite constant between the series.
2. The mean strengths and their CoV's are quite different.

The table represents 170 tests and using these and 70 further test results for similar nails from the same manufacturer gives an average withdrawal strength of 14.3 MPa with a CoV of 16.0 %. If these are taken as the 'true' values, as discussed for the simulation above, the CoV's are no more different than could be expected based on 10-30 tests. However, the mean values should be less different if statistical effects should be the only reason for the difference – especially considering the CoV is 16 % and not 20 % as used in the simulation. Therefore, there is an effect of the series not accounted for by the density of the timber.

3.2 Example – Declared Values for Nails

For nails the declared characteristic strength parameters for withdrawal, pull-through and yield moment are collected from DoP's from various suppliers. Six nail types (1-6) as described in Table 2 from each of six suppliers (A-F) are considered. They are all gun-nails and the heads are either D-shaped or round-eccentric.

Figure 1 shows the results for the withdrawal strength. The values are normalized by the mean value of all declared strengths in order to focus on the principles rather than specific brands (which are only identified by the colour). The parameters are determined by four different test institutes. The values are very different for quite similar products. Some values are very high compared to the bulk and must be regarded to be wrong. If these values are used in actual design, they will compromise safety of the structure.

Tab. 2 Characteristics of the six nail types investigated. (EP = electroplated, zinc thickness about 12 μm, HDG = hot dip galvanized, zinc thickness about 55 μm).

Nail type	1	2	3	4	5	6
$d \times l$	2.8 x 51	2.8 x 63	2.8 x 70	3.1 x 75	3.1 x 90	3.1 x 90
Surface	EP ringed	EP ringed	Bright ringed	EP ringed	HDG ringed	EP smooth

Some difference might be due to the shape of the rings and their sharpness that might influence the real strength. Nail type 6 is smooth, so the values are naturally lower. For these, some suppliers use the - presumably conservative - Eurocode formula. Others has measured the values, one of which is very high and another is below the Eurocode value.

Similar figures for head pull through and yield moment is given in [16]. They are similarly scattered, which is especially surprising for the yield moment, where there is no influence of the timber.

In the examples in section 4.2 and 4.3 it is shown that there is very little difference between different brands of ring shank nails when the test conditions are equal.

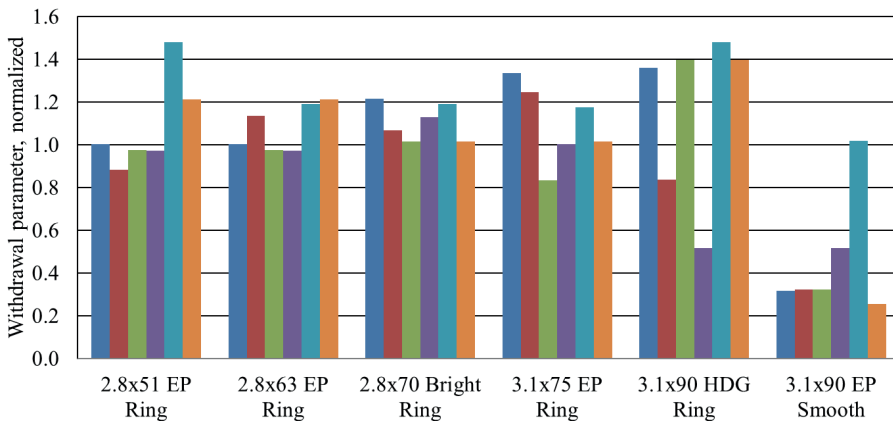


Fig. 1 Withdrawal parameters normalized by the mean value of the parameter.

3.3 Discussion – Declared Values

The procedures for performing tests to determine strength parameters are clearly not sufficiently accurate to ensure reasonably consistent results. This ought to be dealt with in the CEN-committees responsible for the standards. In order to ensure the safety until the standards has been improved, it could be considered to give upper limits to the strength parameters in the National Annexes to Eurocode 5. This is allowed when safety is compromised.

One problem is the statistical uncertainties when using only 20 tests to establish the characteristic value of a strength parameter, where a large contribution to the uncertainty is the scatter of the coefficient of variation (CoV). Using fixed values for the CoV will be much more reasonable.

Another problem is how to select the timber specimens used for withdrawal and head pull-through tests. The selection is specified in EN ISO 8970 [12], but it only deals with the density and the moisture content. There are no methods to take other features that matter for the strength of fasteners in the timber, like the growth ring width, into account as the influence is not known very well. In the next section, it is

discussed the use of reference fasteners to eliminate the problem of selection and thereby ensure consistent strength parameters.

4. Reference Fasteners, Structural Timber

The large difference between test results – and thereby the declared strength parameters – for fasteners that are known to have identical or almost identical properties, is unacceptable. The uncertainty related to the properties of the selected timber specimens and inaccuracy of the test methods can be reduced very significantly if the testing to determine strength parameters is carried out using a pair of fasteners in each specimen. The pair shall consist of the fastener in question and a reference fastener, where the strength of the reference fastener is determined by more extensive testing than usual.

The test results then enable to determine a ratio between the strength of the fastener in question and the reference fastener. This ratio will be much less dependent on the timber sample and the test method than the present method, so it is much easier to reproduce the result.

The reference fastener ought to be fairly similar to the fastener for which the strength parameter should be determined. A ring shank nail should therefore be compared with a reference ring shank nail of about the same diameter, and so on.

The coefficient of variation (CoV) should be established from the extensive testing of the reference fastener and used as a known value for all similar fasteners, because it, as mentioned in section 3, is very reasonable to assume that they are similar. Since the CoV is the same, the characteristic value of the fastener in question can then be determined directly by multiplying the ratio between the mean values to the characteristic value of the reference fastener.

The ratio can be determined either as the ratio between the two mean values or the mean of the ratios for each specimen. The latter method was expected to be the most accurate because the influence of the individual specimen is then reduced, but the random effects appear to overshadow this, so the first and simpler method will give the same result.

The repeatability is studied in the following two examples, which shows that the uncertainties become very small when two (or more) fasteners of similar type are tested in the same specimens.

Introduction of reference fasteners requires that reference fasteners are chosen and tested extensively. The main problem is presumably that a significant stock must be kept and samples distributed to the test labs on request. The gain will be that strength parameters can be determined with high confidence based on relatively few tests because it is only the mean value that is of interest.

A statistical problem arises when engineering sense tells that two fasteners have the same strength, since there is no conventional method to show that two distributions are similar, i.e. have the same mean value. The methods can only show that they

are not similar. This problem could be solved pragmatically by allowing a margin depending on the number of tests. Inspiration can be found in EN 15228 [17], which gives a method to check if impregnation of structural timber influences the strength properties. It in turn refers to ISO 12491 [18] and allows with 75 % confidence level a 10 % difference for a sample size of 50 specimens. This seems quite 'generous'.

4.1 Example – Comparing two Batches

In tests with structural timber and LVL three nails of the same type are used in each specimen. Two are from the same batch and the third from another batch, but with the same specifications. The results are presented in detail in [16] and the results for structural timber represents Series 2 in Table 1.

For both timber and LVL, the mean values become very similar but the CoV's somewhat different, as would be expected based on the simulations described above. However, when the three ratios between the nails in each specimen were determined (second method above) the ratio for the two nails from the same batch are closer to unity than the two others. This could indicate an interaction between the timber and the nail, even the difference between the nails are minor, but this effect is not present in the next example. This advocates for using the first and simpler method when determining the ratio between a fastener and the reference fastener.

4.2 Example – Ring Shank Nails and Screws

In each of five (long) specimens of timber, 14 fasteners are inserted in each specimen. The fasteners, see Figure 2, are two types of ring shank nails (R1, R2) and four types of screws (S1-S4). Three types of smooth nails (-) are not dealt with here. The fasteners were positioned as shown in Figure 3. R1 is used in four positions (a-d), R2 and S1 (a, b) in two positions.

The measured withdrawal strengths are given in Table 3. Results for nail R2 is Series 6 in Table 1, except the strengths in Table 1 are adjusted for density. The results are taken from [19].

It is seen that the mean values for each position are very similar for all nails and all screws, respectively, especially taking into account that there are only five observations at each position. The mean values for each board are very different (and not strongly correlated with the density), showing the difficulty of choosing representative timber specimens. The coefficients of variation for similar conditions are quite different, for nails varying between 9 % and 28 %, even the nails giving these extreme values are identical. This again confirms the findings from the numerical simulation discussed above.

The results show that repeating a test with the same fastener in the same timber sample gives very consistent mean values for each fastener. This is essential for the reference fastener system.

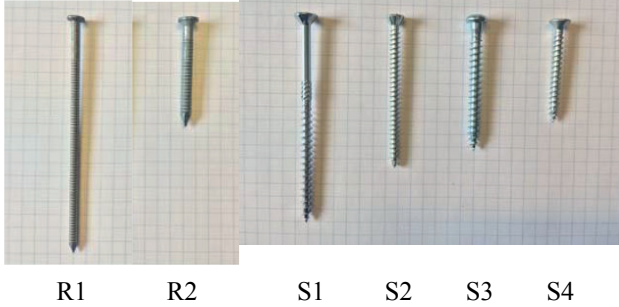


Fig. 2. The fasteners used. The longest nail is 90 mm.

R1a	R2a	R2b	–	–	–	R1b	R1c	S1a	S1b	S2	S3	S4	R1d
-----	-----	-----	---	---	---	-----	-----	-----	-----	----	----	----	-----

Fig. 3 Position of the fasteners along the length of the timber specimen. The blank positions contained smooth nails.

They also show that the withdrawal capacity of the two types of nails and the four types of screws do not deviate more than two results for the same nail. The largest difference is between the identical nails R1b and R1d.

For nails, the similar values could be because they are from the same manufacturer, but as discussed in section 4.3 there seems to be little difference between different brands of ring shank nails.

The four types of screws are quite different and from two different manufactures, so the results seem to indicate that 'screws are screws' such that there is no point in testing them individually. It is remarkably that the withdrawal strengths of the different screws along each board are almost identical – the CoV is only about 5 %, where it for nails on average is 13 %. This supports that 'screws are screws', it is only the properties of the timber that causes differences in the withdrawal strength.

However, testing screws against a reference screw does no harm – it will just reveal the withdrawal capacity is the same. And if a certain product really is better, it will be revealed with much higher confidence than using the present system.

The ratio in Table 3 is taken between the mean values for nails and screws for each board. It is in the range 0.54 to 0.74 with a mean value of 0.65.

Tab. 3 Measured withdrawal strengths (MPa) for ring shank nails and screws when the point length is ignored. The numbers in bold are the common values for all the results. The Ratio is between nails and screws, using the mean value for each board. The density (kg/m³) is at time of test, conditioned at 65 % RH.

Board	Ring shank nails						Board mean	CoV
	R1a	R1b	R1c	R1d	R2a	R2b		
1	10.4	15.9	13.0	15.0	11.3	12.0	12.9	0.17
2	16.9	14.9	14.9	15.1	16.0	11.7	14.9	0.12
3	12.8	13.0	12.6	15.6	14.5	13.0	13.6	0.09
4	11.2	6.8	11.7	13.2	8.7	12.6	10.7	0.23
5	16.3	15.6	17.4	16.7	16.6	15.0	16.3	0.05
<i>Mean</i>	13.5	13.2	13.9	15.1	13.4	12.9	13.7	0.13
<i>CoV</i>	0.22	0.28	0.16	0.09	0.25	0.10	0.18	

Board	Screws					Board mean	CoV	Ratio Nail/ Screw	Density
	S1a	S1b	S2	S3	S4				
1	22.6	25.3	25.2	22.7	23.8	23.9	0.05	0.54	406
2	21.1	21.6	20.3	21.8	21.1	21.2	0.03	0.70	410
3	18.4	17.9	17.9	19.0	18.7	18.4	0.03	0.74	379
4	18.1	16.8	17.3	19.6	18.3	18.0	0.06	0.59	387
5	22.1	21.9	23.1	24.8	25.4	23.4	0.07	0.69	437
<i>Mean</i>	20.5	20.7	20.7	21.6	21.5	21.0	0.05	0.65	404
<i>CoV</i>	0.10	0.17	0.16	0.11	0.15	0.13			0.055

4.2.1 Moisture Content

The same testes are carried out with timber conditioned at 85 % RH instead of 65 %. The specimens are from the same five boards, which are split lengthwise, and then conditioned at 65 % and 85 % respectively.

Higher moisture content seems to affect all nails and all screws similarly and all the CoV's increases somewhat. Even the specimens were paired, there is little correlation between the results from the same board at different moisture content.

The major finding is that the mean value for nails is reduced by 2 % (i.e. unchanged) whereas it decreases by 12 % for screws. The ratios between nails and screws becomes more scattered and is in the range 0.65 to 0.95 with the mean value 0.73.

4.2.2 LVL

The same tests are carried out with LVL. For nails, the CoV's are reduced, as would be expected. The slight tendency seen in Table 3 for nail R2 to be slightly weaker than R1 is enhanced, but still within one standard deviation.

For screws, the CoV's stays about 5 % along each board and the overall CoV is reduced from 13 % in Table 3 to only 6 %. There are even smaller differences between the mean values for the screws than in timber.

Due to the low CoV's it could be tempting to use LVL to establish the ratio between the fastener in question. This requires of course that it can be generally shown that the factor is the same in structural timber and LVL.

The ratio between nails and screws increases and is in the range of 0.73 to 0.87 with the mean value 0.79. This means that nails are relatively more efficient in LVL, but the CoV is still larger than for screws. This means that nails cannot be tested against a reference screw, so it is, as anticipated, necessary with a selection of reference fasteners.

4.3 Example – 7 Ring Shank Nails

In another study [20] seven different 3.1x90 mm ring shank nails, similar to type R1 in Figure 2, were tested using each nail 3 times in each of 10 boards (lamellas in a gluelam beam). The results from board no 10, which happened to have a very high mean density (491 kg/m³), is not included in the analysis because they were scattered and incomplete. A twisted nail included in the testing is not included here. The mean density at 12 % MC of the other boards are 420 kg/m³ with a CoV of 7.1 %, so very similar to those test summarized in Table 1.

The results confirms the findings based on Table 3, namely that identical fastenres placed next to each other in a board obtain very similar strengths, that the difference between the strengths between brands is minor and that the difference between boards is significant. The common mean value is 14.6 MPa with a CoV of 28 %. The larger CoV than for nails in Table 3 is due to a larger dependency on the board. Between the 27 nails in each board the CoV is between 7 and 20 %. In Table 3 is between 5 and 23 %, but that is for only 6 nails in each board. It is to be expected that the span decreases with more tests, as discussed in section 3.

The results for each nail normalized with the mean value for all nails in that board are shown in Figure 4. The nails are seen to be very similar, especially when considering that nail no. 8 and no. 9 are identical nails sold under different names. A closer examination revealed that no. 9 by chance was made with a fresh tool so the rings were sharper than normal, so the difference represents a natural variation.

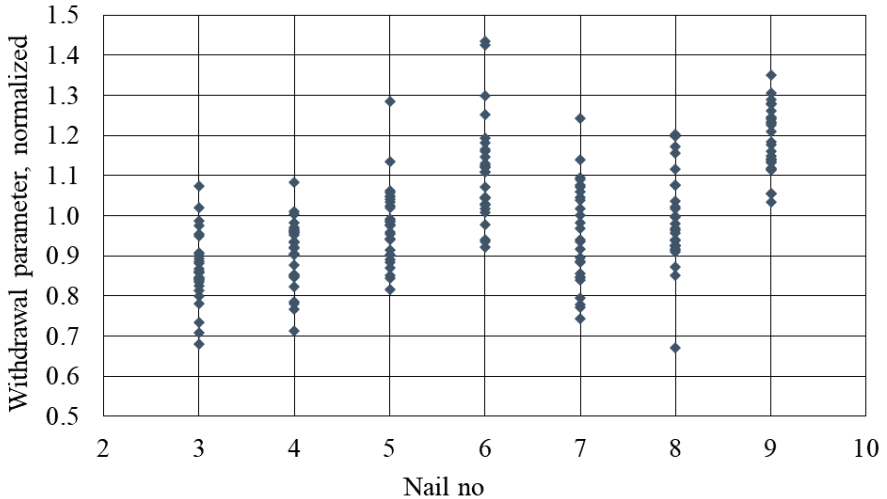


Fig. 4 Measured withdrawal strengths (normalized with board mean) for 7 different 3.1×90 mm ring shank nails.

5. Reference Fasteners, other Wood Materials

As mentioned the harmonized standard EN 14592 [6] only applies to structural timber and there is no consolidated method to declare strength parameters for fasteners used in e.g. plywood and LVL. In principle, it is required that each combination of fastener and wood material should be tested. The needed parameters are the embedment strength, the head pull-through strength and sometimes the withdrawal strength.

By means of reference fasteners it is possible to establish a system that enables the designer to derive the relevant strength parameters for any fastener in any engineered wood material from fairly simple tests carried out independently by the manufactures of fasteners and wood materials, respectively.

5.1 Wood Material Manufacturer

The manufacturers of engineered wood materials can characterize their product's properties with respect to fasteners by carrying out tests with the relevant reference fasteners in representative specimens of their product(s). The outcome should be a characteristic strength parameter for each reference fastener, determined as given in the present standards. Also, the coefficient of variation must be established for each product, unless it appears that it is similar for e.g. all types of LVL. Then it can be defined in a standard.

The specimens used could cover a product family, for which the properties are nearly the same. All the relevant reference fasteners should be tested in each

specimen. This will simplify the tests and might strengthen the evaluation, because the effect of the individual properties of each specimen will be clearer.

5.2 Fastener Manufacturer

The manufactures of fasteners can characterize their product's properties with respect to a type of engineered wood material by testing their fastener paired with the relevant reference fastener in a 'typical' sample of the relevant wood material. Since the outcome is a factor based on ratios it is not necessary to have reference materials, but it is advisable that the wood specimens used for the testing originates from different manufactures.

Perhaps it is not necessary to test the fasteners in all types of wood based panels. This will require that the panel types can be 'ranked' for each reference fastener so interpolation can be used. It could be that a value for particle boards could be determined based on the values for plywood and MDF.

5.3 The Designer

The structural engineer, who needs the strength parameters of a particular fastener in a specific wood material in order to design a connection, can obtain them by multiplying the factor relating the fastener to the reference fastener by the strength parameter for the reference fastener obtained for the wood material.

5.4 Establishing of Reference Fastener System

The procedures for using reference fasteners as an alternative to the present system could perhaps be given in an EAD or a CEN/TS (technical specification). The document should specify the reference fasteners, the selection of wood specimens and the statistical methods necessary to ensure that the adjusted strength parameters are characteristic values in the Eurocode sense.

The system is voluntary and will only be of value if some of the major manufacturers of wood products and fasteners joins in form a start.

The document could also give equations for calculation of safe strength parameters where such equations are available and well documented.

This should be seen as an intermediate step until the method can be included in Eurocode 5 and the harmonized standards for both fasteners and wood based products.

6. Dimensions and Tolerances

The characteristics of a fastener needed to determine the axial and lateral load carrying capacity from the equations given in Eurocode 5 [1] can be subdivided into

1. Geometrical dimensions
2. Strength parameters

It is important that the declaration of dimensions and strength parameters fit together, otherwise the load carrying capacity calculated from Eurocode 5 [1] becomes incorrect.

6.1 Nominal and Target Dimension

Each dimension will in principle have both a *target* value and a *nominal* value. The fasteners are produced aiming at the *target* values, whereas the nominal value is the value given in the product declaration and therefore the one the designer will use in the Eurocode equations. It is preferable if the target and the nominal values are identical, but the nominal value may for convenience differ from the target value, providing that the strength parameters given in the CE-marking are adjusted accordingly, as discussed in the following. (Different target and nominal values could e.g. be relevant for a connector screw with diameter 4.8 mm, which is given the nominal diameter 5 mm because it is meant for brackets with 5 mm holes).

The embedment strength cannot be adjusted because it is not a declared value, so the real effective diameter need to be declared ($d_{\text{eff}} = 1.1 d_{\text{core}}$ according to [1]).

6.2 Tolerances

The target values will necessarily have tolerances. EN 14592 [6] defines allowable tolerances as a range around the target value. It is part of the presumption for the equations in Eurocode 5 that these tolerances are met, so when an EAD like [9] as mentioned in section 2.1 allows larger tolerances the presumptions are not met. It would not mean a great deal if it was real tolerances and the mean value over time equals the target value, since it is then just a small increase of the coefficient of variation. But generous tolerances tend to implicate that the mean value is approaching the lower boundary and then the load carrying capacity is systematically reduced.

In the future two types of tolerances should be considered. In some cases, the production tolerance is most appropriately defined by a range around a mean value, where the actual mean value - over a period of time - should not differ systematically from the target value. This is probably the most relevant criteria for diameters. In other cases, a one-sided tolerance is better because it is the maximum or minimum value that is crucial. This might apply to the length, the threaded length and the head area.

6.3 Determining Strength Parameters

The strength parameters should be determined such that the design load carrying capacity of a fastener, when using equations in Eurocode 5 [1], can be calculated using nominal values for the geometric dimensions. This involves the actual dimension of the tested fastener, the target dimension and the nominal dimension.

As an example, the withdrawal capacity of a nail is considered. The test result for the load carrying capacity is $F_{x,\text{obs}}$, the actual diameter d_{obs} and $t_{\text{pen,obs}}$ is the actual penetration length. The real withdrawal strength is then $f_{\text{ax,obs}} = F_{\text{ax,obs}} / (d_{\text{obs}} t_{\text{pen,obs}})$.

This is also the value that should be determined for a reference fastener or will be obtained from an equation that can substitute tests.

In case the target and nominal diameters, d_{tar} and d_{nom} , are different the declared strength must be adjusted such that when it is multiplied by the nominal diameter, the result is the real capacity if the diameter equals the target value. This is obtained by declaring $f_{ax,dec} = f_{ax,obs} d_{tar}/d_{nom}$.

If the real diameter is systematically lower than the target because it is the lower bound tolerance that is aimed at in production, then the lower bound should be used as the target value above. This would ensure safety and encourage defining and using smaller production tolerances than allowed. It is, however, simpler to require that the real mean diameter equals the target value, so 'tolerances are tolerances'.

A proposal for a more consistent system to declare fastener properties, which has not yet been discussed, is given in document N044 from CEN TC250 / SC5 /WG5 [21]. It includes also discussion of methods to correct for timber properties and steel strengths.

7. Discussion

Confidence among structural engineers on how to design timber connections is very important for the competition with concrete and steel. Regarding strength parameters for timber fasteners it is presently somewhat confusing to find the necessary information and conditions when the fasteners are not CE-marked according to the harmonized standard EN 14592 [6]. Only structural timber of softwood is fully covered.

For wood materials, where the parameters are available, the values for similar products of different brands can deviate a lot, so the designer need to assume a specific product, knowing that the contractor might use a different product with other parameter values, even it looks the same. The difference might to a large extent be due to uncertainties in the test methods used to determine the parameters, especially the selection of timber specimens. Some declared values are therefore incorrect and perhaps too high, so safety is compromised.

Using the ETA system as basis for the CE-marking should enable bypassing shortcomings of harmonised standards, but the system is also used to change rules in the harmonized standard and Eurocode 5 which are applicable. This is both confusing for the designer and principally improper.

The test results referred to indicates that there is very little, if any, difference between different brands of screws and probably also of different brands of ring shank nails, when tested under the same conditions.

It is made likely that the differences can be reduced very significantly by testing relative to reference fasteners, for which the strength parameters are determined by extensive testing. This will ensure that similar products get the same strength

parameters. It will also make it much easier to give consistent values for other wood materials that structural timber.

Introducing classes for fastener strengths giving all necessary strength parameters, similar to e.g. C24 for structural timber, will enable the designer to use non-product specific assumptions and makes it easy for the contractors to choose a product complying with the assumptions. This will support 'ease of use'.

There is also a need for more specific rules for declaration of dimensions and handling of tolerances. It will not change the load carrying capacities much, but contributes to fair competition between fastener manufacturers (and their test-labs).

8. References

- [1] EN 1995-1-1: Eurocode 5: Design of timber structures - Part 1-1: General – Common rules and rules for buildings, European Committee for Standardization (CEN), 2004, Brussels, Belgium.
- [2] Sandhaas C., and Görlacher R., “Nailed joints: investigation on input parameters for design”, *Proceedings of the International Conference on Connections in Timber Engineering – From Research to Standards*, September 2017, Graz, Austria.
- [3] Bader T.K., Bocquet J.-F., Schweigler M., and Lemaitre R., “Numerical modeling of the load distribution in multiple fastener joints.” *Proceedings of the International Conference on Connections in Timber Engineering – From Research to Standards*, September 2017, Graz, Austria.
- [4] Quenneville P., “Brittle failure of connections loaded parallel to grain.” *Proceedings of the International Conference on Connections in Timber Engineering – From Research to Standards*, September 2017, Graz, Austria.
- [5] Jockwer R., and Dietsch P., “Brittle failure of connections loaded perpendicular to grain.” *Proceedings of the International Conference on Connections in Timber Engineering – From Research to Standards*, September 2017, Graz, Austria.
- [6] EN 14592+A1: Timber structures – Dowel-type fasteners – Requirements, European Committee for Standardization (CEN), 2012, Brussels, Belgium.
- [7] EN 13986+A1: Wood-based panels for use in construction – Characteristics, evaluation of conformity and marking, European Committee for Standardization (CEN), 2015, Brussels, Belgium.
- [8] EN 320: Particleboards and fibreboards – Determination of resistance to axial withdrawal of screws, European Committee for Standardization (CEN), 2011, Brussels, Belgium.
- [9] EOTA, Screws for use in Timber constructions, EAD-130118-00-0603, 2017.
- [10] EOTA, Nails and screws for use in nailing plates in timber structures, EAD 130033-00-0603, 2015.

- [11] EOTA, Dowel-type fasteners with resin coating, EAD 130019-00-0603, 2017.
- [12] EN ISO 8970: Timber structures – Testing of joints made with mechanical fasteners – Requirements for wood density, European Committee for Standardization (CEN), 2010, Brussels, Belgium.
- [13] Munch-Andersen J., Sørensen J. D., and Sørensen F., “Estimation of load-bearing capacity of timber connections.” *Proceedings of the 43rd CIB W18 Meeting*, August 2010, Nelson, New Zealand.
- [14] Munch-Andersen J., and Sørensen J. D., “Pull-through capacity in plywood and OSB”, *Proceedings of the 44th CIB W18 Meeting*, Aug.-Sept. 2011, Alghero, Italy.
- [15] EN 338: Structural timber – Strength classes, European Committee for Standardization (CEN), 2016, Brussels, Belgium.
- [16] Munch-Andersen J., and Svensson S., “Accurate strength parameters for fasteners with examples for ring shank nails”, *Proceedings of the WCTE 2016*, August 2016, Vienna, Austria.
- [17] EN 15228: Structural timber – Structural timber preservative treated against biological attack, European Committee for Standardization (CEN), 2009, Brussels, Belgium.
- [18] ISO 12491: Statistical methods for quality control of building materials and components. ISO, 1997.
- [19] Christiansen L. G., and Sivertsen J., Søms udtræksstyrke i træ ved varierende relativ fugtighed, BSc thesis, 2017, Department of Civil Engineering, DTU (in Danish).
- [20] Madsen J., and Wendt-Larsen M., Eksperimentel undersøgelse og teoretisk bestemmelse af friktions indvirken i træsamlinger, BSc thesis, 2012, Department of Civil Engineering, DTU (in Danish).
- [21] Munch-Andersen, J., Characteristics defining relevant properties of dowel-type fasteners, CEN TC250 / SC5 /WG5 / N044.

Nailed Joints: Investigation on Parameters for Johansen Model

Carmen Sandhaas
Senior Researcher
Karlsruhe Institute of Technology
Karlsruhe, Germany

Rainer Görlacher
Academic Director
Karlsruhe Institute of Technology
Karlsruhe, Germany

This contribution has already been published at the INTER conference 2017 in Kyoto, Japan, as paper 50-7-3.

Summary

A comprehensive database containing more than 8000 tests carried out for certification purposes of nails has been analysed with regard to parameters needed for design of nailed joints. An equation to calculate the characteristic yield moment covering all nail types has been proposed. Investigations on the withdrawal and head pull-through parameters revealed that the correlation with the density is weak and the scatter is significant. Consequently, at the current state of the art, tests to obtain declared values need to be carried out.

1. Introduction

In Eurocode 5, nailed joints are designed using the Johansen model extended with the rope effect, the so-called European Yield Model (EYM). Necessary input parameters are hence, apart from geometrical data, embedment strength f_h , yield moment M_y and withdrawal and head pull-through capacity F_{ax} resp. F_{head} . Generally, empirical equations based on regression analyses have been derived for all four parameters f_h , M_y , F_{ax} and F_{head} . However, especially for ring shank nails, no consistent rules are given in the current version of Eurocode 5. Values for yield moments or withdrawal parameters, for instance, must be taken from technical documents of the single nails. This is not only cumbersome for practitioners, it also requires a considerable testing effort from producers.

The aim of this contribution is to propose more straightforward equations regarding the parameters wire tension strength f_u , nail tension capacity F_t , yield moment M_y , withdrawal parameter f_{ax} and head pull-through parameter f_{head} , which have to be experimentally established in current certification practice. Based on an extensive database comprising more than 8000 test results carried out for certification

purposes, regression analyses have been carried out. Potential benefits are more robust design models covering a large range of nails, reduced testing and simplified design equations. Prerequisite to all derived equations are sufficient spacings and end and edge distances to avoid splitting.

2. State-of-the-Art

Joint design in the current Eurocode 5 is based on Johansen's model [1] that firstly had been applied to nailed joints by Moeller [2]. Since then, considerable research effort has been put into further development of methods to establish the ultimate characteristic load and deformation behaviour as discussed in Ehlbeck [3], who gives a concise and comprehensive summary of the state of the art in the late seventies. Ehlbeck already discussed input parameters necessary for the design of nailed joints such as embedment strength and yield moment as well as the contribution of the rope effect to the joint capacity and hence the withdrawal performance of non-smooth shank nails. The background discussed by Ehlbeck is still representative today as research efforts concerning bolted and screwed joints have been and still are in the focus whereas nailed joints are less represented in current research. An exception to this is the work done by Whale and Smith in the eighties concerning embedment strength [4, 5] and investigations by Blaß in the early nineties concerning group effects in nailed joints [6, 7].

In current certification practice, all five parameters, f_u , M_y , F_t , f_{ax} and f_{head} , are tested according to EN 14592 where a minimum value for the wire strength of $f_u = 600$ MPa is required. The evaluated values on the characteristic level are then declared in technical documents. For smooth shank nails however, the characteristic yield moment $M_{y,Rk}$ can also be calculated. For round nails for instance, Eurocode 5 gives the following Eq. (1):

$$M_{y,Rk} = 0.3 \cdot f_u \cdot d^{2.6} \quad (1)$$

where f_u is the wire tension strength and d is the nominal nail diameter.

Eq. (1) is based on work done by Werner and Siebert [8] and it is valid only when a tension strength of the wire of 600 MPa is inserted. This value of 600 MPa is mandatory even if the actual value is higher which is the case for diameters less than 4 mm. The exponent of 2.6 in Eq. (1) reflects an observed increase of yield strength (up to 1000 MPa for 2 mm nails) with decreasing nail diameter which can be explained with work hardening due to cold drawing.

Also for the parameters f_{ax} and f_{head} , regression equations are given in Eurocode 5 for short term loaded smooth shank nails:

$$f_{ax,k} = 20 \cdot 10^{-6} \cdot \rho_k^2 \quad \text{and} \quad f_{head,k} = 70 \cdot 10^{-6} \cdot \rho_k^2 \quad (2)$$

The withdrawal and head pull-through parameters for non-smooth shank nails are, analogously to M_y and F_t , defined in the individual declarations of performance of

the producers. Considering the head pull-through parameter, this applies as well although the head shape may be the same for non-smooth and smooth shank nails.

3. Database

The global database consists of in total 8416 tests taken from 96 reports on mostly ring shank nails (rings 77 %, spiral nails with threads 5 %) and wires (11 %). Special ring shank nails with smooth intermediate shanks as shown in Fig. 1 on the left constituted 5.3 % of the overall database, whereas smooth shank nails constituted only 1 % of the database and square nails only 0.3 %. For smooth shank nails, only wire strength was tested and no other parameters are available. Nails from 33 different producers were considered and the tests were carried out between 1997 and 2013. It is not considered useful to enlarge the database with older results as both steel grades and production technologies may have changed since then and any analyses would not be representative of modern nails. The geometrical properties given in Fig. 1 on the right are also recorded in the database. The number of tests per parameter is given in Tab. 1 As properties of nails made from stainless steel do not differ significantly from all other nails, see for example Fig. 2, no difference will be made in analyses.

With regards to the individual parameters, wire strength f_u , calculated with the wire diameter, and nail tension capacity F_t are measured maximum values. The given yield moment M_y is the value at a measured deformation angle of 45° or the reached maximum bending angle before rupture of the nails. It should be noted that issues concerning test execution and precision of measured angles lead to uncertainties about the measured values as for instance, machine slip as well as elastic bending is included in the measurement during testing [9]. Withdrawal capacity F_{ax} and head pull-through capacity F_{head} were evaluated using softwood (*Picea abies*), stored at 65/20 and with the recorded densities. F_{ax} again is the measured maximum value whereas F_{head} is the maximum value or the value at a deformation of the testing machine of 15 mm.

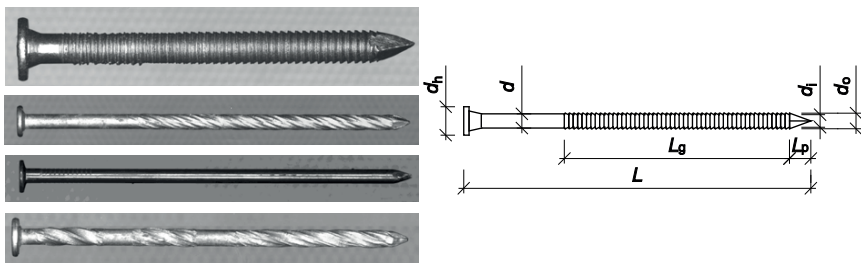


Fig. 1 Left: Nail shapes in database. From top to bottom: ring shank nail, spiral nail, smooth shank nail, special spiral nail. Right: Geometrical properties with d = nominal nail diameter; d_i = inner diameter; d_o = outer diameter; d_h = head diameter; L_g = length of non-smooth shank, L_p = tip length.

Tab. 1 Composition of database.

	Wire tension strength f_u	Yield moment M_y^+	Nail tension capacity F_t	Withdrawal capacity F_{ax}	Head pull-through capacity $F_{head}^\#$
No. of tests	1076	2844	1160	2316	1020
Of which stainless steel	203	369	195	300	60
Of which hdg*	–	265	178	310	220

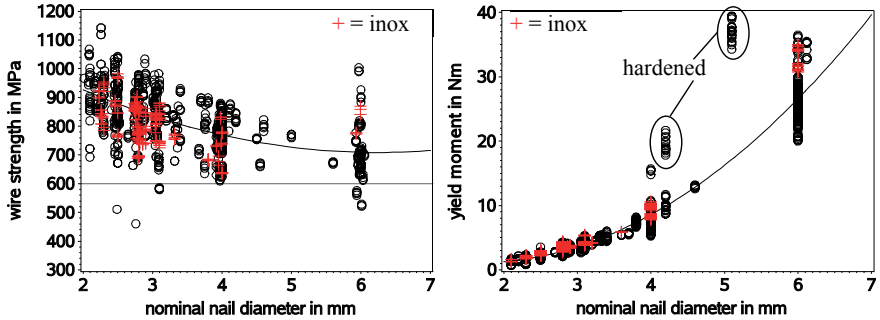


Fig. 2 Influence of stainless steel on wire strength (left) and on yield moment (right). Experimental values are shown and on the right, hardened nails are identified.

4. Analysis and Discussion

4.1 Wire Strength and Tension Capacity

Similar to Werner and Siebert [8], a decrease of wire and nail strength with increasing diameter can be observed in Fig. 3 where the nail strength $f_{u,nail}$ has been calculated using the tension capacity F_t and the nominal diameter d . The nail tension strength calculated with the nominal diameter d (and not with the inner diameter d_i) is slightly lower than the original wire strength. The decrease of tension strength with increasing diameter can be explained with work hardening due to cold drawing. As multiple passes are needed for smaller diameter nails, strength values are increasing with decreasing diameter.

For design purposes, wire strength tests are not needed. Tension tests on nails are sufficient to guarantee tension properties, calculated with the nominal diameter d . Producers may need wire tests however in order to control delivered steel grades. Furthermore, the significant difference between bright wire tension strength and subsequent tension strength of hot-dip galvanised (hdg) nails, the crosses in Fig. 3, is obvious, especially for small diameter nails where a major part of the diameter is affected by heat. For hot-dip galvanised nails, it is indispensable to carry out tension tests on finished nails as wire strength has no significance. The same

applies to hardened nails (special nails) where the wire strength is not correlated to the nail strength.

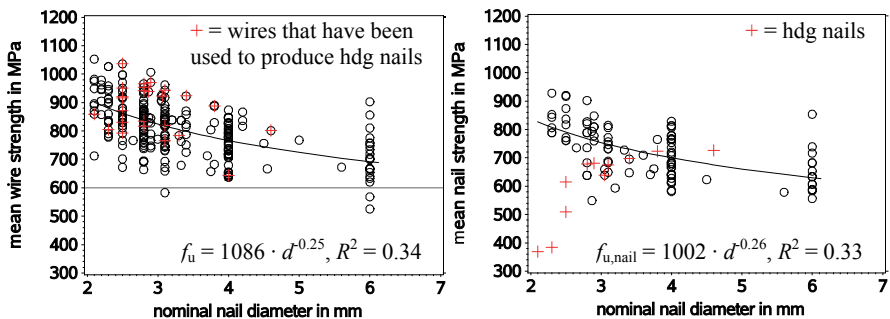


Fig. 3 Left: Mean tension strength of wire versus nominal nail diameter d . Right: Mean tension strength of nail calculated with F_t and nominal diameter d . Data from 78 test series (403 single tests f_w , 916 single tests F_t). Regression excludes hdg nails.

4.2 Yield Moment

A nonlinear regression analysis to derive an expression for M_y has been carried out. The dependent variables have been the nominal diameter d and $f_{u,nail}$ which is the tension strength calculated from the nail tension capacity F_t and the nominal diameter d . Only such a procedure is realistic as both inner diameter d_i and yield strength f_y are unknown values in practice. As an assignment of single M_y values to single F_t values within one testing series is not possible, mean values of both M_y and $f_{u,nail}$ form the basis of the regression analysis. The influence of nail types and steel qualities on the resulting regression equation has been investigated and no significant differences were observed (differences in independent variables of max 1.6 %). Therefore, no differentiation has been made within the database, e.g. with respect to different nail types or normal and stainless steel. The hardened nails highlighted in Fig. 2 on the right could not be included in the analysis as on these nails, only M_y has been tested and no data was available to calculate $f_{u,nail}$. It is expected that they would fit in the following equations if their actual tension strength would be used, which could be experimentally determined very easily. The nonlinear regression based on mean values of 105 test series resulted to (with $R^2 = 0.995$):

$$M_y = 0.185 \cdot f_{u,nail} \cdot d^{2.99} \quad (3)$$

Fig. 4 on the left shows the experimental versus the predicted values. The very good agreement between tests and model resulting in a bisect line with small scatter

can be seen. Eq. (3) is similar (with a difference in the pre-factor of 0.9) to the mechanical equation for a full plastic moment of a round section, Eq. (4):

$$M_{pl} = \frac{1}{6} \cdot f_y \cdot d^3 \quad (4)$$

Blaß and Colling [10] proposed Eq. (4) to calculate the yield moment of dowels defining an effective yield strength $f_{y,ef}$. A good agreement between test results and calculated values was found when $f_{y,ef}$ is put to $f_{u,nail}$ and the following Eq. (5) is proposed for nails:

$$M_y = \frac{1}{6} \cdot f_{y,ef} \cdot d^3 \quad \text{with} \quad f_{y,ef} = f_{u,nail} \quad (5)$$

Fig. 4 on the right shows the ratio between the individual experimental results and the calculated values using Eq. (5) and the mean nail tension strength $f_{u,nail,mean}$ per series. The observed 5-percentile of the ratio is 0.995 (64 of 1034 ratios are smaller than 1) and therefore, the 5-percentile is slightly exceeded.

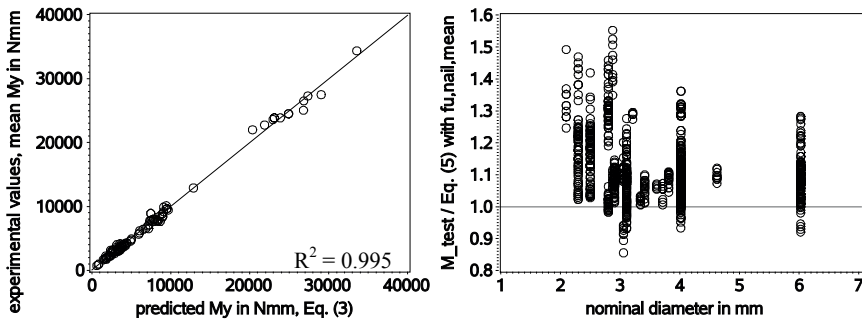


Fig. 4 Left: Experimental and predicted values (Eq. (3)) for the yield moment M_y . Right: The y-axis shows the ratio of individual experimentally determined yield moments over calculated yield moments using Eq. (5) and the mean nail tension strength values $f_{u,nail,mean}$ per series. The x-axis shows the nominal nail diameter. Data from 105 test series (1034 single tests M_y , 1035 single tests F_V).

Based on the procedure prescribed in EN 14358 [11], 5-percentile values have been estimated. The characteristic values were calculated from the test values assuming a lognormal distribution and a standard deviation of $s_y = 0.05$ for both the yield moment and the tension strength. This makes sense because both values are describing the same steel property and the differences in the variation are random. Fig. 5 shows the ratio between experimental and calculated yield moments using Eq. (5) versus the characteristic nail tension strength $f_{u,nail,k}$. The ratio is based on characteristic values $M_{y,k}$ per test series and Eq. (5) with $f_{u,nail,k}$. The 5-percentile of

the ratio is 1.00. Eq. (5) is therefore reflecting accurately the relationship between tension strength, nail diameter and yield moment and it is able to predict the characteristic yield moment $M_{y,k}$ using $f_{u,nail,k}$ as characteristic effective yield strength.

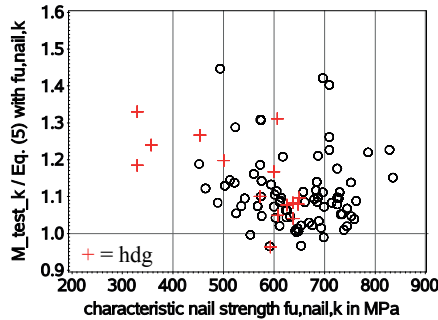


Fig. 5 Ratio between characteristic experimental and characteristic calculated yield moments (Eq. (5)) in dependence of the characteristic nail tension strength $f_{u,nail,k}$. Data from 105 test series (1034 single tests M_y , 1035 single tests F_j).

Fig. 5 also shows that the characteristic tension strength of the nails varies in a wide range and it would hence not be economically efficient to define a minimum tension strength for all nails. It would rather be reasonable to define technical classes to calculate the characteristic yield moment with a characteristic effective yield strength $f_{y,ef,k}$ which is based on characteristic tension strength values, see vertical lines in Fig. 5.

Concerning Eurocode 5, three options to regulate the yield moment of nails exist:

- No equation is given and the practitioners have to take the characteristic yield moments from the individual declarations of performance.
- Eq. (5) is inserted in Eurocode 5 where the characteristic tension strength $f_{u,nail,k}$ has to be taken from the declarations of performance.
- Technical classes are defined prescribing different characteristic tension strength values, where however, additional notes need to be given similar to prEN 14592 [12]. For instance, it must be clearly stated that small diameter nails may have significantly higher tension strength values than 6 mm nails (see also Fig. 3 on the right). Tab. 2 gives some examples on how such classes could be defined.

Tab. 2 Possible definition of technical yield strength classes (YSC) for effective yield strength $f_{y,ef}$ (in MPa) of dowel-type fasteners.

YSC1	YSC2	YSC3	YSC4	YSC5	YSC6	YSC7
300	400	500	600	700	800	900
Mild steel dowels						
hdg nails	-	$d = 6 \text{ mm}$ \longrightarrow			$d = 2 \text{ mm}$	
						Staples

4.3 Withdrawal Parameter

For dowel type fasteners, the withdrawal parameter f_{ax} is calculated from the withdrawal capacity F_{ax} by the following equation:

$$f_{ax} = \frac{F_{ax}}{d \cdot L_{ef}} \quad (6)$$

where d is the nominal diameter and L_{ef} is defined as the length of the threaded part in the pointside member ($L_{ef} = t_{pen}$ (acc. EC 5 [13]) = l_d (acc. EN 1382 [14])). That means that the tip of the nails has to be subtracted from the penetration length. Fig. 6 shows the tip length L_p versus the nail diameter d of all test data. The tip length is between d and $2 \cdot d$ with a mean value of $1.4 \cdot d$.

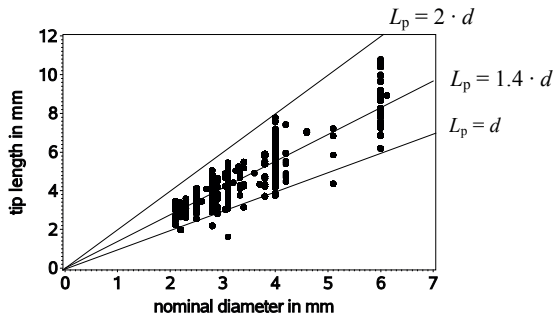


Fig. 6 Tip length L_p versus nominal diameter d , 5483 values (L_p has not always been recorded).

Pearson's correlation coefficients of f_{ax} are given in

Tab. 3. The influence of L_{ef} , L_p and d is weak and also the ring depth, which is expressed as the ratio between inner (d_i) and outer (d_o) diameter, shows no correlation ($R = -0.00$) with f_{ax} . Only the density ρ correlates with f_{ax} ($R = 0.33$). For most types of fasteners, the withdrawal parameter is indeed a function of the wood density, as can be seen in Eq. (2). Fig. 7 shows f_{ax} in dependence of the density ρ . It can be seen that the range of tested densities is not fully representative

for all softwood strength classes according to EN 338 [15] where classes with densities below 300 kg/m^3 and higher than 500 kg/m^3 exist, while the test values are between 329 and 472 kg/m^3 .

In order to give a closer look at the relationship between f_{ax} and ρ , a nonlinear regression has been carried out ($R^2 = 0.11$) which is shown in Fig. 7 and where the exponent of 1.38 corresponds to the correction factors proposed in prEN 14592 [12] (there Table D.1):

$$f_{ax} = 3.6 \cdot 10^{-3} \cdot \rho^{1.38} \tag{7}$$

Tab. 3 Correlation matrix for withdrawal parameter.

	ρ	L_{ef}	L_p	ratio d_i/d_o	d
f_{ax}	0.33	-0.02	-0.20	-0.00	-0.18

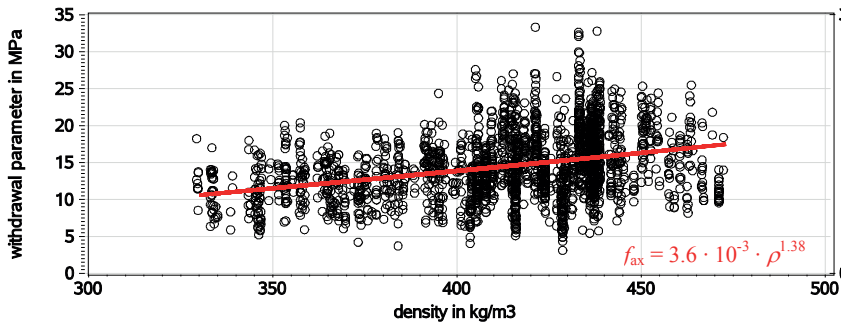


Fig. 7 Withdrawal parameter versus density, 2316 tests.

Still, with a correlation coefficient of 0.33 and a R^2 -value of 0.11, the scatter is rather high and the relationship between f_{ax} and ρ is not very strong. One reason for this is that the differences between the nails of different producers are much higher than the differences caused by the density. This is visualised in Fig. 8 where the withdrawal parameters are given per test series with increasing nominal diameters. In Fig. 8, it can be also seen that the scatter within one test series is smaller for 4 to 6 mm nails than for smaller diameter nails. Additional influence effects were observed during testing. For instance, it has been observed that rather non-measurable factors guarantee good withdrawal parameters. Above all, the sharpness of the rings that can be felt when passing the nails through the fingers defines good performance. In the database, no information is available concerning the quality and sharpness of the rings or threads, and measuring it would increase testing efforts considerably.

Based on the procedure prescribed in EN 14358 [11], 5-percentile values have been estimated assuming a lognormal distribution. The individual withdrawal parameters have been adjusted to a reference density of $\rho_{ref} = 350 \text{ kg/m}^3$ using Eq. (7):

$$f_{ax,corr} = f_{ax} \cdot \left(\frac{350}{\rho} \right)^{1.38} \quad (8)$$

Fig. 9 shows the characteristic withdrawal parameter $f_{ax,k}$ per test series versus the nominal diameter and the five nail types are identified. Spiral, special spiral and square nails did not reach characteristic values larger than 8 MPa. Furthermore, the scatter is higher for smaller diameter nails which has already been seen in Fig. 8.

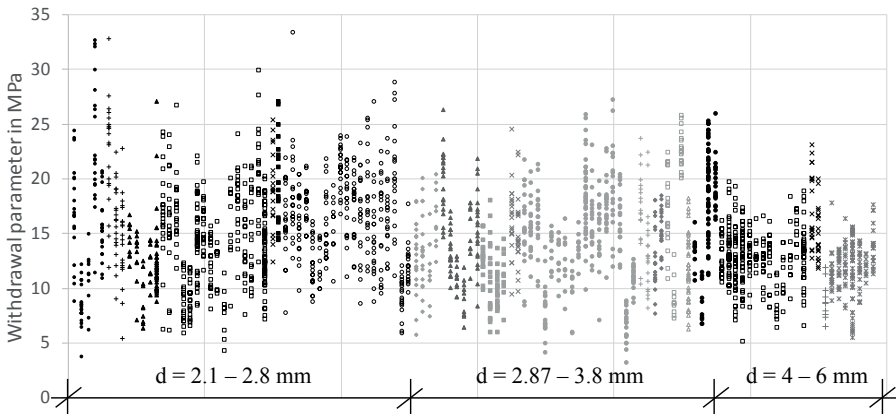


Fig. 8 2316 withdrawal parameters are shown per test series and with increasing diameters.

Based on the actual database and the analyses shown, it can be concluded that also in future, tests have to be carried out and values for f_{ax} have to be taken from technical documents. At the moment, no test results are available where one nail type has been tested using a large range of wood densities or where the detailed nail geometry including information on the ring sharpness has been measured. Consequently, no thorough analyses can be carried out concerning these influence parameters.

With regard to code implementation, technical classes could be introduced so that designers do not need to consult declarations of performance to get withdrawal parameters. The horizontal lines in Fig. 9 correspond to the withdrawal classes for all fastener types in accordance with prEN 14592 [12], where values of 4.5, 6, 7, 8, 10 and 12 MPa are given. The decrease of variation with increasing diameter is observed also on the 5-percentile level. Considering the still persistent high scatter in Figs. 7 to 9, the necessity of determining f_{ax} with the effective penetration depth

(i.e. subtracting the tip length) for joint design purposes remains worth discussing. If a nonlinear regression is carried out where f_{ax} is calculated with the full penetration depth, differences of 10 % to 20 % to Eq. (7) are evaluated which disappear in the scatter within one diameter or density range.

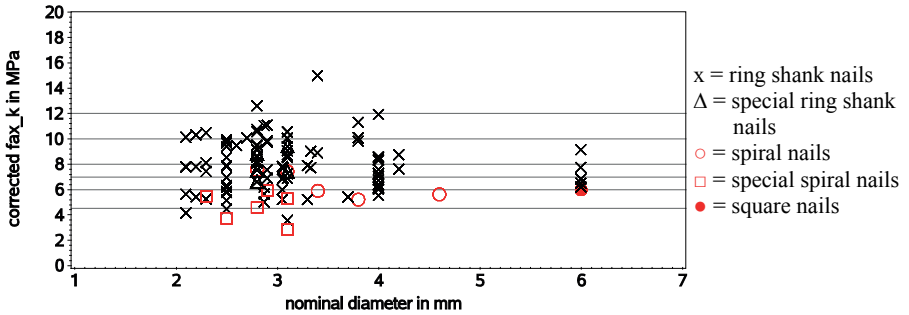


Fig. 9 Characteristic withdrawal parameter f_{ax} versus nominal diameter. f_{ax} has been corrected with $(350/\rho)^{1.38}$. Withdrawal classes from prEN 14592 [12] are shown, see horizontal lines at 4.5, 6, 7, 8, 10 and 12 MPa. Data from 118 test series (2316 single tests f_{ax}).

4.4 Head Pull-Through Parameter

Similar to the withdrawal parameter, also the head pull-through parameter is considered to be a function of the wood density, Eq. (2). Therefore, again a correlation between head pull-through parameter f_{head} and density ρ , Fig. 10 and Tab. 4, has been carried out, where f_{head} has been calculated as follows with d_h = head diameter:

$$f_{head} = \frac{F_{head}}{d_h^2} \quad (9)$$

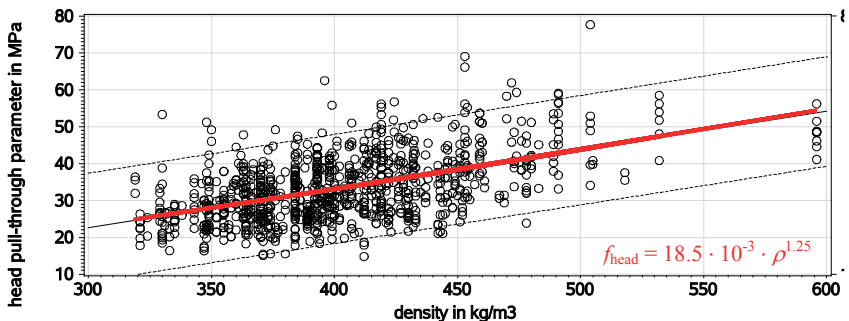


Fig. 10 Head pull-through parameter versus density, 1020 single tests.

Tab. 4 Correlation matrix for head pull-through.

	ρ	d_h	d	d_h/d
f_{head}	0.52	-0.27	-0.27	0.08

Considering Tab. 4, the ratio of head diameter d_h over nominal diameter d (where d_h is approximately $2 \cdot d$) shows no influence on f_{head} . The head shape however may have an influence, but this parameter has not been recorded. No head pull-through tests were carried out using standard ring shank nails with trumpet heads that are used to fasten steel plates. Tab. 4 gives a Pearson's correlation coefficient for the density ρ of $R=0.52$ and Eq. (10) gives the result of a nonlinear regression considering the complete database of 1020 results (with $R^2=0.28$). Eq. (10) is shown in Fig. 10.

$$f_{\text{head}} = 18.5 \cdot 10^{-3} \cdot \rho^{1.25} \quad (10)$$

If the same regression is carried out excluding the few results for high densities $> 550 \text{ kg/m}^3$, Eq. (10) does not change significantly and gives slightly lower values of f_{head} for higher densities (difference at 500 kg/m^3 is 6%). These slight differences are included in the 95 %-confidence interval shown in Fig. 10.

Again, based on the procedure prescribed in EN 14358 [11], 5-percentile values have been estimated assuming a lognormal distribution. The individual head pull-through parameters have been adjusted to a reference density of $\rho_{\text{ref}} = 350 \text{ kg/m}^3$ using Eq. (10):

$$f_{\text{head,corr}} = f_{\text{head}} \cdot \left(\frac{350}{\rho} \right)^{1.25} \quad (11)$$

Fig. 11 shows the characteristic head pull-through parameter $f_{\text{head,k}}$ per test series versus the nominal diameter and the four nail types are identified. Again, the scatter is higher for smaller diameter nails. Fig. 11 also shows a decrease of f_{head} with increasing nail diameter which can be also concluded from Tab. 4 where the correlation coefficient for d (and its related parameter d_h) is -0.27 indicating a relationship between f_{head} and diameter.

Similar to the withdrawal parameter and based on the actual database and the analyses shown, it can be concluded that also in future, tests have to be carried out and values for f_{head} have to be taken from technical documents. With regard to code implementation, technical classes could be introduced also for head pull-through. The horizontal lines in Fig. 11 correspond to the withdrawal classes for all fastener types in accordance with prEN 14592 [12], where values of 10, 12.5, 15, 18, 20, 25 and 30 MPa are given. Considering the persistent scatter of f_{head} in Fig. 11 although head shapes do not differ significantly (round and flat shape and d_h approx. $2 \cdot d$), the random selection of the used timber seems to have a significant influence.

Parameters such as annual ring widths and orientation of tangential and radial directions may impact on the experimental values and the question remains if high f_{head} values above 20 MPa are reliable. A lower bound value of 15 MPa seems to be possible which could be used, without further testing, for all nails with non-smooth shanks as long as $d_h/d > 1.8$.

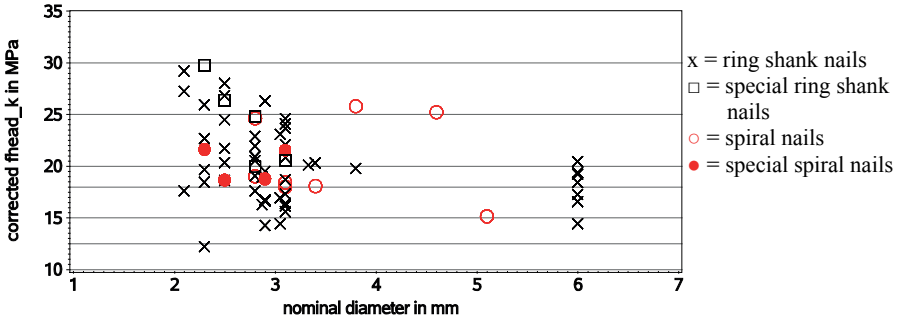


Fig. 11 Characteristic head pull-through parameter f_{head} versus nominal diameter. f_{head} has been corrected with $(350/\rho)^{1.25}$. Head pull-through classes from prEN 14592 [12] are shown, see horizontal lines at 10, 12.5, 15, 18, 20, 25 and 30 MPa. Data from 67 test series (1020 single tests f_{ax}).

5. Conclusions

A comprehensive database containing test results on mainly ring shank nails has been analysed. The following recommendations can be given concerning input parameters for joint design in accordance with the European Yield Model:

- Wire tension strength: These tests are not needed. However, producers may still require wire tests to control delivered steel grades.
- Nail tension capacity F_t : Tension tests on finalised nails need to be carried out and subsequently, a nail tension strength $f_{u,\text{nail}}$ can be calculated using the nominal diameter. This tension strength corresponds to an “effective yield strength $f_{y,\text{ef}}$ ”
- Yield moment M_y : The equation defining the theoretical full plastic bending capacity of a round section using an effective yield strength, Eq. (5), can be inserted in Eurocode 5 for all nail types except square nails where no tests were available. So it would be no longer necessary to determine M_y by tests, where the results are often very different between the testing institutes because of not clearly defined testing conditions (e. g. free bending length between $1 \cdot d$ and $3 \cdot d$ or technical difficulties of measuring the exact bending angle). The nominal diameter and the nail tension strength is needed to calculate the yield moment in accordance with Eq. (5). The nail tension strength, which can

be determined with a repetitious accuracy, must be taken from individual DoPs. Additionally, yield strength classes could be defined giving different nail tension strength values.

- Withdrawal parameter: Considering the analysed database with its limitations, it is proposed to include technical classes in Eurocode 5 to facilitate design of nailed joints. Additionally, individual values can be taken from DoPs. For design purposes, it is recommended to limit the characteristic withdrawal parameter especially for nails with small diameters to a certain limit (e.g. 8 N/mm^2) even if tested values are sometimes higher (see Fig. 9), because the withdrawal strength is very sensible to wood characteristics (not totally explained by the density) and production tolerances.
- Head pull-through parameter: The conclusions are analogous to those for the withdrawal parameter. Also here, the insertion of technical classes is proposed.

6. Acknowledgements

This work has been carried out within COST Action FP1402 and the authors would like to thank Elke Mergny, who started to assemble the database in the framework of a Short Term Scientific Mission which was paid by the same COST Action.

7. References

- [1] Johansen K.W., *Theory of timber connections*, Publication 9, International Association of Bridge and Structural Engineering (IABSE), 1949, Basel, Switzerland.
- [2] Moeller T., *En ny metod foer beraekning av spikfoerband*. Handlingar no. 117, Chalmers Tekniska Hoegskola, 1951, Göteborg, Sweden.
- [3] Ehlbeck J., *Nailed joints in wood structures*, Bulletin no. 166, Wood Research and Wood Construction Laboratory, Virginia Polytechnic Institute and State University, 1979, USA.
- [4] Whale L.R.J., and Smith I., *Mechanical timber joints*. Report 18/86, TRADA, 1986, High Wycombe, UK.
- [5] Whale L.R.J., and Smith I., "The derivation of design clauses for nailed and bolted joints in Eurocode 5", p. 19-7-6, *Proceedings of the 19th CIB-W18 Meeting*, 1986, Florence, Italy.
- [6] Blaß H.J., "Load distribution in nailed joints", p. 23-7-2, *Proceedings of the 23rd CIB-W18 Meeting*, 1990, Lisbon, Portugal.
- [7] Blaß H.J., "Traglastberechnung von Nagelverbindungen", *Holz als Roh- und Werkstoff*, 1991, Vol. 49, Iss. 3, pp. 91-98, doi:10.1007/BF02614345, (in German).

- [8] Werner H., and Siebert W., "Neue Untersuchungen mit Nägeln für den Holzbau", *Holz als Roh- und Werkstoff*, 1991, Vol. 49, Iss. 5, pp. 191-198 (in German).
- [9] Steilner M., and Blaß H.J., "A method to determine the plastic bending angle of dowel-type fasteners", *Materials and joints in timber structures. Recent developments in technology*, RILEM book series Vol. 9, 2014, pp. 301-306.
- [10] Blaß H. J., and Colling F., "Load-carrying capacity of dowelled connections", Paper 48-7-3, *Proceedings of the 48th INTER Meeting*, 2015, pp. 115-129, Sibenik, Croatia.
- [11] EN 14358: *Timber structures – Calculation of characteristic 5-percentile values and acceptance criteria for a sample*, European Committee for Standardization (CEN), 2007, Brussels Belgium.
- [12] prEN 14592: *Timber structures – Dowel-type fasteners - Requirements*. European Committee for Standardization (CEN), 2017, Brussels, Belgium.
- [13] EN 1995 1-1: *Eurocode 5. Design of timber structures - Part 1-1: General - Common rules and rules for buildings*, European Committee for Standardization (CEN), 2010, Brussels, Belgium.
- [14] EN 1382: *Timber structures – Test methods – Withdrawal capacity of timber fasteners*, European Committee for Standardization (CEN), 2016, Brussels, Belgium.
- [15] EN 338, *Structural timber – Strength classes*, European Committee for Standardization (CEN), 2009, Brussels, Belgium.

Design Approaches for Dowel-Type Connections in CLT Structures and their Verification

Andreas Ringhofer ^{*)}

**Post Doc; Research Associate
Institute of Timber Engineering and Wood Technology
Graz University of Technology
Graz, Austria**

Reinhard Brandner ^{*)}

**Assistant Professor; Deputy Head of the Institute
Institute of Timber Engineering and Wood Technology
Graz University of Technology
Graz, Austria**

Hans Joachim Blaß

**Professor; Head of the Institute
Research Center for Steel, Timber and Masonry
Karlsruhe Institute of Technology (KIT)
Karlsruhe, Germany**

^{*)} joint first authorship

Summary

Within the last 20 years, cross laminated timber (CLT) has become one of the most important building products in modern timber engineering. By the end of this decade its annual worldwide production volume is expected exceeding 1,000,000 m³. There is a strong interest of the industry, engineers, architects and constructors to implement CLT in European product, design and execution standards. This is part of the currently ongoing revision of Eurocode 5, supported by COST Action FP1402. In this context and in addition to the ULS and SLS verification of the panels themselves, provisions regarding the design of joints in CLT composed by dowel-type fasteners are of utmost importance.

Within this contribution, we aim on collecting, discussing and validating related approaches for characteristic values in literature for joints and single dowel-type fasteners in CLT. In addition, these models – especially dedicated to the withdrawal and embedment strength of dowels, nails and self-tapping screws – are compared with current regulations on dowel-type fasteners for solid timber and glulam as given in Eurocode 5. These comparisons are made in order to identify a pending need of modification of current EC 5 equations and state-of-the-art regulations.

Regarding the joint design, minimum spacing, edge and end distances as well as additional geometrical conditions, regulations on the effective number of fasteners in a group and minimum penetration depths are summarized. Finally, conclusions in respect of the single fastener properties, withdrawal and embedment strength, are made together with comments on regulations ensuring the integrity of CLT structures. Overall, we aim on presenting a compilation of the current state-of-the-art knowledge on dowel-type fasteners in CLT as basis for implementing design provisions for CLT in the new connection chapter of Eurocode 5.

1. Introduction

Cross laminated timber (CLT) is a planar, large dimension engineered timber product, designed for structural purposes and capable of bearing loads in- and out-of-plane. CLT, with dimensions $t_{CLT} \times w_{CLT} \times \ell_{CLT}$, is commonly composed of an uneven number N of orthogonal layers ($t_\ell \times w_\ell$) of finger-jointed laminations or wood-based panels. Adjacent laminations within the same layer may also feature narrow face bonding; without narrow face bonding gaps between the laminations may occur. The orthogonal layers are typically bonded at their side face forming rigid composite elements; flexible composites featuring layers connected by nails, staples or other fasteners are also on the market but not focused on within this contribution. Current approvals of European CLT products allow gaps in width (w_{gap}) up to 6 mm. Some CLT products feature also laminations with one or more stress reliefs, usually 2.5 mm wide; see Fig. 1 and EN 16351 [1].

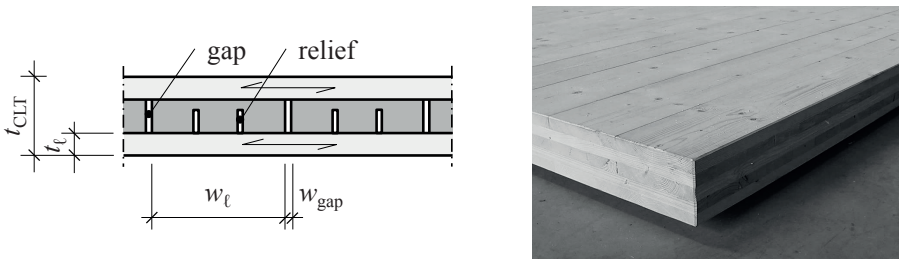


Fig. 1 (left) Principal CLT layout and some definitions of geometry and execution; (right) typical five-layer CLT element

CLT has been used in manifold applications but primary as large dimension wall, floor and roof element in single and multi-story buildings, halls and bridges. Although only 20 years on the market, this product has been changing the timber engineering sector in many ways, e.g.:

- by allowing architects thinking rather in planes and volumes than in lines;

- by supporting the timber engineering sector with a stand-alone structural element enabling assembling of constructions amazingly fast, dry, clean and with high precision;
- by providing all subsequent crafts conditions for easy and fast mounting and manipulation, e.g. of additional layers (e.g. insulation as well as installation layer and façade) and building services in general; and
- by offering end-users and investors highest building quality and a sustainable, natural living and working environment.

CLT has been revolutionizing the timber engineering sector in analogy to the invention of particle boards in furniture industry which at that time initiated also big changes. There are several analogies between CLT and particle boards e.g. the homogeneity of both products in comparison with the base material, i.e. a reduced variation in physical / mechanical properties. Both products are planar, feature a significantly reduced swelling and shrinkage in-plane and utilize base material (quality) which would be hard to use otherwise. Their industrial production processes are relatively simple and the final products can be relatively easy manipulated and assembled.

Apart from all these mutuality, differences in respect to scale, reliability and safety requirements, service life and exposure shall be considered as well.

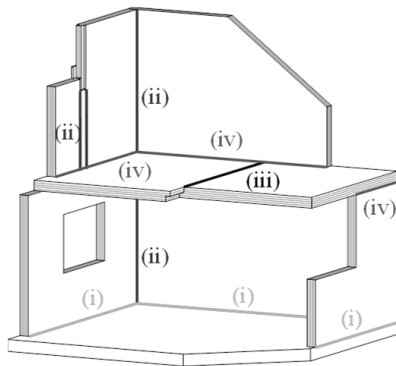
At the time the particle board entered the market also a significant change in furniture design could be observed, again by thinking in planes and volumes (boxes) rather than in lines and frames. New joint and fastener solutions, which were optimized for particle boards, together with a high degree in standardizing products and processes enabled extensive industrialization and economically prized furniture production.

CLT is on the way to catch up also these two very important steps: standardization (e.g. of layer thicknesses ($t_t = 20, 30, 40$ mm), layups, base material quality and design approaches) and by developing a connection technique optimized for CLT; in respect to the latter, there is still much room for further developments and improvements.

Aiming on versatile applicable joint solutions in CLT structures, a first step could be differentiating into principal joint lines (see also Fig. 2).

Considering this and looking at structures as a whole, the possibilities in realizing integer CLT structures also depend on the principle construction system. Single family houses, residential, office and school buildings up to three to five stories are commonly erected as platform-frame systems (indirect vertical load transfer between wall elements of vertically adjacent stories via soft floor elements).

Higher or heavily-loaded buildings are commonly designed as balloon-frame systems (direct vertical load transfer between wall elements of vertically adjacent stories).



- (i) wall-to-foundation
- (ii) wall-to-wall
- (iii) floor-to-floor
- (iv) wall-to-floor

Fig. 2 Definition of joints exemplarily for a CLT platform-frame structure (Brandner et al. 2016 [2]; adapted)

Although CLT is currently used in superstructures hardly possible in timber one decade ago, a connection technique underlining the possibilities building with CLT is still widely missing. In fact, current commonly applied fastener and joint solutions, like angle brackets and hold-downs, are borrowed from light-weight timber constructions; these connectors together with a wall-floor-wall joint in a typical platform-frame CLT structure are shown in Fig. 3. In optimizing angle brackets for CLT structures a first step could be adapting the geometry to resist both, shear and uplift forces, consolidating the tasks of current angle brackets (shear load transmission) and hold-downs (transmission of uplift forces) in one connector (Flatscher and Schickhofer [3]).

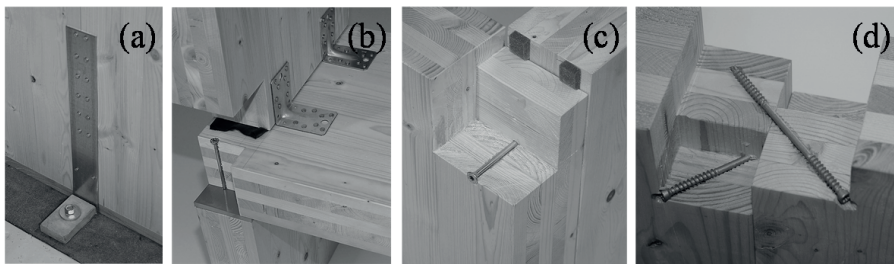


Fig. 3 (a) wall-foundation joint with hold-down; (b) wall-floor-wall joint with angle brackets and partially-threaded self-tapping screws; (c) wall-wall edge-joint with partially-threaded self-tapping screws, (d) wall-wall joint with double-threaded self-tapping screws; Schickhofer et al. (2010) [4]

Apart from angle brackets, hold-downs and line joints realized by means of partially-, fully- or double-threaded self-tapping screws (see Fig. 3), for CLT structures also other joint solutions and first CLT system connectors are available;

e.g. solutions with (self-drilling) smooth dowels / tight-fitting bolts and inner metal plates (e.g. Bernasconi [5]), the system connectors X-RAD (Polastri et al. [6], [7]; <http://www.rothoblaas.com/products/fastening/x-rad> 2017-07-07) or SHERPA CLT Connector (Kraler et al. [8]; http://de.sherpa-connector.com/clt_connector 2017-07-07), as well as special joint solutions, e.g. embedded steel tubes in combination with glued- or screwed-in rods (Schickhofer et al. 2010 [4]); see Fig. 4.

All these joint solutions have in common a connection between metal elements and CLT achieved via dowel-type fasteners, e.g. profiled nails (annular ringed shank nails or helically threaded nails), fully-, partially- or double-threaded self-tapping screws, smooth dowels or tight-fitting bolts as well as screwed- or glued-in rods, which are either loaded axially, laterally or combined. Retailers like Rothoblaas, Simpson Strong Tie, etc. support engineers with comprehensive (software) design tools and tabularized characteristic performance-based joint properties; a detailed verification of the single dowel-type fasteners themselves – fixing angle brackets, hold-downs or system connectors to CLT – is thus not required. However, the anchorage potential of single fasteners in CLT as described e.g. by the embedment strength and the withdrawal strength are essential parameters for the development of CLT connectors and for verification of line-joints realized with self-tapping screws or (self-drilling) dowels as well as individual joint solutions.

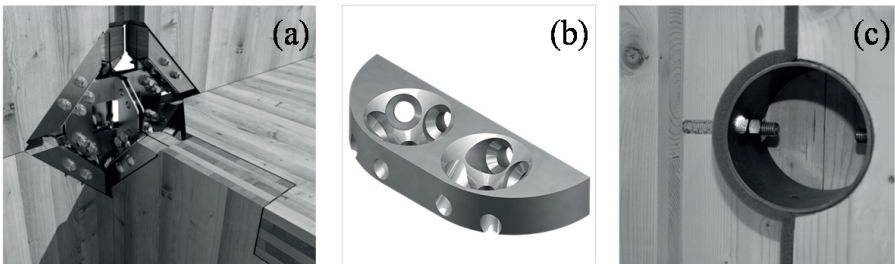


Fig. 4 (a) X-RAD system connector for balloon-frame CLT structures (Rothoblaas © [9]); (b) SHERPA CLT-connector (Sherpa © [10]); (c) embedded steel tube and glued-in rods (Schickhofer et al. 2010 [4])

Joints decisively impact the behavior of CLT structures. Whereas in light-weight timber structures wall and floor diaphragms behave more flexible, CLT diaphragms (walls and floors) are characterized by high stiffness and high resistance in shear, tension and compression in-plane. Consequently, in CLT structures ductility and energy dissipation have to be provided by adequate joint solutions, the contribution from CLT itself is negligible. Considering the main requirements on joints, as they are high resistance, high stiffness and high ductility, the significant difference in the behavior of light-frame and CLT diaphragms is necessitating new ways of thinking in developing adequate joint solutions for CLT.

In view of ongoing harmonization and standardization processes and the upcoming new version of the European Timber Design Code, Eurocode 5 (series of standards EN 1995-x-x), it is intended to reorganize the chapter on connections by providing a tool-box, supporting the engineer step-by-step with required basic characteristic values for different anchoring materials. A prerequisite therefore are generic approaches instead of models limited to each individual timber product.

In view of that, the next chapters are organized by providing at first some general notes on dowel-type fastener behavior in CLT; what is special and what can be treated equally to solid timber and glulam. In that respect potential failure modes are listed and discussed in conjunction with CLT. Following this, we summarize and discuss the state-of-the-art of axially and laterally loaded dowel type fasteners anchored in CLT, emphasizing the withdrawal and embedment behavior, respectively. Some suggestions for harmonization of current regulations on solid timber and glulam with CLT are made. Finally, we summarize also current suggestions and regulations on the joint design and requirements for securing structural integrity before summary and concluding remarks are given.

2. CLT Specialties and Characteristics Common with Glulam and Solid Timber

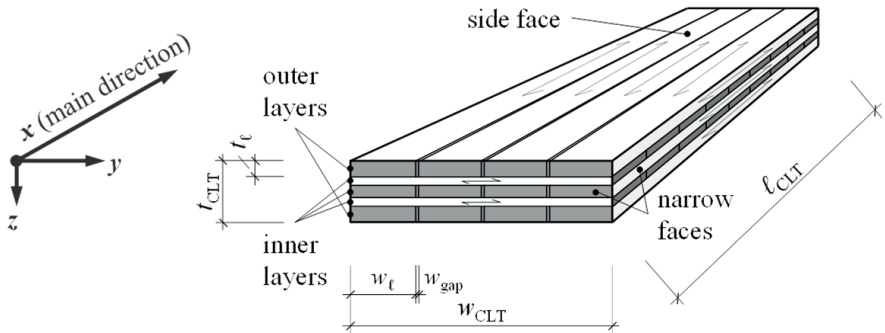


Fig. 5 Principal CLT element: terms, dimensions, coordinate system

CLT as well as glued laminated timber (glulam; GLT) are composed of solid timber laminations, typically of board dimension. Similarities in design provisions between solid timber (ST), CLT and GLT are expected, but the orthogonal layup of CLT demands additional attention. At first, differentiation in the positioning of fasteners in CLT side face (fastener axis oriented out-of-plane) and narrow face (fastener axis oriented in-plane) is necessary; see Fig. 5 (we will see later in a proposed generic approach for withdrawal properties that this differentiation would also make sense for glulam and other laminated products). Furthermore, the influence of gaps and potential stress reliefs has to be taken into account as placement of fasteners in gaps, in particular if inserted in the narrow face and

parallel to the grain, may lead to significant losses in fastener performance. According to approvals of current European CLT products, in the outer (top) layers gap widths up to 4 mm are allowed whereas in the inner (core) layers the gap width is limited to 6 mm. The European product standard for CLT, EN 16351 [1], limits gap widths generally to 6 mm. CLT producers aim on minimizing gap widths which is reflected already in Blaß and Uibel [11], Uibel and Blaß [12], [13] where inner layers featured a mean and 95%-quantile gap width of 2 mm and 3 to 4.6 mm, respectively, whereas the 95 %-quantile in the outer layers was only 1.0 to 2.1 mm.

Fasteners inserted via the CLT side face and loaded laterally behave rather ductile, facilitating that all fasteners in a group of fasteners contribute to the load-bearing capacity to their full extent, i.e. the effective number n_{ef} is equal to n , the number of fasteners inserted; see also Fig. 6. This ductile behavior is due to the orthogonal layup where transverse layers act as reinforcement and prevent early failures in tension perpendicular to grain and block or row shear.

Apart from a generally observed minor influence of gaps (Blaß and Uibel [11] and Uibel and Blaß [12], [13]), fasteners inserted via the CLT side face can be designed similar to solid timber and glulam. Considering also that typical insertion angles are (30°) 45° to 90°, the influence of the angle β between load and grain orientation of outer layers in case of laterally loaded fasteners, as well as the thread-grain angle α in case of axially loaded fasteners (see Fig. 7), is small and with some conservatism even negligible; more on that later.

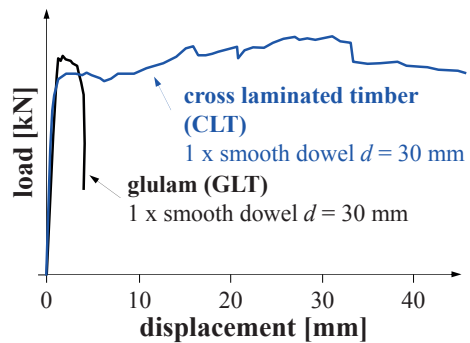


Fig. 6 Load-displacement behaviour of laterally loaded smooth dowels in the CLT side face (Schickhofer et al. 2010 [4]; adapted)

To reduce the influence of gaps on fastener performance, i.e. to reduce the probability that the effective anchorage length of a fastener is solely placed in gaps, it is suggested to penetrate a minimum of three layers ($M=3$, with M as the number of penetrated CLT layers); see Blaß and Uibel [11].

By anchoring fasteners in the CLT narrow face, the possibility of penetrating layers with grain oriented parallel to the fastener axis has to be taken into account. This circumstance influences also the probability that a fastener is inserted in a gap, i.e. the influence of gaps on the fastener performance in the narrow face is higher than in the side face. Furthermore, in a group of fasteners or even for one single fastener different thread-grain angles are possible; see Fig. 8.

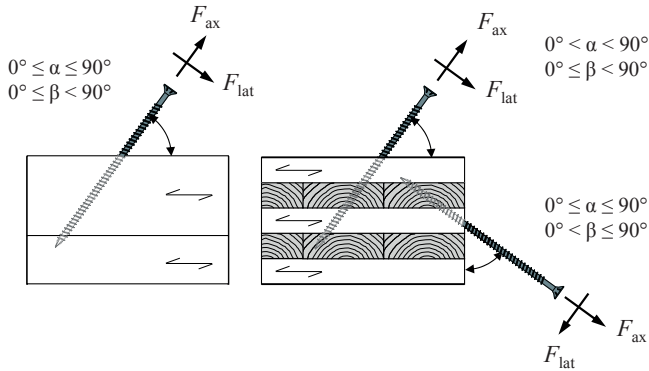


Fig. 7 Definition of thread-grain angle α and the angle between load and grain orientation of outer layers β , exemplarily for a screw inserted in side and narrow face of CLT

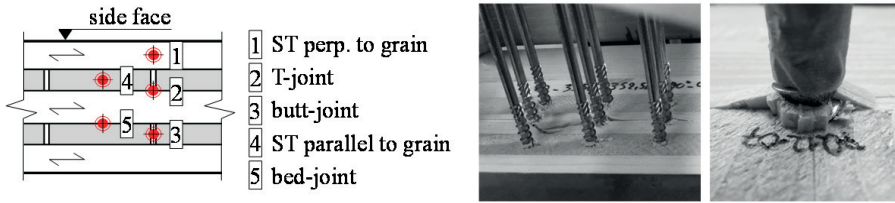


Fig. 8 (left) possible positions of dowel-type fasteners oriented perpendicular to the grain of outer layers in the CLT narrow-face; (middle) group of axially loaded self-tapping screws in the CLT narrow face, and (right) single screw featuring different thread-grain angles (Brandner [14]; adapted)

Laterally loaded fasteners in the CLT narrow face can be either loaded in-plane, i.e. by being loaded parallel to the CLT wide surface, or out-of-plane, i.e. by being loaded perpendicular to the CLT wide surface. In the latter case the possibility of tension perpendicular to grain failures before the capacity of fasteners is reached shall be taken into account.

In general, when discussing the performance of a connection composed by laterally or axially loaded dowel-type fasteners, the following potential failure mechanism can be differentiated; see Table 1.

Table 1 Summary of potential failure mechanism in case of laterally or laterally loaded single or group of fasteners

Loading	Failure mode	Failing material
Axial	Withdrawal	Timber
	Head-pull-through	Timber
	Fastener tension	Steel
	Fastener buckling	Steel (Timber)
	Tension perpendicular to grain (splitting)	Timber
	Block shear and row shear	Timber
Lateral	Embedment	Timber
	Yield in bending	Steel
	Block shear, row shear, plug shear	Timber
	Tension perpendicular to grain (splitting)	Timber

As failures of the fastener itself (steel failures) do not depend on the applied timber products we focus further on failure modes of CLT surrounding the fastener, in particular on the embedment and withdrawal capacity, as the related properties are of major importance for the description of laterally and axially loaded fasteners, respectively.

The density as indicating property for fastener performance in timber has to be differentiated between side and narrow face insertion. For fasteners in the side face, penetrating several layers, the characteristic density of CLT is proposed; see Blaß and Uibel [11] and Uibel and Blaß [13] who defined the characteristic density of CLT, based on laminations with strength class C24 and a characteristic density of $\rho_{12,\ell,k} = 350 \text{ kg/m}^3$ according to EN 338 [15], with $\rho_{12,CLT,k} = 400 \text{ kg/m}^3$. Following the proposal of PT SC5.T1 [16] for the new version of EN 1995-1-1 [17], for CLT made of C24 or T14 laminations according to EN 338 [15] a value of $\rho_{12,CLT,k} = 385 \text{ kg/m}^3$, based on the relationship $\rho_{12,CLT,k} = 1.1 \rho_{12,\ell,k}$, analogously to glulam, is proposed. For adjustment of models for withdrawal and embedment properties to density, corresponding corrections are presented. In contrast to CLT side face, as fasteners inserted via the CLT narrow face anchor mostly only in one lamination, for calculation of embedment and withdrawal capacity the characteristic density of the laminations themselves thus applies, e.g. for C24 or T14 according to EN 338 [15]: $\rho_{12,\ell,k} = 350 \text{ kg/m}^3$.

3. Withdrawal Strength of Axially loaded Dowel-Type Fasteners in CLT

3.1 Definitions, General Comments and Overview

Within this section, we focus on threaded or profiled dowel-type fasteners, enabling a composite action with the surrounding timber material and thus an appropriate performance when loaded in axial direction, i.e. self-tapping screws and profiled nails. Note: glued-in rods or glued-in metal plates, which also show a reasonable performance in case of axial loading, are not discussed in this paper. The composite action between the axially loaded fastener and the timber component is expressed by the withdrawal strength f_{ax} . In contrast to the withdrawal parameter, $f_1 = f_{ax} \pi$, the withdrawal strength f_{ax} is defined as

$$f_{ax} = \frac{F_{ax,max}}{\ell_{ef} d \pi}, \quad (1)$$

with $F_{ax,max}$ as the fastener's capacity in axial direction (equal to the withdrawal resistance $F_{ax,\alpha,Rk}$ according to EC 5 [17]), d as its relevant (nominal) diameter and ℓ_{ef} as its effective inserted thread length; the latter either including the fastener's tip length or not – as it is discussed later on.

Blaß and Uibel [11] (also published in Uibel and Blaß, [12], [13], [18]) were the first who investigated the performance of dowel-type fasteners, situated in different positions in the side and narrow face of CLT. Their analyses comprised variations in fastener type (dowels, self-tapping screws and nails), both angles α and β , different layouts of Central European CLT (also including solid wood-based panels, $N=3 \div 7$), randomly distributed gap widths $w_{gap,mean}$ up to 2.0 mm and different nominal diameters d . With regard to single fastener properties, outcomes were used for determining empirical regression functions as well as characteristic approaches for withdrawal and embedment strength as basis for the design of dowel-type fasteners inserted in CLT.

In respect to self-tapping screws and their axial load-bearing behavior in CLT, within the last years further comprehensive studies were conducted at Graz University of Technology, c. f. Ringhofer [19]. Amongst other topics, several experimental campaigns are compiled dealing with a detailed analysis of selected parameters relevant for the screws' load-bearing behavior. This especially concerns the following parameters, the number of penetrated layers M (Reichelt [20]; Ringhofer et al. [21]), the thread-grain angle α and the gap configuration (gap type and width; see Grabner [22]; Brandner [14]; Brandner et al. [23] and Silva et al. [24]). Based on a detailed statistical analysis on available comprehensive data on screw withdrawal tests an empirical, generic approach, presented in Ringhofer et al. [25]) and Ringhofer [19], was established and successfully validated by means of independently derived data sets.

In the following Sections 3.2 and 3.3 we summarize the main findings and recommendations of both research programs dedicated to the withdrawal behavior of dowel-type fasteners as carried out at KIT and Graz University of Technology.

Furthermore, we compare related models with those currently given in EC 5 [17] for determining the characteristic withdrawal strength particularly of axially loaded self-tapping screws situated in solid timber or glulam.

Apart from the European research programs also the work done by Kennedy et al. [26] is worth being mentioned since it represents one of the few non-European research activities regarding the determination of mechanical properties of single fasteners situated in (the side face of) CLT elements.

3.2 Axially Loaded Self-Tapping Screws in CLT Elements

The experimental program presented in Blaß and Uibel [11] and dedicated to the withdrawal strength of axially loaded self-tapping single screws with outer thread diameters $d = \{6, 8, 12\}$ mm can be separated into two campaigns: one where the focus was on CLT side face insertion and one where the screws were situated in the CLT narrow face. The impact of gaps between laminations of one layer on the mechanical screw performance was investigated by four alternative possibilities of screw insertion, covering the number of penetrated gaps $N_{\text{gap}} = \{0, 1, 2, 3\}$ (CLT side face) as well as the gap type (CLT narrow face, insertion in T- and butt-joints, c. f. Fig. 8) while the mean gap width $w_{\text{gap,mean}}$ varied randomly between 0.2 and 2.0 mm. For screws situated in the CLT side face, this was exclusively done for perpendicular-to-grain insertion while for those situated in the CLT narrow face, both limits of screw axis position to the single layer's grain direction, $\alpha = \{0, 90\}^\circ$ were examined. Specimens made of 3- and 5-layered CLT panels with five different layouts were used for 387 withdrawal tests. Subsequently, empirical regression functions for predicting the withdrawal strength f_{ax} were determined based on the test results; the characteristic approach is presented in Eq. (2):

$$f_{\text{ax,k}} = \frac{9.02 d^{-0.2} \ell_{\text{ef}}^{-0.1}}{1.35 \cos^2 \varepsilon + \sin^2 \varepsilon}, \text{ and } f_{\text{ax,k,corr}} = f_{\text{ax,k}} \left(\frac{\rho_k}{350} \right)^{0.75} \quad (2)$$

and ε as primary insertion angle, e.g. for screws in CLT narrow face: $\varepsilon = 0^\circ$ (on a conservative but general basis), and for screws in CLT side face $\varepsilon = 90^\circ$. As given in Eq. (2), for this approach a multiplicative power model is applied. Apart from ε , it identifies the outer thread diameter, the timber density as well as the effective inserted thread length as influencing parameters. While influences from diameter and density were adapted to the test results (both have a disproportional influence on f_{ax} respectively), Blaß and Uibel [11] adopted the impact of ℓ_{ef} on f_{ax} from the results of a previous testing campaign conducted in solid timber, c. f. Blaß et al. [27] and Eq. (4). Note: with regard to the definition of f_{ax} given in Eq. (1), it is worth mentioning that Blaß and Uibel [11] determined their experimental withdrawal strengths with ℓ_{ef} including the tip length, thus leading to a conservative interpretation of test results.

Due to material homogenization, the smaller probability of gap insertion along ℓ_{ef} as well as to the fact that parallel-to-grain insertion is impossible, the withdrawal strength of screws situated in the CLT side face is of course significantly higher

than of screws situated in the CLT narrow face. This is expressed by the factor 1.35 in Eq. (2), whose magnitude results from a data fit to those CLT narrow face test series with the worst results for withdrawal strength (parallel-to-grain insertion in gaps).

The examinations carried out at Graz University of Technology base on similar parameter configuration as in Blaß and Uibel [11] but additionally comprised variations in thread-grain angle α within the limits $\{0, 90\}^\circ$ for CLT side and narrow face insertion, as well as systematic examinations of the number of penetrated layers' (and their orientation) and the gap width's (for the types shown in Fig. 8). Amongst others, corresponding outcomes were applied for deriving a new generic approach for determining the withdrawal capacity of axially loaded self-tapping screws as presented in Ringhofer et al. [25] and Ringhofer [19] and shown in Eqs. (3–5):

$$f_{ax,k} = k_{ax,k} k_{sys,k} 8.67 d^{-0.33}, \text{ and } f_{ax,k,corr} = f_{ax,k} \left(\frac{\rho_k}{350} \right)^{k_p} \quad (3)$$

$$k_{ax,k} = \begin{cases} 1.00 & \text{for } 45^\circ \leq \alpha \leq 90^\circ \\ 0.64 k_{gap,k} + \frac{1-0.64 k_{gap,k}}{45} \alpha & \text{for } 0^\circ \leq \alpha \leq 45^\circ \end{cases}, k_{sys,k} = \begin{cases} 1.00 & \text{ST} \\ 1.10 & \text{CLT, } N \geq 3 \\ 1.13 & \text{GLT, } N \geq 5 \end{cases} \quad (4)$$

$$k_{gap,k} = \begin{cases} 0.90 & \text{CLT narrow face} \\ 1.00 & \text{else} \end{cases}, k_p = \begin{cases} 1.10 & 0^\circ < \alpha \leq 90^\circ \\ 1.25 - 0.05 d & \alpha = 0^\circ \end{cases} \quad (5)$$

This new generic approach comprises the following features, which are different from current approaches:

- Firstly, density correction by the power factor k_p is kept more flexible; in-depth analyses identified thread-grain angle and outer thread diameter as important influencing parameters.
- Secondly, for screws penetrating more than one layer when applied laminated timber products a significant homogenization was found. Apart from the density, so far the only parameter indicating the anchorage material, a stochastically determined system factor k_{sys} is introduced, see Eq. (4). It allows adjusting the withdrawal capacity related to the base material density, i.e. the density of the laminations, according to the screw application, i.e. it increases the withdrawal capacity the more layers are penetrated by the screw. This circumstance neither can be covered by inserting the product density instead of the base material density nor would this procedure be meaningful. This commitment – aimed to cover screw application in laminated timber products in general – reflects the generic character of this approach as opportunity to decrease the number of models for different applications without a loss of accuracy due to simplification.

- Thirdly, the systematic variation of gap width and type, especially in case of CLT narrow face insertion, enabled the determination of a probabilistic model quantitatively and explicitly describing the related negative impact on withdrawal strength f_{ax} , c. f. Brandner [14]. Considering currently given limits in regard to gaps and stress reliefs, c. f. Chapter 1, and further assumptions (e.g. the variabilities of density and withdrawal strength), a corresponding simplification in form of the multiplicative factor k_{gap} is applied; see Eq. (5).

Besides the explained differences, the impact of both remaining influencing parameters, the outer thread diameter and thread-grain angle, is treated in a traditional way, i.e. diameter adjustment by a negative power parameter and a bilinear model with discontinuity at $\alpha = 45^\circ$ for considering the influence of the thread-grain angle. Of course and in-line with Blaß and Uibel [11], the placement of screws in the side face of CLT elements leads to significantly higher withdrawal strengths than that in their narrow face. Deviating from Blaß and Uibel [11], Eq. (3) does not contain ℓ_{ef} as influencing parameter since no related impact on f_{ax} could be observed as far as the tip length is not part of ℓ_{ef} .

We now compare quantitatively the approaches given in Eq. (2) and Eq. (3), with special focus on screw insertion in CLT elements, with the current model for determining the characteristic withdrawal strength according to EC 5 [17]; see Eq. (6), which is based on Blaß et al. [27] and 1,212 withdrawal tests on axially loaded screws inserted in solid timber at different outer thread diameters, effective insertion lengths (counted by neglecting the tip length) and axis-to-grain angles.

$$f_{ax,k} = \frac{18.0 d^{-0.5} \ell_{ef}^{-0.1} k_d}{1.2 \cos^2 \alpha + \sin^2 \alpha}, \text{ with } f_{ax,k,corr} = f_{ax,k} \left(\frac{\rho_k}{350} \right)^{0.80} \text{ and } k_d = \min \left\{ \frac{d}{8}, 1 \right\} \quad (6)$$

In fact, the approach in Eq. (6) is very similar to Eq. (2) (the impact of d is more pronounced while the density is considered in a quite similar way). In comparison to Eq. (4), the thread-grain influence is modelled according to Hankinson [28] instead of a bi-linear approach, and there is the additional coefficient k_d , which decreases f_{ax} in case of $d < 8$ mm, which, together with the limitation to thread-grain angles $\alpha \geq 30^\circ$ in EC 5 [17] is not part of Blaß et al. [27]. Since the product CLT is not covered by the current version of EC 5 [17], Eq. (6) does not specifically consider a related application. Nevertheless, selected parameter characteristics enable a reasonable model comparison, which is illustrated in Fig. 9 to Fig. 11 in dependence of representative characteristic densities (which means single lamella strength classes; for CLT side face insertion, the relationship $\rho_{12,CLT,k} = 1.1 \rho_{12,t,k}$, was applied) and outer thread diameters. Furthermore, ℓ_{ef} was constantly set to $10 d$, as a related specification is necessary when applying Eq. (2) and Eq. (6).

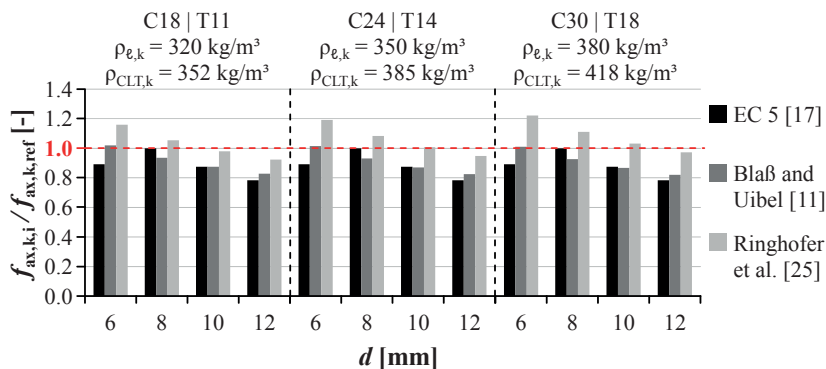


Fig. 9 Comparison of characteristic withdrawal strength according to EC 5 [17] with Blaß and Uibel [11] and Ringhofer et al. [25]) related to that of EC 5 [17] for $d = 8$ mm vs. outer thread diameter of self-tapping screws; CLT side face and perpendicular-to-grain insertion ($\alpha = 90^\circ$)

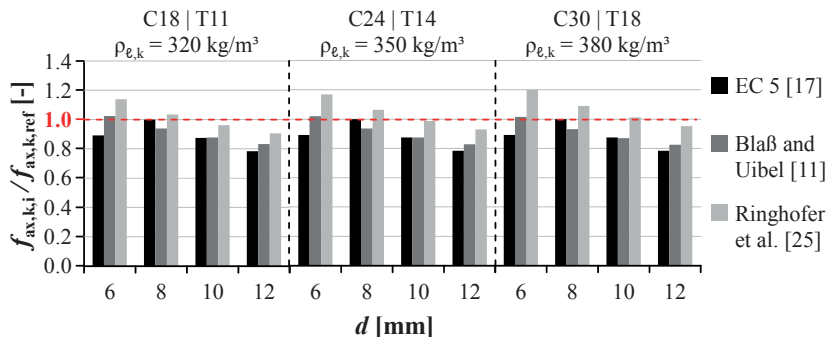


Fig. 10 Comparison of characteristic withdrawal strength according to EC 5 [17] with Blaß and Uibel [11] and Ringhofer et al. [25]) related to that of EC 5 [17] for $d = 8$ mm vs. outer thread diameter of self-tapping screws; CLT narrow face and perpendicular-to-grain insertion ($\alpha = 90^\circ$)

With regard to the comparison of characteristic withdrawal strengths for both perpendicular-to-grain insertions, once through several layers (CLT side face, Fig. 9) and once into one layer (CLT narrow face, Fig. 10), two points are worth being discussed in detail:

Firstly and even though input parameter treatment differs in the size of the power values to some extent, characteristic withdrawal strengths determined by Eq. (2) and Eq. (6) result in a nearly equal value if practically relevant outer thread diameters $d = \{8, 10, 12\}$ mm are considered.

Secondly, the new approach presented in Eq. (3) leads to remarkably higher values of $f_{ax,k}$ if compared to the two others. Furthermore, this is independent from timber density and outer thread diameter and – in case of Fig. 9 – it confirms the aforementioned statement of increased withdrawal strength due to the application of k_{sys} according to Eq. (4).

In Fig. 11, which concerns the parallel-to-grain insertion in CLT narrow face and thus only comprises approaches which take the impact of gaps on f_{ax} into account, the situation is different: here, the generic approach presented in Eq. (3) results in significantly smaller withdrawal strengths than those determined by Eq. (2), irrespective of conducted parameter variations. This conservative estimation can be explained by a less pronounced relationship between density and withdrawal strength in case of $\alpha = 0^\circ$ combined with a higher difference of f_{ax} between perpendicular- and parallel-to-grain insertion, c. f. Eq. (4) and Eq. (5).

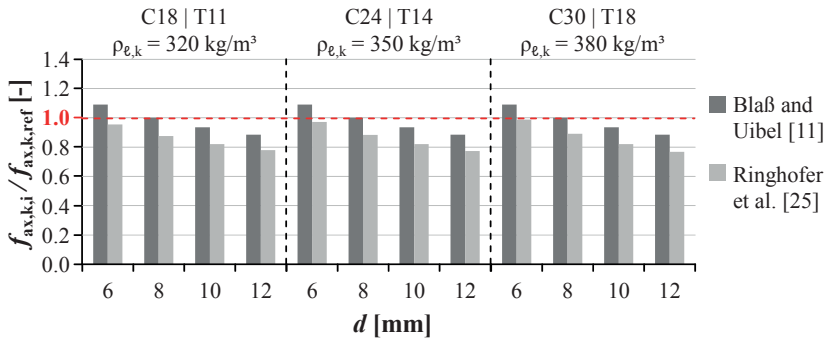


Fig. 11 Comparison of characteristic withdrawal strength according to Blaß and Uibel [11] with Ringhofer et al. [25] related to that of Blaß and Uibel [11] for $d = 8$ mm vs. outer thread diameter of self-tapping screws; CLT narrow face and parallel-to-grain insertion

3.3 Axially Loaded Profiled Nails in CLT Elements

With regard to the performance of axially loaded, profiled nails situated in the side and narrow face of CLT elements, examinations comparable to those for self-tapping screws were not conducted at Graz University of Technology. Thus, the study presented in Blaß and Uibel [11] is the exclusive source for withdrawal properties of nails in CLT discussed in this section. Since their program dedicated to the axial load situation did not distinguish between self-tapping screws and nails, it is referred to Section 3.2 for a related explanation. The sole deviations to self-tapping screws are of course the smaller nominal diameters $d = \{3.1, 4.0, 6.0\}$ mm of the nails (loadbearing class III, according to DIN 1052, 1988) as well as the

higher number of tests (523) carried out in three- and five-layered CLT panels with in total five different layouts. The characteristic approach proposed by Blaß and Uibel [11] again bases on an empirical regression model adjusted to the test results and is shown in Eq. (7):

$$f_{ax,k} = \frac{4.04 d^{-0.4}}{3.33 \cos^2 \varepsilon + \sin^2 \varepsilon}, \text{ with } f_{ax,k,corr} = f_{ax,k} \left(\frac{\rho_k}{350} \right)^{0.80} \quad (7)$$

and ε as primary insertion angle, e.g. for nails in CLT narrow face: $\varepsilon = 0^\circ$ (on a conservative but general basis), and for nails in CLT side face $\varepsilon = 90^\circ$. Apart from the pre-factor 3.33, which is significantly higher than that for self-tapping screws in Eq. (2) – possibly caused by smaller nominal diameters while the average gap width was kept constant – the considered influencing parameters as well as their treatment are very similar to those given in Eq. (2).

Fig. 12 subsequently compares characteristic withdrawal strengths of profiled nails determined according to Eq. (7) in dependence of the nominal diameter, the single layer’s characteristic density as well as the position in the CLT panel (side vs. narrow face). It again highlights the significant difference of withdrawal strength in dependence of the nail location, which is not only caused by the aforementioned pre-factor but also by applying a higher characteristic (product) density $\rho_{12,CLT,k} = 1.1 \rho_{12,t,k}$, for CLT side face if compared to narrow face insertion.

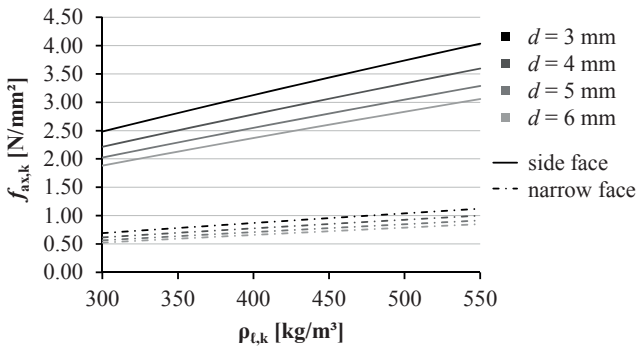


Fig. 12 Characteristic withdrawal strength vs. characteristic density $\rho_{t,k}$ of profiled nails: comparison between CLT side and narrow face insertion in dependence of the nominal nail diameter; according to Blaß and Uibel [11]

In contrast to self-tapping screws or smooth shank nails, the currently valid version of EC 5 [17] refers to design values published in the manufacturers’ declarations of performance (DoP) instead of providing a product-independent approach for determining the characteristic withdrawal strength of profiled nails. This can be

explained by significant differences in withdrawal strength of nails from different producers, which are higher than the ones caused by a variation of common influencing parameters such as the timber density or the nominal diameter, c. f. Sandhaas and Görlacher (2017). In this recently published source, it is reported that the related variability disabled the derivation of a reasonable generic approach. With regard to the average withdrawal strength of profiled nails, Sandhaas and Görlacher (2017) determined a nonlinear, empirical regression model for estimating this property, which is based on a comprehensive test database available at KIT and given in Eq. (8), see:

$$f_{ax,k} = 3.60 \cdot 10^{-3} \rho^{1.38}, \quad (8)$$

with ρ as the density of solid timber as material applied for the tests. According to Sandhaas and Görlacher (2017), this approach has a rather limited predictive quality due to a poor correlation between density and withdrawal strength. Nevertheless, it represents the average declared withdrawal strength of profiled nails in solid timber and shall be applied for a comparison with the one for CLT as published by Blaß and Uibel [11], see Eq. (9):

$$f_{ax} = \frac{0.16 d^{-0.4} \rho^{0.8}}{3.1 \cos^2 \varepsilon + \sin^2 \varepsilon}. \quad (9)$$

This comparison is subsequently illustrated in Fig. 13 in dependence of the nominal nail diameter and the layer density at $\varepsilon = 90^\circ$ and identifies remarkably higher values of f_{ax} determined by Eq. (8), especially for average timber densities of common softwood strength classes (C24 and above) according to EN 338 [15].

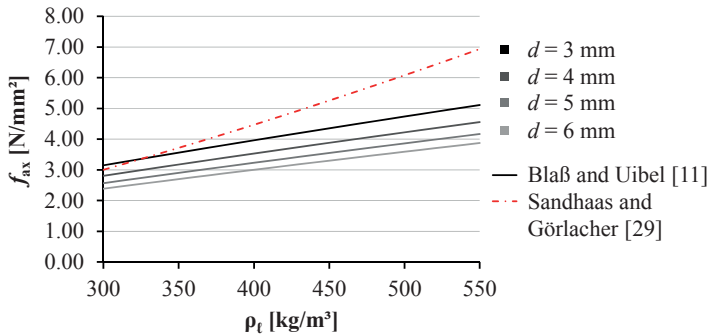


Fig. 13 Comparison of withdrawal strength of profiled nails estimated by Eq. (7) with the approach published in Sandhaas and Görlacher [29] in dependence of nominal diameter and layer density; $\varepsilon = 90^\circ$

4. Embedment Strength of Laterally loaded Dowel-Type Fasteners in CLT

4.1 General Comments and Overview

Blaß and Uibel [11] and Uibel and Blaß [12], [13], [18] were the first investigating laterally-loaded dowel-type fasteners in CLT side and narrow face by means of Central European CLT and solid wood-based panels. More recently, Kennedy et al. [26] report on investigations conducted in North America on laterally-loaded threaded-fasteners inserted in CLT side face.

In the following we summarize the main findings from the comprehensive report of Blaß and Uibel [11] as introduced in Section 3.1 and compare the proposed relationships with current design provisions for solid timber and glulam as given in EC 5 [17].

In general, the embedment strength represents a system property, the resistance of timber against impressed laterally loaded fasteners. In cases of fasteners penetrating several layers in CLT side face or two or more different laminations in the CLT narrow face, featuring different angles between fastener axis and load, this kind of system property even comprises different contributions of layers and laminations as different load-grain angles may be concerned.

4.2 Laterally loaded Dowel-Type Fasteners in CLT Side Face

4.2.1 Smooth Dowels and Tight-Fitting Bolts

Blaß and Uibel [11] tested smooth dowels with diameters $d = 8$ to 24 mm in three- and five-layer CLT elements, positioned apart or in gaps involving one to three layers, and loaded at 0° , 45° and 90° in respect to the outer layer's grain orientation. Thereby, a minor influence of the number of gaps on the embedment strength was observed together with homogenized properties with increasing number of penetrated layers.

By means of regression analysis, for the characteristic embedment strength $f_{h,k,CLT}$ of dowels inserted in CLT side face two models were found: the first, considering explicitly the CLT layup, and the second, more simplified approach, representing the investigated CLT layups and tested configurations on an average basis, see

$$f_{h,k,CLT} = \frac{32(1 - 0.015d)}{1.1\sin^2\beta + \cos^2\beta}, \text{ with } f_{h,k,CLT,corr} = f_{h,k,CLT} \left(\frac{\rho_k}{400} \right)^{1.2} \quad (10)$$

with β as angle between load and grain of outer layers and $\rho_k = 400 \text{ kg/m}^3$. This regression model is limited to the investigated parameters, the layup parameter of tested panels, i.e. the sum of layer thicknesses oriented parallel to outer layers vs. the sum of layer thicknesses oriented perpendicular to outer layers, $\sum t_{\ell,x,i} / \sum t_{\ell,y,i}$, which was between 0.95 and 2.1, and the maximum layer thickness, which was $\max[t_{\ell,i}] = 40 \text{ mm}$.

The influence of density on the embedment strength was found to be equal to solid timber; see additional tests in Blaß and Uibel [11] as well as Blaß et al. [27]. An

adjustment of Eq. (10) to $\rho_{CLT,k} = 385 \text{ kg/m}^3$, as currently proposed by PT SC5.T1 [16], would lower the resistance by 4 %.

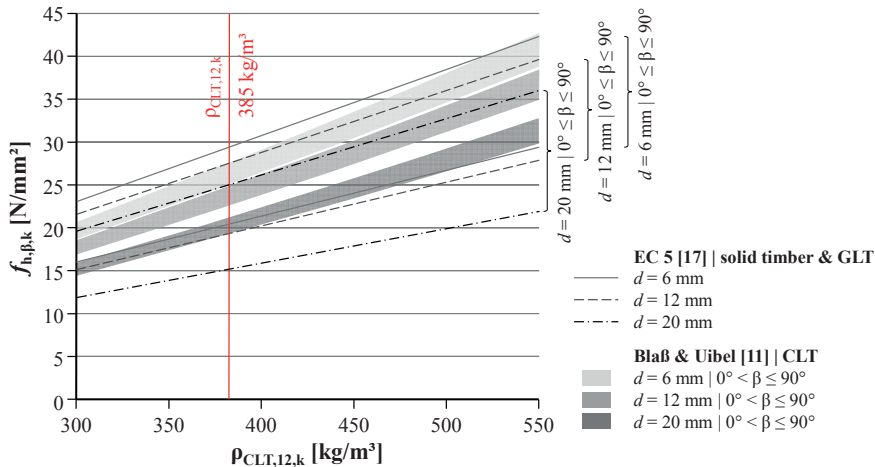


Fig. 14 Characteristic embedment strength vs. characteristic density of smooth dowels and tight-fitting bolts: comparison between EC 5 [17] (solid timber and GLT) with Blaß and Uibel [11] and Uibel and Blaß [12], [13]; CLT side face)

Fig. 14 compares the characteristic embedment strength according to Eq. (10) with the current regulation for solid timber and glulam according to EC 5 [17]; see Eq. (11). In both equations, a similar relationship between dowel diameter and embedment strength is observed. In contrast, the influence of the load-grain angle β on the embedment strength is found to be much smaller for dowels inserted in CLT side face than in solid timber and glulam. This is because the embedment strength determined on dowels inserted in CLT side face comprises both, the influence of layers oriented parallel and perpendicular to loading direction.

$$f_{h,k,EC5} = \frac{0.082(1-0.01 d)\rho_k}{k_{90} \sin^2 \beta + \cos^2 \beta} \xrightarrow{\text{with } \rho_k = 400 \text{ kg/m}^3 \text{ softwood}} f_{h,k,EC5} = \frac{32.8(1-0.01 d)}{(1.35 + 0.015 d)\sin^2 \beta + \cos^2 \beta} \quad (11)$$

Furthermore, the characteristic embedment strength of dowels with smaller diameters are closer to current regulations for dowels at $\beta = 0^\circ$ whereas the characteristic embedment strength of dowels with larger diameters is in-between current regulations for dowels at $0^\circ \leq \beta \leq 90^\circ$. This outcome may be explained in two ways: at first, splitting failures, as being more frequent for dowels with smaller diameter and loaded parallel to grain, are prevented in CLT by the orthogonal layup. Secondly, an influence of gaps on the embedment strength of dowels with smaller diameter could not be observed; the smallest diameter tested was $d = 8 \text{ mm}$.

Overall, regulation of embedment strength for smooth dowels and tight-fitting bolts inserted in CLT side face is suggested equal to solid timber and glulam, with adjustment factors for very small dowel diameters, accounting for a potential negative influence of gaps, and an adapted k_{90} -factor (see Eq. (11)), taking into account the joint action of layers featuring different load-grain angles in CLT.

4.2.2 Profiled Nails and Self-Tapping Screws

Blaß and Uibel [11] and Uibel and Blaß [12], [13] report also on embedment tests with self-tapping screws and smooth nails in the side face of wood-based panels with layer thicknesses $t_{\ell,i} \leq 7$ mm. The thin layers together with the reinforcing transverse layers lead to rather high characteristic embedment strengths $f_{h,k,CLT}$ in comparison with $f_{h,k,EC5}$ for glulam and solid timber according to EC 5 [17], see

$$f_{h,k,CLT} = 60 d^{-0.5}, \text{ with } f_{h,k,CLT,corr} = f_{h,k,CLT} \left(\frac{\rho_k}{400} \right)^{1.05} \quad (12)$$

$$f_{h,k,EC5} = 0.082 \rho_k d^{-0.3} \xrightarrow{\text{with } \rho_k = 400 \text{ kg/m}^3} f_{h,k,EC5} = 32.8 d^{-0.3}$$

In CLT all nails and screws were inserted without predrilling. Although the embedment tests were conducted with smooth nails, Eq. (12) for CLT is limited to profiled nails, e.g. helically threaded nails and annular ringed shank nails.

As already observed in previous investigations, for dowel-type fasteners without predrilling, no influence of load-grain angle on embedment strength is observed.

In their design proposal, Blaß and Uibel [11] and Uibel and Blaß [13] limit Eq. (12) to layer thicknesses of $t_{\ell,i} \leq 9$ mm. Thus, for common CLT with standard layer thicknesses of $t_{\ell,ref} = 20, 30$ and 40 mm this equation is of minor concern. In case of CLT featuring layers with $t_{\ell,i} > 9$ mm, Blaß and Uibel [11] suggest calculating the embedment strength of laterally loaded profiled nails and self-tapping screws, inserted without predrilling, equal to solid timber. This again allows harmonizing regulations for solid timber, glulam and CLT.

4.3 Laterally Loaded Dowel-Type Fasteners in CLT Narrow Face

4.3.1 General Comments

In contrast to CLT side face, in CLT narrow face positioning of fasteners parallel and/or perpendicular to grain within and between single laminations as well as between layers is possible. Furthermore, gaps may have a more significant influence on the embedment strength of fasteners positioned in narrow face than in side face.

Laterally loaded dowel-type fasteners positioned in the CLT narrow face can be loaded in-plane, out-of-plane or a combination of both; see Fig. 15. If loaded out-of-plane, tension perpendicular to grain stresses potentially causing early splitting

and delamination of layers have to be considered; minimum requirements on layer and CLT thickness are presented later in Chapter 5. As the fasteners are inserted in or between laminations, for calculation of the characteristic embedment strength the characteristic density of the laminations, $\rho_{k,\ell}$, applies.

Although Uibel and Blaß in Schickhofer et al. [4] recommend not using smooth dowels, tight-fitting bolts or profiled nails in the narrow face of CLT, neither for bearing axial nor lateral loads, the models derived from testing are briefly presented.

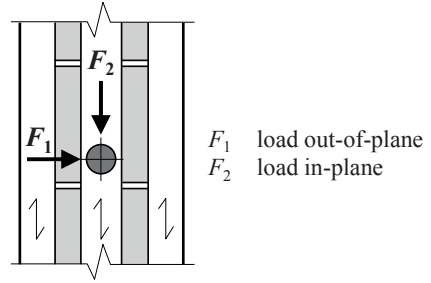


Fig. 15 Laterally loaded dowel-type fasteners in CLT narrow face: principal load directions

4.3.2 Smooth Dowels and Tight-Fitting Bolts

For laterally loaded dowels in CLT narrow face the following relevant parameters were identified (Blaß and Uibel [11]):

- angle between dowel axis and grain of the penetrated CLT layer;
- ratio between dowel diameter and thickness of the penetrated CLT layer, $d / t_{\ell,i}$;
- position of dowels relative to longitudinal and lateral gaps as well as stress reliefs.

During testing, Blaß and Uibel [11] frequently observed splitting failures, due to tension stresses perpendicular to grain, in combination with rolling shear of the penetrated layer in case of dowels inserted parallel to grain. Low resistances were found for dowels inserted perpendicular to grain, featuring a diameter d close to the penetrated layer thickness $t_{\ell,i}$ and loaded out-of-plane. This is because of the adjacent layers with grain oriented parallel to dowel axis, which are activated in compression perpendicular to grain.

From all tested configurations (dowels inserted parallel / perpendicular to grain, in / close to gaps within / between layers) the lowest resistances were observed when dowels with diameter $d < t_{\ell,i}$ were inserted parallel to grain and loaded in-plane. Based on these outcomes and by means of regression analysis the following conservative but universally applicable approach, independent of the load-grain angle, was defined:

$$f_{h,k,CLT} = 9(1 - 0.017 d), \text{ with } f_{h,k,CLT,corr} = f_{h,k,CLT} \left(\frac{\rho_{k,\ell}}{350} \right)^{0.91} \quad (13)$$

4.3.3 Profiled Nails and Self-Tapping Screws

By testing the embedment strength of dowel-type fasteners in the CLT narrow face, smooth nails and self-tapping screws, inserted without predrilling, were used; see Blaß and Uibel [11] and Uibel and Blaß [18], [13]. The embedment strength of screws was determined for the threaded part.

By testing the same load configurations as for dowels, the lowest resistances were again observed when nails or screws with diameters $d < t_{l,i}$ were inserted parallel to grain and loaded in-plane. Based on these outcomes and by means of regression analysis the following conservative but universally applicable approach, independent of the load-grain angle, was defined:

$$f_{h,k,CLT} = 20 d^{-0.5}, \text{ with } f_{h,k,CLT,corr} = f_{h,k,CLT} \left(\frac{\rho_{k,\ell}}{350} \right)^{0.56} \quad (14)$$

In contrast to EC 5 [17] where the effective (core) diameter of screws, d_{ef} , shall be used, according to Eq. (14) the nominal (outer) diameter d applies for both, nails and screws.

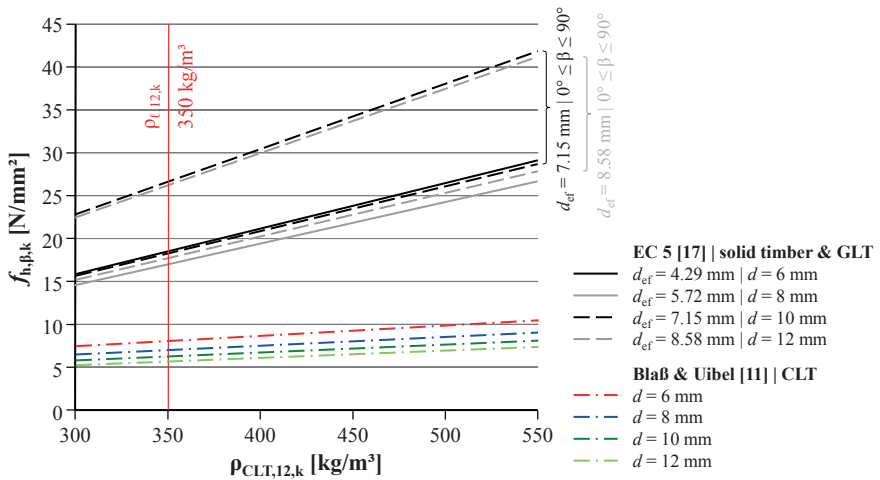


Fig. 16 Characteristic embedment strength vs. characteristic density of self-tapping screws: comparison between EC 5 [17] (solid timber and GLT) with Blaß and Uibel [11] (CLT narrow face); $d_{ef} = 1.1$ ($0.65 d$) assumed; note: acc. to EC 5 [17] screws with $d_{ef} \leq 6$ mm are treated like nails (inserted without predrilling; no influence of load-grain angle), with $d_{ef} > 6$ mm as dowels (inserted with predrilling; influence of load-grain angle)

In comparison to the embedment strength of nails and screws positioned in CLT side face (see Eq. (12)), in CLT narrow face only 1/3 of the resistance can be utilized. This is also reflected in Fig. 16 were a comparison between the approach of Blaß and Uibel [11] and Uibel and Blaß [13] with that in EC 5 [17] for screws inserted in solid timber and glulam is presented.

Aiming on harmonizing the regulations for embedment strength of fasteners positioned in solid timber, glulam and CLT, for laterally loaded self-tapping screws (and nails) in CLT narrow face an additional coefficient $k_{\text{lat,CLT,NF}}$, taking into account the load configuration delivering the lowest embedment strength, and by additionally neglecting the influence of the load-grain angle, as anchored in EC 5 [17], is proposed, see

$$f_{\text{h,k,CLT,NF}} = k_{\text{lat,CLT,NF}} f_{\text{h,k,0,ST \& GLT}}, \text{ with } k_{\text{lat,CLT,NF}} = 0.25 \quad (15)$$

with $f_{\text{h,k,CLT,NF}}$ and $f_{\text{h,k,0,ST \& GLT}}$ as the characteristic embedment strength of laterally loaded self-tapping screws in the narrow face of CLT and the characteristic embedment strength in solid timber and glulam (GLT) at a load-grain angle of $\beta = 0^\circ$, respectively.

5. Joint Design

5.1 Introduction and Overview

In addition to withdrawal and embedment strength, as timber-related relevant fastener properties which are necessary for determining the single fastener's load-bearing capacity (according to Eq. (10) for axial and e.g. according to Johansen [30] for lateral loading), for an appropriate design of joints, comprising groups of fasteners, in CLT there are further specifics required which are also related to timber. These additional specifics and verifications are often directly linked to joint failure modes. One required verification is the resistance of the component's net cross-section. Another verification is the load-bearing capacity of the group of fasteners, which concerns their effective number, n_{ef} , as well as the minimum spacing and the edge and end distances, a_i . It is worth pointing out that both properties, n_{ef} and a_i , are closely related to each other, i.e. $n_{\text{ef}} = n$ can be only achieved if the single fastener in conjunction with the anchorage material provides enough ductility for load redistribution and the minimum spacing (especially parallel to grain, a_1) is fulfilled, preventing unfavorable failure modes such as splitting parallel-to-grain or block shear.

With regard to the state-of-the-art knowledge on both, n_{ef} and a_i , many aspects are already covered by the report of Blaß and Uibel [11]. This source contains a comprehensive study aiming on the lateral load-bearing behavior of connections composed by dowels, nails and screws, situated in the side and narrow faces of CLT elements. Further and more recent publications, focusing on predominately axially loaded joints, are e.g. Mahlkecht and Brandner [31], Plüss and Brandner [33] and Brandner [14]. The main outcomes and recommendations from

these publications are summarized and discussed in the following Sections 5.2 and 5.3.

Other publications which frequently examine dowel-type connections in CLT are more related to their cyclic load-bearing behavior and not to n_{ef} and a_i , e.g. Flatscher et al. [34] and Gavric et al. [35].

5.2 Laterally Loaded Dowel-Type Joints in CLT

Blaß and Uibel [11] conducted a comprehensive test program on laterally loaded connections in order to validate the applicability of their approaches for the characteristic embedment strength of dowels, self-tapping screws and nails for design purposes as well as for determining dowels and verifying nails and screws minimum spacing for CLT; see Fig. 17.

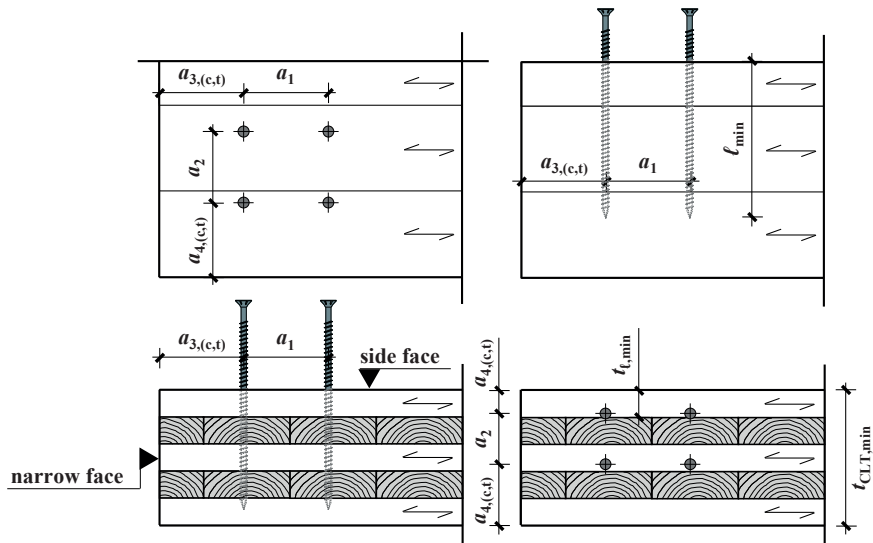


Fig. 17 Definition of minimum spacing, edge and end distances and further geometrical boundary conditions, exemplarily for self-tapping screws; according to Blaß and Uibel [11]

Apart from the applied fasteners and their position within the CLT element (side vs. narrow face), Blaß and Uibel [11] also varied the type of connection (steel-to-timber joints with inner and outer steel plate as well as CLT-CLT lap joints, both with one or two shear planes), the fastener diameter (dowels: $d = \{8, 12, 16, 20, 24\}$ mm; screws: $d = \{8, 12\}$ mm; profiled nails: $d = \{4, 6\}$ mm), the number of fasteners in the group, n , as well as their spacing, edge and end distances and further geometrical boundary conditions, which are illustrated in Fig. 17.

The observations made by Blaß and Uibel [11] during testing joints of laterally loaded dowel-type fasteners in the CLT side face are summarized briefly:

- Apart from some specimen which failed in the zone of load introduction, other failure modes observed by testing joints with dowels were some tension failure in layers close to the shear plane, successive shear & rolling shear failures and some block shear failures, whereby block shear failure emerged without regularity.
- As the number of dowels placed parallel to the outer layer's grain direction did not influence the load-bearing capacity, Blaß and Uibel [11] concluded that the effective number of fasteners n_{ef} can be set equal to their total number n .
- The load-carrying capacity of joints with dowels was predicted by means of the theory of Johansen [30] and the characteristic embedment strength $f_{h,k}$ according to Eq. (10). This characteristic embedment strength $f_{h,k}$ only implicitly represents an inhomogeneous stress distribution along the fastener axis due to penetrated alternating orthogonal layers. Despite these circumstance and although the joint's failure modes differed widely from failure modes observed by testing single dowels, overall good to conservative predictions of the load-carrying capacity of dowel joints were made.
- Good validation for the embedment strength as input parameter in Johansen's [30] theory was also achieved for the majority of tested joints with self-tapping screws and nails. This also concerned the withdrawal strength as basis for the rope effect. The regulation of $n_{ef} = n$ is also proposed for these fasteners.

Similar to joints in CLT side face, proposals made by Blaß and Uibel [11] for the CLT narrow face could also successfully validated. Two important observations made during testing are summarized in brief:

- Joints with dowels situated in layers perpendicular to grain and loaded parallel to grain failed by splitting already at small deformations. However, due to the implicit conservatism in predictions according to Blaß and Uibel [11] even these failure modes are covered but it is pointed out that the given recommendations are only proven for tested CLT layouts and configurations.
- Tests with laterally loaded self-tapping screws situated in the CLT narrow face showed that for some configurations minimum spacing determined by insertion tests in advance were too small. Consequently, Blaß and Uibel [11] increased the corresponding values.

Minimum spacing, edge and end distances and further geometrical boundary conditions, as defined in Fig. 17, as outcome of the comprehensive test campaigns and proposal in Blaß and Uibel [11], [37] are summarized in Table 2 and Table 3.

Table 2 Minimum spacing, edge and end distances of dowel-type fasteners in CLT; according to Blaß and Uibel [11], [37]

Fastener	Position	a_1	a_2	$a_{3,t}$	$a_{3,c}$	$a_{4,t}$	$a_{4,c}$
Self-tapping screws	Side face	$4 d$	$2.5 d$	$6 d$	$6 d$	$6 d$	$2.5 d$
	Narrow face	$10 d$	$3 d$	$12 d$	$7 d$	$5 d$	$5 d$
(Profiled) nails	Side face	$(3 + 3 \cos \beta) d$	$3 d$	$(7 + 3 \cos \beta) d$	$6 d$	$(3 + 4 \sin \beta) d$	$3 d$
Dowels	Side face	$(3 + 2 \cos \beta) d$	$4 d$	$5 d$	$\min[3 d, 4 d \sin \beta]$	$3 d$	$3 d$
	Narrow face	$4 d$	$3 d$	$5 d$	$3 d$	–	$3 d$

Table 3 Further geometrical boundary conditions for dowel-type fasteners in the narrow face of CLT; according to Blaß and Uibel [11], [37]

Fastener type	$t_{\text{CLT},\text{min}}$	$t_{\text{t},\text{min}}$	ℓ_{min}^*
Self-tapping screws	$10 d$	$d \leq 8 \text{ mm}: 2 d$ $d > 8 \text{ mm}: 3 d$	$10 d$
Dowels	$6 d$	d	$5 d$

* Dowels: minimum timber thickness, screws: minimum insertion depth

5.3 Axially Loaded Dowel-Type Joints in CLT Restricted to Self-Tapping Screws

In respect to axially-loaded fasteners, it has to be outlined that a_i , n_{ef} and additional geometrical boundary conditions in Blaß and Uibel [11] are only based on insertion tests (in respect to a_i for nails and screws) as well as tested lap-joints. Additional experimental campaigns were conducted at Graz University of Technology in order to validate the recommendations given by Blaß and Uibel [11] also for axially loaded (concentrated) joints in CLT. This concerned joints with self-tapping screws since these fasteners are exclusively applied for the transmission of heavy loads as well as for efficient system connectors, c. f. Chapter 1. The related studies are summarized separately in dependence of the screw position in the CLT panel:

Mahlknecht and Brandner [31] investigated concentrated joints of screws inserted via the CLT side face, by varying the minimum spacing $\{a_1, a_2\}$, the insertion depth ℓ_{min} as well as the number of screws, n . Despite the orthogonal layup of CLT and although the screws penetrated several layers, brittle block shear failure modes, as combination of rolling shear failure and failure in tension perpendicular to grain,

were observed up to spacing $a_1 = a_2 < 7 d$ and depending on ℓ_{\min} ; c. f. Fig. 18. This failure mode, which is perhaps even more relevant for solid timber and GLT, misses so far a verification approach; a first proposal for solid timber and glulam is presented in Mahlkecht et al. [32].

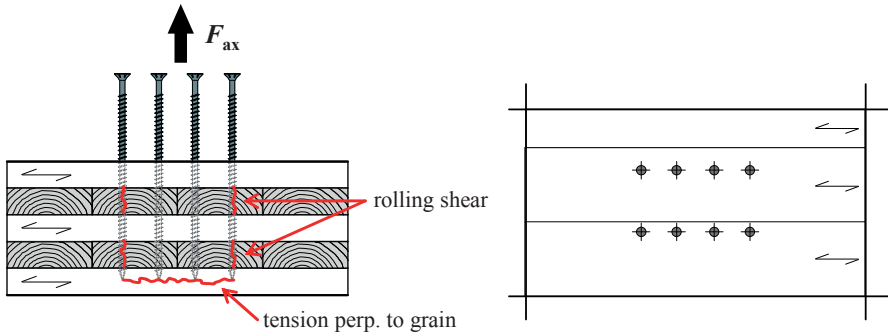


Fig. 18 Block shear failure of axially loaded groups of self-tapping screws situated in the CLT side face

Plüss [36] conducted comprehensive tests on concentrated groups of axially-loaded screws in the CLT narrow face. The CLT layout, the number of fasteners, the thread-fiber angle as well as the spacing between the fasteners were varied. Table 4 summarizes recommendations for a_i as given by Plüss and Brandner [33]. Not surprisingly, a_1 decreasing with α was observed. Comparing the recommendations given in

for lateral and in Table 4 for axial loading for the worst case of $\alpha = 90^\circ$, Table 4 gives slightly smaller minimum requirements.

Table 4 Minimum spacing of axially loaded self-tapping screws situated in the narrow face of CLT in dependence of α ; according to Plüss and Brandner [33]

α	a_1	a_2
0°	$2.5 d$	$5 d / 2.5 d^*$
45°	$5 d$	
90°	$7 d$	
$0^\circ 90^\circ$	$5 d$	
$45^\circ 45^\circ$	$5 d$	

* $5 d$ if inserted in the same layer, $2.5 d$ if inserted in different layers

With regard to the effective number of axially loaded self-tapping screws situated in CLT and basing on a successful verification by Mahlkecht and Brandner [31] (so far block shear failure can be prevented) and Plüss and Brandner [33], Brandner et al. 2016 [2] propose Eq. (16) for a related determination:

$$F_{ax,n} = 0.90 \sum_{i=1}^R F_{ax,ref,i} n_i, \quad (16)$$

with R as the number of different thread-fiber angles, n_i as the number of screws per thread-fiber angle and $F_{ax,ref,i}$ as reference withdrawal capacity of a single fastener for a specific thread-fiber angle. Note: laboratory tests indicated even $n_{ef} \geq n$, which is dedicated to the homogenization occurring with increasing number of screws in a group. The pre-factor 0.9 shall cover inevitable inaccuracies in practical joint execution.

6. Conclusions

Based on the compiled state-of-knowledge on axially and laterally loaded dowel-type fasteners in CLT as well as the comparisons made with current regulations on dowel-type fasteners in solid timber and glulam according to EC 5 [17], the following conclusions are made:

- It is suggested to regulate the embedment as well as the withdrawal strengths of dowel-type fasteners in CLT in analogy to solid timber and glulam. Therefore, generic approaches as exemplarily presented for the withdrawal capacity of self-tapping screws in Eqs. (3–5), should be defined. Some suggestions how to regulate the embedment strength of dowel-type fasteners in CLT based on that of solid timber are already presented in Chapter 4. For profiled nails, recent studies as well as the provisions in EC 5 [17] indicate the necessity of performance testing for axial loading.
- Based on current test experience the following suggestions can be made for applications of dowel-type fasteners in respect to loading and positioning in CLT:

Table 5 Dowel-type fasteners in CLT side and narrow face: recommended applications according to Schickhofer et al. [4]

	Side face	Narrow face
Profiled nails	for axial and lateral loads	not applicable
Smooth dowels and tight-fitting bolts	only for lateral loads	not applicable
Self-tapping screws	for axial and lateral loads	for axial and lateral loads

- In respect to laterally loaded joints composed by dowel-type fasteners in CLT, the ductile behavior in case of side face insertion, which is due to the orthogonal reinforcing layout of CLT, enables $n_{ef} = n$. For laterally loaded fasteners in the CLT narrow face, n_{ef} should be calculated according to the design provisions for solid timber, as e.g. given in EC 5 [17]. For axially loaded self-tapping screws inserted in CLT side or narrow face a suggestion for n_{ef} is given in Eq. (16).

Regulations on minimum spacing and edge and end distances have to consider the specific structure of CLT, i.e. the orthogonal layout and the influence of gaps. Proposals together with additional geometrical regulations can be found in

- to Table 4.
- Apart from regulations on single fastener properties and joints, to ensure the integrity of solid timber constructions with CLT the following maximum spacing e_{max} between joints are recommended:

Table 6 Execution requirements for CLT joints according to ÖNORM B 1995-1-1 [38]

joint type	e_{max} [mm]
CLT to CLT with screws	500
CLT to GLT with screws	500
CLT to steel girders with screws	750
CLT to solid components with angle brackets	1,000

7. Acknowledgements

The publication, as part of the proceedings from the Conference of COST Action FP1402 "International Conference on Connections in Timber Engineering – From Research to Standards", held on the 13th September 2017 at Graz University of Technology, Graz, Austria, was written in the framework of the COST Action FP1402 "Basis of Structural Timber Design – from Research to Standards", chaired by Philipp Dietsch, Technische Universität München (www.costfp1402.tum.de).

8. References

- [1] EN 16351: 2015, "Timber structures – Cross laminated timber – Requirements", CEN, 2015.
- [2] Brandner R., Flatscher G., Ringhofer A., Schickhofer G., and Thiel A., "Cross laminated timber (CLT): overview and development", *European Journal of Wood and Wood Products*, Vol. 74, 2016, pp. 331–351, DOI 10.1007/s00107-015-0999-5.
- [3] Flatscher G., and Schickhofer G., "Displacement-Based Determination of

Laterally Loaded Cross Laminated Timber (CLT) Wall Systems”, 3rd *INTER-Meeting*, 2016, Graz, Austria.

- [4] Schickhofer G., Bogensperger T., and Moosbrugger T. (eds., 2010) “*BSPhandbuch: Holz-Massivbauweise in Brettsperrholz – Nachweise auf Basis des neuen europäischen Normenkonzepts*”, Verlag der Technischen Universität Graz, Graz, Austria, 2010 (in German).
- [5] Bernasconi A., “Überbauung Via Cenni Mailand – 4 Holzhochhäuser mit je 9 Geschossen”, *Internationales Holzbau-Forum*, 2012, Garmisch Partenkirchen, Germany (in German).
- [6] Polastri A., Angeli A., and Gianni D. R., “A new construction system for CLT structures”, *World Conference on Timber Engineering (WCTE)*, Quebec City, Canada, 2014.
- [7] Polastri A., Giongo I., Angeli A., and Brandner R., “Mechanical characterization of a pre-fabricated connection system for cross laminated timber structures in seismic regions”, *Engineering Structures*, 2017 (accepted).
- [8] Kraler A., Kögl J., Maderebner R., and Flach M., “SHERPA-CLT-Connector for cross laminated timber (CLT) elements”, *World Conference on Timber Engineering (WCTE)*, 2014, Quebec City, Canada.
- [9] Rothoblaas, “*Wood Connectors and Timber Plates*”, catalogue, 2015.
- [10] Sherpa, “*Sherpa Manual*”, catalogue, 2013.
- [11] Blaß H. J., and Uibel T. “Tragfähigkeit von stiftförmigen Verbindungsmitteln in Brettsperrholz”, *Karlsruher Berichte zum Ingenieurholzbau*, Band 8, Universitätsverlag Karlsruhe, 2007, ISBN 978-3-86644-129-3 (in German).
- [12] Uibel T., and Blaß H. J., “Load carrying capacity of joints with dowel type fasteners in solid wood panels”, *Proceedings of the CIB Working Commission W18–Timber Structures*, 39th meeting, 2006, Florence, Italy.
- [13] Uibel T., and Blaß H. J., “*Joints with dowel type fasteners in CLT structures*”, In: Harris R., Ringhofer A., and Schickhofer G. (eds.) *COST Action FP1004: focus solid timber solutions – European conference on cross laminated timber (CLT)*, The University of Bath, Bath, 2013.
- [14] Brandner R., “Group action of axially loaded screws in the narrow face of cross laminated timber”, *World Conference on Timber Engineering (WCTE)*, Vienna, Austria, 2016.
- [15] EN 338: 2016, “Structural timber – Strength classes”, CEN, 2016.
- [16] PT SC5.T1, “Working draft of design of cross laminated timber in a revised Eurocode 5-1-1”, 2017, Version: 2017-07-1.
- [17] EN 1995-1-1: 2004 + AC:2006 + A1:2008 + A2:2014, “Eurocode 5: Design of timber structures – Part 1-1: General – Common rules and rules for buildings”,

CEN, 2014.

- [18] Uibel T., and Blaß H. J., “Edge joints with dowel type fasteners in cross-laminated timber”, *Proceedings of the CIB Working Commission W18–Timber Structures*. 40th meeting, 2007, Bled, Slovenia.
- [19] Ringhofer A., “Axially Loaded Self-Tapping Screws in Solid Timber and Laminated Timber Products”, Dissertation, Graz University of Technology, Graz, 2017.
- [20] Reichelt B., “Einfluss der Sperrwirkung auf den Auszieh Widerstand selbstbohrender Holzschrauben”, Master thesis, Graz University of Technology, 2012 (in German).
- [21] Ringhofer A., Brandner R., and Schickhofer G., “Withdrawal resistance of self-tapping screws in unidirectional and orthogonal layered timber products”, *Journal of Material Structures*, Vol. 48, 2015, pp. 1435–1447.
- [22] Grabner M., “Einflussparameter auf den Auszieh Widerstand selbstbohrender Holzschrauben in BSP-Schmalflächen”, Master thesis, Graz University of Technology, 2013 (in German).
- [23] Brandner R., Ringhofer A., Grabner M., “Probabilistic Models for the Withdrawal Behavior of Single Self-Tapping Screws in the Narrow Face of Cross Laminated Timber”, *European Journal of Wood and Wood Products*, 2017, doi:10.1007/s00107-017-1226-3.
- [24] Silva C., Branco J. M., Ringhofer A., Lourenco P. B., Schickhofer G., “The influences of moisture content variation, number and width of gaps on the withdrawal resistance of self tapping screws inserted in cross laminated timber”, *Construction and Building Materials*, Vol. 125, 2016, pp. 1205-1215.
- [25] Ringhofer A., Brandner R., and Schickhofer G., “A universal approach for withdrawal properties of self-tapping screws in solid timber and laminated timber products”, *2nd INTER-Meeting*, Sibenik, Croatia, 2015.
- [26] Kennedy S., Salenikovich A., Munoz W., and Mohammad M., “Design equations for dowel embedment strength and withdrawal resistance for threaded fasteners in CLT”, *World Conference on Timber Engineering (WCTE)*, Quebec City, Canada, 2014.
- [27] Blaß H. J., Bejtka I., and Uibel T., “Tragfähigkeit von Verbindungen mit selbstbohrenden Holzschrauben mit Vollgewinde”, *Karlsruher Berichte zum Ingenieurholzbau*, Band 4, Universitätsverlag Karlsruhe, 2006, ISBN 3-86644-034-0 (in German).
- [28] Hankinson R. L., “Investigation of crushing strength of spruce at various angles to the grain”, In: *Air Service Information Circular 3*, number 259. Materials Section Paper No. 130.
- [29] Sandhaas C., and Görlacher R., “Nailed joints: Investigation on parameters for Johansen model”, *4th INTER-Meeting*, 2017, Kyoto, Japan.

- [30] Johansen K. W., “Theory of timber connections”, *International Association for Bridge and Structural Engineering*, Vol. 9, 1949, pp. 249–262.
- [31] Mahlknrecht U., and Brandner R., “Untersuchungen des mechanischen Verhaltens von Schrauben-Verbindungsmittelgruppen in VH, BSH und BSP”, Research Report, holz.bau forschungs gmbh, Graz, 2013 (in German).
- [32] Mahlknrecht U., Brandner R., Ringhofer A., and Schickhofer G., “Resistance and failure modes of axially loaded groups of screws”, In: Aicher S., Reinhardt H. W., and Garrecht H. (eds) *Materials and joints in timber structures*, RILEM Book series 9, 2014, doi:10.1007/978-94-007-7811-5_27.
- [33] Plüss Y., and Brandner R., “Untersuchungen zum Tragverhalten von axial beanspruchten Schraubengruppen in der Schmalseite von Brettspertholz (BSP)”, In: *20. Internationales Holzbau-Forum IHF*, Garmisch-Partenkirchen, Germany, 2014 (in German).
- [34] Flatscher G., Bratulic K., Schickhofer G., „Screwed joints in cross laminated timber structures“, *World Conference on Timber Engineering (WCTE)*, Quebec City, Canada, 2014.
- [35] Gavric I., Fragiacomio M., Ceccotti A., “Cyclic behavior of typical screwed connections for cross-laminated (CLT) structures”, *European Journal of Wood and Wood Products*, Vol. 73, 2015, pp. 179–191, DOI 10.1007/s00107-014-0877-6.
- [36] Plüss Y., “Prüftechnische Ermittlung des Tragverhaltens von Schraubengruppen in der BSP-Schmalfläche”, Master thesis, Graz University of Technology, 2014 (in German).
- [37] Blaß H. J., and Uibel T., “Bemessungsvorschläge für Verbindungsmittel in Brettspertholz”, *Bauen mit Holz*, Vol. 111, 2009, pp. 46-53 (in German).
- [38] ÖNORM B 1995-1-1, “Eurocode 5: Design of timber structures – Part 1-1: General – Common rules and rules for buildings – National specifications for the implementation of ÖNORM EN 1995-1-1, national comments and national supplements”, ASI, 2015 (in German).

Performance of Dowel-Type Fasteners for Hybrid Timber Structures

Alfredo M. P. G. Dias
Assistant Professor
University of Coimbra
Coimbra, Portugal

Summary

One of the most popular Timber-Concrete connection types is the dowel type fastener, due to many factors, such as for example, simplicity, low cost and adequate performance in most conditions. This connection type was traditionally used in timber structures and was adopted for composite structures from the early ages. The basic phenomena governing the mechanical behavior of timber-timber and timber-concrete connections with dowel type fasteners are similar, however, the last show some relevant specificities due largely to the presence of concrete. Such specificities have a non-negligible influence in the performance and consequently in modelling and design. In this paper such specificities are discussed, as well as, their consequences in the modelling. Based on this analysis proposals are made for models to estimate the connections' load carrying capacity and slip modulus.

1. Introduction

Timber-concrete structures have become increasingly popular all over the world in both rehabilitation and new construction [1]. One of the critical components of this composite system are the connections, which shall transmit the load between timber and concrete with the minimal deformation [2]. From the early ages of Timber-Concrete Composites (TCC) the adoption of timber-timber connection solutions was an option, namely the dowel-type fasteners. These were in many cases combined with solutions specific for TCC such as notches [3]. Different dowel type fasteners have been tried and used in TCC, namely, screws, dowels, nails or bolts [4]. These are simple, relatively cheap and available everywhere, being suitable in a wide range of applications [5], leading to a significant use in practice.

The design methods available for timber-timber connections have also been adopted. The mechanical performance of the TCC connections is, however, different from the one from timber-timber connections, mostly due to the concrete behavior. This has necessarily a direct influence in the modelling and design of TCC connections.

In this paper a comparative analysis will be made between timber-timber and TCC connections. The focus will be on the differences and similarities in the mechanical performance as well as the consequences from these differences to the modelling and design.

2. Mechanical Performance

The basic phenomena involved with the performance of TCC connections do have significant similarities with the ones of timber-timber connections, namely in what regard to the load transmission mechanisms which are rather similar. As mentioned before the most significant differences are related to the concrete mechanical behavior. Concrete is a brittle material, with low plastic deformation capacity, associated with a high elasticity modulus when compared with that of timber. The ratio between timber and concrete elasticity modulus is generally higher than 2 leading to completely different deformation levels in the two materials. Another difference with implication in the performance is the production, usually the fastener is cast in concrete side and inserted after predrilling in timber side. This leads to a perfect fitting in the concrete side and to a partially fitting in timber side.

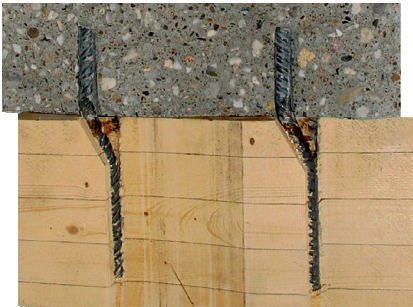


Fig. 1 Tested TCC connection

Fig. 1 shows a TCC connection after being tested, evidencing the damage in timber and concrete.

From the image it is clear the formation of the two plastic hinges as predicted from Johansen model [6]. The damage is visible in both materials, but clearly it is much more significant in timber side. Significant embedding takes place on timber while on concrete side only some crushing signs are visible.

Another important aspect is the pull-out of the fastener in both timber and concrete side. No signs of pull out can be found in any of the materials, which is perfectly in line with the observations and measurements from the experimental tests on which, no significant pull-out could be identified [2]. In this particular situation the dowel used was obtained from profiled steel bars, developed to increase the anchor forces in concrete. Similar tests were performed with smooth bars and similar behavior was observed. On the other hand, in timber the dowels were inserted into tight fitting predrilled holes. In these conditions the bar profile could increase the damage in the timber and lead to a lower pull-out capacity, but such situation could not be observed in the tests [2].

2.1 Load Carrying Capacity

The load carrying capacity of dowel type fasteners is mostly governed by the development of the bending-shear transmission mechanisms. In spite of that, other phenomena such as the friction or the rope effect do also contribute.

The basic load transmission is similar in timber-timber and TCC connections. There are, however, two main differences, the lower deformation in concrete side and the crushing of concrete. The lower deformability in concrete side will lead to a more effective load transmission and consequently to a collapse for a higher load level. Additionally, the crushing of concrete will lead to a fastener length without contact with concrete and consequently to a less effective load transmission.

In terms of secondary transmission mechanisms the friction component will also increase with the higher contact which results from the lower deformability. Similarly, the higher axially load carrying capacity and low axial deformation will contribute to increase the rope effect in this type of connections. In Fig. 2 results from numerical simulation in a TCC connection with different levels of friction/axial boundary in the fastener [7] are presented.

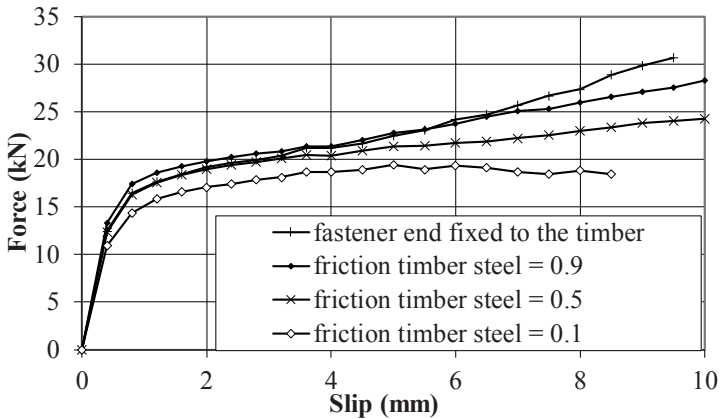


Fig. 2 Influence of the friction and pull out strength in the connection performance [7]

It is clear from the numerical load slip curves that these effects do have a non-negligible influence in the connection's load carrying capacity. On the other hand, the analysis of experimental load slip curves do show high hardening level, which results largely from the contribution of the secondary load transmission mechanisms. In Fig. 3 a number of such experimental curves for both smooth and profiled bars are shown, where this effect is visible.

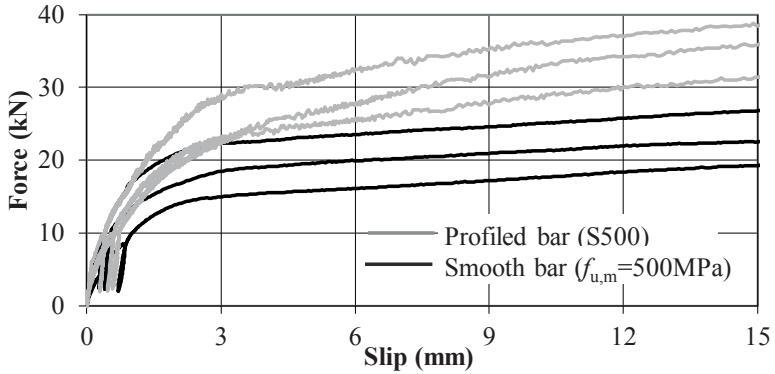


Fig. 3 Experimental load slip curves for smooth and profiled bars [7]

It is also clear, from the experimental load slip curves, that the hardening for profiled bars is higher than the one for smooth bars.

In some particular conditions the load carrying capacity can be governed by global failure in concrete side. Indeed, when non reinforced concrete is used, in combination with high fastener diameter/concrete thickness rates, then concrete collapse due to cracking is likely to occur. In this case the plastic deformation is suddenly interrupted by the premature brittle collapse of concrete [8].

In Fig. 4 load slip curves for various connectors and types of steel are given, clearly when higher diameters or steel grades are used the probability of premature concrete cracking increases, with the consequent reduction in the connection’s load carrying capacity.

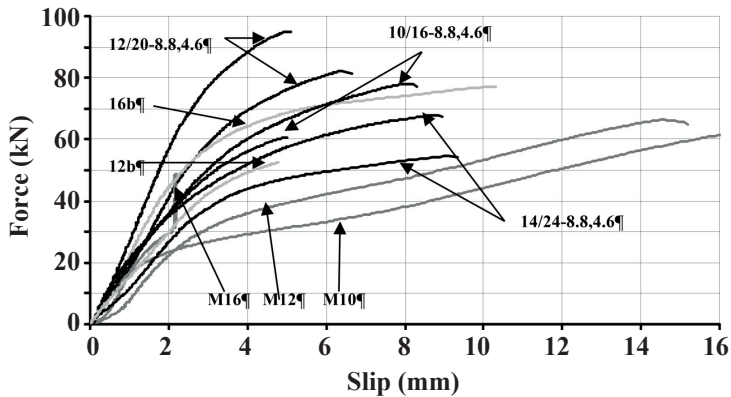


Fig. 4 Load slip curves of tests with global collapse of concrete [8]

Globally an increase is observed in TCC connection load carrying capacity when compared to a similar timber-timber connection [7].

2.2 Slip Modulus

The slip modulus of a connection is usually determined as indicated in ISO EN 26891 [9], based on the slip values measured for load levels up to 40% of the maximum estimated loads, on which, mostly elastic phenomena are involved. In this situation the higher elasticity modulus and lower deformability of concrete will necessarily lead to lower global deformation and consequently to a higher connection stiffness.

In practice the deformation in concrete side is much lower than the one in timber side and the global performance of the connection, in the elastic range, is close to the one of a steel-timber connection [10].

2.3 Ductility

The ductility is an important property in TCC connections. Despite the lower ductility of the timber member, that usually governs the failure mechanism, some increase in the ductility may be expected if ductile connections, such as for example nails or low diameter dowels, are used [11].

The higher axially load carrying capacity of TCC connections significantly contributes to increase their ductility. For the reasons mentioned before this ductility might be limited if brittle failure occurs on concrete. Such failure type rarely occur in practice due to the connection configuration (fastener diameter/concrete thickness ratio) and to the existence of reinforcement steel when larger diameters are used (Fig. 2, Fig. 3 and Fig. 4).

3. Calculation Models

The models available for timber-timber connections are often adopted as a base approach for TCC connections, for both analysis and design. Their accuracy increases when these models are adapted to take into consideration the specific phenomena from TCC connections, such as the concrete crushing or its lower deformability.

3.1 Load Carrying Capacity

There are various models available to estimate the load carrying capacity of TCC connections with dowel type fasteners. A comprehensive review was undertaken by Dias [12]. The Johansen model [6] based on the limit plastic approach showed the best results. In order to use it for TCC connections some adaptations are required. On the timber side the application is direct, while on the concrete side adaptations are required. To this end three approaches are usually followed to take the concrete specificities into account:

- Elastic perfectly plastic behavior (a)
- Elastic perfectly rigid behavior (b)

- Elastic behavior with a gap between the two materials (simulating crushing)
(c)

Due to the actual configuration of the TCC connections only the failure mode with two plastic hinges will usually apply, the corresponding equations can be derived and are given below:

$$(a) F_{p,c} = \sqrt{\frac{2\beta}{1+\beta}} \sqrt{2M_y f_h d} \quad (1)$$

$$(b) F_{e,c} = \sqrt{4M_y f_h d} \quad (2)$$

$$(c) F_{cr,c} = f_h d \left(-e + \sqrt{\frac{4M_y}{f_h d} + e^2} \right) \quad (3)$$

Where f_h is the timber embedding strength, β is the ratio between the embedding strength of concrete and the embedding strength of timber, M_y is the fastener yield moment, and d is the fastener diameter

Dias [12] compared the results obtained with these models with experimental data assuming a conservative approach to the embedding strength of concrete. Similar analysis can be done using a concrete embedding strength obtained from Eurocode 2 [13] (a ratio between embedding and compression strength of 3), which is in line with values given in bibliography [14]. The mean ratios between numerical and experimental data, as well as the correlations between the two sets of data, obtained in these conditions, are indicated in Tab. 1.

Tab. 1 Comparison between numerical and experimental values of the connection load carrying capacity

No. tests	Model	$F_{model}/F_{experimental}$	Correlation
126	$F_{p,c}$	0.77	0.71
	$F_{e,c}$	0.89	0.70
	$F_{cr,c}$	0.78	0.70

The best correlation was obtained for the model assuming elastic perfectly plastic behavior of concrete, while the worst was obtained for the model assuming elastic perfectly rigid behavior of concrete. All the models lead to lower values than those obtained in the experimental tests. The most relevant reason for this difference is probably related to the secondary transmission mechanisms such as friction or rope effects that were not considered.

Once these secondary transmission mechanisms have a significant influence in TCC connections performance, it was decided to consider them as a part of Johansen model, similarly to what is indicated in EN1995 part 1-1 [15] for timber-timber connections. In Tab. 2 the percentages that should be considered in order to have a ratio between the numerical and experimental values equal to one are given.

Tab. 2 Contribution of the rope effect (in % of the Johansen part) that lead to a ration between numerical and experimental equal to 1

Model	Rope effect
$F_{p,c}$	30 %
$F_{e,c}$	13 %
$F_{cr,c}$	29 %

From the low axial movement that was observed in the tests, rope effect contributions similar or higher to those assumed for timber-timber connections shall be expected. The values obtained here are in line with the maximum ones allowed in EN 1995 which are 15 % for round nails and 100 % for screws.

This analysis indicates that the elastic perfectly plastic behavior of the connections tends to overestimate the load carrying capacity of the connections, when primary and secondary load transmission mechanisms are considered. For these reasons it is not the best solution to estimate the load carrying capacity of TCC connections. Due to difficulties in the estimation of the crushing length on concrete and higher correlation obtained with the model assuming elastic perfectly plastic behavior of concrete, this last options seems to be the best one to estimate the load carrying capacity of TCC connections.

In Fig. 5 the experimental results against the numerical ones assuming elastic perfectly plastic behavior of concrete and a contribution from the rope effect equal to 30 % of the Johansen part are plotted.

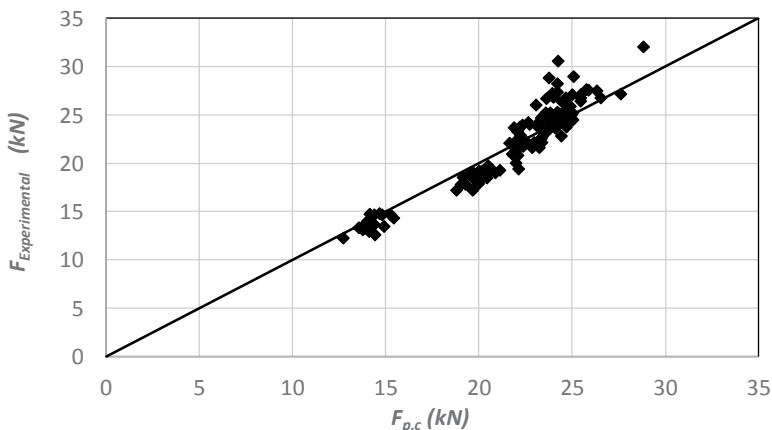


Fig. 5 Experimental and numerical results considering the contribution of the rope effect

3.2 Slip Modulus

There are essentially two approaches for the estimation of the connection slip modulus: beam on elastic foundation and empirical model given in EN 1995 part 1-1 [13].

Many derivations of the beam on elastic foundation have been tried after the first application by Keunzy in 1955 [16]. A specific one for TCC connections was proposed by Gelfi [14] (Equation 4).

A completely different approach was proposed by Ehlbeck and Larsen [17] based on a large amount of test data available. The original proposal for timber-timber connections is usually adapted to TCC connections by assuming no deformation on concrete side (Equation 5).

$$K_{bef} = \frac{12\lambda_c^2\lambda_t^2 EI}{3(\lambda_c^2 + \lambda_t^2)(\lambda_c + \lambda_t)} \quad (4)$$

$$K_{EC5} = 2 \times \rho_m^{1.5} \frac{d}{23} \quad (5)$$

where

$$\lambda_t^4 = \frac{k_{ft}}{4EI}$$

$$\lambda_c^4 = \frac{k_{fc}}{4EI}$$

k_t and k_c are the foundation modulus of timber and concrete respectively, EI is the bending stiffness of the fastener, ρ_m is density of the timber, and d is the fastener diameter.

Dias [7] compared the experimental results with the one obtained by these two models, the mean values of the correlations between numerical and experimental data, as well as, of the ratio between numerical and experimental results are indicated in Tab. 3.

Tab. 3 Comparison between numerical and experimental values of the connection load slip

No. tests	Model	F _{model} /F _{experimental}	Correlation
126	Beam on elastic foundation ¹	0.89	0.367
	EN1995	1.13	0.497

The empirical model from EN 1995 tends to overestimate the TCC slip modulus; however this overestimation is not significant when all the uncertainties and variabilities are considered. On the other hand, the beam of elastic foundation is more complex and requires data that is usually unavailable such as the material foundation modulus.

For these reasons the EN 1995 empirical model is suggested as the best option for the estimation of the TCC connections' slip modulus.

4. Conclusions

The analysis undertaken in this paper shows that the mechanical performance of timber-timber and TCC connections made with dowel type fasteners have multiple similarities. In spite of that, there is also a number of differences which are closely related to the specificities of concrete.

These specificities have a non-negligible influence in the performance of TCC connections. Consequently, the models used to estimate the TCC mechanical performance do also need to take these aspects into account with.

In terms of load carrying capacity the analysis indicates that the most adequate model for the determination of the load carrying capacity is the Johansen model given in EN 1995 for timber-timber connections, assuming elastic perfectly plastic behavior of concrete. There is a non-negligible underestimation of the experimental results which is, at least partially, due to secondary load transmission mechanisms such as friction or rope effect. If these parameters are considered in the model its prediction accuracy shows a significant increase.

The most adequate model for the estimation of the connections' load slip was also found to be the one given in EN 1995 part 1-1. It has an empirical base, but when adapted for TCC connections, it yields to the best results.

5. Acknowledgements

This work was partly financed by FEDER funds through the Competitiveness Factors Operational Programme – COMPETE and by national funds through FCT – Foundation for Science and Technology within the scope of the Project POCI-01-0145-FEDER-007633.

6. References

- [1] Dias A.M.P.G., et al., "Timber-concrete-composites increasing the use of timber in construction", *European Journal of Wood and Wood Products*, 2015, pp. 1-9.
- [2] Dias, A.M.P.G., et al., "Load-carrying capacity of timber-concrete joints with Dowel-type fasteners", *ASCE Journal of Structural Engineering*, Vol. 133, Iss. 5, 2007, pp. 720-727.
- [3] Wacker J.P., Dias A.M.P.G., and Hosteng T.K., *Investigation of Early Timber-Concrete Composite Bridges in the United States*, 3rd International Conference on Timber Bridges, 2017, Skelleftea, Sweden.
- [4] Monteiro S.R.S., Dias A.M.P.G., and Negrao J.H.J.O., "Assessment of Timber-Concrete Connections Made with Glued Notches: Test Set-Up and Numerical Modeling", *Experimental Techniques*, 2013, Vol. 37, Iss. 2, pp. 50-65.

- [5] Dias A.M.P.G., "Analysis of the Nonlinear Behavior of Timber-Concrete Connections", *ASCE Journal of Structural Engineering*, 2012, Vol. 138, Iss.9, pp. 1128-1137.
- [6] Johansen K.W., *Theory of timber connections*. Publication 9, International Association of Bridge and Structural Engineering, 1949, pp. 249-262.
- [7] Dias A.M.P.G., *Mechanical behaviour of timber-concrete joints*, Delft University of Technology, 2005, Delft.
- [8] Dias A.M.P.G., et al., "Experimental shear-friction tests on dowel type fasteners timber-concrete joints", *Proceedings of the 8th Conference on Timber Engineering - WCTE 2004*, 2004, Lahti, Finland.
- [9] ISO EN 26891: *Timber structures - Joints made with mechanical fasteners - General principles for the determination of strength and deformation characteristics*, European Committee for Standardization (CEN), 1991, Brussels, Belgium.
- [10] Dias A.M.P.G., et al., "Stiffness of dowel-type fasteners in timber-concrete joints", *Proceedings of the Institution of Civil Engineers-Structures and Buildings*, Vol. 163, Iss. 4, 2010, pp. 257-266.
- [11] Dias A.M.P.G., and Jorge L.F.C., "The effect of ductile connectors on the behaviour of timber-concrete composite beams", *Engineering Structures*, 2011, Vol. 33, Iss. 11, pp. 3033-3042.
- [12] Dias A.M.P.G., *Mechanical behaviour of timber-concrete joints*, PhD Thesis, Delft University of Technology, 2005, Delft, The Netherlands.
- [13] EN 1992-1-1, *Eurocode 2 - Design of concrete structures - Part 1-1: General - Common rules and rules for buildings*, European Committee for Standardization (CEN), 2004, Brussels, Belgium.
- [14] Gelfi P., Giuriani E., and Marini A., "Stud shear connection design for composite concrete slab and wood beams", *ASCE Journal of Structural Engineering*, 2002, Vol. 128, Iss. 12, pp. 1544-1550.
- [15] EN 1995-1-1: *Eurocode 5 - Design of timber structures - Part 1-1: General - Common rules and rules for buildings*, European Committee for Standardization (CEN), 2004, Brussels, Belgium.
- [16] Kuenzi E.W., *Theoretical design of a nailed or bolted joint under lateral load*, 1955, USDA Forest Product Laboratory: Madison, Wisconsin, USA.
- [17] Ehlbeck J., and Larsen H.J., "Eurocode 5 – Design of timber structures: Joints" *Proceedings of the International workshop on wood connectors*, 1993, Madison, USA.

Push-out vs. Beam: Can the Results of Experimental Stiffness of TCC-Connectors be Transferred?

Jörg Schänzlin
Head of the institute of timber design
Hochschule Biberach
Biberach a.d.R., Germany

Simon Mönch
Research assistant
Institute of Structural Design, University of Stuttgart
Stuttgart, Germany

Summary

In timber concrete composite systems the flexibility of the connectors has to be considered in the determination of the deformations and of the internal stresses. Since this stiffness is a quite important parameter this value is often determined by push-out tests. When comparing the effective stiffness re-evaluated from the results of bending tests on notched connections and the stiffness obtained from push-out tests, the effective stiffness in a bending test is lower than the stiffness in a push-out test. Since the forces are transferred at the joint from one cross section to the other and the normal stresses are distributed over the whole cross section shear deformations might influence the effective stiffness. In order to cover this influence the basic equations of the shear-analogy method have been transformed into an effective stiffness of the connectors, so the differences between the stiffness of the connector obtained by re-evaluation of bending tests and by push-out tests can be minimized.

1. Introduction

In timber-concrete-composite systems the limitation of the deflection in the long term is one of the most important parameters in designing the elements. Since timber, concrete and the connection creep and timber and concrete shrink and swell, the long term behavior has to be studied in detail. For that reason several models have been developed in order to describe the long term behavior of this type of composite (see among others [1] or [2]). In these models the rheological models of the components have been linked together. As example, in [1] the rheological models according to [3] and according to [4] have been connected by the differential equation of the slip between timber and concrete (see [5]).

One important part of the development of these models is the verification and the comparison with the "reality". For this comparison, test results are compared with

the results of the models. In [6] short term as well as long term tests of different connections have been performed as e.g. notches with a reinforcement bar (see Fig. 1).

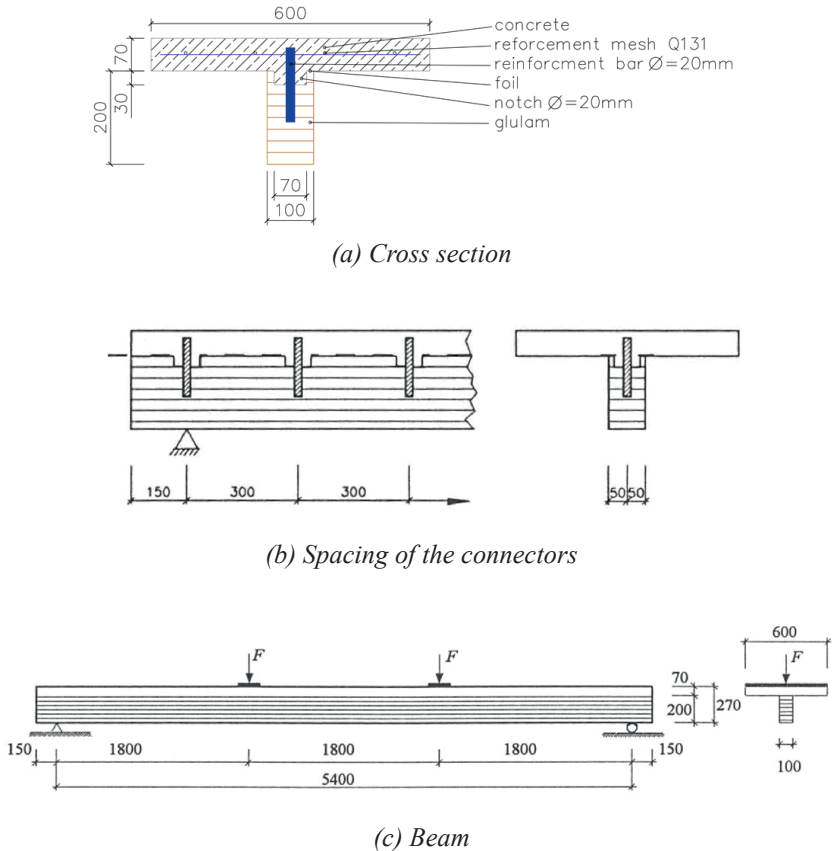
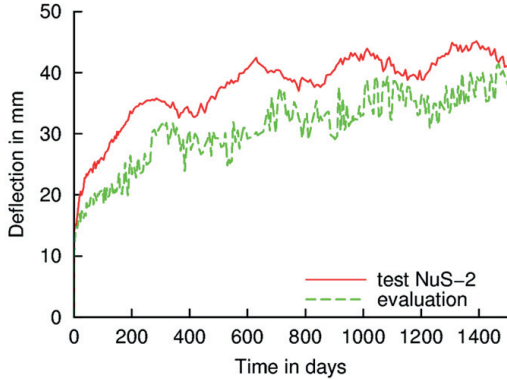
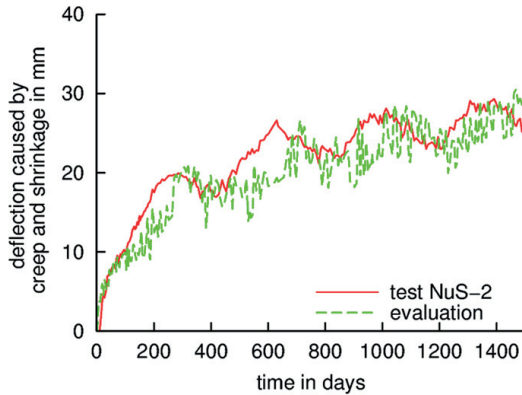


Fig.1 Test set-up of the long term tests by [6] (taken from [6], Fig. a redrawn and translated)

The beam was loaded with a permanent load of 2×7.8 kN for a period between 27.04.1995 and 19.10.1999. Among others the mid span deflection was monitored during the whole time. When the results of these tests are compared with the results of the evaluation of the deflection, differences between the measurement and the evaluation appear (see Fig. 2(a)).



(a) Total deflection



(b) Increase of the deflection

Fig. 2 Comparison between the measured deflection and the evaluated deflection

As can be seen in Fig. 2(a) the evaluation underestimates the deformation. However if only the increase of the deflection is regarded, the results of the model lead to a sufficient accuracy between the model and the tests (see Fig. 2(b)). Therefore the major differences between the model and the evaluation are caused by an underestimation of the elastic deflection.

2. Identification of the Stiffness

For the re-evaluation of the deflection of these tests following input values are necessary:

- geometrical values
- stiffness values of the cross sections
- properties of the connection
- load

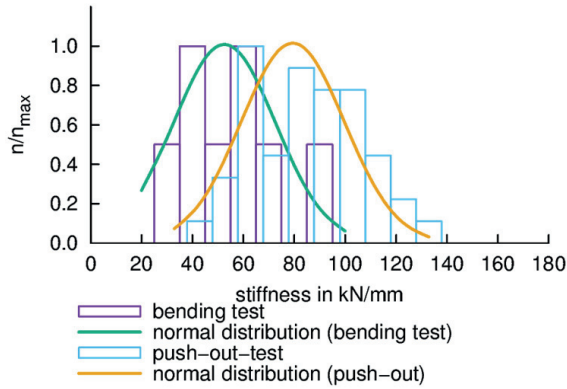
The geometrical values as well as the load are given. The stiffness values of the timber cross section are often measured by a bending test as in [6], whereas the stiffness of the concrete is determined by testing of a cube. Concerning the connections the properties of the push-out tests are assumed to be valid in a beam. However the stiffness is one parameter which is not directly determined but transferred from the push-out test. In order to explain the difference in the deflection of the tested beam and the evaluation the hypothesis was proposed, that there is a difference between the stiffness in a push-out test and a bending test. In order to accept or reject this hypothesis the stiffness of the connectors is re-evaluated from the bending tests by comparing the deformation.

For the re-evaluation of the effective stiffness of the connectors based on the bending tests according to [6] the solution of the differential equation of the slip was used (see [5]). The advantage of this method is that all possible systems can be modeled by adopting the boundary conditions of the differential equation to the boundary conditions in the tests, e.g. the single loads can be considered in the evaluation of forces. Additionally the connectors in this test are installed in a distance less than 5 % of the span of the beam (see [7]), so the connectors can be smeared along the beam axis.

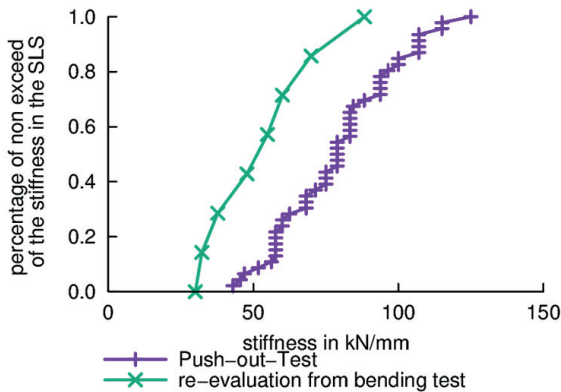
As shown in Fig. 2(a) there are differences between the measured and the evaluated deformation of a beam. So the re-evaluated stiffness is lower than the ones obtained from push-out tests. The mean value of the stiffness and the standard deviation are given in Tab. 1.

Tab. 1 Mean value and coefficient of variation of the stiffness of the connector notch & reinforcement bar (see Fig. 1)

	push-out tests	re-evaluation by bending tests
number of tests	46	8
mean value	70 kN/mm	52.6 kN/mm
standard deviation	20.3 kN/mm	20.0 kN/mm
CoV	0.25	0.38



(a) Distribution of the stiffness

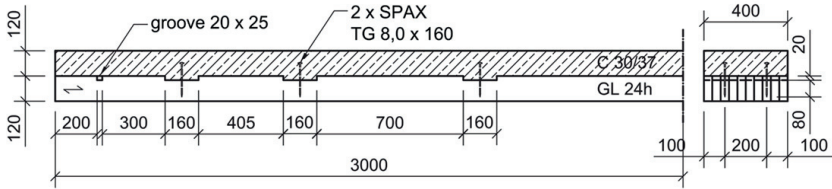


(b) Cumulative distribution of the stiffness

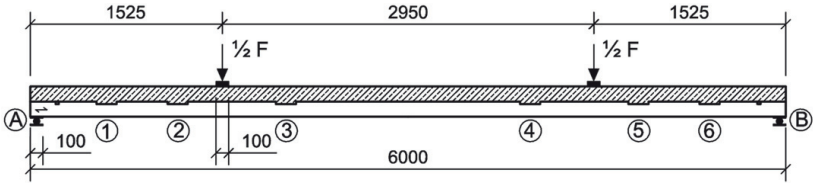
Fig. 3 Comparison of the stiffness in the serviceability limit state determined from push-out tests and re-evaluated from bending tests of the tests in [6])

As can be seen in Fig. 3 and from Tab. 1 the stiffness of the connection between timber and concrete in the bending tests is lower than the stiffness in the push-out test.

If the same approach is applied to the tests performed by [8] (see Fig. 4) a comparable difference in the evaluated stiffness appears (see Fig. 5 and Tab. 2).



(a) cross-section and dimensions



(b) Test-setup

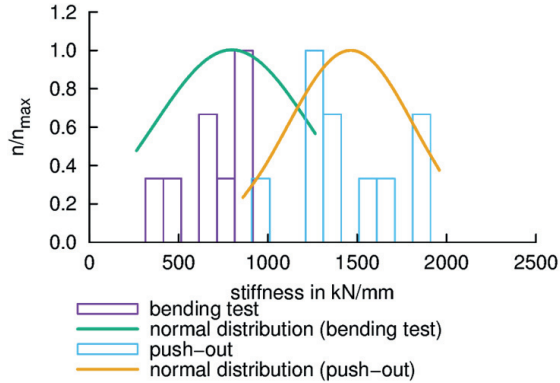
Fig. 4 Test-setup in [8] (taken from [8])

For the evaluation of the required stiffness of the connection the system was modeled as a strut & tie model with the software SOFISTIK in order to cover the non-linear behavior of concrete in tension.

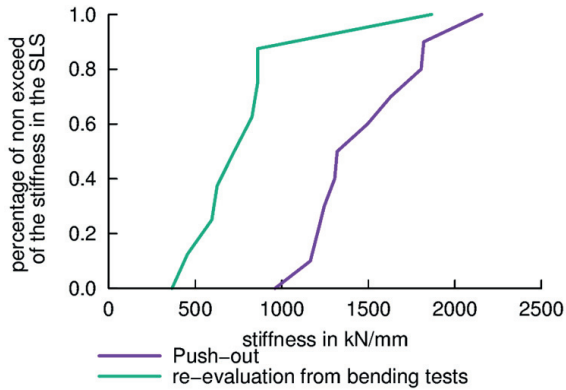
Tab. 2 Mean value and coefficient of variation of the stiffness of the notch as connector in the tests by [8]

	push-out tests	re-evaluation by bending tests
number of tests	11	9
mean value	1464 kN/mm/m width	797 kN/mm/m width
standard deviation	354 kN/mm/m width	437 kN/mm/m width
CoV	0.24	0.54

As can be seen by the comparison of both test series with notched connections the stiffness obtained by push-out-tests are higher than the effective stiffness in the beam obtained by the re-evaluation based on the deflection in the serviceability limit state. So the deformation of the beam can be underestimated, if the parameters obtained from the push-out tests are used without any modification as can be seen in Fig. 2(a).



(a) Distribution of the stiffness

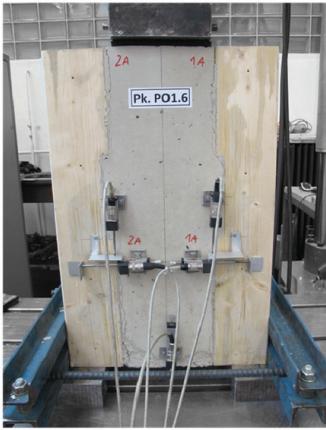


(b) Cumulative distribution of the stiffness

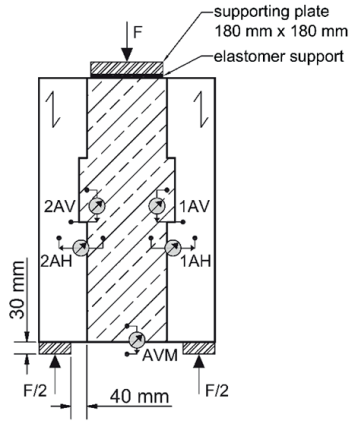
Fig. 5 Comparison of the stiffness in the serviceability limit state determined from push-out tests and re-evaluated from bending tests based on the tests performed in [8]

3. Possible Reason for the Differences

In normal tests the slip between the composite elements is measured directly at the joint between timber and concrete (see Fig. 6).



(a) test setup



(b) sketch

Fig. 6 Typical test setup (see [8])

So the load slip behavior in the joint can be described. However in the design the cross sections are reduced to their centroidal axis. If the stiffness of the joint is used as stiffness in the calculation, the influence of the cross section between the joint and the centroidal axis is neglected.

As a result, there might be shear deformations with lead to a reduction of the effective stiffness of the connection between the centroids of the cross sections (see Fig. 7).

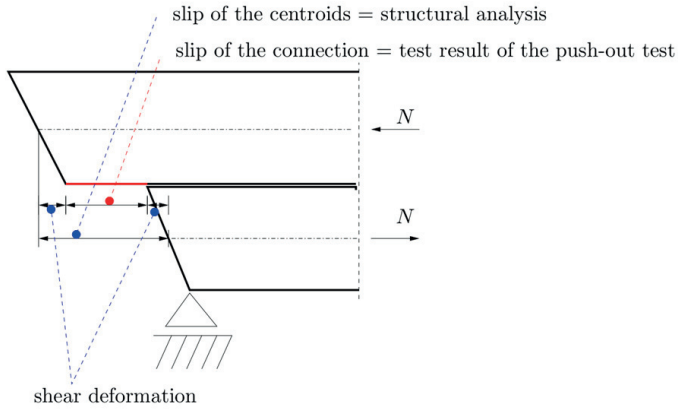


Fig. 7 Effective stiffness of the connectors

The shear deformation is normally neglected in the determination of the internal forces, except in the shear-analogy-method according to [9] and [10] (see also [11]). In this method the bending stiffness of a composite beam is split up into the bending stiffness of the single cross sections and the stiffness caused by the composite action. In order to consider the slip of the connector effective shear stiffness is derived (see Fig. 8). This shear stiffness is determined by adding all deformation caused by constant shear force in the cross section and comparing this effective shear deformation with the shear deformation of a homogeneous cross section.

$$\Delta u = \frac{a^2 T}{GA^*} = \sum \frac{T}{k_i} + \frac{h_0 \cdot T}{2 \cdot G_0 \cdot b_0} + \sum_{i=2}^{n-1} \frac{h_i \cdot T}{2 \cdot G_i \cdot b_i} + \frac{h_n \cdot T}{2 \cdot G_n \cdot b_n}$$

$$\frac{1}{GA^*} = \frac{1}{a^2} \cdot \left[\sum \frac{1}{k_i} + \frac{h_0}{2 \cdot G_0 \cdot b_0} + \sum_{i=2}^{n-1} \frac{h_i}{2 \cdot G_i \cdot b_i} + \frac{h_n}{2 \cdot G_n \cdot b_n} \right], \quad (1)$$

where GA^* is the effective shear stiffness of the connection, a the distance of the centroids of the outer layers, k the stiffness of the connectors smeared along the beam axis, h_i , b_i and G_i the height, the width and the shear modulus of the layer i .

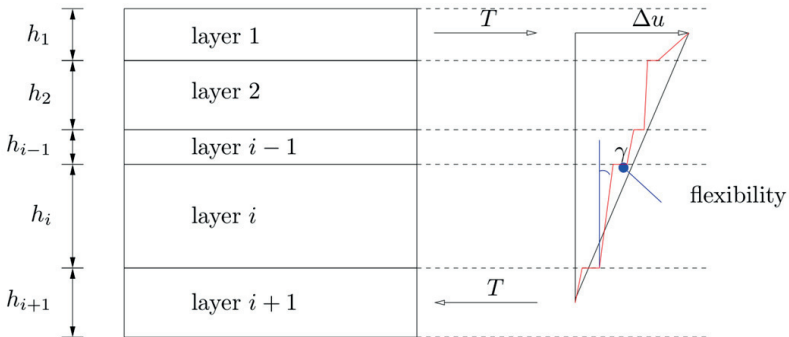


Fig. 8 Determination of the effective shear stiffness in the shear-analogy-method

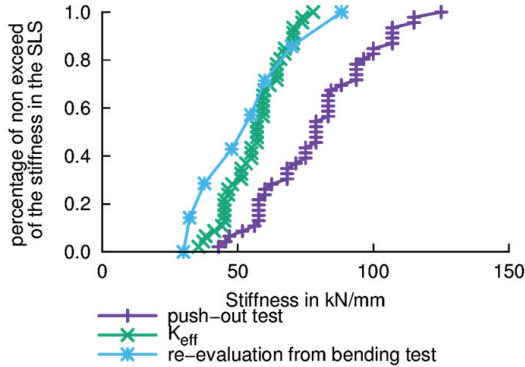
In the shear-analogy-method this shear stiffness is considered in the subsystem representing the composite action of the composite beam. In difference to the other design methods the influence of the shear deformation can be considered.

In order to consider the shear deformation in the other design methods Eq. (1) can be transformed into an effective stiffness of the connection for a composite beam with two layers

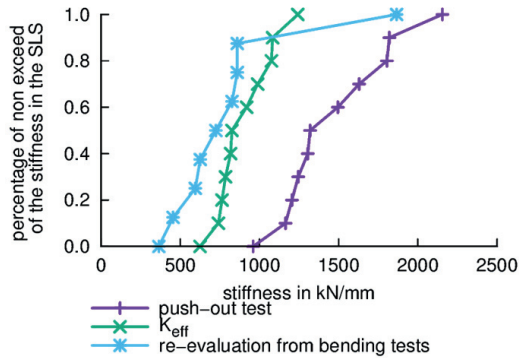
$$\frac{1}{GA^*} = \frac{1}{a^2} \cdot \left[\frac{1}{k_{\text{joint}}} + \frac{h_0}{2 \cdot G_0 \cdot b_0} + \frac{h_1}{2 \cdot G_1 \cdot b_1} \right] = \frac{1}{a^2} \cdot \frac{1}{k_{\text{eff}}}$$

$$\frac{1}{k_{\text{eff}}} = \frac{1}{k_{\text{joint}}} + \frac{h_0}{2 \cdot G_0 \cdot b_0} + \frac{h_1}{2 \cdot G_1 \cdot b_1} \quad (2)$$

where k_{eff} is the effective stiffness with respect to the local shear deformation, smeared along the beam axis, k_{joint} is the stiffness of joint between timber and concrete, smeared along the beam axis, h_i , b_i and G_i the height, the width and the shear modulus of the layer i . With this equation an effective stiffness of the connectors with respect to the shear deformation can be determined. In Fig. 9 the effective stiffness of the connectors of the tests by [6] and [8] are given. As can be seen the difference of the stiffness between the values obtained from the push-out tests and re-evaluated from the bending tests decreases.



(a) [6]



(b) [8]

Fig. 9 Modified stiffness of the connector

4. Effect of the Effective Stiffness of the Connector

As shown the effective stiffness of the connector may be influenced by the shear deformation of the cross section. Since the stiffness of the connector and the

influence of the shear deformation are in serial order, the resulting stiffness can only be increased if the stiffness of both components is increased. Therefore the maximum composite action is limited by the shear deformation of both cross sections. In Fig. 10 the maximum γ -value according [12] is evaluated for a solid timber deck made of C24 and C20/25.

As can be seen in Fig. 10 the influence of the shear deformation increases with increasing height of the cross section of timber, since the shear stiffness of timber is lower compared to the shear stiffness of concrete. Additionally a full composite action cannot be achieved, since the shear deformation limits the effective stiffness in the joint between timber and concrete.

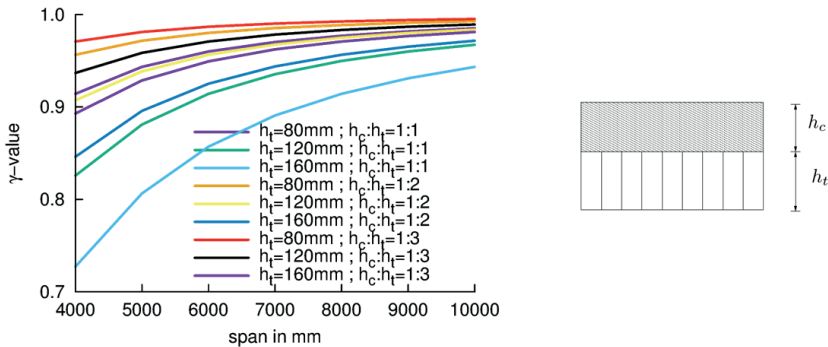


Fig. 10 Maximum γ -value for solid timber-concrete decks due to shear deformation for timber C24 and concrete C20/25

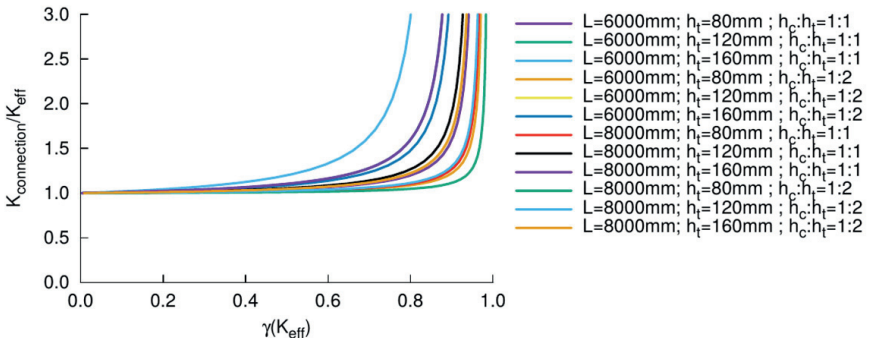


Fig. 11 Ratio of the connection stiffness K to K_{eff} including the shear deformation depending on the γ -value according to [12] in a solid TCC-deck (timber C24; concrete: C20/25)

In Fig. 11 the required connection stiffness is determined depending on the γ -value. As can be seen the influence of the shear deformation in the solid timber deck can

be neglected up to a γ -value of 0.6. For larger γ -values a consideration of the shear deformation is recommended.

5. Summary & Outlook

The properties of a connection between timber and concrete are often determined by push-out tests, since the properties of the connection can be determined in an easier way than their determination by the re-evaluation of bending tests. As one important parameter the slip between the timber and the concrete is measured. However in the common design methods the slip between the centroidal axes of the cross sections is an input value. However there might be shear deformations in the cross section between the joint and the centroidal axis of the cross section, the slip at the joint is not always the same as the slip of the centroids of both cross sections. Consequently the effective stiffness of the connectors including this shear deformation might be lower than the stiffness obtained from the push-out test.

In order to cover this influence the effective shear stiffness in a composite system and the basic equations of the shear analogy method have been transferred into an effective stiffness of the connector. It has been shown, that the effective stiffness of the connectors with respect to the shear deformations leads to comparable stiffness as re-evaluated from bending tests. However it has to be highlighted that this influence can be neglected for lower stiffness of the connectors compared to the stiffness of the cross section of the beam.

Both tests series shown have in common, that the composite action is quite high compared to the bending stiffness of the single cross sections. Additionally the influence of cracking of concrete was quite low. However both influences may also have an influence on the effective stiffness of the connectors. Beside that the connections in both test series are notched connections. In these cases the shear forces are transferred at the surface of the cross sections and distributed over the whole cross section. If the connector transfers the shear forces into the cross section as e.g. in the case of inclined screws, the influence of the shear deformation might be reduced.

6. References

- [1] Schänzlin J., *Zum Langzeitverhalten von Brettstapel-Beton-Verbunddecken*, PhD thesis, 2003, Institute for Structural Design, University of Stuttgart (in German).
- [2] Fragiaco M., *Comportamento a lungo termine di travi composte legno-calcestruzzo*, PhD thesis, 2000, University of Trieste (in Italian).
- [3] Hanhijärvi A., *Modelling of creep deformation mechanisms in wood*, PhD thesis, 1995, Helsinki University of Technology, Technical Research Centre of Finland VTT Publications. Espoo (SF).
- [4] DIN EN 1992-1-1:2011-01 Eurocode 2: *Bemessung und Konstruktion von Stahlbeton- und Spannbetontragwerken; Teil 1-1: Allgemeine Bemessungs-*

regeln und Regeln für den Hochbau; German version EN 1992-1-1:2004 + AC:2010. 2011.

- [5] Dabaon M., Tschemmerneegg F., Hassen K., and Lateef T. A., „Zur Tragfähigkeit von Verbundträgern bei teilweiser Verdübelung“, *Stahlbau*, Vol. 62, 1993, pp. 3–9 (in German).
- [6] Blass H.-J., Ehlbeck J., Linden M.L.R., and Schlager M., „Trag- und Verformungsverhalten von Holz-Beton-Verbundkonstruktionen“, *Bauen mit Holz*, No. 5, 1996, pp. 392 – 399 (in German).
- [7] Dias A., Fragiaco M., Harris R., Kuklic P., Rajcic V., and Schänzlin J., *Technical Specification – 2nd Draft – Eurocode 5: Design of Timber Structures – Part 1-3: Structural design of timber concrete composite structures – Working Draft / Project Team CEN/TC 250-SC5.T2*. 2017.
- [8] Kudla K., *Kerven als Verbindungsmittel für Holz-Beton-Verbundstraßenbrücken*, PhD thesis, 2017, Institute for Structural Design, University of Stuttgart (in German).
- [9] Kreuzinger H., „Die Holz-Beton-Verbundbauweise“, Informationsdienst Holz (ed.): *Fachtagung Holzbau 1999-2000, Holzbau für das neue Jahrhundert*, 2000, pp. 70–83.
- [10] Scholz A., *Ein Beitrag zur Berechnung von Flächentragwerken aus Holz*, PhD thesis, 2003, TU München (in German).
- [11] DIN EN 1995-1-1 / NA: *Nationaler Anhang - Eurocode 5: Bemessung und Konstruktion von Holzbauten - Teil 1-1: Allgemeines- Allgemeine Regeln und Regeln für den Hochbau*. DIN-Deutsches Institut für Normung e.V., 2013 (in German).
- [12] DIN EN 1995-1-1: *Eurocode 5: Bemessung und Konstruktion von Holzbauten - Teil 1-1: Allgemeines – Allgemeine Regeln und Regeln für den Hochbau*. DIN-Deutsches Institut für Normung e.V., 2010 (in German).

Numerical Modeling of the Load Distribution in Multiple Fastener Joints

Thomas K. Bader
Associate Professor
Department of Building Technology, Linnaeus University
Växjö, Sweden

Jean-François Bocquet
Associate Professor
ENSTIB / LERMAB, University of Lorraine
Epinal, France

Michael Schweigler
Doctoral student
Institute for Mechanics of Materials and Structures,
Technische Universität Wien
Vienna, Austria

Romain Lemaître
Doctoral student
ENSTIB / LERMAB, University of Lorraine
Epinal, France

Summary

Numerical modeling approaches, for the determination of load distribution in laterally loaded joints, as well as for the assignment of stiffness properties of joints for the structural analysis, are summarized in this contribution. The effect of the nonlinearity and the load-to-grain orientation dependence of connection slip, of elastic deformation in the surrounding wood matrix, and of the deviation between load and displacement direction are discussed. Comparison of various models demonstrates the pronounced effect of the load-to-grain orientation dependence and the nonlinearity in connection slip on the load distribution, particularly in case of moment loading. The effect of elastic deformation in the wood matrix on the load distribution increases with increased size of joints, even more pronounced when joints are loaded by a shear force perpendicular to the grain. In case of normal force loading, the non-uniform load distribution due to elastic deformation in the wood matrix reduces rapidly with increased relative joint displacement. Pros and cons of the modeling approaches as well as necessary input data are discussed in relation to the design process and European standardization.

1. Introduction

In the design of timber structures, engineers are permanently facing the question of how to distribute loads in multiple fastener joints. This is decisive for assigning joint properties in the analysis of timber structure based on fastener properties, as well as in the verification of fasteners in joints subjected to a set of internal forces. The way how this is achieved, naturally depends on regulations in the timber engineering design standard (EN1995-1-1, EC 5 [1]). The latter is currently primarily designed towards the behavior of single fasteners, rather than towards the behavior of multiple fastener joints. In practical applications, multiple fastener joints are mostly loaded by a combination of internal forces, which from a beam theory point of view includes normal force, shear forces and bending moments. Regarding standardization, load distribution in joints is currently not explicitly regulated in EC 5.

Design regulations and assumptions on the single fastener behavior, however, strongly affect the possibilities of modeling the load distribution in joints. EC 5, in its current version, prescribes a limit state approach for the determination of the strength of single fastener connections. Since the limit state approach does not give deformations, an empirical equation for their elastic stiffness in the serviceability limit state (SLS) is given. The stiffness however does not depend on the load orientation with respect to the grain, and consequently, an isotropic and most commonly elastic load distribution model is used in engineering practice. The combination of an elastic and isotropic distribution model based on the polar moment of inertia with plastic limit loads might be questioned, even when using reduced stiffness of the fasteners in the ultimate limit state (ULS) design, while ultimate limit loads of joints could be suitably estimated with limit state approaches. However, pronounced nonlinearities in the single fastener behavior with hardening under loading perpendicular to the grain are not accounted for. Thus, in order to enhance the modeling of load distribution in multiple fastener joints, also regulations for the modeling of the single fastener behavior must be improved.

Beam-on-nonlinear foundation models have shown to be able to predict nonlinear single fastener load-deformation behavior based on a kinematically compatible experimental dataset of the embedment behavior of wood and the bending behavior of steel fasteners [2]. Thus, numerical modeling can give access to the *nonlinear slip behavior of fasteners* loaded under arbitrary angles to the grain. The nonlinear relationships can be exploited in the load distribution modeling, avoiding the need for assigning different linear stiffness for SLS and ULS design, respectively. Particularly when joints are subjected to a bending moment, fasteners are loaded at various angles to the grain. Consequently, load distribution is governed by the load-to-grain orientation dependence of the load-deformation behavior of the single fastener (Ohashi and Sakamoto, 1989 in [3]).

Another effect of the anisotropic material behavior of wood is the *deviation of the force and displacement orientation* in case of loading at an angle between the principal material orientations. This has been investigated experimentally for wood embedment behavior [4] and single dowel connection behavior [2] as well as numerically for a group of fasteners [5]. Not only 3dimensional Finite Element Method (FEM) modeling but also 3dimensional beam-on-foundation modeling with appropriate input datasets can be used to represent this behavior and its effect on the load distribution.

Fasteners typically introduce stress peaks in the wood, which lead to local plastic deformations and local relative displacements between the connected members, while the rest of the wooden matrix deforms elastically. Thus, finally, it is the effect of the *elastic deformations of the wooden matrix* in-between the fasteners of a joint, which affects the load distribution. Jorissen [6] showed that even the size of bending deformation of the steel fastener affects the load distribution in case of normal forces. This is related to the different degree of nonlinearity in the single fastener behavior, depending on the fastener bending failure mode. Thus, in case of unreinforced connections with a risk for brittle failure modes, the strength of multiple fastener joints *may be lower than the summation of the individual load-carrying capacities of each fastener* (EC 5 8.1.2(2) [1]).

As outlined above, the load distribution in multiple fastener joints depends on the mechanical properties of their components, which can be simplified in the numerical model in many different ways, depending on the material models and the type of internal forces considered. Herein, we will focus on in-plane loading, namely bending moment M_y , shear force V_z and normal force N_x , while out-of-plane loading is not considered. Previously proposed as well as novel 3dimensional and 2dimensional approaches will be reviewed and discussed. The contribution focuses on the load distribution in an integer wooden matrix without cracks. This is a prerequisite for the calculation of realistic stresses in the timber matrix, which allow assessing the risk for brittle failure.

The paper is organized as follows. Load distribution models including the effect of orientation dependent nonlinearity in the single fastener behavior, the elastic behavior of the wooden matrix, and the deviation of load and displacement direction will be reviewed and discussed, starting from the most general case with opportunities for simplification. This will show possibilities to reduce the amount of required input data and modeling efforts. Selected models will be applied to the cases of loading by an in-plane bending moment, normal force, shear force, and a combination of internal forces. Mechanical causalities in the above described cases of load distribution will be discussed, before recommendations for standardization and engineering design, including standardized material properties and consideration of the stochastic nature of component properties, will be proposed at the end of this paper.

2. Modeling of Load Distribution – Approaches and Simplification

2.1 General

Various numerical models for the determination of the load distribution and the corresponding input data are summarized in Figure 1 and will be discussed in the following, starting with the most complex model and subsequently increasing simplifications.

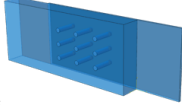
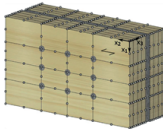
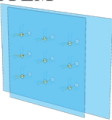
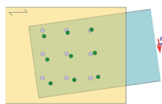
numerical model	features / benefits	input data	
(2.2) 3dimensional solid FEM model 	load distribution steel dowel deformation stress state in matrix ✓ nonlinear slip ✓ elastic matrix deformation ✓ load-displacement orientation	constitutive model for wood, incl. elasticity, plasticity, (brittle failure) constitutive model for steel, incl. elasticity and plasticity contact model for dowel-wood interaction	MATERIAL level
(2.3) 3dimensional FEM with beam-on-foundation 	load distribution steel dowel deformation stress state in matrix ✓ nonlinear slip ✓ elastic matrix deformation ✓ load-displacement orientation	nonlinear embedment behavior of wood; constitutive model for steel, incl. elasticity and plasticity	
(2.4) 3 or 2dimensional FEM with nonlinear coupled springs 	load distribution approximated stress state in matrix ✓ nonlinear slip ✓ elastic matrix deformation ✓ load-displacement orientation	nonlinear slip curves of single fasteners elastic material model for wood (contact model for dowel-wood interaction with 3dimensional shell)	SINGLE FASTENER level
(2.5) Nonlinear springs with rigid matrix 	load distribution NO stress state in matrix ✓ nonlinear slip ✗ elastic matrix deformation ✓ load-displacement orientation	nonlinear slip curves of single fasteners	
(2.6) Isotropic or anisotropic linear elastic connector $F_j = \frac{M_{y,joint}}{I_p} r_j$ $F_j = \frac{K_{oj} r_j}{K_r} M_{y,joint}$	LINEAR load distribution ✗ nonlinear slip ✗ elastic matrix deformation ✗ load-displacement orientation	LINEAR slip stiffness of single fastener	

Fig. 1 Overview of models for the determination of load distribution in joints with laterally loaded fasteners.

There are basically two possible starting points with respect to modeling of load distribution in joints, which are either the *material level* (2.2 and 2.3 in Figure 1) or the *single fastener level* (2.4-2.6 in Figure 1). The former can either relate to basic material properties of wood or to a phenomenological modeling of the embedment

behavior, as it is used in beam-on-foundation approaches [2]. In both cases, the single fastener behavior is derived as a consequence of the material properties and the global loading of the joint. Alternatively, load distribution modeling starts at the single fastener level, with knowledge about the nonlinear fastener slip behavior, without accounting for local bending deformations of the fastener (see Figure 1).

Herein, in-plane loading situations of joints will be discussed, which requires knowledge of material properties or of laterally loaded single-fastener slip curves. Consequently, a coupling of properties in principal material directions parallel and perpendicular to the grain must be taken into account in constitutive and phenomenological material models. Input data used in example calculations within this contribution are visualized in Figure 2. They encompass material properties of the components and single fastener slip curves.

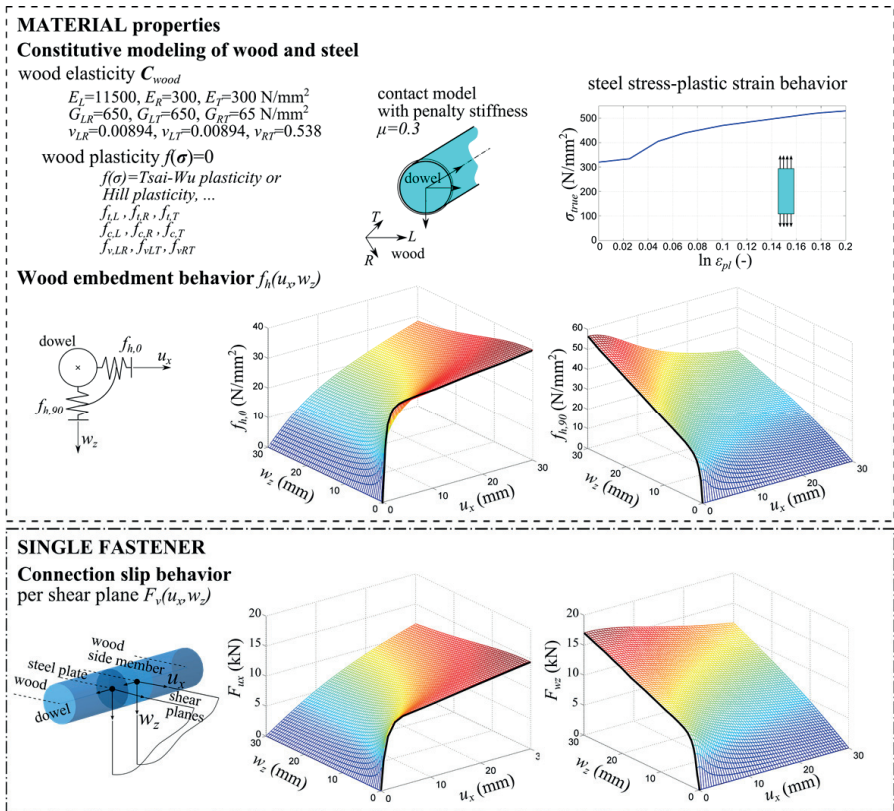


Fig. 2 Input data for numerical modeling of load distribution.

Stiffness properties of wood have been considered as mean values of glued laminated timber strength class GL24h [7] and Poisson's ratios were taken from literature [8]. A huge variability of Poisson's ratios of wood is reported in literature. However, a negligible effect of the Poisson effect on the load distribution is expected. Having at hand experimentally determined wood embedment behavior [4] and stress-strain relationship for steel [2], a beam-on-foundation model [2] has been used to determine single dowel connection slip curves, see Figure 2.

2.2 3Dimensional Solid FEM Model

The load distribution in joints could be studied by a 3dimensional discretization of the joint components with solid elements in FEM software. The interaction between the fasteners and the timber is then modeled with a contact criterion, typically by surface-to-surface contact encompassing a penalty friction formulation in the transverse plane and high contact stiffness in the normal direction. A pressure-overclosure relationship could be used to account for the local weakness of the interface (see [9] and [10]). Moreover, appropriate material models for wood and steel are required, which must at least account for elasticity and plasticity in order to reflect the plastic deformation of the timber member that causes plastic bending deformation of the mechanical fastener. The constitutive model for wood is the challenge in this case, since large strains are obtained close to the dowel-wood interface. Besides continuum damage mechanics models [11], classical failure criteria such as Tsai-Wu [9] or Hill [12] have been used to define yield functions, which have mainly been used in combination with ideal-plasticity in connection models. Most of the models were limited to small strain theory and small displacements and are thus most appropriate for the serviceability limit state. The main advantage of these models is naturally, in case of using an appropriate material model, the detailed information about local stresses and deformations. At the same time, this is their main drawback, since these models require long pre- and post-processing as well as long calculation times, which make them inflexible and unpractical for the engineering design of structures.

As another example, the deviation of the load and displacement direction in moment loaded joints has been studied by using a 3dimensional FEM model with an elastic material model for wood [5]. Load distribution was determined by integrating contact forces over the wood borehole surface. This work also included examples of how to combine beam models with 3dimensional solid FEM models.

2.3 3Dimensional Beam-on-Foundation with Wood Matrix Model

The complexity in the local deformation and stress state in wood close to the dowel suggests using a simpler, phenomenological approach to describe the embedment behavior. Thus, beam-on-foundation approaches have been developed (see Figure 1), where nonlinear springs are used to model the contact between wood and steel dowel [13], by making use of mathematical functions for the relative displacement-embedment load behavior (see [14] and [15]). In most of these

equations, the parameters can be related to physical properties derived from uniaxial embedment tests. The simplest approach would be to assume linear tangents with a continuous intermediate nonlinear transition [14]. An initial nonlinear region with increasing stiffness is typically observed in test data. This is linked on the one hand to the quality and the precision of production and assembling, and on the other hand to the stochastic nature of the properties. Mathematical functions enable an integration of this initial behavior [15], which would lead to a more realistic load distribution in multiple fastener joints.

The orthotropic behavior of wood is considered by using spring stiffness that depends on two orthogonal displacements (cf. Figure 2), i.e., a coupling between the two springs for loading in-between the principal material directions is used (see e.g. [16] for modeling with coupled nonlinear springs). Thus, the steel dowel is 3dimensionally embedded in the wood. The discretization of the embedment behavior, i.e., the number of spring elements along the dowel, depends on the side member thickness. Hirai [13] proposed a law to determine the number of springs depending on the thickness of the wood and the dowel diameter. The dowel itself is modeled by 1dimensional beam elements, which makes it possible to reduce the number of elements compared to a 3dimensional model. An elastic-plastic material behavior is assigned to these beam elements.

The single fasteners are embedded in wood and steel members using 3dimensional solid elements with orthotropic elastic material behavior, in order to account for the elastic deformation of the wood matrix in the load distribution. Moreover, the non-uniform stress distribution over the thickness of the wood members is preserved in this model. However, the borehole in the timber as well as a contact behavior of the steel dowel to the wood is not explicitly accounted for.

2.4 Spring Model (one Spring per Shear Plane) with Elastic Wood Matrix Model

The local behavior of the steel dowel-wood interface could in a next step be simplified by a spring that accounts for the local relative displacement between the components (see Figures 1 and 2). The spring element must however appropriately reflect the coupling between spring properties parallel and perpendicular to the grain [16], which herein is formulated in a nonlinear elastic manner using single dowel slip curves predicted by the beam-on-foundation approach (cf. Figure 2 and [17]). The steel dowel is represented by quasi-rigid beam elements and the structural members could be reduced to 2dimensional elastic shell elements, since the non-uniform stress distribution over the thickness of the timber side members will be neglected in this model.

Another possible simplification relates to the local contact behavior of the steel dowel-wood interface, namely the loss of contact on one side due to plastic deformations in the wood. A surface-to-surface contact model is necessary for this purpose, which requires continuum shell elements for the timber side members in the numerical model. Alternatively, special grids with nonlinear springs could be

designed (see [18] and [19]) or the contact could even be neglected and a kinematic coupling of the dowel and the surrounding wood could be applied. The latter has been used in the calculations presented herein. This introduces compression and tension stresses in the wood, and consequently, corrupts the stress state in the wood close to the interface with the dowel. It is however computationally much more efficient for the determination of the load distribution. The herein used spring behavior shown in Figure 2 does not consider a deviation of the displacement and load direction, while a different set of spring forces could be used to predict this effect on the load distribution.

2.5 Spring Model with Rigid Wood Matrix

The wood matrix behavior is further simplified by neglecting its elastic deformations and assuming it to be rigid. The same applies to the steel plate in steel-to-timber connections (see [19] and [21]). Consequently, the load distribution modeling strongly simplifies and can be solved by kinematic compatibility and equilibrium considerations. An incremental procedure is however necessary for the calculation of joint slip curves, due to the nonlinearity in the connection slip behavior. A global relative displacement in two directions and a relative in-plane rotation of the joint is distributed to the individual fasteners, yielding relative displacements of fasteners and their direction with respect to the grain direction of the timber. The latter quantities are subsequently used to assign single fastener loads from their slip curve (cf. Figure 2). Summing up of the loads finally yields internal forces of the joints, which are a consequence of the global relative displacement. On the contrary, calculation of load distribution for a given set of internal forces requires an iterative solution method. The procedure has been implemented in *Matlab* [19].

The main advantages of this model are its simple pre- and post-processing and short calculation times. Thus, the model can be integrated in the structural analysis of timber structures and even more, complex connection situations with different types of fasteners or end-grain contact situations can be considered using appropriate slip curves [19]. However, non-uniform load distribution under uniform normal force or shear force cannot be modelled with this approach, since the elastic deformation of the matrix is neglected.

2.6 Analytical Models with Linear Connection Slip

Assuming a linear instead of the nonlinear connection slip further simplifies the modeling. Preserving the orientation dependence in the slip behavior, i.e., linear elastic stiffness K_α depending on the load-to-grain angle, α , in-between parallel and perpendicular to the grain, the load of a single fastener $F_{M,i}$ due to an in-plane bending moment $M_{y,joint}$ is given by [3]

$$F_{M,i} = \frac{K_{\alpha i} \cdot r_i}{K_r} \cdot M_{y,joint} \quad (1)$$

with the distance of the fastener to the center of rotation r_i and the rotational stiffness K_r of the joint,

$$K_r = \sum_{j=1}^n K_{\alpha_j} \cdot r_j^2. \quad (2)$$

K_α could be determined experimentally for connections or numerically based on embedment data (cf. with experimental data in [4]) with beam-on-foundation approaches. For standardization purposes, an analytical function with stiffness values parallel and perpendicular to the grain in combination with e.g. the Hankinson equation could be used.

As a final simplification, an orientation independent slip behavior of the connection could be assumed, which yields single fastener loads F_j due to an in-plane bending moment $M_{y,joint}$ from [3]

$$F_j = \frac{M_{y,joint}}{I_p} \cdot r_j, \quad (3)$$

with I_p as the so-called polar moment of inertia calculated as the sum of squares of polar radii r_j , which are the radial distances of each fastener to the center of rotation. The rotational elastic stiffness $C_{ser,r}$ of the multi-fastener joint (in this case under serviceability conditions) is calculated as

$$C_{ser,r} = \sum_{j=1}^n K_{ser,j} \cdot r_j^2, \quad (4)$$

with $K_{ser,j}$ as the slip modulus of dowel j .

3. Modeling Load Distribution in Case of in-plane Bending Moment

In the following, selected numerical models described in section 2 will be applied to study the load distribution of multiple fastener joints. As reference connection, a double shear steel-to-timber connection with a 12 mm steel dowel, loaded by a center steel plate, is used. A wood side member thickness of 50 mm and a steel plate thickness of 12 mm were assumed together with material properties as summarized in Figure 2. The spacing of the dowels was increased compared to EC 5 minimum values by two times the dowel diameter, to account for plastic displacements in highly ductile or possibly reinforced connections, see Figure 3 and 4. Regarding load distribution in case of bending moment, three different dowel groups have been calculated with 2x2, 3x3, and 5x5 dowels using the models described in subsections 2.4 and 2.5. Pure moment loading was ensured by using symmetric boundary conditions without constraining the timber matrix.

The effect of the elasticity of the wood matrix could be assessed. The rotational stiffness of the investigated joints as well as the obtained load distribution was found to hardly depend on the elastic deformation of the timber matrix (see Figure 3). Only a slight increase in loads parallel to the grain combined with a slight decrease in loads perpendicular to the grain was observed in the Finite Element model with elastic wood matrix (see 5x5 dowels group in Figure 3).

However, the nonlinear orientation dependent slip curve of the fasteners is governing the load distribution. The high stiffness of the single fastener parallel to the grain (cf. fasteners 2&8 in Figure 3 top right, and 3&23 in Figure 3 bottom left) leads to a stronger loading of these dowels even compared to fasteners that are further away from the center of rotation (cf. fasteners 1&3&7&9 in Figure 3 top right, and 1&5&21&25 in Figure 3 bottom right). An analytical calculation based on the polar moment of inertia (see subsection 2.6) would yield a different load distribution in the initial loading path, since the load distribution would only be linearly related to the distance from the center of rotation, see Eq. (3). Comparison of linear with nonlinear models is discussed in [17] and underlines that an isotropic calculation might lead to an underestimation of loads parallel to the grain. Using a load orientation dependent stiffness K_α would enhance the prediction quality of the linear elastic model, see Eq. (1). The load distribution in the plastic loading path subsequently depends on the limit loads, which are again a function of the load orientation. With respect to the rotational stiffness of multiple fastener joints, the modeling results suggest a negligible influence of the elasticity of the timber matrix in-between the dowels. Except for the very first part of the slip curve, the difference in dowel loads between the models with elastic (2.4) and rigid (2.5) wood matrix was found to be less than 10 % (cf. Figure 3).

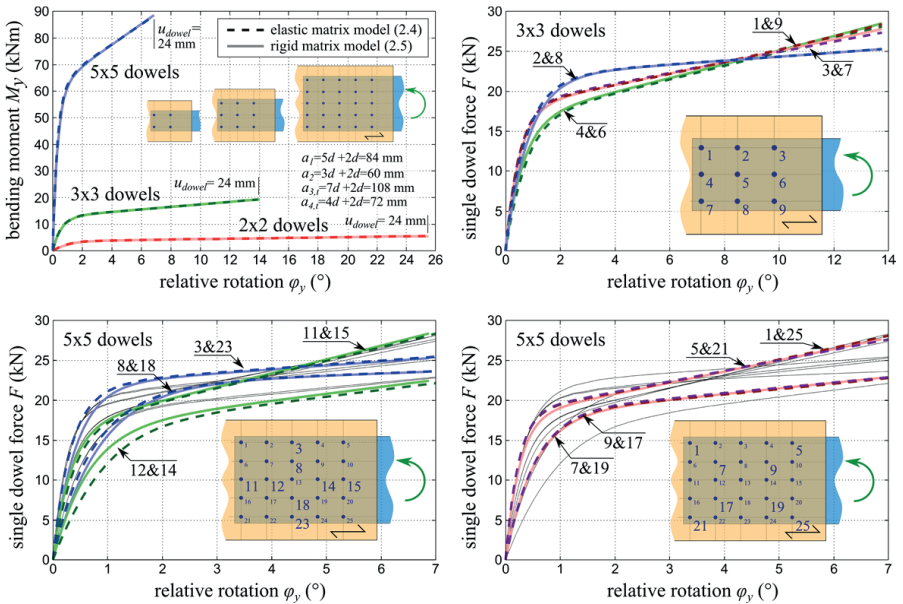


Fig. 3 Load distribution in case of in-plane bending moment – calculation examples.

The effect of lateral loads of the single dowels as a consequence of a prescribed displacement path, i.e. the fact that the load orientation does not necessarily follow the displacement orientation in anisotropic materials, could be neglected in the load distribution in case of a pure bending moment. This is due to the fact that these load components are pointing to the center of rotation and thus, they are not adding a contribution to the global moment. However, lateral loads might affect the stress distribution in the timber matrix predicted by the modeling approaches. This effect could be considered by adding the contribution of the lateral loads to the spring properties shown in Figure 2, which would then yield a deviation of load orientation from the prescribed displacement orientation.

4. Modeling Load Distribution in Case of Normal Force and Shear Force

Most research related to load distribution has been conducted for multiple fasteners in a row parallel to the grain, loaded by a normal force. This was done to assess the risk for brittle failure as a consequence of load and stress accumulation [6]. The load distribution effect is however also present in multiple fasteners in a row perpendicular to the grain, loaded by a force at an angle of 90° to the grain, subsequently called shear force. Jorissen [6] used an elastic spring model with nonlinear slip curves and even accounted for a random initial slip in the fasteners. Based on experimental and computational results, Jorissen proposed simplified design rules that comply with the effective number of fasteners concept for loading parallel to the grain. Effective number of fasteners in EC 5 are based on the elastic solution of Lantos (1969) (see [22] for a review of modeling approaches) taking into account longitudinal stiffness of the connected members, the number of fasteners, fastener spacing, and the slip modulus of the single fasteners. Models are based on an effective flexibility of the wood between the fasteners, which is a function of the parallel and lateral spacing, the side member thickness and the Young's modulus of wood in the load direction [6].

Sjödin and Serrano [23] showed the influence of several rows of dowels and the effect of the unloaded edge distance (a_2 and $a_{4,c,t}$ according to EC 5) on the load distribution and proposed two numerical models (based on linear elastic fracture mechanics and based on EC 5 single fastener strength values) for the calculation of the strength of such connections. The effect of lateral spacing and number of rows has also been investigated by means of a 2dimensional FEM model in [18] and [19].

The influence of the elastic deformation of the wood matrix on the load distribution in multiple fastener joints under normal force and shear force is exemplarily demonstrated in Figure 4, using a beam-on-foundation modeling approach (subsection 2.3) for the single dowel, and an elastic FEM model (subsection 2.4) and a rigid matrix model (subsection 2.5) for multiple dowel groups. Input data is visualized in Figure 2. Displacement boundary conditions in the numerical models have been set on the wood at a distance of 50 mm from the dowel, and on the steel plate at the height of the wood end grain. Slip curves of fastener groups are

compared to the theoretical slip curve of the single dowels times the number of dowels (black curves related to model 2.5 in Figure 4).

In case of normal force loading, the non-uniform load distribution vanishes after some millimeters of relative displacement, while due to the low stiffness of wood perpendicular to the grain, in case of shear force, a non-uniform load distribution prevails and limits the strength of the multiple fastener joint. The group effect in the stiffness of joints is clearly visible, and much more dominant under shear loading perpendicular to the grain.

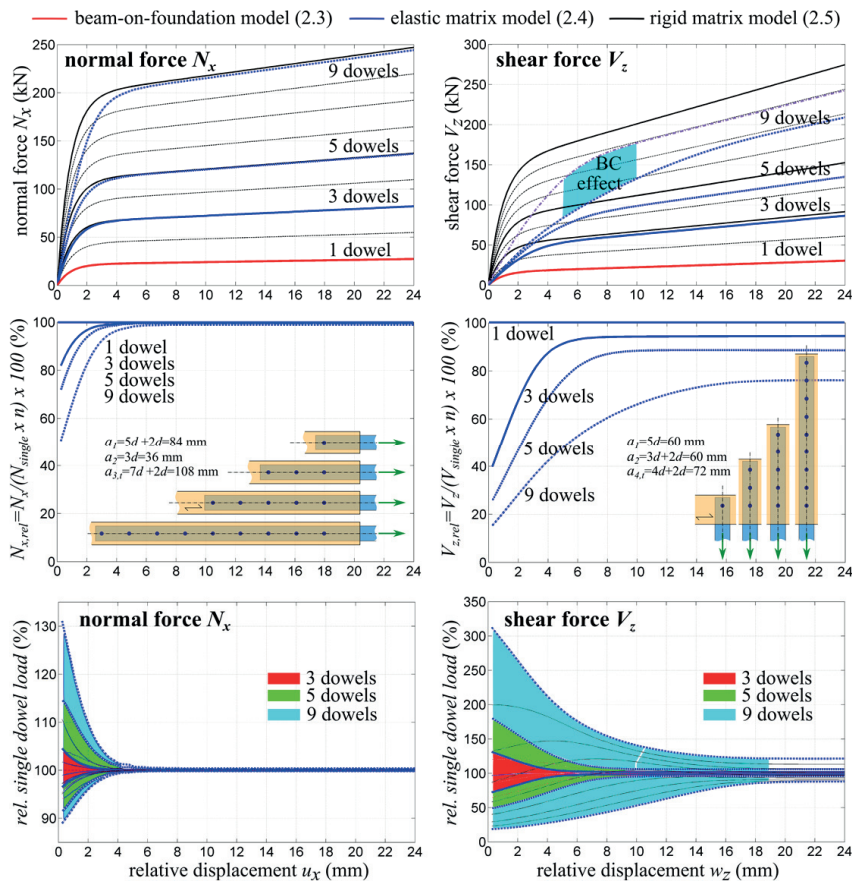


Fig. 4 Load distribution in case of normal force or shear force – calculation example

The load distribution, relative to a mean value of single dowel forces, is shown in Figure 4 bottom and shows a load accumulation in the fastener closest to the displacement boundary condition of the wood, which in this case is the dowel furthest away from the end grain of the wood member. If all dowels had 100 % of the mean value, a uniform load distribution would be given. The examples demonstrate the effect, but the load distribution naturally depends on the boundary conditions of the members. This is illustrated by the slip curve for 9 dowels under shear force loading (BC effect in Figure 4 top). The upper line is calculated with constrained displacements at mid-height of the beam instead of at the top edge of the beam.

5. Modeling of Load Distribution in Case of Complex Loading

In the most general case, a combination of internal forces acts on joints in timber structures. The combination of the above described special cases of single internal forces (sections 3 and 4) naturally depends on load cases of structures. All models presented in Figure 1 could be used for this purpose to describe the interaction in the load distribution on the global behavior of joints. However, some of them are computationally very costly and thus not practical for an engineering design. Thus, calculations presented in the following, were done with the model described in subsection 2.5, i.e., without elastic deformations of the wood matrix.

Based on this model, limit surfaces of joints can be calculated based on limit state criteria. In the following, we are using maximum relative dowel displacements of 1.5 mm, 6 mm, 12 mm and 24 mm as limit criteria to determine limit states of two multiple dowel joints (3x3 and 5x5 dowels with same layout as shown in Figure 2). Calculation results could be visualized in terms of relative displacements and rotation or, as in Figure 5, by means of internal forces of the dowel group.

Limit curves for pairs of internal forces (Figure 5 bottom) clearly show the interaction as well as the hardening behavior, as a consequence of load redistribution in the case of moment loading or of displacement hardening for loading perpendicular to the grain. Neglecting the weak stiffness of wood perpendicular to the grain might slightly affect the interaction with the shear force, particularly as regards the initial stiffness and for larger dowel groups.

The model predicted global behavior of the multiple fastener joint can be further used in the structural analysis of timber structures to account for the interaction of internal forces on the displacement behavior of the single fasteners and the load distribution among them, which finally governs the global behavior. Thus, each internal force (N_x , V_z , M_y) becomes a function of three degrees of freedom, namely the relative displacements u_x , w_z and the relative rotation ϕ_y . Alternatively, the relationship could be formulated in terms of a stiffness matrix, linking internal loads with relative displacements and rotation.

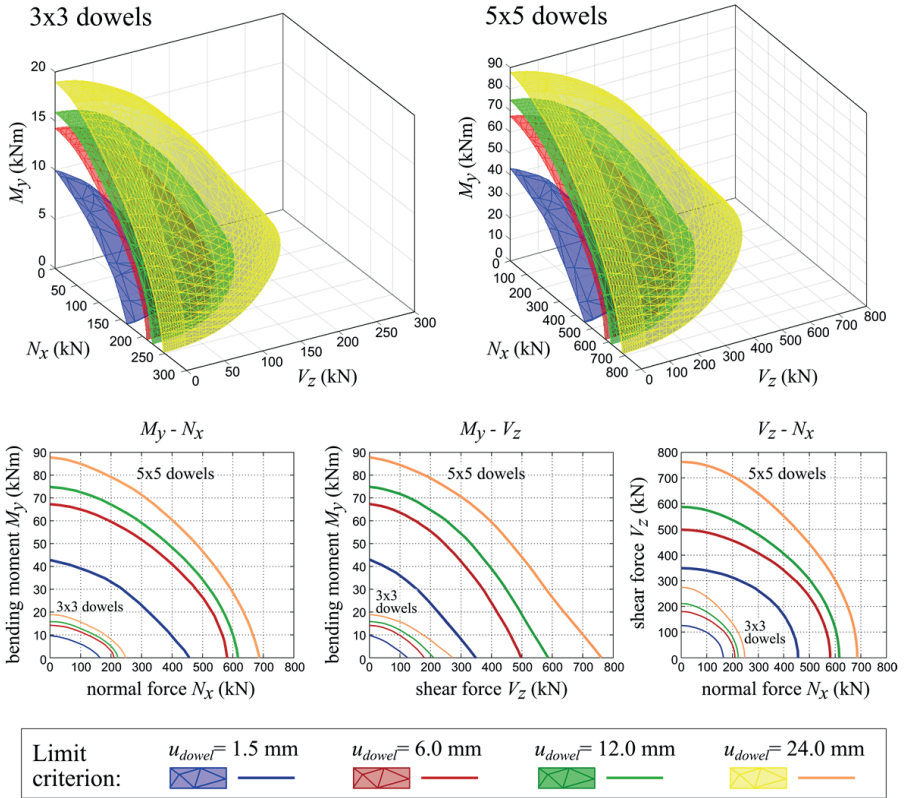


Fig.5 Load distribution in case of combined normal force, shear force and in-plane bending moment.

6. Suggestions for Revisions and Additions in Design and Testing Standards

The presented numerical models of multiple fastener joints are essential for an improved design of connections based on a sound load distribution as a prerequisite for a realistic stress state in the timber matrix. The contribution highlights the need for improved knowledge of the nonlinear embedment and single connection behavior as the main reason for non-uniform load distribution among fasteners, particularly under in-plane bending moment loading. Nonlinear embedment properties together with steel fastener material properties could be exploited in beam-on-foundation models to predict nonlinear slip curves of connections. This would avoid the need for comprehensive experiments for the assignment of stiffness properties of single fasteners by means of derivation of empirical equations. Thus, a revision of embedment testing standards is required to prescribe embedment testing of connections up to large relative displacements and

parameterization methods for the evaluation of test data. This would open up manifold possibilities for an advanced modeling and engineering design of connections, even including their seismic behavior.

The load distribution modeling is not only necessary for the determination of single connection loads in the verification of connections, but also for the assignment of stiffness properties in the structural analysis of timber structures in the first step. The isotropic distribution model was previously shown to be a very crude simplification, underestimating connection loads parallel to the grain under moment loading. A more advanced analytical model using load-to-grain orientation dependent stiffness of connections would considerably enhance load distribution modeling. Moreover, joint stiffness parallel and perpendicular to the grain is reduced with increased number of fasteners, due to the weak elastic stiffness of the timber.

Compared to the currently pursued design of single fastener connections in Eurocode 5, joint models presented herein would allow for an engineering design of multiple fastener joints. The design of connections is currently based on characteristic properties of the components, which yields lower limit strength below the characteristic strength of joints, since possible homogenization effects over the length scales are not accounted for. Herein, we propose to use mean values as input to the models, which consequently yields mean values on the connection and joint level. The variability should subsequently be defined by taking into account the failure mode in combination with appropriate partial safety factors for connections and joints. Since the modification factor only relates to the timber, it should be used to modify the mean values of the timber properties in the model instead of being assigned to the overall joint properties. Consequently, the fastener failure modes will not be modified by uncertainty considerations. There is a potential for the presented models to considerably enhance the elastic-plastic design of timber structures exploiting the ductile capacity of reinforced multiple fastener joints.

Future standardization should provide regulations and allow for both, a simplified analytical as well as for a more advanced numerical modeling of load distribution. A comprehensive comparison of numerical modeling of load distribution with linear elastic load distribution models could be performed to determine errors, and consequently limits, of the simplified linear load distribution model, which should be made transparent in the design standard. A more advanced numerical design of joints should be supported by the standard by providing regulations and input data for beam-on-foundation and load distribution models.

Throughout this paper, we pointed out the need for assessment of brittle failure, which should rest on a reliable prediction of stresses in the matrix, taking into account the non-uniform load distribution. This forms the basis for the design of reinforcement measures to avoid brittle failure. Assessment of brittle failure, particularly in case of combined loading, should build upon the herein proposed numerical models that account for interactions of internal forces.

7. References

- [1] EN 1995-1-1:2004 + AC:2006 + A1:2008, *Eurocode 5: Design of Timber Structures – Part 1-1: General–Common Rules and Rules for Buildings*, European Committee for Standardization (CEN), 2004, Brussels, Belgium.
- [2] Bader T.K., Schweigler M., Serrano E., Dorn M., Enquist B., and Hochreiner G., “Integrative experimental characterization and engineering modeling of single-dowel connections in LVL”, *Construction and Building Materials*, Vol. 107, 2016, pp. 235–246.
- [3] Racher P., “Moment resisting connections”, *Lecture C16 in Timber Engineering STEP 1*, Centrum Hout, 1995, The Netherlands.
- [4] Schweigler M., Bader T.K., Hochreiner G., Unger G., and Eberhardsteiner J., “Load-to-grain angle dependence of the embedment behavior of dowel-type fasteners in laminated veneer lumber”, *Construction and Building Materials*, Vol. 126, 2016, pp. 1020–1033.
- [5] Ormarsson S., and Blond M., “An improved method for calculating force distributions in moment-stiff timber connections”, *Proceedings of the World Conference on Timber Engineering (WCTE)*, 2012, Auckland, New Zealand.
- [6] Jorissen A., *Double shear timber connections with dowel type fasteners*, Delft University, 1998.
- [7] EN 14080:2013, *Timber structures – Glued laminated timber and glued solid timber – Requirements*, European Committee for Standardization (CEN), 2013, Brussels, Belgium.
- [8] Gecys T., Daniunas A., Bader T.K., Wagner L., and Eberhardsteiner J., “3D finite element analysis and experimental investigations of a new type of timber beam-to-beam connection”, *Engineering Structures*, Vol. 86, 2015, pp. 134–145.
- [9] Dorn M., *Investigations on the Serviceability Limit State of Dowel-Type Timber Connections*, PhD thesis, 2012, Vienna University of Technology.
- [10] Iraola B., Cabrero J.M., and Gil B., “Pressure-overclosure law for the simulation of contact in spruce joints”, *Proceedings of the World Conference on Timber Engineering (WCTE 2016)*, 2016, Vienna, Austria, eds.: Eberhardsteiner J., W. Winter, A. Fadaei, M. Pöll, Publisher: Vienna University of Technology, Austria.
- [11] Sandhaas C., *Mechanical behaviour of timber joints with slotted-in steel plates*, PhD thesis, 2012, Delft University.
- [12] Dias A.M.P.G., Van de Kuilen J.W.G., Cruz H.M.P., and Lopes S.M.R., “Numerical modelling of the load-deformation behavior of doweled softwood and hardwood joints”, *Wood and Fiber Science*, Vol. 42, 2010, pp. 480–489.

- [13] Hirai T., “Non-linear load-slip relationship of bolted wood-joints with steel side-members -II- Application of the generalized theory of beam on an elastic foundation”, *Makusu Gakkaishi*, Vol. 29, No. 12, 1983, pp. 839–844.
- [14] Foschi R., “Load-slip characteristics of nails”, *Wood Science*, Vol. 7, No. 1, 1974, pp. 69–76.
- [15] Sauvat N., *Résistance d’assemblages de type tige en structure bois sous chargements cycliques complexes*, PhD thesis, LERMES / CUST, Université Blaise Pascal-Clermont II, 2001, France (in French).
- [16] Vessby J., Serrano E., and Olsson A., “Coupled and uncoupled nonlinear elastic finite element models for monotonically loaded sheathing-to-framing joints in timber based shear walls”, *Engineering Structures*, Vol. 32, 2010, pp. 3433–3442.
- [17] Bader T.K., Schweigler M., Hochreiner G., and Eberhardsteiner J., “Load distribution in multi-dowel connections under moment loading – integrative evaluation of multiscale experiments”, *Proceedings of the World Conference on Timber Engineering (WCTE 2016)*, 2016, Vienna, Austria, eds.: Eberhardsteiner J., Winter W., Fadai A., Pöll M., Publisher: Vienna University of Technology, Austria.
- [18] Hochreiner G., Bader T.K., Schweigler M., and Eberhardsteiner J., “Structural behaviour and design of dowel groups Experimental and numerical identification of stress states and failure mechanisms of the surrounding timber matrix”, *Engineering Structures*, Vol. 131, 2017, pp. 421–437.
- [19] Hochreiner G., Riedl C., Schweigler M., Bader T.K., and Eberhardsteiner J., “Matrix failure of multi-dowel type connections – engineering modelling and parameter study”, *Proceedings of the World Conference on Timber Engineering (WCTE 2016)*, 2016, Vienna, Austria, eds.: Eberhardsteiner J., Winter W., Fadai A., Pöll M., Publisher: Vienna University of Technology, Austria.
- [20] Schweigler M., *A numerical model for slip curves of dowel connections and its application to timber structures*, Master thesis, 2013, Vienna University of Technology.
- [21] Jensen J., *Dowel-type fastener connections in timber structures subjected to short-term loading*, PhD thesis, 1994, Danish Building Research Institute, SBI-Rapport 237.
- [22] Blass H.J., “Multiple fastener joints”. *Lecture C15 in Timber Engineering STEP 1*, Centrum Hout, 1995, The Netherlands.
- [23] Sjödin J., and Serrano E., “A numerical study of methods to predict the capacity of multiple steel-timber dowel joints”, *Holz als Roh- und Werkstoff*, Vol. 66, 2008, pp. 447–454.

Brittle Failures of Connections Loaded Parallel-to-Grain

Pierre Quenneville
Professor

Department of Civil and Environmental Engineering
The University of Auckland
Auckland, New Zealand

Summary

The design of timber connections in most international design standards is based on the computation of the resistance of assumed ductile failure modes further modified for the potential occurrence of brittle failure ones. Research efforts initiated in the mid-1990's to develop separate design equations have culminated in the formulation of a set of comprehensive design equations for small and large diameter dowel connections failing in a brittle manner. The latest New Zealand design standard includes these equations in conjunction with the European Yield Model (EYM) set of equations which allow the designer to predict the resistance and the failure mode of a connection. This paper provides an overview of the brittle failure modes and associated design equations for small and large dowel connections loaded parallel-to-grain.

1. Introduction

There is agreement in principle within the international timber engineering community that design standard sections dealing with timber connections should be based on recognised mechanics models and that these models must identify each potential mode of failure. Failure modes to be considered are the yielding failure or the brittle failures in wood or other components of a connection. The mode with the lowest estimated capacity will be the governing one. Each mode may encompass a range of mechanisms. For example, the yielding modes will encompass the mechanisms associated with the European Yield Model (EYM). The brittle modes will include mechanisms such as block tear out of a fastener group or row shear failure in the line of the fasteners.

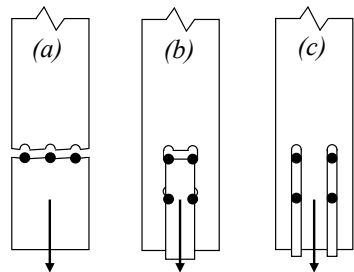


Fig. 1 Observed failure modes for timber bolted connections loaded parallel-to-grain (a) net tension (b) group tear-out (c) row shear (d) yielding

As it is the case, in most design standards [1], [2], the approach for the design of multiple-fastener connections is solely based on the EYM, further modified in certain cases to attempt to account for potential brittle failure modes. As a result of the many recent studies on the brittle behaviour of connections in timber structures [3], [4], [5], failure modes for large diameter dowel fasteners have been identified and are as shown in Figure 1. For small diameter fasteners, the modes of failures identified are shown in Figure 2.

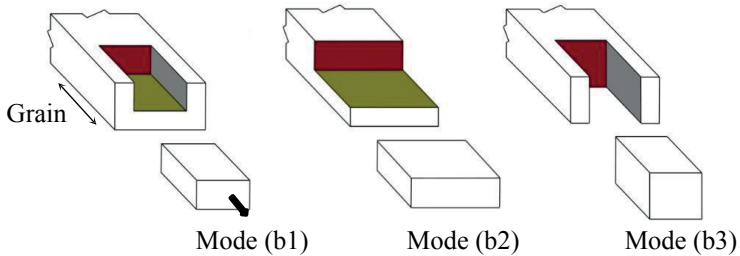


Fig. 2 Different possible failure modes of wood block tear-out [6].

One will have noticed that the failure modes shown in Figure 2 are applicable to both single and double shear connections.

These brittle failure modes have been observed in small [6] and large diameter dowel-type connections, as demonstrated in Fig. 3.

Over 1500 connection specimens have been tested over the last 25 years by the author and students under his supervision, ranging from bolted connections to rivet, nail or screw connections.

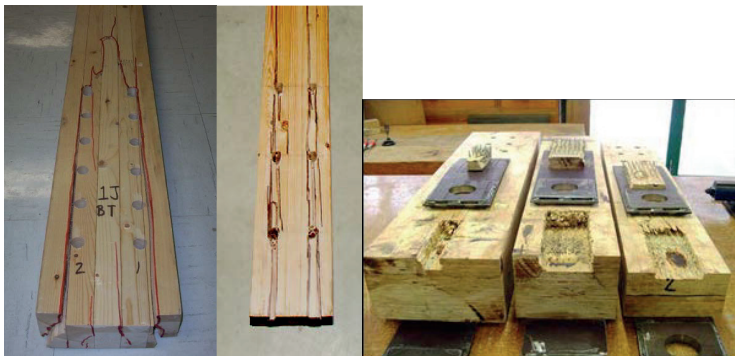


Fig. 3 Wood failure parallel to grain: (a) group tear-out (b) row shear (c) block tear-out bounded by a rivet cluster perimeter;

2. Proposed Design Approaches

The data collected has served to demonstrate that the behavior of connections, either exhibiting yielding or one of the wood failures, is a mixture of the two. If none of the wood failure occurs, i.e. there is no failure in tension or in longitudinal shear in the wood, the fastener will resist the load through bearing and one of the EYM mode of failure will occur. If the resistance of the connection to all brittle failure modes is higher than the resistance of the EYM mode 1, then the resistance of the EYM mode 1 will become the ultimate resistance of the connection. It is the upper limit of the resistance of the fastener (the resistance will include a small addition due to the friction of the connection parts).

2.1. Small Dowel-Type Fasteners

In light of the complexity of predicting the resistance of connections either failing by yielding or through one of the brittle failure, Zarnani [6] proposed the following design approach to predict the resistance of connections with small dowel-type fasteners.

$$N^* \leq N_0 \quad (1)$$

$$N_0 = \begin{cases} N_{0,w,e} & \text{if } N_{0,w,e} < N_{0,y,y} \\ N_{0,y,y} & \text{if } N_{0,w,y} < N_{0,y,y} \leq N_{0,w,e} \\ N_{0,w,y} & \text{if } N_{0,y,y} \leq N_{0,w,y} \leq N_{0,y,u} \\ N_{0,y,u} & \text{if } N_{0,y,u} < N_{0,w,y} \end{cases} \quad (2)$$

where

N^* load applied to the joint

N_0 parallel-to-grain joint resistance

$N_{0,w,e}$ design elastic block tear-out strength

$N_{0,w,y}$ design post-yield block tear-out strength

$N_{0,y,y}$ fastener group design yield strength (governing EYM mode)

$N_{0,y,u}$ fastener group design ultimate yielding strength (EYM mode 1)

It is important to distinguish between the $N_{0,y,y}$ and $N_{0,y,u}$. As shown in Fig. 4, the latter one is the strength associated with the EYM mode 1 failure. It is the ultimate resistance possible for a given connection configuration. The former one, is the strength associated with one of the other EYM failure mode, only if the EYM mode 1 is not the governing one (if the EYM mode 1 is the governing yielding mode, one would expect an elasto-plastic relationship). For small-dowel connection, $N_{0,y,u}$ can be two to three times $N_{0,y,y}$.

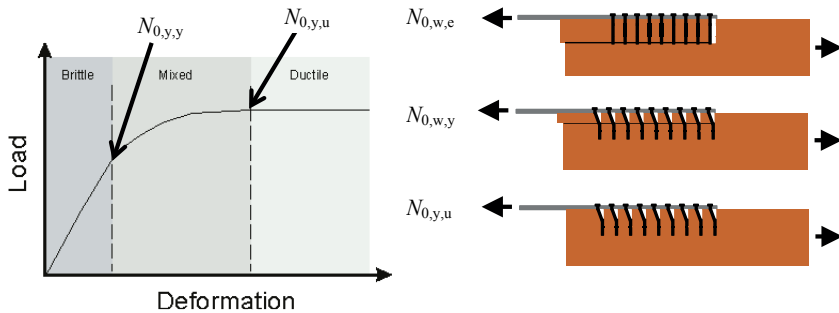


Fig. 4 Potential failure zones of a timber connection.

The values of $N_{0,w,e}$ and $N_{0,w,y}$ are determined from the resistance equations for brittle failure modes. In the instance of small dowel-type fasteners such as rivets, screws and nails, Zarnani [6] proposed a block tear-out model that predicts with excellent results, the resistance of the connection. The model is based on the principle that the failure planes attract a portion of the connection load in proportion to the stiffness of the adjacent timber, as shown in Figure 5.

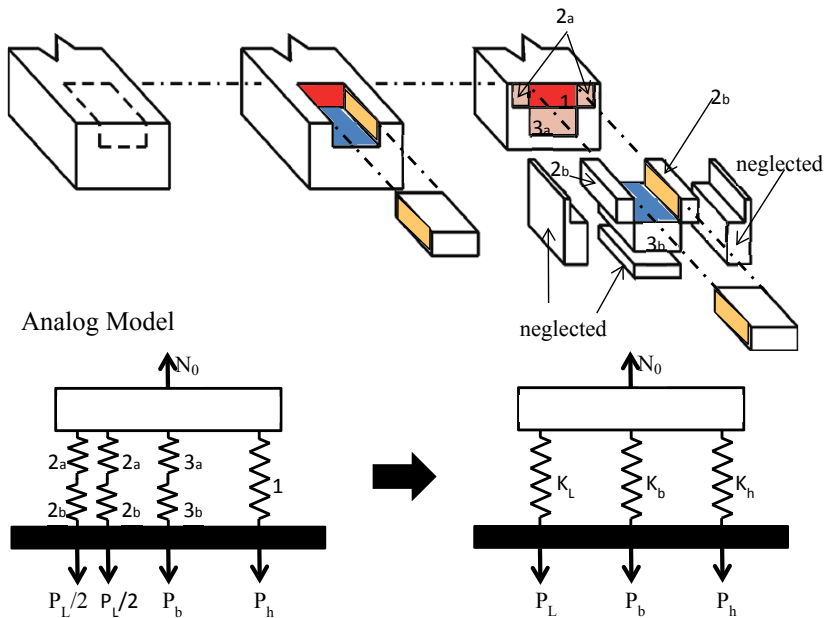


Fig. 5 Stiffness-based failure model for block tear-out [6].

The adjacent timber portion can be loaded in shear or in tension and depending on the connection configuration and member size, a certain portion of the load is channelled to one of the possible failure plane. The connection resistance is the sum of the load carried by each failure plane and this load is attained when a failure plane resistance is reached. The model is based on the two assumptions that:

- a. each of the failure plane carry a portion of the joint force, and
- b. the failure of the joint is triggered by the failure of any one of the failure plane.

The first assumption is evident when one considers the comparison shown in Figure 6. The second one leads to the following formulation:

$$N_0 = P_L + P_b + P_h \tag{3}$$

The first of the following three ratios that reaches a value of 1 triggers a failure (see Figure 5):

- P_L / resistance of shear plane L
- P_h / resistance of tension plane h
- P_b / resistance of shear plane b

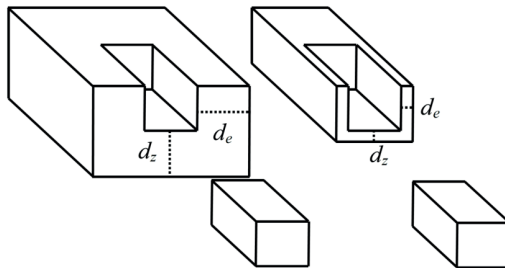


Fig. 6 Failure plane loading concept for block tear-out leading to the first assumption (same block torn-off but different failure plane loading)[6].

Zarnani [6] has developed a set of equations to determine the connection resistance when block tear-out failure occurred based on the above two assumptions.

The reader is referred to the rivet design guide [11] for a very comprehensive design procedure including all yielding and brittle failure modes and numerous design examples.

The design procedure for predicting the resistance of small dowel-type fasteners has been used to predict the resistance of test data available in the literature and from experiments conducted by Zarnani [6]. Figures 7 and 8 show the results of the predictions using the proposed model and design philosophy for both rivet connections (Fig. 7) and nail connections (Fig. 8) in comparison to the existing predictions using the EC 5 design method.

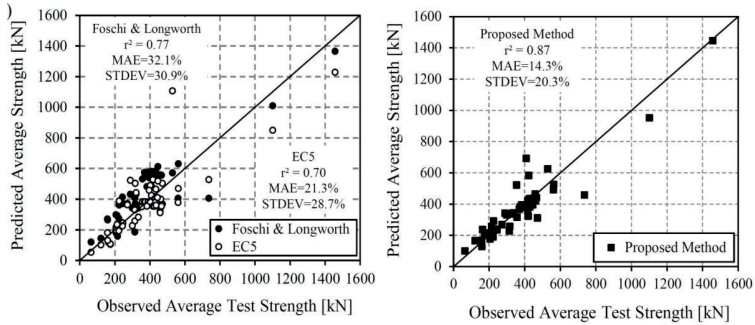


Fig. 7 Predictions vs. observations for rivet connection capacity [6].

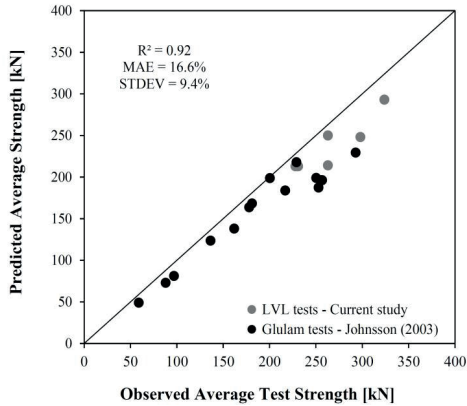


Fig. 8 Predictions vs. observations for nail connection capacity [6].

2.2. Large Dowel-Type Fasteners

For large dowel-type fasteners (bolts, dowels or coach screws with a diameter greater than 6 mm), the following design approach has been proposed by the author:

$$N^* \leq N_{0,y} \quad (4)$$

$$N^* \leq N_{0,w} \quad (5)$$

where

N^* = load applied to the joint

$N_{0,y}$ = design ultimate yielding strength of the fastener group in the joint
(determined using the EYM equations)

- $N_{0,w}$ = design strength of the fastener group
= the minimum of $N_{0,t}$, $N_{0,gt}$ or $N_{0,rs}$ if under a tension load
- $N_{0,t}$ = member design net tension strength
- $N_{0,gt}$ = member design group tear-out strength
- $N_{0,rs}$ = member design row shear strength

One will note that the net tension resistance verification is part of the connection design chapter to prevent any omission of this important verification. In equations 4 and 5, the EYM equations and the net tension failure are not novel and will not be covered here. In equation 5, the row shear resistance is given by the following relationship:

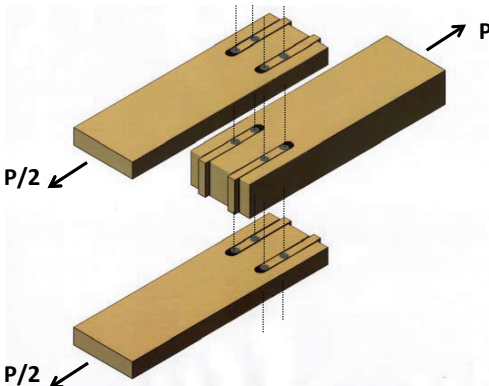
$$N_{0,rs} = \phi_w \cdot RS_{i \min} \cdot n_r \cdot k_1 \cdot k_{12} \tag{6}$$

where

- $RS_{i \min} = \text{minimum} (RS_1, RS_2, \dots, RS_{nr})$, in N
- RS_i is the characteristic row shear strength along 2 shear planes of row i
- $RS_i = 0.75 \cdot f_{s,k} \cdot K_{LS} \cdot n_{fi} \cdot 2 \cdot a_{cri} \cdot t$
- n_r is the number of rows in the member

and ϕ_w , k_1 and k_{12} are the material, load duration and service condition factors respectively, and

- $f_{s,k}$ is the member characteristic shear strength, in MPa
- K_{LS} is the loading surfaces factor (see Figure 11)
- n_{fi} is the number of fasteners in row i
- $a_{cri} = \text{minimum} (a_1, a_{3i})$ for row i , in mm (see Figure 10)
- t is the member thickness, in mm



When using equation 6, one has to verify the row shear resistance in all members of the connection, as shown in Figure 9 and all possible row shear resistances for each of the different rows ($RS_{i \min}$), as shown in Figure 10.

Fig. 9 Potential row shear failures in members of a connection.

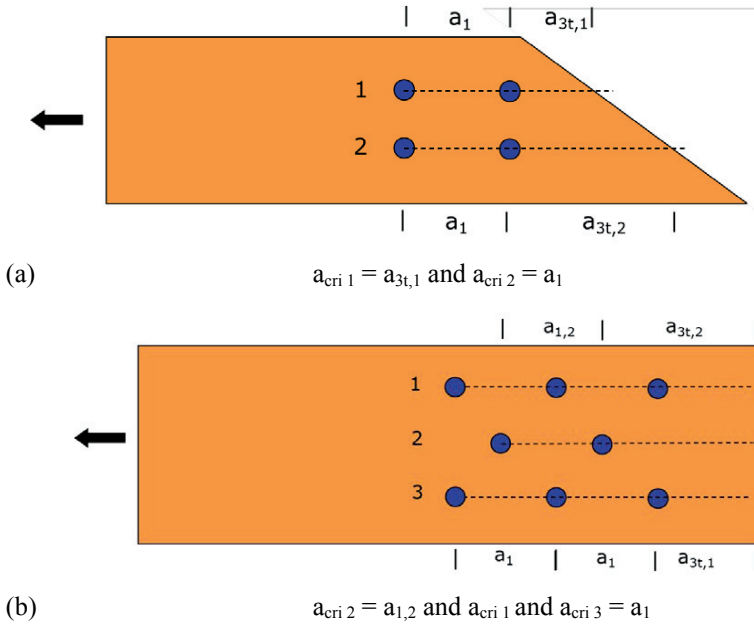


Fig. 10 Definition of a_{cri} for different rows of a joint.

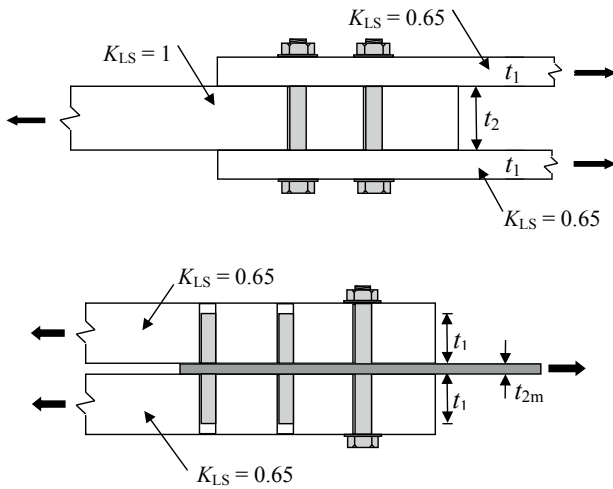


Fig. 11 Definition of K_{LS} factor in row shear equation.

The design equation to predict the resistance of the group tear-out failure mode in large dowel-type connection is given by:

$$N_{0,gt} = \phi_w \cdot (0.5 \cdot (RS_1 + RS_{nr}) + 1.25 \cdot f_{t,k} \cdot A_{GT-net}) \cdot k_1 \cdot k_{12} \quad (7)$$

where

RS_1 is the characteristic row shear strength along 2 shear planes of row 1

RS_{nr} is the characteristic row shear strength along 2 shear planes of row n_r

$f_{t,k}$ is the member characteristic tensile strength, in MPa

A_{GT-net} is the net area between the two outer rows, in mm^2

ϕ_w , k_1 and k_{12} have the same definitions as in equation 6.

Equations 5, 6, and 7 are the result of extensive bolted connection testing conducted since 1995 where each of the configurations parameters have been varied in order to assess its effect on the failure mode and resistance. Figures 12, 13 and 14 are graphs comparing the resistance predictions using the appropriate design formula for the observed connection failure modes and the measured average failure load. The predicted values have been determined using material information available in the design standard. Each point represents the average of 10 specimens.

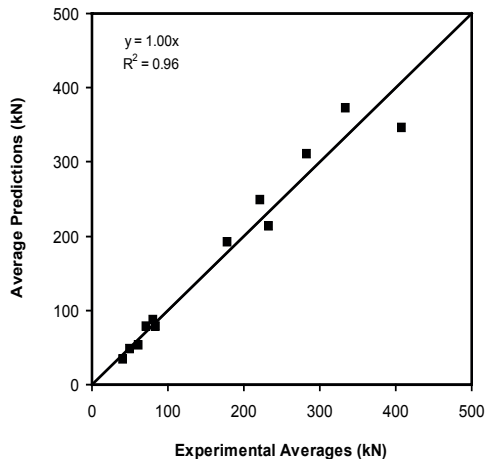


Fig. 12 Predicted averages of connection capacity vs experimental resistance averages for the yielding failure mode

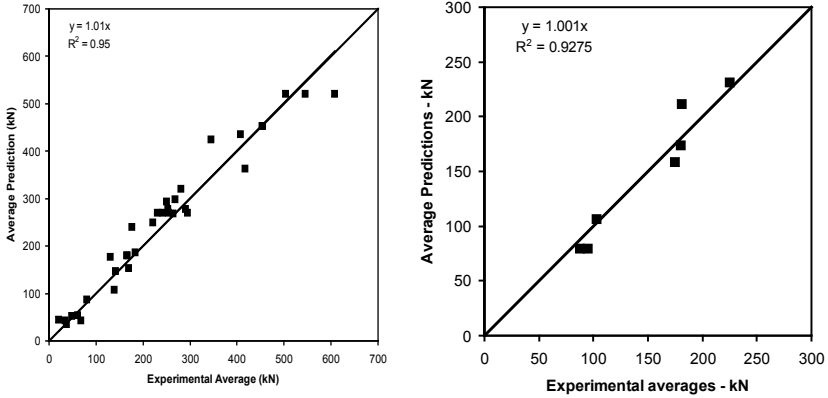


Fig. 13 Predicted averages of bolted connection capacity determined using equation (6) vs average experimental resistance for row shear failures (a) steel-wood-steel connections ($K_{LS} = 1$) (b) wood-steel-wood connections ($K_{LS} = 0.65$).

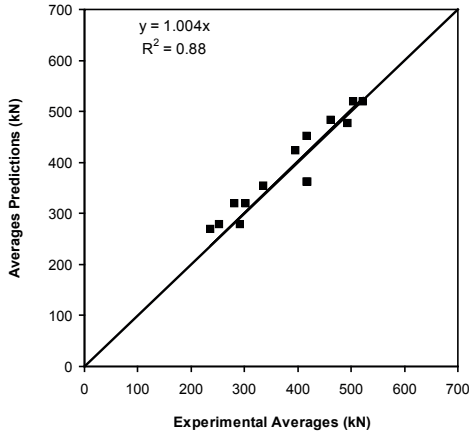


Fig. 14 Predicted averages of bolted connection capacity determined using equation (7) vs average experimental resistance for group tear-out failures.

The prediction of the brittle failure mode resistances for bolted connections using equations 5, 6 and 7 has formed the basis for the updated Canadian design standard since 2009. It is also being incorporated in the proposed connection chapter of the

New Zealand timber design code, along with the design approach for the determination of the resistance of small dowel-type fasteners.

3. Conclusions

The design procedures for timber connections in most design codes are based mainly on the European Yield Model modified by a factor to attempt to account for the potential brittle failure modes. For multi-fastener connections loaded parallel to grain, failure of the wood can be the dominant mode. Two design procedures are proposed to identify the wood and fastener capacities under possible brittle, mixed and ductile failure modes; one for small dowel-type fasteners and the other one, for large dowel-type fasteners. The fastener resistances for yielding and ultimate limit states are determined using the relevant wood embedment strength and fastener moment capacity, as per the EYM theory. The proposed design procedures for determining the resistance of brittle failures have been verified using tests conducted on various fasteners such as bolts, rivets, nails and screws. The proposed design approaches are now part of the proposed connection chapter of the future New Zealand timber design standard.

4. Acknowledgements

The content of this paper is the result of the contribution of numerous graduate students over the last 30 years and funding sources from the Canadian and New Zealand governments.

5. References

- [1] EN 1995-1-1:2004, *Eurocode 5-Design of timber structures*, European Committee for Standardization (CEN), 2004, Brussels, Belgium.
- [2] NDS-1997, *National Design Specification (NDS) for wood construction*, American Forest & Paper Association, Inc., 1997, United States of America.
- [3] Quenneville J.H.P., and Mohammad M., "On the failure modes and strength of steel-wood-steel bolted timber connections loaded parallel-to-grain", *Canadian Journal of Civil Engineering*, Vol. 27, 2000, pp. 761-773.
- [4] Mohammad M., and Quenneville J.H.P., "Bolted wood-steel and wood-steel-wood connections: verification of a new design approach", *Canadian Journal of Civil Engineering*, Vol. 28, 2001, pp. 254-263.
- [5] Reid M.S., *Predictions of two-row multi-bolted timber connections resistance subjected to parallel-to-grain loading*, Master Thesis, 2004, 146 pages, Royal Military College of Canada, Kingston, Canada.
- [6] Zarnani P., *Load-Carrying Capacity and Failure Mode Analysis of Timber Rivet Connections*, Thesis submitted in partial fulfillment for the degree of Doctor of Philosophy, 2013, The University of Auckland, New Zealand.

- [7] Jorissen A., *Double Shear Timber Connections with Dowel Type Fasteners*, Delft University Press, 1998, 264 pages.
- [8] Johnsson H., *Plug shear failure in nailed timber connections*, Doctoral dissertation, 2003, Department of Civil and Environmental Engineering, Lulea University of Technology, Sweden.
- [9] Hanhijärvi A., and Kevarinmäki A., *Timber failure mechanisms in high-capacity dowelled connections of timber to steel*, Espoo, VTT publication 677, 2008, 53 pages.
- [10] CSA O86-09, *Engineering design in wood*, Canadian Standards Association, 2009, Toronto, Canada.
- [11] Zarnani P., and Quenneville P., *EXPAN Timber rivet connections design guide*, 2013, 121 pages., New Zealand.

Brittle Failure of Connections Loaded Perpendicular to Grain

Robert Jockwer
Senior Scientist
ETH Zurich
Zurich, Switzerland

Philipp Dietsch
Team Leader Timber Structures
Technical University of Munich
Munich, Germany

Summary

Connections loaded perpendicular to grain are prone to brittle failure due to fracture induced by tension perpendicular to grain stresses. Different approaches can be found in design codes and literature to account for the reduction of load-carrying capacity in the design of the structure. In this paper selected design approaches are discussed and their behaviour with regard to different geometrical parameters is analysed. The structural behaviour of connections loaded perpendicular to grain is evaluated on the basis of a test series carried out at ETH Zurich and based on test results from literature. The impact of different geometrical parameters on the load-carrying capacity is demonstrated and the design approaches are benchmarked by the large number of individual test results. Recommendations for a safe design are given at the end of the paper.

1. Introduction

1.1 Failure Modes of Connections and Considerations in Design

Failure in connections can occur either due to local failure of the fasteners or due to failure in the surrounding timber. Design should be aimed at receiving a failure of the fastener in order to be able to adjust the load-carrying capacity by the choice of an adequate fastener diameter and in order to achieve a ductile failure mechanism.

The different failure modes of fasteners in shear were described by Johansen [1] and are given in the European design code for timber structures EN 1995-1-1 (Eurocode 5, EC 5) [2]. The failure modes of the so called European Yield Model (EYM) are defined mainly by the properties and diameter of the fastener and the density and thickness of the timber members.

In addition to the resistance of the fastener, the surrounding timber has to allow for sufficient load distribution in order to prevent splitting and brittle failure in the timber. Minimum spacing and minimum end and edge distances of the fastener are specified in EC 5 in order to prevent the premature splitting of the timber. The

effect of splitting of multiple fasteners loaded in a row parallel to grain is accounted for by a reduction factor for the load-carrying capacity that is leading to a reduction of the number of effective fasteners. For fasteners in a row loaded perpendicular to grain, such a reduction in form of an effective number of fasteners is not included. Instead a simple design approach is given to account for the risk of tension perpendicular to grain splitting at connections loaded perpendicular to grain.

In this study the different impacts on the fracture and failure of connections loaded perpendicular to grain are evaluated and discussed and recommendation for a safe design are given.

1.2 Tension Perpendicular to Grain Failure of Connections

Due to its anisotropic material behaviour wood shows very high strength and stiffness when being loaded in direction of the grain but only moderate or low strength and stiffness when being loaded perpendicular to the grain direction. Especially in tension perpendicular to grain, not only low strength and stiffness but also brittle failure behaviour can be observed. That is why an economic design should avoid any loading in tension in direction perpendicular to grain. Since the strength of timber in tension perpendicular to grain is generally low and shows high variability conservative values are specified in different design codes e.g. the Swiss SIA 265 [3]. The values given in the product standards for solid timber EN 338 [4] or glued laminated timber EN 14080 [5] corresponding to EC 5 give representative values that may not be adequate to design the specific case of stress singularities near concentrated loads and cracks.

In connections loaded perpendicular to grain very high tensile stresses perpendicular to grain occur that may initiate cracking and cause failure of the timber member. A typical crack pattern occurring at connections loaded perpendicular to grain is illustrated in Fig. 1.

The magnitude of the tensile stresses perpendicular to grain depends mainly on the relative distance h_e/h of the most distant row of fasteners from the beam edge loaded in tension (lower beam edge in Fig. 1). The force has to be transferred from the connection into the beam by shear and perpendicular to grain stresses. Depending on the position of the connection along the beam height, the transfer of forces induces compression or tension stresses perpendicular to grain. In order to avoid tension stresses perpendicular to grain and in order to reduce the risk of cracking and failure of members, the connection should be

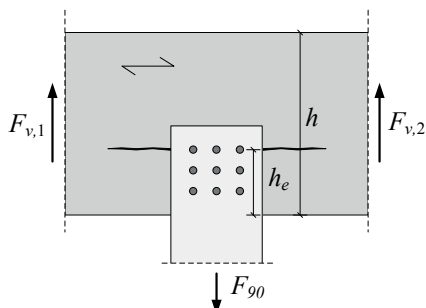


Fig. 1 Typical crack pattern at a connection loaded perpendicular to grain.

positioned at sufficient distance from the beam edge loaded in tension. If that is not possible the connection should be reinforced in order to prevent fracture and to bridge possible cracks.

1.3 Reinforcement

In order to prevent cracking and premature failure members loaded in tension perpendicular to grain should be reinforced. Recommendations for the reinforcement of connections loaded perpendicular to grain can be found e.g. in the former German design code for timber structures DIN 1052 [6] or in the German national annex to EC 5 [7] and are currently under development for the next generation of EC 5 [8].

The reinforcement can be distinguished into internal and external reinforcement. Internal reinforcement can be achieved by means of glued-in rods or fully-threaded screws or rods. The reduction of cross-section by this internal reinforcement should be accounted for in the design. External reinforcement can be realized e.g. by means of wood based panels (e.g. plywood or laminated veneer lumber) or boards glued to the timber member or pressed-in punched metal plates. When designing the glued on external reinforcement it needs to be accounted for the unequal stress distribution in the glue line and the resulting unequal distribution of forces in the reinforcing panel. When determining the tensile forces in the reinforcing elements, the tensile capacity of the timber may be neglected.

1.4 Types of Connections Loaded Perpendicular to Grain

Connections where a load component is introduced into a beam at an angle to grain occur e.g. at primary to secondary beam connections, to hang up loads or members to beams. Other examples, although only of temporary use, are mounting joints for lifting and assembling large timber elements or CLT panels.

Connections with slotted in metal steel plates are often made by means of dowels. External steel plates are used e.g. in combination with bolts or screws. Punched metal plates are used e.g. for truss structures made of solid timber elements. Three dimensional nailing plates like joist hangers are often nailed or screwed.

2. Theoretical Description of the Load-Carrying Behaviour of Connections Loaded Perpendicular to Grain

2.1 General

The structural behaviour of connections loaded perpendicular to grain has been extensively studied by several authors in various studies. The studies differ with regard to the intended goal and the development of concise design rules. Different geometrical and material parameters are used depending on the complexity of the approaches.

In DIN 1052 [6] an empirically based design approach was included, that was developed on the basis of tests on nailed connections on full size glulam beams. In

EC5 [2] a theoretically based design approach is given, that is based on the fracture mechanical model of a connection with a single dowel. This approach was developed further in order to account for additional geometrical parameters by Ballerini [9].

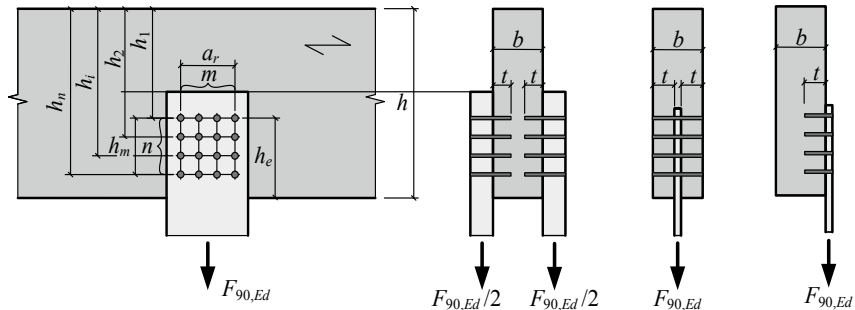


Fig. 2 Denotation at a connection loaded perpendicular to grain with cross-sectional views of a two sided, central or one-sided arrangement of the tensile members.

These three design approaches were selected for further discussion due to their existing implementation in design codes, the consideration of a wide range of geometrical parameters and the availability of relevant material parameters.

2.2 Strength Based Design Approach

A first empirically based design approach was presented by Möhler and Siebert [10,11]. The approach is based on studies and tests described in [10,12]. The size effect of the volume loaded in tension perpendicular to grain is accounted for based on studies by Barret et al. [13] by an exponent of the effectively loaded tension area $(t_{ef}h)^{0.8}$.

The design approach was further developed by Ehlbeck et al. [14,15] and is included in the DIN 1052 [6].

$$\frac{F_{90,Ed}}{R_{90,d}} \leq 1 \quad (1)$$

$$R_{90,d} = k_s k_r \left(6.5 + \frac{18k_c^2}{h^2} \right) (t_{ef}h)^{0.8} f_{t,90,d} \quad (2)$$

$$k_s = \max \left\{ 1; 0.7 + \frac{1.4a_r}{h} \right\} \quad (3)$$

$$k_r = \frac{n}{\sum_{i=1}^n \left(\frac{h_i}{h} \right)^2} \quad (4)$$

The individual configuration of the fastener layout is considered by the two factors k_s and k_r in Eq. (3) and (4), respectively: The factor k_s accounts for the height of the connection h_m as well as the number n of fasteners in the connections. The factor is based on the assumption that the contribution of each single fastener to the entire amount of tension perpendicular to grain stresses is reduced with the square of the ratio between the distance h_1 of the closest row of fasteners to the unloaded beam edge and the distance h_i of each fastener row i to the unloaded beam edge.

The tests being the basis for this design approach showed that connections with stiffer fasteners allowed for higher load-carrying capacities. The effective length of the fasteners, necessary to determine the value t_{ef} , was chosen in dependency of the diameter of the fasteners. For more slender fasteners the effective length of the fasteners decreases in proportion to the width of the beam. For stouter fasteners the full fastener length can be accounted for.

If more than one connection loaded perpendicular to grain is located in a single beam, there can be an interaction between neighbouring connections. If the clear distance l_1 between two neighbouring connections is larger than twice the beam height, no interaction has to be accounted for. In contrast, for distances smaller than half the beam height both connections have to be treated as one single connection of greater width. For intermediate clear distances l_1 the impact of neighbouring connections may be accounted for by the following reduction factor per connection:

$$k_g = \frac{l_1}{4h} + 0.5 \quad (5)$$

For connections located close to the beam end with a clear end distance $a_3 < h$, only half the load-carrying capacity may be accounted for.

The design approach in Eq. (2) is valid only for relative connection height $h_c/h \leq 0.7$. Connections with $h_c/h > 0.7$ showed only a minor risk of failure due to cracking, i.e. no special design with regard to tension perpendicular to grain stresses is necessary.

In contrast connections with $h_c/h < 0.2$ should be avoided and – if absolutely necessary – loaded only in short durations of load (e.g. wind loads).

2.3 Fracture Mechanics Based Design Approach

A fracture mechanics based design approach for connections loaded perpendicular to grain was proposed by van der Put [16,17]. Based on the equilibrium of energies during growth of a crack of infinitesimal length, the energy released during crack growth can be calculated from the variation of elastic energies in the beam.

The example of a crack of length x with a crack growth by Δx is illustrated in Fig. 3. The resistance of the timber against fracture can be described by the critical fracture energy G_c , the shear stiffness G and the modulus of elasticity E_0 in direction parallel to grain as well as the beam height, the beam width and the relative connection height. In a general approach proposed by Jensen [18] the crack length x is considered in addition.

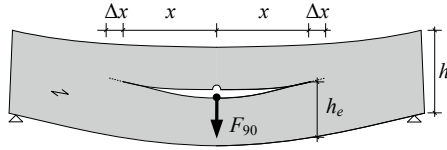


Fig. 3 Typical crack pattern with denotation of the crack length x and crack growth Δx for a connection with a single dowel.

The approach proposed by van der Put [16] is a simplification of Eq. (6) in which the impact of crack length is disregarded ($x = 0$). The resulting very simple approach in Eq. (7) is the maximum of the load-carrying capacity at crack initiation at the connection in midspan.

$$F_{90,crit} = 2b \sqrt{\frac{GG_c h_e}{0.6 \left(1 - \frac{h_e}{h}\right) + 1.5 \frac{G}{E_0} \left(\frac{x}{h_e}\right)^2 \left(1 - \left(\frac{h_e}{h}\right)^3\right)}} \quad (6)$$

$$F_{90,crit} = 2b \sqrt{\frac{GG_c h_e}{0.6 \left(1 - \frac{h_e}{h}\right)}} \quad (7)$$

Other geometrical parameters like the width or the configuration of the connection are not included in the fracture mechanical basis of these approaches. Instead the cracks at a connection with one single point-like dowel-type fastener are described. It can be seen from the tests and the design approach in Eq. (2) that this case with $a_r = 0$ and $h_m = 0$ is the most unfavourable configuration of the fastener layout with regard to the load-carrying capacity. Therefore the design approach in Eq. (7) allows for a conservative design.

The material property values used in Eq. (7) can be either calculated from property values determined in standardized tests, or calibrated on the basis of tests on connections loaded perpendicular to grain. When calculating the theoretical values of a material strength parameter $C_1 = (G \cdot G_c / 0.6)^{0.5}$ for Eq. (7), pure crack opening failure in fracture mode 1 can be assumed with $G_{c,mean} = G_{1,mean} = 0.3 \text{ N/mm}$ for spruce softwood [19]. The theoretical value of the material parameter is $C_{1,mean} = (G \cdot G_{1,mean} / 0.6)^{0.5} = (650 \cdot 0.3 / 0.6)^{0.5} \approx 18 \text{ N/mm}^{1.5}$. This value is higher than the value proposed by van der Put and Leijten [17] with $C_{1,mean} \approx 15 \text{ N/mm}^{1.5}$, which was back calculated from tests. Leijten and Jorissen [20] studied the material property values more in detail and made a comparison with different other design models. A characteristic value of the material strength property $C_{1,k} \approx 10 \text{ N/mm}^{1.5}$ was proposed in [20] for consideration in design codes. For the implementation of Eq. (7) in Eurocode 5, $C_{1,k} \approx 14 \text{ N/mm}^{1.5}$ was chosen. This factor overestimates the load-carrying capacity compared to results from tests as discussed in [21].

An additional adaptation of Eq. (7) was done during implementation into Eurocode 5: The verification is not based on the load applied to the connection $F_{90,Ed}$ but it is based on the shear forces reacting $F_{v,Ed}$ on both sides of the connection loaded perpendicular to grain as shown in Eq. (8) and (9), see also Fig. 1.

$$F_{v,Ed} \leq F_{90,Rd} \quad (8)$$

$$F_{v,Ed} = \max \{ F_{v,Ed,1}; F_{v,Ed,2} \} \quad (9)$$

The corresponding resistance of the connection is only half the value compared to Eq. (7):

$$F_{90,Rk} = C_{1,k} b w \sqrt{\frac{h_c}{1 - \frac{h_c}{h}}} \quad \text{with } C_{1,k} = 14 \text{ N/mm}^{1.5} \quad (10)$$

For connections with punched metal plate fasteners the resistance can be increased by a factor w in dependency of the width parallel to grain w_{pl} of the punched metal plate:

$$w = \max \left\{ \left(\frac{w_{pl}}{100} \right)^{0.35}; 1.0 \right\} \quad \text{for punched metal plates} \quad (11)$$

$$w = 1.0 \quad \text{for all other types of fasteners} \quad (12)$$

Using the shear force reactions $F_{v,Ed}$ instead of the load applied to the connection $F_{90,Ed}$ for the verification in Eq. (8) allows to account for the effect of neighbouring connections, connections close to the support or connections at a cantilever. The impact on the load-carrying capacity of such configurations is conservative.

2.4 Extension of the Fracture Mechanical Approach

Ballerini [9] made further developments of the approach by van der Put [16] and Jensen et al. [18]. Assuming a different force and moment distribution in the reduced cross-section at the cracked connection, Ballerini proposed a different exponent of the relative connection height in his approach compared to Eq. (7). Based on own tests and results from literature, he proposed a design value of the material parameter $C_{1,d} = 8.6 \text{ N/mm}^{1.5}$.

$$R_{90,d} = 2b C_{1,d} f_w f_r \sqrt{\frac{h_c}{1 - \left(\frac{h_c}{h} \right)^3}} \quad (13)$$

where:

$$f_w = \min \left\{ \begin{array}{l} 1 + 0.75 \left(\frac{a_r + l_1}{h} \right) \\ 2.2 \end{array} \right. \quad (14)$$

$$f_r = 1 + 1.75 \frac{\kappa}{1 + \kappa} \quad \text{with} \quad \kappa = \frac{n \cdot h_m}{1000} \quad \text{and} \quad h_m \text{ in [mm]} \quad (15)$$

The parameters f_w and f_r were introduced by Ballerini in order to account for the influence of the width (a_r) and the height (h_m) of the connection, respectively. In addition the clear distance (h) between two neighbouring connections is considered. The derivation of the parameters f_w and f_r is purely empirical on the basis of a large number of test results.

3. Structural Behaviour of Connections Loaded Perp. to Grain

3.1 Tests Carried out at ETH Zurich

The structural behaviour of connections loaded perpendicular to grain was studied in a test series at ETH Zurich. In this test series the relative connection height h_e/h was varied between 60 %, 70 % and 80 % of the beam height and two different arrangements of the dowels in the connection with a slotted in metal steel plate were tested: a horizontal configuration with $m = 4$ rows and $n = 2$ columns (Fig. 4 left) and a vertical configuration with $m = 2$ rows and $n = 4$ columns (Fig. 4 right) of dowels with diameter $d = 12$ mm. The beam height was $h = 440$ mm and the width $b = 140$ mm.

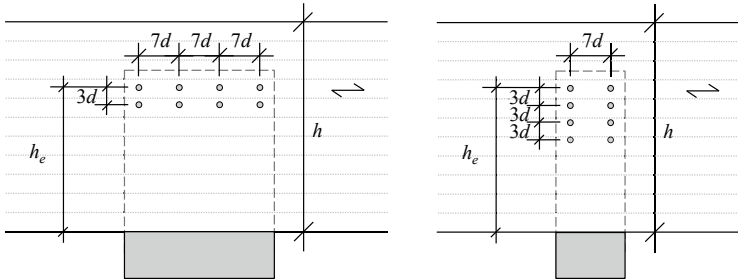


Fig. 4 Geometry of the connections tested at ETH Zurich.

The load-displacement behaviour of the beam, the crack opening and the relative pull-out of the steel plate were measured by means of LVDT. The deformations on the surface of the beam were recorded by means of optical measurements. These deformations were used to study the crack initiation and growth during load application. Results of these measurements are summarized in [22,23].

In Fig. 5 the load-deformation behaviour of three specimen with different relative connection height is shown. The deformation was measured at the steel plate and it can be seen that with increasing relative connection height higher load-carrying capacities and larger deformations were reached. The full load-carrying capacity of the connection with yielding of the fasteners is reached for the connection with

$h_c/h = 0.8$. In contrast the connection with $h_c/h = 0.6$ fails due to instable crack growth already at small deformations of the fasteners. The connection with $h_c/h = 0.8$ shows a more stable crack growth with increasing load until the full load-carrying capacity of the fasteners is reached. Some of these connections with $h_c/h = 0.8$ failed due to shear failure in the reduced cross-section.

Tests showed that cracking occurs also for relative connection heights h_c/h larger than 70 % as well as for connections with reinforcement. Nevertheless, the crack initiation is not followed by an unstable crack growth causing failure of the entire beam, but instead further loading is possible.

3.2 Tests Reported in Literature

The large number of tests reported in literature offers the possibility to analyse the impact of individual parameters on the structural behaviour and to calculate fractile values for the design. For the following evaluations individual results from tests on glulam beams reported in [11,24–31] were used. A summary of the tests is given in [32].

The majority of the tests were performed as 3-point bending tests with the connection in the central position of the beam span. A small number of tests were performed with an eccentric position of the connection [24,30,31] or with the connection at a cantilever beam [24,31].

The majority of the tests were carried out on beams with rather small beam height $h \leq 400$ mm and beam widths $b \leq 80$ mm. The small beam width in combination with relatively large fastener diameter caused mostly an embedment failure mode of the fasteners. This constant load introduction over the entire width of the beam leads to a linear dependency of the load-carrying capacity on the beam width. For more slender fastener an early crack initiation around the fasteners can be expected. Mostly bolts with external steel plates were used in the tests, besides dowels, nails and connectors.

3.3 Comparison of Test Results and Design Approaches

3.3.1 Geometry of the Connection

The impact of the geometry of the connection on the load-carrying capacity is shown in Fig. 6. In the two diagrams on the top the impact of the connection width

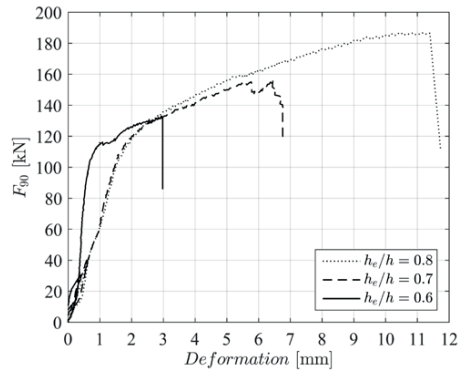


Fig. 5 Load in dependency of the deformation of the slotted in steel plate for three different relative connection heights.

a_r on the relative load-carrying capacity in comparison to a reference with $a_r/h = 0.5$ is shown. In the two diagrams below the impact of the number of rows of fasteners on the relative load-carrying capacity in comparison to a reference with $n = 1$ row is shown. The test results are normalized by means of the design approach by Ballerini in Eq. (13) (Figures on the left) and Ehlbeck et al. in Eq. (2) (right), respective, and can be compared with the solid lines representing the corresponding design approach. The impact of the parameter is underestimated by the design approaches if the test results are located in average above the solid lines, whereas the impact of the parameter is overestimated by the design approaches if the test results are located in average below the solid lines.

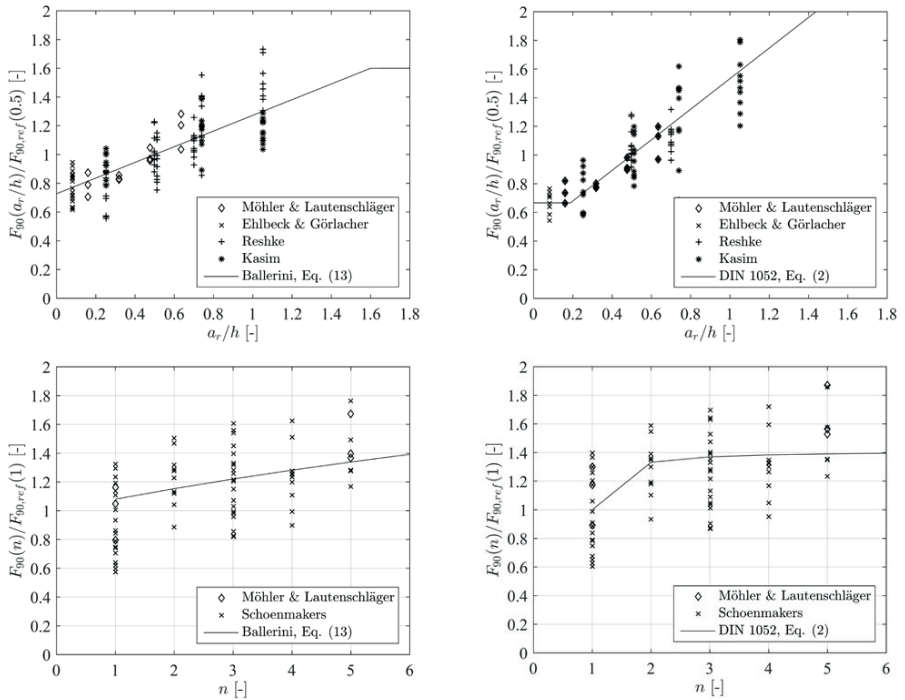


Fig. 6 Impact of the connection width a_r (top) and number of rows of fasteners n (bottom) on the relative load-carrying capacity and comparison with design approaches according to Eq. (13) (left) and Eq. (2) (right).

It can be seen that with increasing width a_r of the connection and with increasing number of rows of fasteners the load-carrying capacity is increasing. The different behaviour of the design approaches in dependency of the connection width and number of rows of fasteners can be explained by the empirical background and the

limited number of tests considered in the derivation of the parameters accounting for the impact of the connection geometry in these design approaches.

The design approach given in EC 5 on the basis of [16] was derived for ($h_m = 0$ and $a_r = 0$ together with $n = 1$ and $m = 1$), leading to conservative results with increasing value of these parameters.

3.3.2 Influence of the Position of the Connection

The impact of the position of the connection loaded perpendicular to grain along the beam axis is considered only by the design approach given in Eurocode 5 as explained in Chapter 2.2. The evaluation of the test results shows no considerable impact of the position of the connection along the span of the beam, see Fig. 7. Only in one test series on connections with small end-distances at a cantilever beam, lower load-carrying capacities were reached compared to tests with connections at midspan.

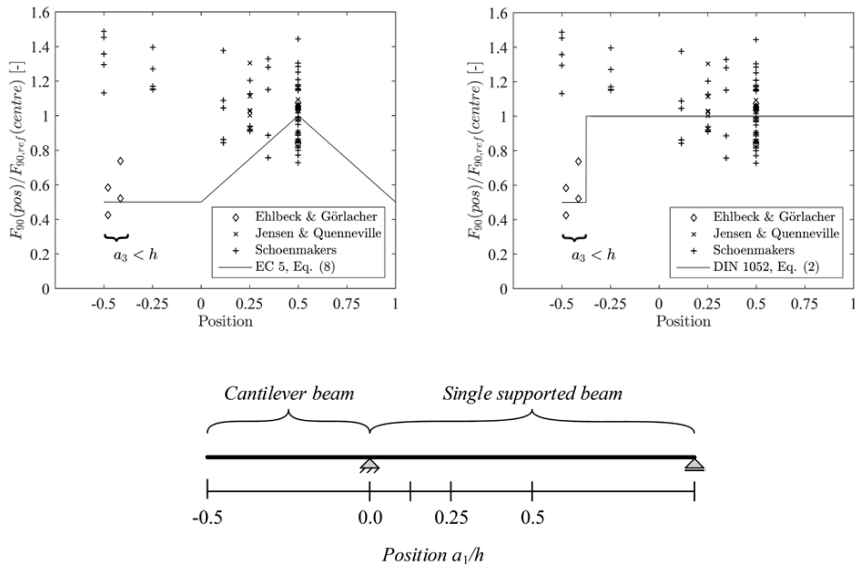


Fig. 7 Impact of the position of the connection along the beam axis on the relative load-carrying capacity according to EC 5 (left) and according to DIN 1052 (right).

3.3.3 Influence of Neighbouring Connections

The load-carrying capacity of neighbouring connections increases with increasing distances between the connections. Two neighbouring connections with a small clear distance ($l_1 = a_1/h \leq 0.5$) show approximately the same resistance as one single connection. For larger distances the load-carrying capacity of each individual connection increases but does not reach the full capacity of one single connection. Due to the limited number of available test results no precise statement about the impact of neighbouring connections is possible.

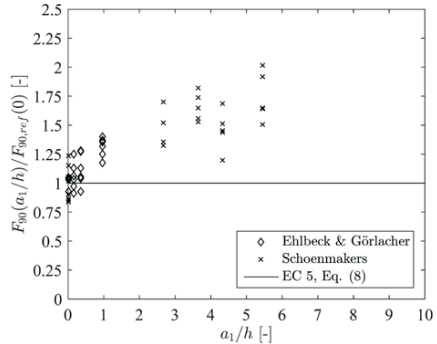


Fig. 8 Impact of the distance a_1/h between two neighbouring connection on the total load-carrying capacity.

3.4 Characteristic Values of the Material Property Values

Each of the design approaches presented requires different material property values and an individual calibration for the design, due to the differences in the underlying theory and partially empirical background. The approach based on strength theory in Eq. (2) uses tension perpendicular to grain strength, which is strongly dependent on the tested volume and is topic of various discussions among experts (e.g. [33,34]). The use of the general strength value $f_{t,90,k}$ given in the product standards (EN 338 [4] and EN 14080 [5]) should be treated with caution.

The approaches with a fracture mechanical background in Eq. (7) and (13) are based on the fracture energy and the shear modulus of the wood. The fracture with crack opening in mode I is the relevant failure mode. Together with the values of shear modulus taken from EN 14080 [5] for the common glulam strength grades, it would be possible to estimate the load-carrying capacity based on fracture energy values given in literature e.g. by Larsen and Gustafsson [19].

With the help of the large number of test results it is possible to back-calculate the material parameters used in the different design approaches. The design approaches can be benchmarked based on the variability of these material parameters and possible dependencies on certain parameters can be determined. In case of an ideal design approach the material parameter back-calculated from tests would show a very low variation, which could be explained by the natural variability of the material timber. However, the existing design approaches lead to material properties with a relatively high variation and with dependencies on certain geometrical properties.

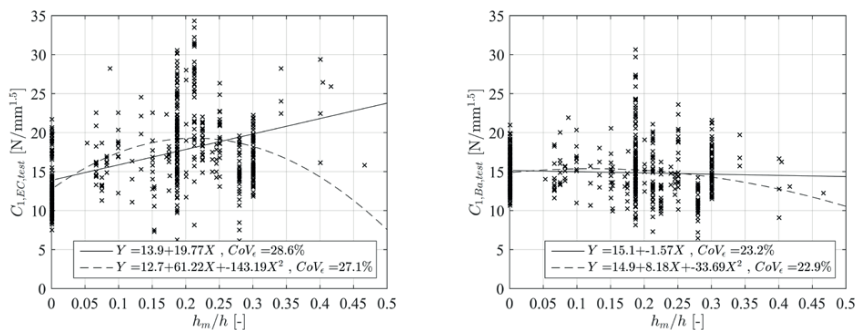


Fig. 9 Material property values in dependency of the relative connection height h_m/h back-calculated from test results for EC 5 in Eq. (8) (left) and Ballerini in Eq. (13) (right) together with linear and quadratic regression functions.

The material parameters $C_{1,EC,test}$ and $C_{1,Ba,test}$ back-calculated from the test results by means of the design approaches in Eq. (8) (Eurocode 5) and (13) (Ballerini), respectively, are shown in Fig. 9 in dependency of the connection height h_m/h . All test selected for this evaluation were made on softwood glulam and no dependency on additional material parameters was accounted for.

The material parameter back-calculated from the design approach by Ballerini shows very little dependency on the geometry of the connection, which means that these properties are accounted for in an adequate way by the two parameters f_w and f_r in Eq. (14) and (15).

The approach give in Eurocode 5 does not account for the beneficial impact of larger connection width or connection height and hence, underestimates the load-carrying capacities of such connections.

4. Considerations for the Design of Connections Loaded Perpendicular to Grain

The design approach proposed by Ballerini [9] in Eq. (13) considers various geometrical parameters and configurations of connections and shows the best agreement with test results. Based on the tests under short term duration of load a characteristic material property value of $C_{1,Ba,k} \approx 10 \text{ N/mm}^{1.5}$ can be found for the design approach by Ballerini in Eq. (13) as shown in Fig. 10. In case it is decided to keep the current approach in EC 5, despite its limits in consideration of connection geometry, a value of $C_{1,EC5,k} \approx 9.5 \text{ N/mm}^{1.5}$ is proposed.

For the determination of design values, the characteristic 5 %-fractile values have to be reduced by the partial safety factor for the material γ_M and the modification factor k_{mod} for the consideration of duration of load effects and the impact of

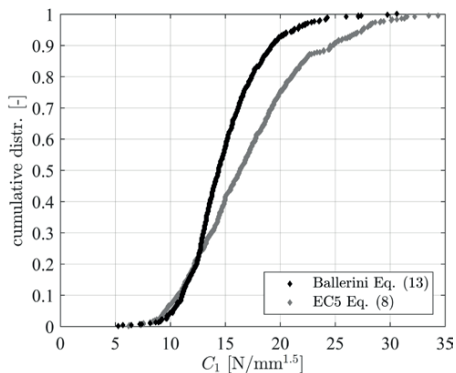


Fig. 10 Cumulative distribution of material parameter C_1 calculated from test results.

5. Conclusion

The most relevant geometrical parameters with regard to the load-carrying capacity of connections loaded perpendicular to grain are height h and width b of the beam, relative connection height h_c/h , connection width a_r and connection height h_m . In case of multiple connections the distance between them has an important influence as well. The position of the connection along the beam span or at a cantilever beam is of minor relevance with regard to the load-carrying capacity.

The various design approaches from literature can be separated into approaches based on strength criteria (like the approach given in DIN 1052) and into approaches based on fracture mechanics theory (like the approach given in EC 5 or the approach by Ballerini). A good fit between a large number of test results and the design approach by Ballerini was found.

Reinforcement is an easy and efficient possibility to restore the load-carrying capacity of beams with connections loaded perpendicular to grain.

6. Acknowledgement

The work presented in this paper was developed during a Short Term Scientific Mission at Technical University of Munich supported by COST Action FP 1402 (www.costfp1402.tum.de). The students C. Thiede and D. Gisler are thanked for their contributions in the frame of their master thesis.

service classes. It is well known that timber is prone to cracking if loaded in tension perpendicular to grain and if exposed to varying moisture content. Hence, the application of connections loaded perpendicular to grain should be limited to situations with low variation in moisture content. Otherwise reinforcement should be installed in order to avoid cracking and to maintain the load-carrying capacity even after cracks occur [8]. Reinforcement can also help to avoid premature failure in cases of long duration of loads since knowledge about the behaviour of connections loaded perpendicular to grain under long duration of load is scarce.

7. References

- [1] Johansen K. W., "Theory of Timber Connections", *IABSE Publications*, Vol. 9, 1949, pp. 249–262.
- [2] EN 1995-1-1: *Eurocode 5: Design of timber structures - Part 1-1: General - Common rules and rules for buildings*, European Committee for Standardization (CEN), 2004, Brussels, Belgium.
- [3] SIA 265: *Timber Structures*, SIA Swiss Society of Engineers and Architects, 2012, Zurich, Switzerland.
- [4] EN 338: *Structural timber - Strength classes*, European Committee for Standardization (CEN), 2009, Brussels, Belgium.
- [5] EN 14080: *Timber structures - Glued laminated timber and glued solid timber - Requirements*, European Committee for Standardization (CEN), 2013, Brussels, Belgium.
- [6] DIN 1052: *Entwurf, Berechnung und Bemessung von Holzbauwerken - Allgemeine Bemessungsregeln und Bemessungsregeln für den Hochbau*, DIN Deutsche Institut für Normung e.V., 2008, Berlin, Germany (in German).
- [7] DIN EN 1995-1-1/NA: *National Annex - Nationally determined parameters - Eurocode 5: Design of timber structures - Part 1-1: General - Common rules and rules for buildings*, DIN Deutsche Institut für Normung e.V., 2013, Berlin, Germany.
- [8] Dietsch P., and Brunauer A., "Reinforcement of timber structures - a new section for EC5", *Proceedings of the International Conference on Connections in Timber Engineering - from Research to Standards*, September 2017, Graz, Austria.
- [9] Ballerini M., "A new prediction formula for the splitting strength of beams loaded by dowel-type connections", *Proceedings of the 37th CIB-W18 Meeting*, 2004, Edingburgh, Scotland.
- [10] Möhler K., and Siebert W., *Ausbildung von Queranschlüssen bei angehängten Lasten an Brettschichtträgern oder Vollholzbalken*, Technical Report, 1980, Lehrstuhl für Ingenieurholzbau und Baukonstruktion, Technical University Karlsruhe, Karlsruhe, Germany (in German).
- [11] Möhler K., and Siebert W., "Queranschlüsse bei Brettschichtträgern oder Vollholzbalken", *Bauen mit Holz*, Vol. 83, 1981, pp. 84–89 (in German).
- [12] Möhler K., and Lautenschläger R., "*Großflächige Queranschlüsse bei Brettschichtholz*", Technical Report, 1978, Lehrstuhl für Ingenieurholzbau und Baukonstruktion, Technical University Karlsruhe, Karlsruhe, Germany (in German).
- [13] Barrett J.D., Foschi R.O., and Fox S.P., "Perpendicular-to-grain strength of Douglas-Fir", *Canadian Journal of Civil Engineering*, Vol. 2, 1975, pp. 50–57.

- [14] Ehlbeck J., Görlacher R., and Werner H., "*Determination of perpendicular to grain stresses in joints with dowel-type fasteners - A draft proposal for design rules*", *Proceedings of the 22nd CIB-W18 Meeting*, 1989, Berlin, Germany.
- [15] Ehlbeck J., and Görlacher R., "Empfehlung zum einheitlichen genaueren Quernachweis für Anschlüsse mit mechanischen Verbindungsmitteln", *Bauen mit Holz*. Vol. 93, 1991, pp. 825–828 (in German).
- [16] Van der Put T.A.C.M., "Tension perpendicular to the grain at notches and joints", *Proceedings of the 23rd CIB-W18 Meeting*, 1990, Lisbon, Portugal.
- [17] Van der Put T.A.C.M., and Leijten A.J.M., "Evaluation of perpendicular to grain failure of beams caused by concentrated loads of joints", *Proceedings of the 33rd CIB-W18 Meeting*, 2000, Delft, The Netherlands.
- [18] Jensen J.L., Gustafsson P.-J., and Larsen H.J., "A tension fracture model for joints with rods or dowels loaded perpendicular to grain", *Proceedings of the 36th CIB-W18 Meeting*, 2003, Colorado, USA.
- [19] Larsen H.J., and Gustafsson P.J., "The fracture energy of wood in tension perpendicular to the grain", *Proceedings of the 23rd CIB-W18 Meeting*, 1990, Lisbon, Portugal.
- [20] Leijten A.J.M., and Jorissen A., "Splitting strength of beams loaded by connections perpendicular to grain, model validation", *Proceedings of the 34th CIB-W18 Meeting*, 2001, Venice, Italy.
- [21] Jensen J.L., and Quenneville P., "Splitting of beams loaded perpendicular to grain by connections—some issues with EC 5", *Proceedings of the 44th CIB-W18 Meeting*, 2011, Alghero, Italy.
- [22] Jockwer R., Frangi A., and Steiger R., "Evaluation of the reliability of design approaches for connections perpendicular to the grain", *Proceedings of the 48th INTER Meeting*, 2015, Šibenik, Croatia.
- [23] Jockwer R., and Frangi A., *Tragsicherheit von Queranschlüssen: Entwicklung eines praxisingerechten Bemessungsverfahrens*, Techn. Report, 2016, WHFF Projekt Nr. 2013.15., Zürich, Schweiz (in German).
- [24] Ehlbeck J., and Görlacher R., *Tragverhalten von Queranschlüssen mittels Stahlformteilen, insbesondere Balkenschuhen, im Holzbau*, Forschungsbericht, Versuchsanstalt für Stahl, Holz und Steine, Abteilung Ingenieurholzbau, Universität Fridericiana Karlsruhe, 1983, Germany (in German).
- [25] Ballerini M., "A new set of experimental tests on beams loaded perpendicular-to-grain by dowel-type joints", *Proceedings of the 32nd CIB-W18 Meeting*, 1999, Graz, Austria.
- [26] Ballerini M., and Giovanella A., "Beams transversally loaded by dowel-type joints: influence on splitting strength of beam thickness and dowel size", *Proceedings of the 36th CIB-W18 Meeting*, 2003, Colorado, USA.

- [27] Reshke R., *Bolted timber connections loaded perpendicular to grain: influence of joint configuration parameters on strength*, 1999, Department of Civil Engineering, Royal Military College of Canada, Kingston, Ontario, Canada.
- [28] Kasim M.H., *Bolted timber connections loaded perpendicular-to-grain - Effect of row spacing on resistance*, 2002, Department of Civil Engineering, Royal Military College of Canada, Kingston, Ontario, Canada.
- [29] Habkirk R., *Bolted wood connections loaded perpendicular-to-grain - Effect of wood species*, 2006, Department of Civil Engineering, Royal Military College of Canada, Kingston, Ontario, Canada.
- [30] Jensen J.L., and Quenneville P., "Experimental investigations on row shear and splitting in bolted connections", *Construction and Building Materials*, Vol. 25, 2011, pp. 2420–2425.
- [31] Schoenmakers J.C.M., *Fracture and failure mechanisms in timber loaded perpendicular to the grain by mechanical connections*, PhD thesis, 2010, Technische Universiteit Eindhoven.
- [32] Jockwer R., "Review of design recommendations for connections loaded perpendicular to the grain", Report of Short Term Scientific Mission at Technical University Munich within COST Action FP1402 "Basis of Structural Timber Design" - from research to standards, TU Munich, 2016, Munich, Germany.
- [33] Aicher S., Dill-Langer G., and Klöck W., "Evaluation of different size effect models for tension perpendicular to grain strength of glulam", *Proceedings of the 35th CIB-W18 Meeting*, 2002, Kyoto, Japan.
- [34] Mistler H.-L., "Design of glulam beams according to EN 1995 with regard to perpendicular-to-grain tensile strength: comparison with research results", *European Journal of Wood and Wood Products*, Vol. 74, 2016, pp. 169–175.

Reinforcement of Timber Structures – a New Section for EC 5

Philipp Dietsch
Team Leader Timber Structures
Technical University of Munich
Munich, Germany

Alfons Brunauer
Technical Director Timber Engineering
WIEHAG GmbH
Altheim, Austria

Summary

The reinforcement of timber structures has seen considerable research and development in recent years. New materials and methods for reinforcement have been developed and are now used in practice. Eurocode 5 in its current edition, however, lacks approaches to design reinforcement for timber members. To close this gap, the standardization committee responsible for drafting Eurocode 5, has decided to establish a Working Group (WG) on this item. This Working Group is supported by a Project Team, mandated to draft the associated sections for Eurocode 5. This contribution reports on the approach to this task, the work items of WG 7 “Reinforcement”, the current status and the work scheduled for the coming years. The proposed structure of the new section as well as design approaches and related background information are presented.

1. Introduction

The reinforcement of timber structures has seen considerable research and development in recent years, see e.g. [1]. New materials like fully-threaded, self-tapping screws and screwed-in rods or laminated veneer lumber offer potential also in view of their use as reinforcement. The European timber design standard, Eurocode 5, in its current edition [2] lacks approaches to design reinforcement for timber members. The standardized use of reinforcement is enabled only in a few European countries by means of non-contradictory information (NCI), given in the National Annexes to Eurocode 5 [3], [4]. Closing the obvious gap between recent developments and practical needs on the one side and missing standardization on the other, reinforcement for stresses perpendicular to the grain was classified high priority when defining the list of work items to be dealt with during the upcoming revision of Eurocode 5 [5]. In 2011, the European standardization committee responsible for Eurocode 5, CEN/TC 250/SC 5, decided to form a Working Group 7 “Reinforcement”. In addition, reinforcement of timber members was prioritized for Phase 1 (of 4 phases) of the standardization work to be mandated by

the European Commission. Within Phase 1, two Project Teams to draft new sections for Eurocode 5 were established and equipped with experts, namely PT SC5.T1 – to draft the sections on cross laminated timber and reinforcement – and SC5.T2 – to draft a new part on timber-concrete composites.

2. Approach

Standardization is the culmination of successful research and development that has seen positive application and acceptance in practice, see Fig. 1. According to the European position on standardization [6], harmonized technical rules shall be prepared for “common design cases” and shall contain “only commonly accepted results of research and validated through sufficient practical experience”. The target audience for such rules is “competent civil, structural and geotechnical engineers, typically qualified professionals able to work independently in relevant fields”.

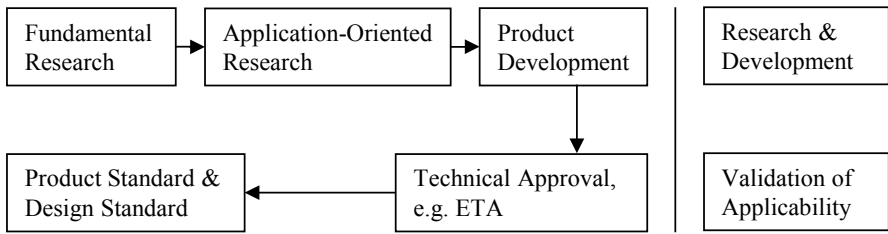


Fig. 1 Development of products or methods and their legalization

3. Organization

Different committees and groups of experts are contributing to European standardization in the field of the design of structures, see Fig. 2 for the example of Timber structures. In the following, a short description of the main structure and organisation within these committees and groups is given. For an in-depth description of the structure, the interested reader is referred to [7].

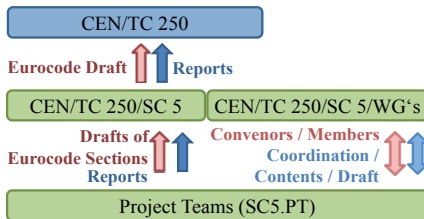


Fig. 2 Responsibilities in CEN/TC 250/ SC 5

CEN/TC 250 is the head committee, responsible for the development and definition of the design rules of common building and civil engineering structures. This committee is substructured into 11 sub-committees (SCs), each sub-committee being responsible for the development and revision of one Eurocode.

CEN/TC 250/SC 5 is responsible for all parts of Eurocode 5 (EN 1995). The members of these sub-committees are delegates sent by National Standardization Bodies (NSBs) that are members of CEN. For the technical work, each sub-committee is supported by Working Groups (WGs) that deal with specific items within the Eurocode the SC is responsible for. Within CEN/TC 250/SC 5 for example, WG 1 is responsible for cross laminated timber, WG 5 is responsible for connections and WG 7 is responsible for reinforcement of timber structures, see [7] for a full overview. The Working Groups are responsible to develop the work programme, i.e. the items to be covered within their responsibility. In this connection, the WGs are meant to serve as institution for technical discussions resulting in technical proposals (methods, design approaches, design equations and details) for the section(s) under their responsibility. To achieve this objective, the WGs are staffed with experts sent by the National Standardization Bodies. These experts may have a dual role as National Delegates within the SC and as experts in a WG or work solely as the latter. CEN/TC 250/SC 5/WG 7 “Reinforcement” currently has 21 members (experts and observers), about five experts contribute actively to the work.

The drafting of the standard text based on the technical proposals developed and agreed within the WGs is the responsibility of Project Teams (PTs), consisting of five members and one leader. The work of the Project Teams is supported by the European Commission, hence they are established in a tender process. Within a given time frame, the PTs have to deliver a draft of a new or revised Eurocode or a specific section of the same. In other words, the PTs have to bring the technical proposals into standard text including harmonized notations, terminology and references, adhering to the principles of “Ease-of-Use” [6]. In addition, the Project Teams have to develop so-called “background documents” describing the technical reasoning and scientific background of all new or changed technical contents under their scope. From the members in Project Team SC5.T1 “Cross-laminated timber and reinforcement”, three members are actively involved in the drafting of the section on reinforcement while four members actively contribute to the drafting of the section on CLT. The liaison between the SCs, WGs and PTs can be summarized as follows: the SC is the responsible control institution while the WGs and PTs are the executive institutions developing the technical contents (WGs) and the drafts of the standard (PTs).

4. Work Items

4.1 General

Adhering to the principles described in section 2, CEN/TC 250/SC 5/WG 7 “Reinforcement” decided to prioritize the following applications and reinforcement methods for preparation for the revised Eurocode 5. These items were also classified high priority during a pan-European survey carried out amongst a multitude of stakeholders in 2010 [5].

4.2 Applications

- Reinforcement of double tapered, curved and pitched cambered beams
- Reinforcement of notched beams
- Reinforcement of holes in beams
- Reinforcement of connections with a force component perp. to the grain
- Reinforcement of connections ($n = n_{ef}$)
- Reinforcement of members with concentrated compression stresses perpendicular to the grain

4.3 Materials and Methods

- Fully-threaded screws or screwed-in threaded rods
- Glued-in rods
- Glued-on timber, plywood, LVL

The choice of materials is explained by the precondition that (1) test procedures as well as (2) a product standard or Technical Approval / Assessment for the product / material are available. Without these, rules in a design standard cannot be used since the basic input parameters are missing. This situation can best be described by a 3-step pyramid, see Fig. 3 and [8].



Fig. 3 Sketch of the 3-step pyramid applied in internat. standardization for the construction sector

This pyramid is based on (1) test standards (containing rules on how to test products). Relating to these, product standards (2) are developed (giving strength and stiffness parameters, boundary conditions and rules for production and quality control). The design standards (3) represent the tip of this pyramid

(providing design equations and formulating specific requirements in e.g. spacing, edge distance, minimum anchorage length, etc.).

5. Current Status and Work Plan

By the end of April 2017, all currently active Project Teams had to send the second drafts to their contractual partner, the Netherlands Standardization Institute (NEN). NEN delivered the drafts to the respective CEN/TC 250/SCs for review and comments within a two-month period (May - June). The SCs can draw upon the National Standardization Bodies (NSBs) for additional review and comments to the drafts. The Project Team is requested to answer all comments received during the work on the final draft, implementing all comments and proposals that are deemed useful and technically sound. The final draft has to be delivered to NEN in October

2017. NEN will directly forward this document to the National Standardization Bodies (NSBs) for a three-month enquiry. Following that, the PTs have two months to prepare the final documents, taking into account the comments received from the NSBs. The delivery of the final documents and the background documents, marking the end of the work of the PTs, is in April 2018.

6. Structure of the Second Draft

EN 1995-1-1 [2] in its current version does not contain provisions on reinforcement. Hence, a decision on the structure of this new section had to be taken. The obvious approach is to write a separate but continuous section on the design of reinforcement for timber members. This solution, however might not fully suit the designers needs in terms of applicability and navigation, hence might not fully obey to the principles on “Ease-of-Use”. The current proposal, which was accepted by WG 7 “Reinforcement”, is to integrate the provisions on reinforcement into the existing main part, i.e. following the sequence of a typical design task: general considerations – design of members in the unreinforced state – design of reinforcement for these members. Fig. 4 contains the proposed structure.

7. Contents of the Second Draft

7.1 General

In the following, the core contents of the sections on reinforcement are given in form of *italic writing*, followed by relevant background information on these clauses. For a comprehensive overview of the current state of the art in the design of reinforcement including design equations and extensive background information, the interested reader is referred to [9] and [10]. The Figures shown do not represent the Figures for the standard text as they also include graphical representations produced to exemplify background information. Since the strength verifications required for the reinforcement are rather independent of the member or detail to be reinforced, these are presented in consolidated form in the first Section *General*. An exception is the reinforcement of members with compression stresses perpendicular to the grain, hence (and in difference to the proposed standard structure) the proposed standard text and necessary amendments to existing sections will be presented in consolidated form at the end of this Section.

- 6 Ultimate limit states
 - 6.1 Design of cross-sections subjected to stress in one principal direction
 - 6.1.5 Compression perpendicular to the grain
 - 6.1.5.1 General
 - 6.1.5.2 Reinforcement of members with compression stresses perpendicular to the grain**
 - 6.4 Design of members with special requirements based on geometrical form**
 - 6.4.1 General**
 - 6.4.2 Effects of moisture content changes**
 - 6.4.3 Design of cross-sections in members with varying cross-section or curved shape
 - 6.4.3.1 General
 - 6.4.3.2 Single tapered beams
 - 6.4.3.3 Double tapered, curved and pitched cambered beams
 - 6.4.3.4 Reinforcement of double tapered, curved and pitched cambered beams**
 - 6.4.4 Notched members
 - 6.4.4.1 General
 - 6.4.4.2 Beams with a notch at the support
 - 6.4.4.3 Reinforcement of rectangular notches in members with rectangular cross-section**
 - 6.4.5 Holes in beams
 - 6.4.5.1 General
 - 6.4.5.2 Holes in beams with rectangular cross-section
 - 6.4.5.3 Reinforcement of holes in beams with rectangular cross-section**
- 8 Connections with metal fasteners
 - 8.1 General
 - 8.1.4 Connection forces at an angle to the grain
 - 8.1.4.1 Design of connections with a tensile force component perpendicular to the grain
 - 8.1.4.2 Reinforcement of connections with a tensile force component perpendicular to the grain**
 - 8.5 Bolted connections
 - 8.5.1 Laterally loaded bolts
 - 8.5.1.1 *General and bolted timber-to-timber connections*
 - 8.7 Screwed Connections
 - 8.7.1 *Axially loaded screws*

*Fig. 4 Proposed structure for sections on reinforcement (new sections in **bold**, sections on reinforcement in **bold italic**, sections with proposed additions in italic)*

General

Standard text:

- *In the following clauses, the tensile capacity perpendicular to the grain of the timber is neglected in the determination of the load on the reinforcement.*
- *Pitched cambered beams, notched members and holes in beams should be reinforced for tensile stresses perpendicular to the grain. Curved and double tapered beams should be reinforced if the design tensile stresses perpendicular to the grain exceed 60 % of the design tensile strength perpendicular to the grain.*

Background for the clauses given above:

Within the approaches given, the tensile capacity perpendicular to the grain of the timber is neglected, i.e. a cracked cross-section is assumed in direction of tensile stresses perpendicular to the grain. This is in difference to the method presented in [11] in which only the force components, exceeding the tensile strength perpendicular to the grain of the timber, are applied for the design of the reinforcement. Before cracking of the cross-section perpendicular to the grain, a proportional share of tensile stresses perpendicular to the grain is transferred by the timber. The share depends on the stiffness of the reinforcement embedded in or around the timber compared to the stiffness of the timber member but also on the distance of the cross-section under consideration to the next reinforcing element.

Even if the verification of systematic, load-dependent tensile stresses perpendicular to the grain can be met, it is state of the art to reinforce double tapered, curved and pitched cambered beams against tensile stresses perpendicular to the grain. Reason is the superposition of the load-dependent stresses with moisture induced stresses perpendicular to the grain due to e.g. changing climatic conditions or a drying of the beam after the opening of the building, see e.g. [12]. In the lack of a method to reliably predict the magnitude of tensile stresses perpendicular to the grain, it was custom to apply reinforcement if the maximum load-dependent tensile stresses perpendicular to the grain exceeded 60 % of the design tensile strength perpendicular to the grain.

Since end-grain is exposed bare at a notch and in holes, the superposition of moisture induced stresses and load-dependent tensile stresses perpendicular to the grain around notches and holes can be significant [13]. Therefore, many authors recommend that notches and holes in beams should always be reinforced.

- *The following internal, dowel-type reinforcement may be applied:*
 - *glued-in threaded rods and screwed-in threaded rods with wood screw thread according to European Technical Assessment;*
 - *fully-threaded screws according to EN 14592 or European Technical Assessment.*

- *The following plane reinforcement may be applied:*
 - *glued-on plywood according to EN 13986;*
 - *glued-on structural laminated veneer lumber according to EN 14374;*
 - *glued-on laminations made of either structural solid timber according to EN 14081-1 or plywood according to EN 13986 or structural laminated veneer lumber according to EN 14374.*
 - *pressed-in punched metal plate fasteners.*

The list of applicable internal or external reinforcements is – amongst other factors – based on the necessity of a continuous interconnection between the timber and the reinforcement as well as sufficient stiffness of this connection (to prevent cracking). Due to the latter argument, perforated metal plates or wood-based panels, both nailed onto the timber member, are not adequate as reinforcement, see e.g [13], [14].

- *The distance between the peak tensile stresses perpendicular to the grain and the dowel-type reinforcement should be minimized but should not be below the minimum values given in the following. For fully-threaded screws and screwed-in threaded rods, the spacing rules should be taken from the (Table 8.6 in [2]) or from the Technical Assessment. For glued-in threaded rods, the spacing between glued-in threaded rods, a_2 , should not be less than $3 \cdot d$. The edge distance in grain direction, $a_{3,c}$, as well as the edge distance perpendicular to the grain, $a_{4,c}$, should not be less than $2.5 \cdot d$.*
- *For inclined dowel-type reinforcement, the spacing may be determined based on the centre of gravity of the dowel-type reinforcement in the section of the timber member under consideration, see Fig. 6.*
- *The reduction in the cross-sectional area due to internal reinforcement should be considered in the design of the timber member.*
- *In block glued members, each component within the block should be reinforced, either by internal dowel-type reinforcement or by plane reinforcement glued to both side faces of each component. The reduction in the cross-sectional area due to glued in plane reinforcement should be considered in the design of the block glued member.*

The reinforcing effect of dowel-type or plane reinforcement is strongly dependent on the distance between the reinforcement and the location of peak stresses. Edge and end distances of glued-in steel rods are partly reduced compared to the minimum edge and end distances given in Chapter 8 of [2], since such reinforcement is loaded by axial forces and its continuous interconnection with the wood prevents splitting [14]. The reinforcing effect of the applicable reinforcement elements over the width of a timber member is limited; hence each component of a block-glued timber member should be reinforced separately.

- The design tensile force in a reinforcement should satisfy the following Expression:

$$\frac{F_{t,90,Ed}}{F_{t,90,Rd}} \leq 1.0 \quad (1)$$

where

$F_{t,90,Ed}$ is the design tensile force in the reinforcement, according to the expressions given in the following sections;

$F_{t,90,Rd}$ is the design tensile resistance of dowel-type or plane reinforcement according to expressions (2) – (4).

- The design resistance of dowel-type reinforcement or plane reinforcement should be taken as the minimum value found from the following Expressions:
 - For fully-threaded screws or fully-threaded rods (see also 8.7 in [2]):

$$F_{t,90,Rd} = n_r \cdot \min \left\{ \begin{array}{l} f_{ax,d} \cdot d \cdot l_{ad} \\ f_{tens,d} \end{array} \right. \quad (2)$$

- For glued-in steel rods:

$$F_{t,90,Rd} = n_r \cdot \min \left\{ \begin{array}{l} f_{g1,d} \cdot \pi \cdot d \cdot l_{ad} \\ f_{u,d} \cdot \pi \cdot r_{cd}^2 \\ f_{y,d} \cdot \pi \cdot r_d^2 \end{array} \right. \quad (3)$$

- For glued-on plane reinforcement:

$$F_{t,90,Rd} = n_r \cdot \min \left\{ \begin{array}{l} f_{g2,d} \cdot l_{ad} \cdot b_r \\ \frac{f_{t,d}}{k_k} \cdot b_r \cdot t_r \end{array} \right. \quad (4)$$

with:

$$l_{ad} = \min \left\{ \begin{array}{l} l_{ad,t} \\ l_{ad,c} \end{array} \right. \quad (\text{determined in accordance with the geometry of the detail to be reinforced, see e.g. Fig. 5 - 8}) \quad (5)$$

where:

n_r is the number of reinforcing elements (typically 2, resp. 4 with the exception of curved and pitched cambered beams, where $n = 1$);

$f_{ax,d}$ is the design withdrawal strength of the fully-threaded screw/rod;

$f_{tens,d}$ is the design tensile capacity of the fully-threaded screw/rod;

$f_{u,d}$ is the design ultimate strength of the steel rod;

- $f_{y,d}$ is the design yield strength of the steel rod;
- $f_{g1,d}$; $f_{g2,d}$ are design strengths of the glue line;
- $f_{t,d}$ is the design tensile strength of the plane reinforcement;
- d is the outer thread diameter of the fully-threaded screw or steel rod (≤ 20 mm);
- r_{cd} is the core radius of the steel rod;
- r_d is the shank radius of the steel rod;
- b_r is the width of the plane reinforcement;
- t_r is the thickness of the plane reinforcement;
- k_k is a factor to account for non-uniform distribution of stresses in the plane reinforcement. Without further verification, $k_k = 2.0$ may be assumed (for reinforcement of connections with a tensile force component perpendicular to the grain, $k_k = 1.5$ may be assumed, for reinforcement of curved or pitched cambered beams, $k_k = 1.0$ may be assumed);

- Reinforcement with punched metal plate fasteners should be designed in analogy to equation (4) and should be placed according to the rules for plane reinforcement given in the following sections.

The assembly of all equations to determine the resistance of the reinforcement in one place was undertaken with the aim to realize a homogeneous set of equations, independent of the member or detail to be reinforced and to enable a better overview of equations to determine resistances including all corresponding factors (ease-of-use). The factor k_k is applied to take into account the characteristics of the non-uniform distribution of stresses and the concentration of stresses at the panel edge facing the peak stresses in the timber member [15].

7.2 Effects of Moisture Content Changes

Standard text:

- The effects of moisture content changes in the timber (e.g. shrinkage cracks) shall be taken into account.

Background for the clause given above:

Changes in wood moisture content lead to changes of virtually all physical and mechanical properties (e.g. strength and stiffness properties) of wood. An additional effect of changes of the wood moisture content is the shrinkage or swelling of the material and the associated internal stresses. If these stresses locally exceed the very low tensile strength perpendicular to the grain of wood, the result will be a stress relief in form of cracks, which can reduce the load-carrying capacity of structural timber elements in e.g. shear or tension perpendicular to the grain. Multiple evaluations of damages in timber structures, e.g. [16], [17], [18], show,

that a prevalent type of damage is pronounced cracking in timber elements. Almost half of the damages in large-span glued laminated timber structures can be attributed to low or high moisture content or severe changes of the same.

- *The effects of moisture content changes in the timber should be minimized. Potential measures to reduce the effects of moisture content changes include:*
 - *Before being used in construction, timber should be dried as near as practicable to the moisture content appropriate to its climatic condition in the building in use, unless the structure is able to dry without any effect on the load-carrying capacity of its members;*
 - *During transport, storage and assembly, timber should be protected to minimize detrimental changes of moisture content in the timber;*
 - *In dry environments, controlled drying of the timber to service conditions should be planned.*

NOTE: In the case of structures or members sensitive to moisture changes, temporary moisture control is recommended.

- *The effects of reinforcement (or connections) that restrain moisture induced deformations of the timber member should be minimized.*

NOTE: External plane reinforcement glued onto the entire surface area under tensile stresses perpendicular to the grain decelerates the process of moisture changes or drying of the timber member, hence such reinforcement may be favourable in applications with permanently dry or frequently changing climate.

The most common effect of detrimental moisture content changes is shrinkage cracks. Shrinkage cracks can be attributed to two different phenomena.

1. Large moisture gradient over the timber cross-section due to strong and fast wetting or drying (the latter prevailing in closed and heated buildings) of the timber member, e.g. throughout the process production – transport – storage – assembly – interior works – opening – operation (heating). Careful planning and moisture control during this process is recommended, especially if a dry environment is to be expected in the finished building. Specifications on moisture control could be given in an execution standard for timber structures.
2. Prevention of free shrinkage or swelling deformation of the cross section by restraining forces, e.g. from connections covering larger heights or dowel-type reinforcement. In these cases, equilibrium of tensile and compressive moisture induced stresses is impeded, resulting in stresses of higher magnitude and eventually in deep shrinkage cracks.

Due to the fact that there is currently lack of a method to reliably predict the magnitude of tensile stresses perpendicular to the grain from moisture changes it was decided to introduce the term *effects of moisture content changes*.

- *Potential measures to reduce restraining effects from reinforcement include:*
 - *larger distances between reinforcement;*
 - *reduction of height of the reinforced areas in the timber member;*
 - *reducing the angle between dowel-type reinforcement and grain direction of the timber member.*

The restraining effect of dowel-type reinforcement was experimentally and analytically investigated in [19] and [20], demonstrating the positive effect of measures such as increased distance, reduced height or inclined positioning of dowel-type reinforcement. Attention should be paid to the additional stresses induced by the inclined reinforcement in the deformed timber beam (positive compression stresses perpendicular to the grain in the case of decreasing inclination, i.e. angle between load and grain, in the deformed shape vs. detrimental tensile stresses perpendicular to the grain in the case of increasing inclination in the deformed shape), see [21].

In the original draft, the proposed clauses on the effects of moisture content changes are separated into general clauses applicable to all timber elements (proposed as a new section 2.3.3 *Effects of moisture content changes* within Section 2.3 *Basic Variables*) and clauses applicable to reinforced timber elements (proposed for Section 6.4.2 *Effects of moisture content changes in reinforced beams*). For reasons of representation, this differentiation was omitted in this contribution.

7.3 Reinforcement of Double Tapered, Curved and Pitched Cambered Beams

Standard text:

- *For beams in which reinforcement to carry the full tensile stresses perpendicular to the grain is applied, the design tensile force in the reinforcement, $F_{t,90,Ed}$, should be calculated as follows:*

$$F_{t,90,Ed} = k_{kA} \cdot \sigma_{t,90,d} \cdot b \cdot a_1 \quad (6)$$

where

$\sigma_{t,90,d}$ *is the design tensile stress perp. to the grain (acc. to Eq. 6.54 in [2]);*

b *is the beam width;*

a_1 *is the spacing of the reinforcement in longitudinal direction of the beam at the height of its axis, see Fig. 5;*

k_{kA} *is a factor to account for the distribution of tensile stresses perpendicular to the grain along the beam axis*

$k_{kA} = 1.0$ for the inner quarters of the length of the volume exposed to tensile stresses perp. to the grain, measure from the apex, in double tapered, curved and pitched cambered beams;

$k_{kA} = 0.67$ for the outer quarters of the area exposed to tensile stresses perp. to the grain, in double tapered, curved and pitched cambered beams;

Background for the clause given above:

The approach given is based on an integration of the sum of tensile stresses perpendicular to the grain in the plane of zero longitudinal stresses. Since in most design standards, e.g. [2], only expressions to determine the maximum tensile stresses perpendicular to the grain in the apex are given, the distribution of tensile stresses perpendicular to the grain along the beam axis has to be accounted for in simplified format. Depending on the form and loading of the beam, the tensile stresses perpendicular to the grain decrease with increasing distance from the apex (an exception being the not yet standardized curved beams with mechanically fixed apex, i.e. secondary apexes, see below). For simplification, the full tensile stresses perpendicular to the grain are used to design the reinforcement in the inner quarters of the area exposed to tensile stresses perpendicular to the grain. In the outer quarters, the tensile stresses perpendicular to the grain are assumed to reach 2/3 of the maximum tensile stresses perpendicular to the grain, see Fig. 5.

- For curved or pitched cambered beams with mechanically jointed apex, the reinforcement should be designed for:
 - the tensile stresses perpendicular to the grain at the inflection points (secondary apex at the end of the mechanically jointed apex) and
 - the tensile stresses perpendicular to the grain from curvature in the apex.

The reinforcement at the inflection points should cover a length of at least $2 \cdot h_{ap}$ in direction of the apex and $1 \cdot h_{ap}$ in direction of the beam end. The reinforcement from the curvature in the apex should be arranged in the remaining curved parts. Between both areas, distances between the reinforcement may be linearly graded. If the tensile stresses perpendicular to the grain from curvature in the apex are higher than the tensile stresses perpendicular to the grain at the inflection points, the associated reinforcement should be arranged over the whole curved length.

Curved beams with mechanically jointed apex are neither regulated in EN 1995-1-1 [2] nor in NCI such as in [3], [4]. Nevertheless, these beams represent the most widely utilized form in practice. The most common type is curved beams with raised dry joint and mechanically jointed apex to realize the form of a pitched cambered beam. The top edge of the beam features a shorter curved length compared to the curved length of the bottom edge, leading to so-called secondary apexes at the transition points between the curved upper edge and the straight upper

edge of the beam. The approach to design curved beams with mechanically jointed apex and the reinforcement of the same is to examine and verify two different cross-sections:

1. The apex, formed by the curved part of the beam and to be designed in analogy to curved beams;
2. The secondary apex, located at the transition point between curved upper edge and straight upper edge at the end of the mechanically jointed apex. This cross-section is to be designed in analogy to pitched cambered beams.

The length of area to be covered by the reinforcement determined for the two cross-sections is dependent on the length of area of decreasing stresses. The design approach is in the style of the information and results presented in [22], [23].

- *Internal, dowel-type reinforcement should cover the full height of the beam excluding the outer lamellas in bending tension. One reinforcing element should be placed in the cross-section below the apex respectively secondary apex (inflection point). The spacing, a_1 , at the top side of the beam should not be less than 250 mm but not greater than $0,75 \cdot h_{ap}$.*
- *Plane reinforcement, e.g. panels or laminations, should be glued to both sides of the member and should cover the full height of the beam; at maximum it should exclude the outer lamellas.*

The timber-cross-section should not be reduced by reinforcement in the vicinity of the maximum tensile bending stresses. The spacing between the reinforcement is limited to ensure that the reinforcing effect is assured over the whole beam length exposed to tensile stresses perpendicular to the grain, see Fig. 5.

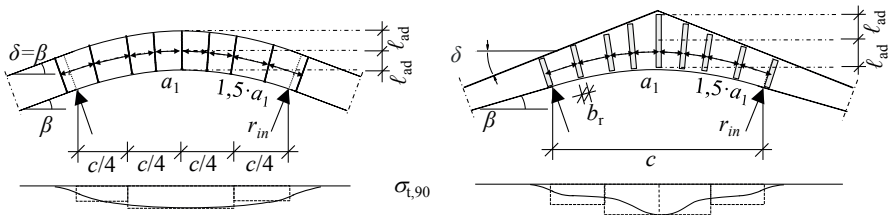


Fig. 5 Curved and pitched cambered beams: stress distribution, reinforcement and geometries

7.4 Reinforcement of Rectangular Notches in Members with Rectangular Cross-Section

Standard text:

- *The reinforcement of a rectangular notch on the loaded side of a member support (see Fig. 6) may be designed for a tensile force $F_{t,90,Ed}$:*

$$F_{t,90,Ed} = 1.3 \cdot V_d \cdot [3 \cdot (1-\alpha)^2 - 2 \cdot (1-\alpha)^3] \quad (7)$$

where

$$\alpha = h_{ef}/h; \text{ see Fig. 6.}$$

Background for the clause given above:

The tensile force perpendicular to the grain, $F_{t,90,Ed}$, can be approximated by integration of the shear stresses below the notch, between the loaded edge and the corner of the notch, see Fig. 6. A more detailed analysis of the magnitude of the tensile stresses perpendicular to the grain around the notch has shown that these stresses are even higher [24]. For relationships $x \leq h_{ef}/3$, the tensile force perpendicular to the grain, $F_{t,90,Ed}$, can be sufficiently estimated by applying an increase factor of 1,3.

- *The reinforcement should cover the full height of the notched edge ($h - h_{ef}$). The minimum length $l_{ad,t} = \min\{l_{ad,c}; 1.5 \cdot x\}$, see Fig. 6.*
- *If the tensile force, $F_{t,90,d}$, according to expression (7) is carried by internal dowel-type reinforcement, only one row of internal reinforcing elements at a distance $a_{3,c}$ from the edge of the notch should be considered. The dowel-type reinforcement may be inclined to reduce the distance between the peak tensile stresses perpendicular to the grain and the dowel-type reinforcement, see Fig. 6.*
- *If the tensile force, $F_{t,90,Ed}$, according to expression (7), is carried by internal dowel-type reinforcement, oriented perpendicular to the grain, the load-carrying capacity is limited to twice the load-carrying capacity of the unreinforced notched beam. In addition, the shear stresses (expression (6.13) in [2]) should be satisfied in the notched part.*
- *Plane reinforcement, e.g. panels or laminations, should be glued to both sides of the member, with the following limits:*

$$0.25 \leq \frac{b_r}{h - h_{ef}} \leq 0.5 \quad (8)$$

where

b_r is the width of the reinforcement panel or lamination in direction of the beam axis at the side of the notch;

h, h_{ef} see Fig. 6.

The depth of the reinforcement should be sufficient such as to ensure adequate load transfer into the reinforcement and from the reinforcement into the support. Only one row of dowel-type reinforcement at a distance $a_{3,c}$ should be considered as reinforcement. The distance between the dowel-type reinforcement and the notch, $a_{3,c}$, should be as small as possible. Reason is the limited distribution length of the tensile stresses perpendicular to the grain outside the corner of the notch. This can

be achieved by inserting the screws at an inclined angle, as the distance requirements are based on the position of the center of gravity of the dowel-type reinforcement in the timber member under consideration, $a_{3,CG}$, see Fig. 6. The limitation of load-carrying capacity of notched members reinforced with dowel-type reinforcement arranged perpendicular to the grain is based on [25], where it was experimentally and analytically verified that the load-carrying capacity of reinforced notched members is not infinite but limited by the shear component on fracture of notched members. The applicable width of reinforcement panels is limited due to the limited distribution length of the tensile stresses perpendicular to the grain outside the corner of the notch. In addition, this limitation is also implicitly directed at assuring panels of adequate thickness to prevent failure due to the stress singularities at the notch.

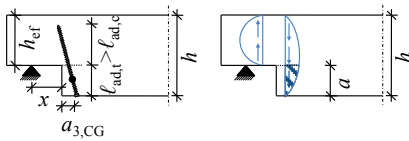


Fig. 6 Notched beam: reinforcement (left) and distribution of shear stresses (right).

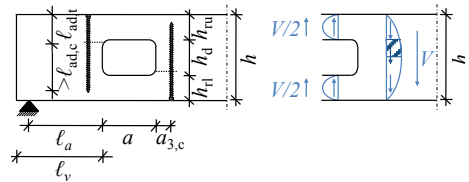


Fig. 7 Hole in beam: reinforcement (left) and distribution of shear stresses (right)

7.5 Reinforcement of Holes in Beams with Rectangular Cross-Section

Standard text:

The reinforcement of holes, which comply with the geometrical boundary conditions given in

- Tab. 1, may be designed for a tensile force, $F_{t,90,Ed}$, according to expression (9).

Tab. 1 Minimum and maximum dimensions of reinforced holes in beams with rectangular cross-section

$l_v \geq h$	$l_z \geq h$, not less than 300 mm ^c	$l_\Lambda \geq h/2$	$h_{r(tru)} \geq 0.25 \cdot h$	$a \leq h$ $a/h_d \leq 2.5$	$h_d \leq 0.3 \cdot h^a$ $h_d \leq 0.4 \cdot h^b$
^a for internal dowel-type reinforcement ^b for plane reinforcement, e.g. panels or laminations ^c l_z is the clear spacing between two holes					

$$F_{t,90,Ed} = F_{t,V,Ed} + F_{t,M,Ed} = \frac{V_d \cdot h_d}{4 \cdot h} \cdot \left[3 - \frac{h_d^2}{h^2} \right] + 0,008 \cdot \frac{M_d}{h_t} \quad (9)$$

where

$$h_r = \min \{h_{rl}; h_{ru}\}.$$

h_d, h, h_{rl}, h_{ru} see Fig. 7.

In the case of rectangular holes, the tensile force, $F_{t,90,Ed}$, should be assumed to act on planes defined by the top and bottom faces of the hole, on the corners prone to tensile stresses perpendicular to the grain (see Fig. 7). In the case of round holes, the tensile force, $F_{t,90,d}$, should be assumed to act under 45° from the center of the hole with regard to the beam axis. All areas prone to splitting from tensile stresses perpendicular to the grain should be analysed. The minimum and maximum dimensions given in

Tab. 1 apply:

- The relevant effective anchorage length, l_{ad} , applied in Expression (9) should be taken as follows, see also Fig. 7:

$$l_{ad} = h_{rl} \text{ or } h_{ru} \quad \text{for rectangular holes;}$$

$$l_{ad} = h_{rl} + 0.15 \cdot h_d \text{ or } h_{ru} + 0.15 \cdot h_d \quad \text{for round holes;}$$

Background for the clause given above:

The tensile force perpendicular to the grain, $F_{t,V,Ed}$, can be approximated by integration of the shear stress between the axis of the member and the corner of the hole prone to cracking. The tensile force perpendicular to the grain, $F_{t,M,Ed}$, has been derived from tests [26]. The limitation of the permissible relative dimensions of the holes in dependency of the type of reinforcement is described in [27], [28].

- The application of internal dowel-type reinforcement, positioned perpendicular to the grain, should be limited to locations in the timber member that are subjected to low shear stresses.
- In members with holes and internal dowel-type reinforcement, the increased shear stresses in the area of the edges of the holes should be accounted for. The maximum shear stress, τ_{max} , to be applied in shear verification (expression (6.13) in [2]), should be calculated as follows:

$$\tau_{max} = \kappa_{max} \cdot \frac{1,5 \cdot V_d}{b_{ef} \cdot (h - h_d)} = 1,84 \cdot \left[1 + \frac{a}{h} \right] \cdot \left(\frac{h_d}{h} \right)^{0,2} \cdot \frac{1,5 \cdot V_d}{b_{ef} \cdot (h - h_d)} \quad (10)$$

where

b_{ef} is the effective beam width, see 6.1.7. [2] (taking into account the impact of shrinkage cracks on shear capacity);

a, h, h_d see Fig. 7. In the case of round holes h_d may be replaced by $0.7 \cdot h_d$.

If the shear verification with τ_{\max} from Expression (10) is not fulfilled, internal reinforcement positioned perpendicular to the grain should not be used.

The limitation of applicability of dowel-type reinforcement, arranged perpendicular to the grain, to areas exposed to low shear stresses is based on the fact that this arrangement leads to restraint of free shrinkage (see Section 7.2). This results in reduced shear capacity of the reinforced timber member which, in the vicinity of holes, is exposed to increased shear stresses. The reinforcing effect of dowel-type or plane reinforcement is strongly dependent on the distance between the reinforcement and the location of peak stresses (in e.g. tension perpendicular to the grain or shear). To reduce this distance, dowel-type reinforcement can be rotated to e.g. 45°. Such an arrangement has additional advantages such that it also enables the transfer of shear stresses as well as a reduced restraining effect in case of shrinkage (see Section 7.2).

In the case of rectangular holes it is necessary to take into account the increased shear stresses around the edges of the holes. A description as well as an associated design equation is given in [29]. In [14] it is recommended to apply the same verification for round holes as well, although this yields results on the safe side. The same publication describes a method to verify the bending stresses above respectively below rectangular holes, including the additional longitudinal stresses from the frame action (lever of the shear force) around the hole (see also [26]).

- *If internal dowel-type reinforcement is arranged according to Fig. 7, the spacing requirements given in Section 7.1 apply.*
- *The relevant effective anchorage length, l_{ad} , of plane reinforcement, applied in Expression (4) should be taken as follows:*

$$l_{\text{ad}} = h_1 \quad \text{for rectangular holes;}$$

$$l_{\text{ad}} = h_1 + 0.15 \cdot h_d \quad \text{for round holes;}$$

where

h_1 is the depth of plane reinforcement above or below a hole.

- *The plane reinforcement, e.g. panels or laminations should be glued to both sides of the member, with the following limits:*

$$0.25 \cdot a \leq b_r \leq 0.6 \cdot l_{t,90} \quad (11)$$

and

$$h_1 \geq \max \begin{cases} 80 \text{ mm} \\ 0.25 \cdot a \end{cases} \quad (12)$$

where:

$$l_{t,90} = 0.5 \cdot (h_d + h) \quad (13)$$

b_r is the width of the reinforcement panel or lamination in direction of the beam axis at the sides of the hole;

a, h_d, h see Fig. 7.

The specifications concerning the edge distance and the permissible number of rows of dowel-type reinforcement and the applicable width of the reinforcement are due to the same conditions as described for notched members, see Section 7.4.

7.6 Reinforcement of Connections with a Tensile Force Component Perpendicular to the Grain

Standard text:

- The reinforcement of connections with a tensile force component perpendicular to the grain (see
- Fig. 8) may be designed for a tensile force $F_{t,90,Ed}$.

$$F_{t,90,Ed} = [1 - 3 \cdot \alpha^2 + 2 \cdot \alpha^3] \cdot F_{90,Ed} \quad (14)$$

where

$$\alpha = h_c/h \text{ see}$$

Fig. 8.

- The depth of the reinforcement ($l_{ad,c} + l_{ad,t}$, see
- Fig. 8) should be larger than $0.7 \cdot h$, measured from the loaded beam edge. In all other cases, the possibility of splitting caused by the tensile force component perpendicular to the grain, should be satisfied at the tip respectively edge of the reinforcement facing the unloaded beam edge.

Background for the clauses given above:

The tensile force perpendicular to the grain, $F_{t,90,Ed}$, is the resultant of the tensile stresses perpendicular to the grain on the plane defined by the loaded edge distance to the centre of the most distant fastener, h_c (see e.g. [30]). According to beam theory, the connection force component perpendicular to the grain results in a step in the shear force distribution. The tensile force perpendicular to the grain, $F_{t,90,Ed}$, is determined by integration of the shear stress in the area between the row of fasteners considered and the unloaded edge. The term in brackets in Eq. (14) is the result of this integration, a derivation can be found in e.g. [31].

The depth of the reinforcement should be sufficient such as to avoid moving the location of tensile failure perpendicular to the grain from the connection to the tip / edge of the reinforcement. In analogy to the experiences and rules for connections with a tensile force component perpendicular to the grain ([2], [3]), no verification is necessary for relationships $(l_{ad,c} + l_{ad,t})/h > 0.7$.

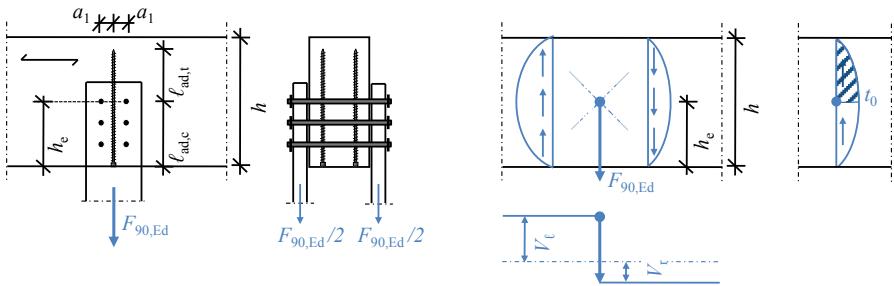


Fig. 8 Reinforced cross-connection: reinforcement (left) and distribution of shear stresses and shear flow (right)

- If the tensile force, $F_{t,90,Ed}$, is carried by internal dowel-type reinforcement, only one row of internal dowel-type reinforcement at a distance $a_{3,c}$ from the edge of the connection should be considered.
- The reinforcement panels or laminations should be glued to the member, with the following limits:

$$0.25 \leq \frac{b_r}{l_{ad}} \leq 0.5 \quad (15)$$

where

$$l_{ad} = \min \{l_{ad,c}; l_{ad,t}\} \quad (16)$$

b_r is the width of the reinforcement panel or lamination in direction of the beam axis at the sides of the connection;

The distance between the dowel-type reinforcement and the connection is limited to take into account the limited distribution length of the tensile stresses perpendicular to the grain outside the connection. The same is valid for the applicable width of reinforcement panels.

7.7 Bolted Connections

Standard text:

- Where splitting of the timber is prevented through sufficient reinforcement perpendicular to the grain, the effective number of fasteners according to (expression (8.34, i.e. determination of n_{ef} in [2]) may be taken as $n_{ef} = n$.
- The tensile force in the reinforcement may be taken as $F_{t,Ek} = 0.3 \cdot F_{v,Rk}$ with $F_{v,Rk}$ determined according to Johansen-Theory (expressions (8.9) – (8.13) in [2]).

Background for the clauses given above:

The load-carrying capacity per dowel in connections with multiple dowels placed in a row parallel to the grain and loaded by a load component parallel to the grain is smaller as the load-carrying capacity of a connection with one single dowel. This reduction in load-carrying capacity in connections with multiple dowel-type fasteners is mainly the result of premature splitting of the timber in the direction of the rows of dowels. The effective number of dowels (according to equation (8.34) in [2]) is based on [32]. Splitting may be prevented by reinforcing the connection area, e.g. by self-tapping screws or wood-based panels. In [33] it is demonstrated that in connections with sufficient reinforcement between the dowels, the timber does not split and the effective number n_{ef} equals the actual number n of dowels in one row. With reference to [34] it is stated in [33] that timber splitting is prevented, if the axial load-carrying capacity $F_{ax,Rk}$ of each screw exceeds 30 % of the lateral load-carrying capacity $F_{v,Rk}$ per shear plane of each dowel. In practice, a distance between the dowel/bolt and the dowel-type reinforcement of twice the dowel/bolt diameter has proven sufficient to enable a safe insertion of the reinforcement.

7.8 Reinforcement of Members with Compression Stresses Perpendicular to the Grain

Standard text:

- *For members with reinforcement by means of fully-threaded screws or screwed-in threaded rods to carry compression stresses perpendicular to the grain, provided:*
 - *an equal distribution of screws or rods in the reinforced contact area,*
 - *a fully supported bearing area or a contact material of adequate stiffness and evenness to provide an equal distribution of the compression force over all screws or rods;*
 - *an angle between screw or rod axis and grain direction $45^\circ \leq \alpha \leq 90^\circ$,*
 - *the screw or rod axis is perpendicular to the contact surface,*
 - *the screw or rod heads are flush with the contact surface,*
 - *penetration of the screw or rod heads is prevented by a contact material of adequate stiffness (e.g. a steel plate of adequate thickness).*

the characteristic resistance of the reinforced contact area should be taken as the minimum value found from the following expression:

$$F_{c,90,Rk} = \min \left\{ \begin{array}{l} k_{c,90} \cdot b \cdot l_{ef,1} \cdot f_{c,90,k} + n \cdot \min \{ F_{ax,a,Rk}; F_{ki,Rk} \} \\ b \cdot l_{ef,2} \cdot f_{c,90,k} \end{array} \right. \quad (17)$$

where

$k_{c,90}$ (according to 6.1.5.1 in [2]);

- b is the contact width, in mm;
- $l_{ef,1}$ is the effective contact length parallel to grain (according to 6.1.5 in [2]), in mm;
- $n = n_0 \cdot n_{90}$ is the number of fully-threaded screws or rods applied for reinforcement;
- n_0 is the number of fully-threaded screws or rods arranged in a row parallel to the grain;
- n_{90} is the number of fully-threaded screws or rods arranged in a row perpendicular to the grain;
- $F_{ax,\alpha,Rk}$ is the characteristic withdrawal capacity (according to 8.7.2 in [2] or Technical Assessment);
- $F_{ki,Rk}$ is the characteristic capacity of the screw in axial compression, in N , see below (or Technical Assessment);
- $l_{ef,2}$ is the effective distribution length parallel to grain in the plane defined by the screw or rod tips, see Fig. 9;

with

$$l_{ef,2} = l_{ad} + (n_0 - 1) \cdot a_1 + \min \{ l_{ad}; a_{3,c} \} \text{ for end supports, see Fig. 9,} \quad (18)$$

$$l_{ef,2} = 2 \cdot l_{ad} + (n_0 - 1) \cdot a_1 \text{ for intermediate supports, see Fig. 9,} \quad (19)$$

where

l_{ad} is the point side penetration length of the threaded part of the screw or rod in the timber member, in mm, see Fig. 9;

$a_1, a_{3,c}$ are the spacing parallel to grain and end distance, in mm.

- Minimum spacing and end and edge distances should be taken from (Table 8.6 in [2] or the Technical Assessment).
- The contact material (e.g. steel plate) should be designed for the load introduced by the screw head.
- If screws or rods are driven into the member from top and bottom and the screws are overlapping at least $10 \cdot d$, the second condition in Expression (17) may be disregarded. The screws should be arranged symmetrical to the bearing area.
- Reinforcement with glued-in rods may be designed in analogy to the clauses given above.

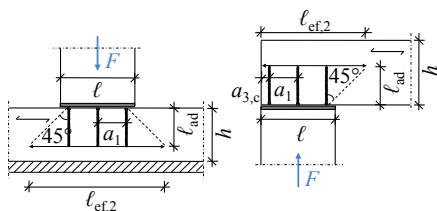


Fig. 9 Reinforced support areas: member on continuous support (left) and discrete support (right)

Background for the clauses:

Structural details in which the timber is loaded in compression perpendicular to the grain are very common, e.g. beam supports or sills/sole plates. The combination of high loads to be transferred over localized areas and low capacities in compression perpendicular to the grain can make it difficult to meet the associated verifications.

Fully-threaded, self-tapping screws or screwed-in rods are a means to improve the stress dispersion into the timber. The main developments in this field were achieved within [35].

In contrast to the design approach applied for reinforcement to carry tensile stresses perpendicular to the grain, the load-carrying capacity of a reinforced support can be determined under the assumption of an additive coaction between the timber under compression stresses perpendicular to the grain and the screws/rods under compression. This assumption is valid if certain deformations of the loaded edge are accepted. In addition, verification of the compression resistance of a fully-threaded screw (pushing-in or buckling) is necessary, see below. Finally it should be verified that the compression capacity perpendicular to the grain of the timber is not exceeded at the screw tips (transition between reinforced and unreinforced section), in a plane defined by an effective length, $l_{ef,2}$. The effective length is not to be interpreted as a support length, hence the factor $k_{c,90}$ is not applicable in this verification [35]. Reason is that at the screw tips, the failure behavior under compression stresses perpendicular to the grain is characterized by transverse deformations (elongation) over the member width. Over supports, this deformation is prevented by the bearing material. The angle of stress distribution applied to determine the effective length used for verification at the screw tips may be taken as 45° , measured from the screw heads. The definition of stress distribution has changed over the years (linear load distribution under 45° , measured from the edge of the steel plate [36]; exponential load distribution, measured from the edge of the steel plate [35]; linear load distribution under 45° , measured from the screw tips, e.g. [37], hence different approaches can still be found in literature. The compression force must be evenly distributed to all screws and the compression stresses at the screw heads have to be absorbed by the bearing material. These two requirements can only be met by a hard bearing material. This can be realized in form of a hard intermediate layer from e.g. steel, designed in adequate thickness and thus capable to transfer the load uniformly. In beam support, the steel plate should be supported by elastomeric bearing material to provide rotational capacity and thus a uniform stress transfer into the steel plate. The screws shall be equally distributed over the bearing area and the screw heads shall be on one line with the

surface of the timber member. The distance requirements are the same as for screws in tension. It is not necessary to take into account an effective number of screws, n_{ef} . Reinforcement driven in from both edges of the beam to enable the transfer of compression perpendicular to grain stresses through the timber member has been studied in [38] and was subsequently introduced into Technical Approvals [39].

For information on the verification of the fully-threaded screws or screwed-in rods in axial compression it is referred to the information given below. In [35] a calculation model to determine the stiffness of reinforced beam supports is proposed as well.

- The characteristic compression resistance (pushing-in or buckling), $F_{c,\alpha,Rk}$, should be taken as:

$$F_{c,\alpha,Rk} = \min \{ F_{ax,\alpha,Rk}; F_{ki,Rk} \} \quad (20)$$

where

$F_{ax,\alpha,Rk}$ is the characteristic withdrawal capacity (according to expression (8.39) respectively (8.40) in [2]);

$F_{ki,Rk} = 1,18 \cdot k_c \cdot N_{pl,k}$ is the characteristic capacity of the screw in axial compression;

$N_{pl,k} = \pi \cdot \frac{d_1^2}{4} \cdot f_{y,k}$ and values according to Tabl 2.

d_1 is the inner thread diameter;

$f_{y,k}$ is the characteristic yield strength of the steel

Table 2: Reduction factors k_c for buckling of screws

Characteristic value of yield strength of steel	Angle α between screw axis and grain	
	$\alpha = 90^\circ$	$\alpha = 0^\circ$
$f_{y,k} = 1000 \text{ N/mm}^2$	$k_c = 0.6$	$k_c = 0.5$
$f_{y,k} = 800 \text{ N/mm}^2$ (e.g. hot dip galvanized steel)	$k_c = 0.65$	$k_c = 0.55$
$f_{y,k} = 500 \text{ N/mm}^2$ (e.g. stainless steel)	$k_c = 0.75$	$k_c = 0.65$

The characteristic compression resistance of a fully-threaded screw is taken as the smaller of the pushing-in or buckling capacity. The pushing-in capacity is

considered equal to the withdrawal capacity of the fully-threaded screw. The full equations to determine the buckling capacity of fully-threaded screws were determined in [35]. The simplification of equations proposed above has been developed in [40]. In [35] information on the (increased) buckling resistance of fully-threaded screws with a clamped head support is given. This can be achieved by e.g. clamping the screw heads into a steel plate featuring holes that are countersunk in the form of the screw heads in such a way as the surface of the screw heads is flush with the lower steel plate surface. In practice this can be a challenge due the necessity of exact manufacturing in combination with the multitude of forms of screw heads available on the market.

8. Conclusions

Despite the current lack of design approaches in Eurocode 5, reinforcement for stresses perpendicular to the grain with fully-threaded, self-tapping screws, glued-in or screwed-in threaded rods or glued-on plywood and LVL should be considered state-of-the art in timber engineering practice. For numerous applications, design procedures are available which have already been clarified to an extent satisfying safety requirements and engineering needs. These are currently being prepared for introduction into the next generation of Eurocode 5. This contribution gives an overview of these developments, applications and related design procedures, including relevant background information. Future research and development should comprise the better quantification of the reinforcing effect of inclined dowel-type reinforcement, a clearer determination of stiffness properties of the reinforcement in the timber before cracking as well as further efforts to better understand and quantify the potentially harmful effect of reinforcement restricting the free shrinkage or swelling of the timber.

9. Acknowledgement

The technical input and comments from the following experts is thankfully acknowledged: Dr. Robert Jockwer (CH), Dr. Tobias Wiegand (DE), Harald Liven (NO) and Prof. João Negrão (PT).

10. References

- [1] Harte A., and Dietsch P. (eds), *Reinforcement of Timber Structures. A state-of-the-art report*, Shaker Verlag, 2015, Aachen, ISBN 978-3-8440-3751-7.
- [2] EN 1995-1-1:2004, *Eurocode 5: Design of timber structures - Part 1-1: General - Common rules and rules for buildings*, + AC (2006) + A1 (2008) + A2 (2014), European committee for standardization (CEN), Brussels, Belgium.
- [3] DIN EN 1995-1-1/NA:2013, *National Annex - Nationally determined parameters - Eurocode 5: Design of timber structures - Part 1-1: General - Common rules and rules for buildings*, DIN Deutsches Institut für Normung e.V., Berlin, Germany.

- [4] ÖNORM B 1995-1-1:2015-06, *Eurocode 5: Design of timber structures - Part 1-1: General - Common rules and rules for buildings - National specifications for the implementation of ÖNORM EN 1995-1-1, national comments and national supplements*, ASI Austrian Standards Institute, Vienna, Austria.
- [5] Dietsch P., and Winter S., “Eurocode 5 - Future Developments towards a more comprehensive code on timber structures”, *Structural Engineering International*, Vol. 22, No. 2, 2012, pp. 223-231.
- [6] CEN/TC 250 N1239, *Position paper on enhancing ease of use of the Structural Eurocodes*, CEN/TC 250 Doc. N1239, 2014, Brussels, Belgium.
- [7] Kleinhenz M., Winter S., and Dietsch P., “Eurocode 5 – a halftime summary of the revision process”, *Proceedings of the World Conference on Timber Engineering (WCTE 2016)*, 2016, Vienna, Austria.
- [8] Harte A., Jockwer R., Stepinac M., et al., “Reinforcement of Timber Structures – the route to standardization”, *Proceedings of the 3rd International Conference on Structural Health Assessment of Timber Structures SHATIS*, 2015, Wroclaw, Poland, ISBN 978-83-7125-255-6.
- [9] Dietsch P., and Brandner R., “Self-tapping screws and threaded rods as reinforcement for structural timber elements – A state-of-the-art report”, *Construction and Building Materials*, Vol. 97, 2015, pp. 78-89.
- [10] Steiger R., Serrano E., et al., “Strengthening of timber structures with glued-in rods”, *Construction and Building Materials*, Vol. 97, 2015, pp. 90-105.
- [11] Brüninghoff H., Schmidt C., and Wiegand T., „Praxisnahe Empfehlungen zur Reduzierung von Querschlüssen bei geleiteten Satteldachbindern aus Brettschichtholz“, *Bauen mit Holz*, Vol. 95, Iss. 11, 1993, pp. 928-937 (in German).
- [12] Ranta-Maunus A., and Gowda S.S., *Curved and cambered glulam beams - Part 2: Long term load tests under cyclically varying humidity*, VTT Publications 171, 1994, Technical Research Centre, Espoo.
- [13] Gustafsson P.J., “Notched beams and holes in glulam beams”, Blaß H.J., et al. (eds): *Timber Engineering STEP 1*, Centrum Hout, Almere, 1995.
- [14] Blaß H.J., Ehlbeck J., Kreuzinger H., and Steck G., *Erläuterungen zu DIN 1052:2004-08*, Bruderverlag, Karlsruhe, 2004 (in German).
- [15] Blaß H.J., and Steck G., „Querzugverstärkungen von Holzbauteilen: Teil 1 – Teil 3“, *Bauen mit Holz*, Vol. 101, 1999, Iss. 3, pp. 42-46, Iss. 4, pp. 44-49, Iss. 5, pp. 46-50 (in German).
- [16] Frühwald E., Serrano E., et al., *Design of safe timber structures – How can we learn from structural failures in concrete, steel and timber?* Report TVBK-3053, 2007, Div. of Struct. Eng, Lund University.

- [17] Blaß H.J., and Frese M., *Schadensanalyse von Hallentragwerken aus Holz*, Vol. 16 of the book series *Karlsruher Berichte zum Ingenieurholzbau*, KIT Scientific Publishing, Karlsruhe, 2010 (in German).
- [18] Dietsch P., and Winter S., “Structural failure in large-span timber structures: a comprehensive analysis of 230 cases”, *Structural Safety, under review*.
- [19] Wallner B., *Versuchstechnische Evaluierung feuchteinduzierter Kräfte in Brettschichtholz verursacht durch das Einbringen von Schraubstangen*, Master thesis, 2012, Institute of Timber Engineering and Wood Technology, Graz University of Technology (in German).
- [20] Dietsch P., “Effect of reinforcement on shrinkage stresses in timber members”, *Construction and Building Materials*, Vol. 150, 2017, pp. 903–915.
- [21] Blaß H.J., and Krüger O., *Schubverstärkung von Holz mit Holzschrauben und Gewindestangen*, Vol. 15 of the book series *Karlsruher Berichte zum Ingenieurholzbau*, KIT Scientific Publishing, Karlsruhe, 2010 (in German).
- [22] BVPI, *Spannungsnachweise bei Satteldachträgern aus Brettschichtholz*, Technische Mitteilung 06 / 011 der Bundesvereinigung der Prüfungenieure für Bautechnik e.V., Berlin, 2010 (in German).
- [23] Dietsch P., and Winter S., *Untersuchung von nicht im Eurocode 5 geregelten Formen von Satteldachträgern im Hinblick auf den Nachweis der Quersugspannungen*, Forschungsbericht, 2015, Lehrstuhl für Holzbau und Baukonstruktion (in German).
- [24] Henrici D., „Beitrag zur Bemessung ausgeklinkter Brettschichtholzträger“, *Bauen mit Holz*, Vol. 92, Iss. 11, 1990, pp. 806-811 (in German).
- [25] Jockwer R., *Structural behaviour of glued laminated timber beams with unreinforced and reinforced notches*, Dissertation, 2014, IBK Report No. 365, ETH Zurich.
- [26] Kolb H., and Epple A., *Verstärkungen von durchbrochenen Brettschichtholzbindern*, Schlussbericht zum Forschungsvorhaben I.4 – 34810, 1985, Forschungs- und Materialprüfungsanstalt Baden-Württemberg, Stuttgart (in German).
- [27] Aicher S., and Höfflin L., “Glulam Beams with Holes Reinforced by Steel Bars”, *Proceedings of the 42nd CIB-W18 Meeting*, CIB-W18/42-12-1, 2009, Zürich, Switzerland.
- [28] Aicher, S., “Glulam Beams with Internally and Externally Reinforced Holes – Test, Detailing and Design”, *Proceedings of the 44th CIB-W18 Meeting*, CIB-W18/44-12-4, 2011, Alghero, Italy.
- [29] Blaß H.J., and Bejtka I., Reinforcements perpendicular to the grain using self-tapping screws, *Proceedings of the 8th World Conference on Timber Engineering (WCTE 2004)*, 2004, Lahti, Finland.

- [30] Ehlbeck J., Görlacher R., and Werner H., „Empfehlung zum einheitlichen genaueren Querkzugnachweis für Anschlüsse mit mechanischen Verbindungsmitteln“, *Bauen mit Holz*, Vol. 93, Iss. 11, 1991, pp. 825-828 (in German).
- [31] Kreuzinger H., „Holzbau“, in: Zilch, K., Diederichs, C.J., and Katzenbach, R. (eds.): *Handbuch für Bauingenieure*, Springer, Berlin, 2002 (in German).
- [32] Jorissen A.J.M., *Double shear timber connections with dowel type fasteners*, Dissertation, 1998, Delft University of Technology, The Netherlands.
- [33] Bejtka I., and Blaß H.J., “Self-tapping screws as reinforcements in connections with dowel-type fasteners”, *Proceedings of the 38th CIB-W18 Meeting*, CIB-W18/38-7-4, 2005, Karlsruhe, Germany.
- [34] Schmid, M., *Anwendung der Bruchmechanik auf Verbindungen mit Holz*, Dissertation, 2002, Universität Karlsruhe (in German).
- [35] Bejtka, I., Blaß, H.J., “Self-tapping screws as reinforcements in beam supports”, *Proceedings of the 39th CIB-W18 Meeting*, CIB-W18/39-7-2, 2006, Florence, Italy.
- [36] Bejtka I., „Querzug- und Querdruckverstärkungen: Aktuelle Forschungsergebnisse“, *Proceedings of Ingenieurholzbau - Karlsruher Tage*, Bruderverlag, Karlsruhe, 2003 (in German).
- [37] ETA-12/0114, *Self-tapping screws for use in timber structures*, SPAX International GmbH & Co. KG, ETA Denmark, 2012.
- [38] Watson C.P., van Berschoten W., Smith T., Pampanin S., and Buchanan A.H., “Stiffness of screw reinforced LVL in compression perpendicular to the grain”, *Proceedings of the 46th CIB-W18 Meeting*, CIB-W18/46-12-4, 2013, Vancouver, Canada.
- [39] DIBt Z-9.1-519, *Allgemeine bauaufsichtliche Zulassung, SPAX-S Schrauben mit Vollgewinde als Holzverbindungsmitel*, Deutsches Institut für Bautechnik, Berlin, 2014 (in German).
- [40] Jockwer R., *Simplification of the design approach for buckling failure of reinforcement in compression*, Short Report, ETH Zurich, 2016.

Summary and Recommendations Regarding the Seismic Design of Timber Connections

Roberto Tomasi
Professor
Norwegian University of Life Science
Ås, Norway

Dag Pasca
M.S. student
Norwegian University of Life Science
Ås, Norway

Summary

The role of connections is crucial in the seismic design of timber structures. In timber structures, the energy dissipation cannot be achieved in timber elements, characterized by brittle failure mechanisms, but from the yielding of the mechanical connection devices, which should be designed adopting hierarchy principles, in order to favor local ductile mechanisms. This design approach, indicated also as capacity design approach, is illustrated in the first part of this paper.

The current version of the European code for seismic design (Eurocode 8, [1]), published in 2004, does not contain complete information on the application of these principles for timber structures. For that reason, a new proposal for the chapter 8 of Eurocode 8, containing different provisions for timber connections is currently under discussion, within the European Standardisation committee. These are summarized in the central part of this paper.

Capacity design rules require that the strength capacity of ductile elements must be lower than the strength capacity of brittle elements, and for this purpose a coefficient, indicated as over-strength factor, has to be introduced in the design. The assessment of this value is still under investigation for different type of timber connections, and some methods and results are reported in the last part of this paper.

1. Introduction

It is now internationally recognized that a well-designed and -manufactured timber building can provide high levels of seismic safety. This because, among other reasons, wood is much lighter than other building materials. The forces acting on a building in case of earthquake are proportional to the mass of the building itself; this means that wooden constructions are subjected to lower seismic loads in comparison to constructions made with other materials.

Wood, however, is an inherently brittle material, especially under tensile loads, and therefore timber elements exhibit almost no potential for energy dissipation. This means that in a timber structure the most efficient way to provide ductility, and consequently exhibit hysteretic dissipation of energy under cyclic loading, are the metal connection systems.

Structures designed according to recent seismic regulations possess resistance margins that allow them to withstand, accepting significant damage but preventing collapse, seismic loads of a level well above the ones used in the design phase. These margins come substantially from the application of hierarchy principles that aim at obtaining a properly highly dissipative plasticization mechanism (capacity design).

Capacity Design (CD) was developed in New Zealand during the nineteen seventies for the seismic design of reinforced concrete structures, and is the most common way of ensuring a dissipative behaviour. The definition of CD according to Eurocode 8 is: *“design method in which elements of the structural system are chosen and suitably designed and detailed for energy dissipation under severe deformations while all other structural elements are provided with sufficient strength so that the chosen means of energy dissipation can be maintained”*. [1]

A common way to explain the concept behind CD is the chain analogy: if we imagine having a chain made of several links, some brittle and some ductile, and apply a tension force to it, then the overall behaviour of the chain will be ductile (large deformation after yielding, and before failure) - if the resistance of the ductile links is lower than the resistance of the brittle links. Otherwise the behaviour of the chain will be brittle (sudden failure after yielding) - if the resistance of the brittle elements is lower than the ductile links. It is then obvious that the designer shall aim to obtain an overall ductile behaviour, by ensuring that the ductile failure mechanisms will activate before the brittle ones do.

The procedure aims to achieve a controlled damage by selecting proper lateral load resisting systems and proper detailing of individual members, and can be summarized as follows:

- a process in which it is decided which objects within a structural system will be permitted to yield (ductile components) and which objects will remain elastic (brittle components);
- ductile components are designed with sufficient deformation capacity to absorb the energy involved;
- brittle components are designed to achieve sufficient strength levels in comparison to the ductile ones.

This is ensured by the application of eq. (1):

$$\gamma_{Rd} \cdot F_{d,Rd} \leq F_{b,Rd} \quad (1)$$

Where $F_{b,Rd}$ and $F_{d,Rd}$ stand for the design resistance of the brittle and the ductile components respectively, whereas γ_{Rd} is the over-strength factor.

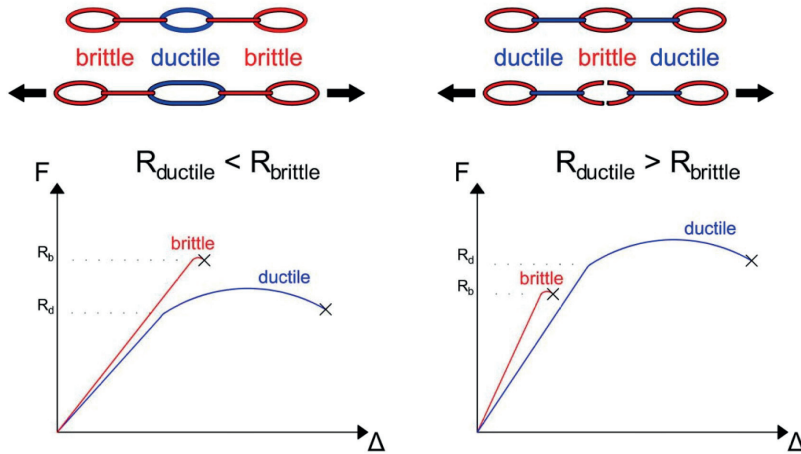


Fig. 1 Concept of Capacity Design

Since the most efficient way to rely on ductility is given by connections systems, a correct design of these elements is a crucial issue for the seismic design of timber structures.

2. The New Provision for Seismic Design of Timber Buildings

The current version of the Eurocode 8 provides, in Chapter 8 for the design timber structures, concise and short instructions, without a complete implementation of the capacity design approach. For this and other reasons a new proposal of this Chapter is currently under discussion within the CEN/TC250/SC8 'Design for Earthquake Actions', sub-group WG3 'Timber'.

The proposal has been partly presented in several papers, which represent follow-up of an ongoing work [2]. In the following are reported some of the principal provisions contained in the proposal regarding timber connections.

2.1 Design Concepts Regarding Timber Connections

The classification of timber buildings is modified specifying that “*Earthquake-resistant timber buildings shall be designed in accordance with one of the following concepts:*

- a) *High- or Medium-dissipative structural behaviour;*
- b) *Low-dissipative structural behaviour.”*

Later it is also specified that “*Other structural types, classified in ductility class M (medium, DCM) or H (high, DCH) may be designed with concept b) provided that the corresponding provisions given in the reference parts of this section for the general rules at building level are satisfied.*”

For the dissipative zones, the current definition specifies that the dissipative zones shall be located in joints and connections, whereas the timber members themselves shall be regarded as behaving elastically. More specifically it is stated that “*The energy dissipation is provided by plasticization of metal fasteners combined with embedment of timber at the interface with the fasteners, and for some systems also by friction. Friction can be taken into account only in presence of devices specifically designed for the transmission of horizontal forces through it; in other cases it shall not be considered.*”

The ductility properties of the dissipative zones should be fulfilled for each structural type in order to ensure that the given values of the behaviour factor (Tab. 1) may be used. Three alternative methods are given.

Method 1: ensuring that “*the dissipative zones, specified in the capacity design rules for each structural type, shall be able to deform plastically for at least three fully reversed cycles at a static ductility ratio reported in Tab. 1, without more than a 20 % reduction of their resistance between the first and third cycles backbone curve. For the same structural type these provisions shall be satisfied by only one type of dissipative sub-assembly/element provided that the Capacity Design Rules as defined in the relevant sections of each structural type are satisfied.*”

The values proposed in Tab. 1 are based on researches conducted so far (see for example [3] and [4] for light frame structures), however more research is needed in order to check their validity.

Method 2: as an alternative, the above given provisions may be regarded as satisfied in the dissipative zones of all structural types classified in ductility class H if the following provisions are met:

a) in doweled, bolted and nailed timber-to-timber and steel-to-timber joints, the minimum thickness of the timber connected members is $10d$ and the fastener-diameter d does not exceed 12 mm;

b) in shear walls and diaphragms of Light-Frame construction, the sheathing material is wood-based with a minimum thickness of $4d$, where the nail diameter d does not exceed 3.1 mm.

If the above requirements are not met, but the minimum member thickness of $8d$ and $3d$ for case a) and case b), respectively, is assured, the dissipative zones of all structural types can be regarded as ductility class M.

Tab. 1 Required static ductility values of dissipative zones tested according to EN 12512 [5], without more than a 20 % reduction of their resistance between the first and third cycles backbone curve for all structural types depending on the Ductility Class.

Structural type	Dissipative sub-assembly/element/connector	Type of ductility	DCM	DCH
CLT buildings	Shear wall	Displacement ductility	3.0	4.0
CLT buildings	Hold-downs, angle brackets, screws	Displacement ductility	3.0	4.0
Light-Frame buildings	Shear wall	Displacement ductility	3.0	5.0
Light-Frame buildings	Fastener (nail/screw/staple)	Displacement ductility	5.0	7.0
Log House buildings	Shear wall	Displacement ductility	2.0	–
Moment resisting frames	Portal Frame	Displacement ductility	2.5	4.0
Moment resisting frames	Beam-column joint	Rotational ductility	6.0	10.0
Post and beam timber buildings	Braced Frame	Displacement ductility	2.0	–
Timber framed walls with masonry infills	Shear wall	Displacement ductility	2.0	–
Vertical cantilever systems made with glulam or CLT wall elements	Shear wall	Displacement ductility	2.5	–

Method 3: as an alternative to method 2 the provisions of method 1 are considered satisfied if the following conditions are met.

- *for the dissipative zones of all ductility class M structural types, of the ductility class H CLT system with segmented wall and for the sheathing-to-framing connection, when a ductile failure mechanism characterized by the*

formation of at least one plastic hinge in the mechanical fasteners is attained for the seismic design load condition;

- for the nailed and screwed connections between the sheathing material and timber frame used in class H in Light-Frame buildings, when a ductile failure mechanism characterized by the formation of at least one plastic hinge in the nail (or screw) is attained for the seismic design load condition;
- for the dissipative zones of all ductility class H structural types, when a ductile failure mechanism characterized by the formation of two plastic hinges in the mechanical fasteners is attained for the seismic design load condition.

Referring to 8.2.2 of EN 1995-1-1 for timber-to-timber and panel-to-timber connections [6], failure modes a, b and c for fasteners in single shear, and g and h for fasteners in double shear characterized by only embedding of timber and no fastener plasticization shall be avoided. Referring to 8.2.3 of EN 1995-1-1 for steel-to-timber connections, failure modes a, c for fasteners in single shear, and f, j and l for fasteners in double shear characterized by only embedding of timber and no fastener plasticization shall be avoided. Special care should be taken in avoiding brittle failures characterized by splitting, shear plug, tear out and tensile fracture of wood in the connection regions. In the case of connections with multiple fasteners in dissipative zones, adequate reinforcement should be added to avoid the aforementioned brittle failure mechanisms.

Another provision is given for dowel-type fasteners transferring most of the load via axial resistance, which cannot be considered as dissipative. Referring to Fig. 2, A and B cannot be considered as dissipative connections, while C can be considered as dissipative.

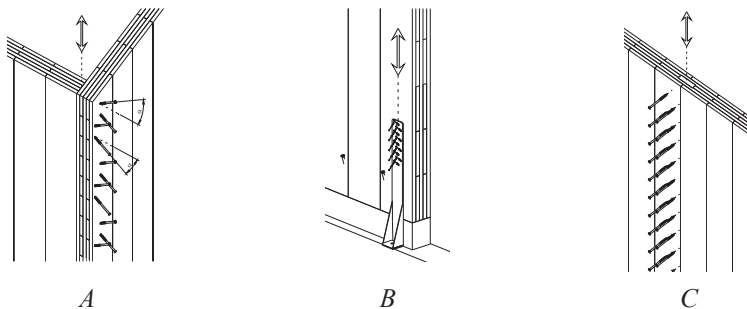


Fig. 2 A and B: fasteners inserted inclined with respect to the direction of the shear force, transferring most of the load via axial resistance, which cannot be considered as dissipative. C: connections inserted perpendicular with respect to the direction of the shear force, transferring most of the load via axial shear resistance, which can be considered as dissipative

3. Assessment of the Over-Strength Factor

Capacity Design rules require that the strength capacity of ductile elements must be lower than the strength capacity of the brittle elements. Due to the scatter in mechanical properties it is however not certain that the dissipative element will be the governing failure mechanism. An unexpected over-strength of a dissipative element could in fact compromise the resistance hierarchy planned by the designer. Therefore, in order to ensure that the chosen dissipative element will activate before the non-dissipative one, the over-strength factor is introduced in equation (1).

The design strength of the ductile part $F_{d,Rd}$ acts, in equation (1), as an action on the design strength of the brittle parts $F_{b,Rd}$, but it is calculated using 5th percentile values of material properties distributions. While using 5th percentile values to calculate resistance properties ensures to stay on the safe side, using them to calculate actions will have the opposite effect. The over-strength factor represents then the amount by which the actual strength of the dissipative element may exceed the design strength.

The first proposed method for the evaluation of the over-strength factor for timber structures from experimental testing can be found in Jorissen and Fragiaco [7]. In this paper, a general overview on ductility and over-strength factor for timber structures is presented using the results on previous work of Jorissen on dowelled connections. The over-strength factor is here defined as the contribution of three terms:

$$\gamma_{Rd} = \frac{R_{d,0.95}}{R_{d,0.05}} \cdot \frac{R_{d,0.05}}{R_{d,k}} \cdot \frac{R_{d,k}}{R_{d,d}} = \gamma_{sc} \cdot \gamma_{an} \cdot \gamma_M \quad (2)$$

Where $R_{d,0.95}$ and $R_{d,0.05}$ are respectively the 95th and 5th percentile of the ductile component strength distribution; $R_{d,k}$ and $R_{d,d}$ are respectively the characteristic and the design values of the

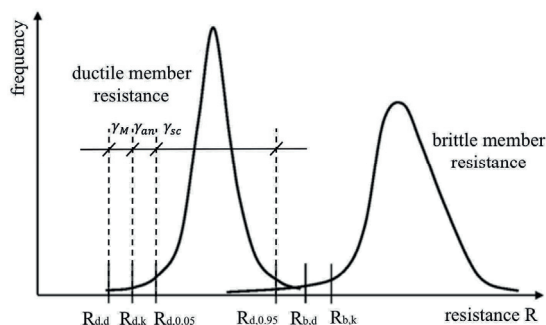


Fig. 3 Concept of over-strength factor according to [7]

analytical prediction of the ductile element strength. The coefficient $\gamma_{sc} = R_{d,0.95} / R_{d,0.05}$ expresses the scatter of the experimental connection strength properties and, therefore, gives an indication on the reliability of the connection. The coefficient $\gamma_{an} = R_{d,0.05} / R_{d,k}$ express instead how well the analytical formula used to evaluate the strength property approximates the

experimental results. Finally, γ_M is the partial material factor that, for verifications of structures designed in accordance with the concept of dissipative structural behaviour (DCM, DCH), should be taken from the accidental load combinations (equal to one). The average values μ , standard deviations σ , 5th and 95th percentile of the connection strength distribution, are calculated according to EN 14358 [8].

A formally different approach is presented in Schick et al, 2013 [9], here the over-strength factor is determined through the following equation:

$$\gamma_{Rd} = \frac{R_m^*}{R_k} \cdot \frac{R_{exp,m}}{R_m^*} \cdot \frac{R_{exp,0.95}}{R_{exp,m}} = \gamma_{mat} \cdot \gamma_{mech} \cdot \gamma_{0.95} \quad (3)$$

Where R_k is the design value according to code provisions, R_m^* is the mean value of resistance calculated with the mean values of material properties (instead of the characteristic ones), $R_{exp,m}$ is the mean value of strength capacity according to test results and $R_{exp,0.95}$ is the 95 % quantile of the experimental distribution of strength.

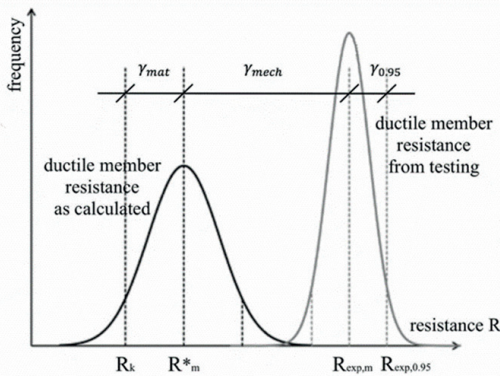


Fig. 4 Concept of over-strength factor according to [9]

The partial coefficient γ_{mat} then takes into account the spread between the characteristic resistance calculated according to design provisions and the one calculated using mean values for the material properties. γ_{mech} considers the “hidden reserves” that is present from the difference between calculated and experimental values. Finally, $\gamma_{0.95}$ is defined as the ratio between the 95th percentile and the mean value from testing. In this method as well the average values μ , standard

deviations σ , 5th and 95th percentile of the connections strength distribution are calculated according to EN 14358 [8].

A closer look at the equation (3) reveals that the differences with the definition found in Jorissen and Fragiacomio [7] is only in how the various contributions to evaluate γ_{Rd} are defined. Ultimately, in in both procedures γ_{Rd} depends only on the ratio $R_{d,0.95}/R_k$.

The survey of the existing literature for the assessment over-strength factor in timber structures revealed a mainly experimental approach to the topic [7, 9-13]. Several authors focused on the mainly used structural systems and the outcomes seem consistent even though, on average, a small number of samples and configurations was tested. On the other hand, only in one research a probabilistic simulation is employed even though this method is widely used for other structural materials and allows for a more extensive and cost-effective investigation [14].

Tab. 2 Overview of the evaluation of the OSF [7, 9-14]

Article	Approach	Connection type	Loading	n° of specimens	n° of configurations	Results (γ_{Rd})
[7]	$\gamma_{Rd} = \frac{R_{d,0.95}}{R_{d,0.05}} \cdot \frac{R_{d,0.05}}{R_{d,k}} \cdot \frac{R_{d,k}}{R_{d,d}}$ $= \gamma_{sc} \cdot \gamma_{an} \cdot \gamma_M$	Doweled connections timber-to-timber C24	Monotonic shear parallel to the grain	10 ÷ 25	14	1.20 ÷ 1.85 Mean 1.60
[9]	$\gamma_{Rd} = \frac{R_m^*}{R_k} \cdot \frac{R_{exp,m}}{R_n^*} \cdot \frac{R_{exp,0.95}}{R_{exp,m}}$ $= \gamma_{mat} \cdot \gamma_{mech} \cdot \gamma_{0.95}$	Nails and staples in light frame elements (OSB, GFB)	Monotonic and cyclic shear	4 ÷ 7 1 ÷ 4	11 10	Mean 2.20 Mean 1.65 (for $\gamma_{mech}=1$)
[10]	$\gamma_{Rd} = \frac{R_{d,0.95}}{R_{d,0.05}} = \gamma_{sc}$	Nailed connections metal angle brackets on CLT panels	Cyclic shear Cyclic uplift	3 2 ÷ 3	1 1	1.3 1.2
[11]		Screwed connections perpendicular CLT panels	Cyclic shear	5	1	1.6
[12]	$\gamma_{Rd} = \frac{R_{d,0.95}}{R_{d,0.05}} = \gamma_{sc}$	Screwed connections on CLT panels	Monotonic and cyclic shear (and withdrawal)	1 monotonic 6 cyclic	12	1.2 ÷ 1.9 Mean 1.74
[13]	$\gamma_{Rd} = \frac{R_{d,0.95}}{R_{d,0.05}} = \gamma_{sc}$	Hold-downs and angle brackets nailed on CLT panels	Monotonic and cyclic shear and tension	1 monotonic 6 cyclic	8	1.25 ÷ 1.45 angle brackets
[14]	Monte Carlo simulation Reliability analysis	Doweled connections timber-steel-timber GL24h	Bending	10 ⁸ simulations	3	1.99 for $\beta=3,80$

In Tab. 2 we can give an overview of the research that used these approaches to evaluate the over-strength factor for different types of connection systems, as hold-downs, angle brackets, and vertical joint between panels [7, 9-14]. The table shows the various researches comparing the approach used, the type of connection tested, number of specimen and configuration, adopted loading protocol and the results of the testing.

The Capacity Design rules and over-strength factor values proposed in the current draft proposal for the new chapter 8 of Eurocode 8 are mainly based on the results of these research experiences and for CLT buildings, for example, an over-strength factor of 1.3 is proposed. It should be noted however that most of the researches [10-13] does not report the values for γ_{an} , and calculates γ_{Rd} with the only contribution of γ_{sc} .

4. Conclusion

The ongoing work on the revision of the Chapter 8 of Eurocode 8 presents new concepts for the seismic design of timber buildings, such as the introduction of capacity design rules for each structural type and of the over-strength factors to be used in the design of the brittle components.

The validity of the new proposal has to be verified in different aspects by means of further research and investigation. Regarding the assessment of the over-strength factor, the experimental investigations should be larger and should include more types of connection systems used in the modern timber buildings. On the other hand studies considering a probabilistic approach (e.g. Monte Carlo simulation) are desirable to this purpose, overcoming some of the distinctive downsides of the experimental approach (e.g. limited number of specimens).

However, the survey on the existing literature shows that the over-strength factors experimentally derived for CLT structures tend to values equal or higher than the value 1.3 proposed in the new chapter 8 of the Eurocode 8.

In the opinion of the authors the adoption of lower values seems reasonable under two circumstances: when the resistance of the dissipative connection is evaluated through experimental tests, and not through the Johansen's equations; and if both the dissipative and the non-dissipative element that appear in the equation are connections. Then, it could be assumed that both connections will be overdesigned by approximately the same quantities and the fact that the European yielding model gives conservative values for the evaluation of the connection resistance could be neglected.

5. References

- [1] EN 1998-1-1, *Eurocode 8: Design of structures for earthquake resistance, Part 1: General rules, seismic actions and rules for buildings*, European Committee for Standardization (CEN), 2004, Brussels Belgium.
- [2] Follesa M., Fragiaco M., Vassallo D., Piazza M., Tomasi R., Casagrande D., and Rossi S., “A proposal for a new Background Document of Chapter 8 of Eurocode 8”, *Proceedings of the 48th International Network on Timber Engineering Research (INTER) Meeting*, 2015, p. 48-102-1 - ISSN: 2199-9740, Šibenik, Croatia.
- [3] Casagrande D., et al., “Capacity design approach for multi-storey timber-frame buildings”, *Proceedings of the International Network on Timber Engineering Research (INTER) Meeting*, 2014, p. 47-15-3, Bath, United Kingdom.
- [4] Casagrande D., Rossi S., Tomasi R., and Mischi G., “A predictive analytical model for the elasto-plastic behaviour of a light timber-frame shear-wall”, *Construction and Building Materials Engineering*, 2015, Elsevier.
- [5] EN 12512: *Timber structures – Test methods – Cyclic testing of joints made with mechanical fasteners*. European Committee for Standardization (CEN), 2001, Brussels Belgium.
- [6] EN 1995-1-1, *Eurocode 5: Design of timber structures – Part 1-1: General rules and rules for buildings*, European Committee for Standardization (CEN), 2009, Brussels Belgium.
- [7] Jorissen A., and Fragiaco M., “General notes on ductility in timber structures”, *Engineering Structures*, Vol. 33, Iss. 11, 2011, pp. 2987-2997.
- [8] EN 14358, *Timber structures. Calculation and verification of characteristic values*. European Committee for Standardization (CEN), 2016, Brussels Belgium.
- [9] Schick M., Vogt T., and Seim W., “Connections and anchoring for wall and slab elements in seismic design”, *Proceedings of the 46th CIB W18 Meeting*, 2013, Vancouver, Canada.
- [10] Sustersic I., Dujic B., and Fragiaco M., “Influence of the Connection Modelling on the Seismic Behaviour of Crosslam Timber Buildings”, *Materials and Joints in Timber Structures*, RILEM book series Vol. 9, 2014, pp. 677-687.
- [11] Fragiaco M., Dujic B., and Sustersic I., “Elastic and ductile design of multi-storey crosslam massive wooden buildings under seismic actions”, *Engineering Structures*, Vol. 33, Iss. 11, 2011, pp. 3043-3053.

- [12] Gavric I., Fragiacomio M., and Ceccotti A. “Strength and deformation characteristics of typical X-lam connections”, *Proceedings of the World Conference on Timber Engineering (WCTE 2012)*, Vol. 2, pp. 146-155, Auckland New Zealand.
- [13] Gavric I., Fragiacomio M., and Ceccotti A. “Cyclic behavior of CLT wall systems: Experimental tests and analytical prediction models”, *Journal of Structural Engineering*, Vol. 141, Iss. 11, 2015, United States.
- [14] Brühl F., Schänzlin J., and Kuhlmann U., “Ductility in Timber Structures: Investigations on Over-Strength Factors”, *Materials and Joints in Timber Structures. Recent developments in technology*, RILEM bookseries Vol. 9, 2014, pp. 181-190.

Conference of COST Action FP1402
Graz University of Technology, Institute of Timber Engineering and Wood Technology
Graz, Austria, 13.09.2017

International Conference on Connections in Timber Engineering – From Research to Standards

Lists of Authors, Reviewers and Participants

List of Authors

- Thomas K. Bader Dr., Associate Professor
Department of Building Technology
Linnaeus University
351 95 Växjö, Sweden
thomas.bader(at)lnu.se
- Hans Joachim Bläß Prof. Dr.-Ing., Head of the Institute
Research Center for Steel, Timber and Masonry
Karlsruhe Institute of Technology (KIT)
Reinhard-Baumeister-Platz 1, 76131 Karlsruhe, Germany
hans.blass(at)kit.edu
- Jean-François Bocquet Associate Professor
ENSTIB / LERMAB, University of Lorraine
27 rue Philippe Séguin, 88026 Epinal cedex, France
jean-francois.bocquet(at)univ-lorraine.fr
- Reinhard Brandner Ass.Prof. Dipl.-Ing.(FH) Dr.techn., Assistant Professor
Institute of Timber Engineering and Wood Technology
Graz University of Technology
Inffeldgasse 24/I, 8010 Graz, Austria
reinhard.brandner(at)tugraz.at
- Alfons Brunauer Dipl.-Ing., Technical Director Timber Engineering
WIEHAG GmbH
Linzer Straße 24, 4950 Altheim, Austria
a.brunauer(at>wiehag.com
- Frank Brühl Dipl.-Ing., Head of WIEHAG Engineering
WIEHAG GmbH
Linzer Straße 24, 4950 Altheim, Austria
f.bruehl(at>wiehag.com
- Alfredo M. P. G. Dias Prof. Dr., Assistant Professor
Departamento de Engenharia Civil – FCTUC
University of Coimbra
Rua Luís Reis Santos – Pólo II da Universidade
3030 – 788 Coimbra Coimbra, Portugal
alfgdias(at)dec.uc.pt
- Philipp Dietsch Dr.-Ing., Team Leader Timber Structures
Chair of Timber Structures and Building Construction
Technical University of Munich
Arcisstraße 21, 80333 München, Germany
dietsch(at)tum.de

Gerhard Fink	Dipl.-Ing. Dr., Assistant Professor School of Engineering Aalto University Rakentajanaukio 4 A, 02150 Espoo, Finland <i>gerhard.fink(at)aalto.fi</i>
Rainer Görlacher	Dr.-Ing., Academic Director Research Center for Steel, Timber and Masonry Karlsruhe Institute of Technology (KIT) Reinhard-Baumeister-Platz 1, 76131 Karlsruhe, Germany <i>rainer.goerlacher(at)kit.edu</i>
Robert Jockwer	Dr., Senior Scientist Institute of Structural Engineering ETH Zurich Stefano-Franscini-Platz 5, 8093 Zurich, Switzerland <i>jockwer(at)ibk.baug.ethz.ch</i>
Jochen Köhler	Dr., Associate Professor Department of Structural Engineering NTNU Richard Birkelands vei 1a, 7491 Trondheim, Norway <i>jochen.kohler(at)ntnu.no</i>
Ulrike Kuhlmann	Prof. Dr.-Ing., Professor Institute of Structural Design Universität Stuttgart Pfaffenwaldring 7, 70569 Stuttgart, Germany <i>u.kuhlmann(at)ke.uni-stuttgart.de</i>
Romain Lemaître	M.Sc., Doctoral student ENSTIB / LERMAB, University of Lorraine 27 rue Philippe Séguin, 88026 Epinal cedex, France <i>romain.lemaitre(at)univ-lorraine.fr</i>
Simon Mönch	M.Sc., Research assistant Institute of Structural Design University of Stuttgart Pfaffenwaldring 7, 70569 Stuttgart, Germany <i>simon.moench(at)ke.uni-stuttgart.de</i>
Jørgen Munch-Andersen	Dr., Senior Advisor Danish Timber Information (TRÆINFORMATION) Lyngby Kirkestræde 14, 2800 Kongens Lyngby, Denmark <i>jma(at)traeinfo.dk</i>

Dag P. Pasca	M.S. student Faculty of Science and Technology Norwegian University of Life Science, Campus Ås Universitetstunet 3, 1430 Ås, Norway <i>dag.pasquale.pasca(at)nmbu.no</i>
Pierre Quenneville	Prof. Dr., Professor of timber design Department of Civil and Environmental Engineering The University of Auckland 20 Symonds Str., Auckland 1010, New Zealand <i>p.quenneville(at)auckland.ac.nz</i>
Andreas Ringhofer	Dipl.-Ing. Dr.techn., Post Doc, Research Associate Institute of Timber Engineering and Wood Technology Graz University of Technology Inffeldgasse 24/I, 8010 Graz, Austria <i>andreas.ringhofer(at)tugraz.at</i>
Carmen Sandhaas	Dr.ir., Senior Researcher Research Center for Steel, Timber and Masonry Karlsruhe Institute of Technology (KIT) Reinhard-Baumeister-Platz 1, 76131 Karlsruhe, Germany <i>carmen.sandhaas(at)kit.edu</i>
Jörg Schänzlin	Prof. Dr.-Ing. habil., Head of the Institute Institute of Timber Design University of Applied Sciences Biberach Karlstrasse 11, 88400 Biberach, Germany <i>schaenzlin(at)hochschule-bc.de</i>
Michael Schweigler	Dipl.-Ing., Research Assistant, Doctoral student Institute for Mechanics of Materials and Structures Vienna University of Technology Karlsplatz 13/202, 1040 Wien, Austria <i>michael.schweigler(at)tuwien.ac.at</i>
Roberto Tomasi	Prof. Dr. Ing., Professor Faculty of Science and Technology Norwegian University of Life Science, Campus Ås Universitetstunet 3, 1430 Ås, Norway <i>roberto.tomasi(at)nmbu.no</i>

List of Reviewers

- Reinhard Brandner Ass.Prof. Dipl.-Ing.(FH) Dr.techn., Assistant Professor
Institute of Timber Engineering and Wood Technology
Graz University of Technology
Inffeldgasse 24/I, 8010 Graz, Austria
reinhard.brandner(at)tugraz.at
- Philipp Dietsch Dr.-Ing., Team Leader Timber Structures
Chair of Timber Structures and Building Construction
Technical University of Munich
Arcisstraße 21, 80333 München, Germany
dietsch(at)tum.de
- Robert Jockwer Dr., Senior Scientist
Institute of Structural Engineering
ETH Zurich
Stefano-Franscini-Platz 5, 8093 Zurich, Switzerland
jockwer(at)ibk.baug.ethz.ch
- Andreas Ringhofer Dipl.-Ing. Dr.techn., Post Doc, Research Associate
Institute of Timber Engineering and Wood Technology
Graz University of Technology
Inffeldgasse 24/I, 8010 Graz, Austria
andreas.ringhofer(at)tugraz.at

List of Participants (status from 18. 08. 2017)

Name	Family Name	Affiliation	E-mail
Ishan	Abeysekera	ARUP	ishan.abeysekera(at)arup.com
Thomas	Bader	Linnaeus University	thomas.bader(at)lnu.se
Bostjan	Ber	University of Maribor	bostjan.ber(at)kager-hisa.si; bostjan.ber(at)kager.si
Stefano	Bezzi	Norwegian University of Life Sciences	stefano.bezzi(at)unitn.it
Andrii	Bidakov	Kharkiv National University	bidakov(at)mail.ru
Hans Joachim	Blaß	KIT	blass(at)kit.edu
Jean-François	Bocquet	LERMAB Epinal	jean-francois.bocquet(at)univ-lorraine.fr
Reinhard Frank	Brandner	TU Graz	reinhard.brandner(at)tugraz.at
	Brühl	Wiehag	f.bruehl(at)wiehag.com
Alfons	Brunauer	Wiehag	a.brunauer(at)wiehag.com
Jose Manuel	Cabrero	Universidad de Navarra	jcabrero(at)unav.es
Wen-Shao	Chang	University of Bath	wsc22(at)bath.ac.uk
Manuela	Chiodega	Rothoblaas GmbH	manuela.chiodega(at)rothoblaas.com
Timo	Claus	University of Kassel	timo.claus(at)uni-kassel.de
Reid	Costley	ISL Engineeringand Land Services LTD	RCostley(at)islengineering.com
Thierry	Descamps	University of Mons	thierry.DESCAMPS(at)umons.ac.be
Philipp	Dietsch	TUM	dietsch(at)tum.de
Julia	Dröscher	DI Josef Koppelhuber	j.droescher(at)koppelhuber.at
Artur	Feio	University Lusiada	arturfeio(at)gmail.com
Gerhard	Fink	Aalto University	gerhard.fink(at)aalto.fi
Steffen	Franke	Bern University of Applied Science	steffen.franke(at)bfh.ch
Alfredo	Geraldes Dias	University of Coimbra	alfgdias(at)dec.uc.pt
Kiril	Gramatikov	UKIM	gramatikov(at)gf.ukim.edu.mk
Andreas	Hettich	HECO-Schrauben GmbH & Co KG	info(at)heco-schrauben.de
Georg	Hochreiner	TU Wien	georg.hochreiner(at)tuwien.ac.at
Daniel	Honfi	Technical Research Institute of Sweden	daniel.honfi(at)sp.se
Bilgin	Icel	Suleyman Demirel University	bilginicel(at)sdu.edu.tr
Tiago	Ilharco	NCREP	tiago.ilharco(at)ncrep.pt
Matteo	Izzi	IVALSA / Uni of Trieste / Uni of Sassari	izzimatteo(at)gmail.com
Mario	Jelec	University of Osijek	mjelec(at)gfos.hr
Robert	Jockwer	ETH Zurich / Empa	jockwer(at)ibk.baug.ethz.ch
André	Jorissen	Eindhoven University of Technology	a.j.m.jorissen(at)tue.nl
Marion	Kleiber	Harrer-Ingenieure, Karlsruhe	m.kleiber(at)harrer-ing.net
Miriam	Kleinhenz	TUM	kleinhenz(at)tum.de
Klemen	Klemenak	Vinzenz Harrer GmbH	klemen.klemenak(at)harrer.at
Sebastian	Knoflach	Mayr-Melnhof Holz GmbH	Sebastian.Knoflach(at)mm-holz.com
Jochen	Köhler	NTNU	jochen.kohler(at)ntnu.no
Josef	Koppelhuber	DI Josef Koppelhuber	office(at)koppelhuber.at
Ewa	Kotwica	BUD-LOGISTIK	ewainga(at)members.pl
Miha	Kramar	Slovenian National Building and Civil Engineering Institute	miha.kramar(at)zag.si
Benjamin	Kreis	ETH Zurich	kreis(at)ibk.baug.ethz.ch; kreis(at)ibk.ethz.ch
Harald	Krenn	KLH Massivholz GmbH	krenn(at)klh.at
Petr	Kuklik	Czech Technical University	kuklik(at)fsv.cvut.cz
Pierre	Landel	RISE	pierre.landel(at)ri.se
Peter	Lang	Rothoblaas GmbH	peter.lang(at)rothoblaas.com
Andrew	Lawrence	ARUP	andrew.lawrence(at)arup.com

Name	Family Name	Affiliation	E-mail
Bernd	Lederwasch	Vinzenz Harrer GmbH	bernd.lederwasch(at)harrer.at
Ildiko	Lukacs	Norwegian University of Life Science	ildiko.lukacs(at)nmbu.no
Chiara	Luzzani	Rothoblaas GmbH	chiara.luzzani(at)rothoblaas.com
Almudena	Majano-Majano	Technical University Madrid	almudena.majano(at)upm.es
Julian	Marcroft	Marcroft Timer Consultancy Ltd.	julian(at)marcrofttimerconsultancy.co.uk
Michael	Mikoschek	HS Augsburg	michael.mikoschek(at)hs-augsburg.de
Franco	Moar	Rothoblaas GmbH	franco.moar(at)rothoblaas.com
Simon	Mönch	University of Stuttgart	simon.moench(at)ke.uni-stuttgart.de
Sandra	Monteiro	University of Coimbra	sandra(at)dec.uc.pt
Thomas	Moosbrugger	Rubner	thomas.moosbrugger(at)rubner.com
Jørgen	Munch-Andersen	Traeinformation	jma(at)traeinfo.dk
Tomasz	Nowak	Wroclaw University of Technology	tomasz.nowak(at)pwr.edu.pl
Tomaz	Pazlar	Slovenian National Building and Civil Engineering Institute	tomaz.pazlar(at)zag.si
Julius	Postupka	Universität Stuttgart	julius.postupka(at)ke.uni-stuttgart.de
Pierre	Quenneville	The University of Auckland	p.quenneville(at)auckland.ac.nz
Henrik	Rasmussen	Lilleheden A/S	hr(at)lilleheden.dk
Andreas	Ringhofer	TU Graz	andreas.ringhofer(at)tugraz.at
Daniel	Roat	Rothoblaas GmbH	Daniel.Roat(at)rothoblaas.com
Vladimir	Rodriguez	Barcelona Tech-UPC	biotectura(at)gmail.com
Jaroslav	Sandanus	Slovak University of Technology	jaroslav.sandanus(at)stuba.sk
Carmen	Sandhaas	KIT	carmen.sandhaas(at)kit.edu
Jörg	Schänzlin	HS Biberach	schaenzlin(at)hochschule-bc.de
Johann	Scheibenreiter	Schmid Schrauben Hainfeld GmbH	Johann.Scheibenreiter(at)schrauben.at
Kay-Uwe	Schober	HS Mainz	kay-uwe.schober(at)hs-mainz.de; schober(at)is-mainz.com
Michael	Schweigler	TU Wien	michael.schweigler(at)tuwien.ac.at
Wendel	Sebastian	University of Bristol	Wendel.Sebastian(at)bristol.ac.uk
Erik	Serrano	Lund University	erik.serrano(at)construction.lth.se
Roman	Shchupakivskyy	Ukraine National Forestry University	roman.shchupakivskyy(at)nltu.edu.ua
Jan	Siem	NTNU	Jan.Siem(at)ntnu.no
Christophe	Sigrist	Bern University of Applied Science	christophe.sigrist(at)bfh.ch
Rossi	Simone	University of Trento	simone.rossi(at)unitn.it
Phil	Snowden	Heyne Tillett Steel	PSnowden(at)hts.uk.com
Kristian	Sogel	Slovak University of Technology	kristian.sogel(at)stuba.sk
Uwe	Stehle	HECO-Schrauben GmbH & Co KG	info(at)heco-schrauben.de
Mislav	Stepinac	University of Zagreb	mstepinac(at)grad.hr; mstepinac(at)gmail.com
Roberto	Tomasi	Norwegian University of Life Sciences	roberto.tomasi(at)unitn.it; roberto.tomasi(at)nmbu.no
Tomi	Toratti	Confederation of Finnish Construction Industries	tomi.toratti(at)puutuoteteollisuus.fi; tomi.toratti(at)woodworkingindustries.fi
Eleftheria	Tsakanika	NTUA	eletsaka(at)central.ntua.gr; etsakanika(at)arch.ntua.gr
Vasileios	Tsipiras	itech	v.tsipiras(at)itech-soft.com
Eero	Tuhkanen	Tallinn University of Technology	eero.tuhkanen(at)ttu.ee
Johannes	Urschitz	Würth Handels GmbH	johannes.urschitz(at)wuertth.at
Simone	Vanzo	Rothoblaas GmbH	simone.vanzo(at)rothoblaas.com
Lukas	Velebil	CTU Prague	lukas.velebil(at)seznam.cz
Markus	Wallner-Novak	FH Joanneum	Markus.Wallner-Novak(at)fh-joanneum.at
Laura	Watzlik	SIHGA GmbH	l.watzlik(at)sihga.com

International Conference on Connections in Timber Engineering From Research to Standards

Significant technical advances and developments in the field of timber connections within the last years have fostered the recent renaissance of timber as a structural material. An increased range of connection types and corresponding applications gives designers both opportunity and challenge. The result is a noticeable trend towards systemized solutions enabling quick and reliable assembly on site.

The objective of this conference is to record the current state-of-the-art for connections in timber engineering, and to illustrate how new developments will be adopted in the next generation of Timber Design Standards. It is an opportunity to have this compendium of contributions from some of the world's leading experts on the design, application and performance of Connections in Timber Engineering.

Verlag der Technischen Universität Graz
www.ub.tugraz.at/Verlag

ISBN (print) 978-3-85125-553-9
ISBN (e-book) 978-3-85125-554-6
DOI 10.3217/978-3-85125-553-9

Sponsorship

